



The  
University  
Of  
Sheffield.

# **Characterising lymphocyte subpopulations and heat shock protein 70 expression in clinical and experimental pulmonary arterial hypertension**

**Amy Joanna Shepherd**

**Department of Cardiovascular Science**

**University of Sheffield**

**Thesis submitted for the degree of Doctor of Philosophy**

**September 2012**

# Summary

Pulmonary arterial hypertension (PAH) is fatal disease of the small pulmonary arteries which is characterised by medial hypertrophy causing an increase in pulmonary vascular resistance and pulmonary artery pressure resulting in right ventricular failure and death. The pathogenesis of PAH has not been fully elucidated to date and there is no current curable pharmacological treatment.

Inflammation is thought to play an important role in the pathogenesis of PAH. The work undertaken in this thesis aimed to investigate the role of T cells in the pathogenesis of PAH by characterising lymphocyte subsets (T and B cell distribution) in treatment-naïve patients with PAH and animal models of disease. I found that the relative frequency of CD8<sup>+</sup> cytotoxic T cells in treatment-naïve Scleroderma associated-PAH patients was significantly decreased compared to corresponding controls. A negative correlation was also noted between the relative frequency of CD4<sup>+</sup> T cells and several clinical parameters. To investigate cause or effect of changes in T cell frequency, I examined a time course of the paigen diet-fed ApoE<sup>-/-</sup>/IL-1R1<sup>-/-</sup> mouse model of PAH, but noted no difference in circulating T cell subset distribution. CD4<sup>+</sup> T cell depletion rendered these animals more susceptible to the development of PAH.

Collectively, these findings suggest that subtypes of PAH are associated with distinct T cell profiles. Alterations in circulating T cell and B cell subsets in clinical PAH, particularly CD8<sup>+</sup> T cells suggest a dysfunctional immune system which could contribute to disease pathogenesis. In experimental models, the propagation of disease progression by depletion of CD4<sup>+</sup> T cells suggests an anti-inflammatory nature of these cells within this disease setting. Future studies are needed to fully understand the exact role that T cells play in the pathogenesis of PAH.

# Acknowledgements

Firstly I wish to thank my supervisors Dr Allan Lawrie and Professor Graham Pockley for their support, guidance and patience throughout my time at Sheffield University. Their encouragement and intellectual guidance has been very much appreciated. Thankyou to the pulmonary vascular lab group for their support, you have been a pleasure to work with and I have greatly enjoyed being part of the group. Special thanks go to Nadine Arnold for her help in the field labs, Kay Hopkinson and Sue Newton for their help in the flow cytometry core facility at Sheffield University and Josephine Pickworth for her help in the lab.

I also wish to thank everyone in the department of Cardiovascular Science at Sheffield University for their encouragement and helpful insights into my project over the years at research in progress meetings. I also appreciate the help and support of the SPVDU and CVBRU for their help in collecting the clinical blood samples and Dr Abdul Hameed for donating serum samples and undertaking haemodynamic assessments. I also wish to thank the NIHR the MRC for their support.

I have made many friends during my 4 years in Sheffield and I appreciate all of their encouraging words and witty banter which have got me through the dull days of thesis writing and labwork, however special thanks have to go to Gemma Foulds and Sara Kohal who over the years have become very special friends to me. I hope to treasure our friendships for many years to come.

I wouldn't have even thought about attempting a PhD if it wasn't for my parent's enthusiasm for science and their support of my career. Their encouragement has been unwavering and much appreciated. And finally, special thanks go to Chris, who has kept my spirits up and been patient with me through the most frustrating moments of writing my thesis.

# Table of contents

Summary .....	i
Acknowledgements.....	ii
Table of contents.....	iii
List of figures.....	vi
Abbreviations .....	x
Chapter 1 General introduction.....	1
1.1 PULMONARY CIRCULATION .....	1
1.2 T CELL IMMUNOBIOLOGY.....	1
1.2.1 <i>Mechanisms of action of Treg cells</i> .....	6
1.3 PULMONARY HYPERTENSION.....	9
1.4 PULMONARY ARTERIAL HYPERTENSION .....	11
1.4.1 <i>Idiopathic pulmonary arterial hypertension</i> .....	11
1.4.2 <i>Pulmonary arterial hypertension secondary to connective tissue disease</i> .....	12
1.5 PATHOBIOLOGY OF PULMONARY ARTERIAL HYPERTENSION.....	14
1.6 MECHANISMS OF PULMONARY ARTERIAL HYPERTENSION PATHOGENESIS .....	16
1.6.1 <i>Genetics</i> .....	16
1.6.1.1 Bone morphogenetic receptor 2 mutations .....	17
1.6.1.2 Activin-receptor-like kinase 1 mutations .....	17
1.6.1.3 Endoglin mutations .....	18
1.6.2 <i>Voltage-gated potassium channels</i> .....	18
1.6.3 <i>Serotonin dysregulation</i> .....	19
1.6.4 <i>Plasma leptin and insulin resistance</i> .....	21
1.6.5 <i>Other mediators</i> .....	22
1.6.6 <i>Inflammatory mediators in pulmonary arterial hypertension</i> .....	23
1.7 B AND T CELL INVOLVEMENT IN THE PATHOGENESIS OF PULMONARY ARTERIAL HYPERTENSION .....	26
1.7.1 <i>T cells and their involvement in the pathogenesis of scleroderma</i> .....	29
1.8 INVOLVEMENT OF HEAT SHOCK PROTEIN 70 IN PULMONARY ARTERIAL HYPERTENSION...	31
1.9 TREATMENTS OF PULMONARY ARTERIAL HYPERTENSION .....	33
1.10 AIMS AND HYPOTHESES.....	34
Chapter 2 Characterising lymphocyte subpopulations in peripheral blood of patients with pulmonary arterial hypertension .....	35
2.1 INTRODUCTION.....	35
2.2 METHODS.....	35
2.2.1 <i>Ethics</i> .....	35
2.2.2 <i>Patient Samples</i> .....	36
2.2.2.1 Lymphocyte subset staining in patient blood and controls.....	37
2.2.3 <i>Treg functional studies</i> .....	43
2.2.3.1 EasySep® Mouse CD4 <sup>+</sup> CD25 <sup>+</sup> Regulatory T Cell Isolation Kit .....	44
2.2.3.2 CD4 <sup>+</sup> CD25 <sup>+</sup> Regulatory T cell Isolation Kit.....	45
2.2.3.3 CD4 <sup>+</sup> CD25 <sup>+</sup> CD127 <sup>dim/-</sup> Regulatory T Cells Isolation Kit II.....	46
2.2.3.4 Complete Kit for Human CD4 <sup>+</sup> CD127 <sup>low</sup> CD25 <sup>+</sup> Regulatory T Cells .....	47
2.2.3.5 Assessment of purity of T regulatory and T responder cell populations .....	47
2.2.3.6 Treg cell suppression assays .....	48
2.2.4 <i>Statistical Analysis</i> .....	51

2.3	RESULTS.....	51
2.3.1	<i>Patient demographics.....</i>	51
2.3.2	<i>T cell subsets in patient and control peripheral blood samples.....</i>	54
2.3.2.1	CD4 <sup>+</sup> T cell subset.....	54
2.3.2.2	CD8 <sup>+</sup> T cell subset.....	55
2.3.2.3	CD4:CD8 T cell ratio.....	57
2.3.3	<i>Activation status of T cell subsets in patient and control peripheral blood samples 58</i>	
2.3.3.1	Activation status of CD3 <sup>+</sup> T cells.....	58
2.3.3.2	Activation status of CD4 <sup>+</sup> T cells.....	59
2.3.3.3	Activation status of CD8 <sup>+</sup> T cells.....	61
2.3.4	<i>T regulatory cells and their activation status in patient and control peripheral blood samples.....</i>	62
2.3.5	<i>B cells and their activation status in patient and control peripheral blood samples 66</i>	
2.3.6	<i>Correlations between clinical data and T cell subsets.....</i>	69
2.3.7	<i>Patient survival analysis.....</i>	73
2.3.8	<i>Lymphocyte subset analysis in patients undergoing PAH treatment.....</i>	74
2.4	DISCUSSION.....	82
2.4.1	<i>Clinical peripheral lymphocyte subset analysis.....</i>	82
2.4.2	<i>Correlation of clinical parameters with proportions of CD4<sup>+</sup> T cells in pulmonary arterial hypertension patients.....</i>	86
2.4.3	<i>Treatments of pulmonary arterial hypertension and their effect on T cell subsets proportions.....</i>	87
2.4.4	<i>Limitations leading to future work.....</i>	89
2.4.4.1	Patient cohorts.....	89
2.4.4.2	Foxp3 expression in T regulatory cells.....	90
2.4.5	<i>Concluding remarks.....</i>	91
Chapter 3 ApoE <sup>-/-</sup> /IL-1R1 <sup>-/-</sup> high fat diet model of pulmonary arterial hypertension ..		92
3.1	INTRODUCTION.....	92
3.2	METHODS.....	95
3.2.1	<i>ApoE<sup>-/-</sup>/IL-1R1<sup>-/-</sup> timecourse study.....</i>	95
3.2.1.1	Cardiac puncture.....	96
3.2.1.2	Lung and splenic tissue preparation.....	96
3.2.1.3	Flow cytometric analysis of T cell subsets in blood and tissue samples.....	97
3.2.1.4	Tissue preparation for analysis by immunohistochemistry.....	99
3.2.1.5	Immunohistochemical analysis.....	100
3.2.1.6	Analysis of Vessel Remodelling.....	102
3.2.2	<i>CD4<sup>+</sup> T cell depletion model.....</i>	103
3.2.2.1	Echocardiography.....	104
3.2.2.2	Cardiac catheterisation.....	105
3.2.2.3	Blood and tissue sample collection, preparation and analysis.....	106
3.2.2.4	CD4 <sup>+</sup> T cell depletion confirmation.....	106
3.2.3	<i>Statistical analysis.....</i>	106
3.3	RESULTS.....	107
3.3.1	<i>ApoE<sup>-/-</sup>/IL-1R1<sup>-/-</sup> timecourse.....</i>	107
3.3.1.1	Haemodynamic and vessel remodelling analysis.....	107
3.3.1.2	Circulating T cell subset analysis.....	111
3.3.1.3	Cell marker expression within lung tissue.....	117
3.3.2	<i>Depletion model.....</i>	119
3.3.2.1	Confirmation of CD4 <sup>+</sup> T cells depletion.....	119

3.3.2.2	Haemodynamic and vessel remodelling analysis.....	120
3.3.2.3	T cell subset analysis in blood and tissue samples.....	124
3.3.2.4	Cell marker expression within lung tissue .....	129
3.4	DISCUSSION.....	130
3.4.1	<i>ApoE<sup>-/-</sup>/IL-1R1<sup>-/-</sup> Timecourse</i> .....	130
3.4.2	<i>CD4 depletion model</i> .....	132
3.4.3	<i>Concluding remarks</i> .....	134
Chapter 4 Heat shock protein 70 expression in pulmonary arterial hypertension... 135		
4.1	INTRODUCTION.....	135
4.2	METHODS.....	138
4.2.1	<i>Serum Hsp70 levels in Pulmonary Arterial Hypertension</i> .....	138
4.2.2	<i>Hsp70 levels in rat monocrotaline serum</i> .....	140
4.2.3	<i>Hsp70 expression in lung tissue from animal models of pulmonary arterial hypertension</i> .....	141
4.2.4	<i>Influence of hypoxia on Hsp70 expression by cultured pulmonary artery endothelial cells</i> .....	143
4.2.4.1	Pulmonary artery endothelial cell culture.....	144
4.2.4.2	Hypoxic cell culture and sample collection .....	144
4.2.4.3	Quantification of Hsp70 in cell lysate and supernatant samples .....	145
4.2.4.4	Quantification of Hsp70 in isolated RNA samples .....	148
4.3	RESULTS .....	151
4.3.1	<i>Circulating Hsp70 levels in pulmonary arterial hypertension</i> .....	151
4.3.2	<i>Hsp70 levels in rat serum</i> .....	152
4.3.3	<i>Hsp70 expression in the lungs of rat and mouse models of pulmonary arterial hypertension</i> .....	153
4.3.4	<i>Effect of hypoxia on cultured pulmonary artery endothelial cell Hsp70 expression</i> .....	156
4.4	DISCUSSION.....	158
Chapter 5 General Discussion .....		163
Appendix 1 .....		169
1.	GENERAL REAGENTS .....	169
2.	CELL CULTURE .....	172
3.	FLOW CYTOMETRY REAGENTS.....	174
4.	ANIMAL STUDY REAGENTS .....	179
5.	IMMUNOHISTOCHEMISTRY BUFFERS AND REAGENTS .....	181
6.	PATIENT TREATMENT PLANS.....	185
Bibliography .....		187

# List of figures

Figure 1.1 T regulatory cell mechanisms of action .....	8
Figure 2.1 Isolation of PBMCs from whole blood.....	38
Figure 2.2 Representative gating hierarchy template and acquisition plots used to define different lymphocyte subsets. ....	41
Figure 2.3 Representative gating hierarchy template and acquisition plots used to define Treg cells. ....	42
Figure 2.4 Proportions of CD4 <sup>+</sup> helper T cells in peripheral blood of PAH patients and controls. ....	55
Figure 2.5 Proportions of CD8 <sup>+</sup> cytotoxic T cells in peripheral blood of PAH patients and controls. ....	56
Figure 2.6 CD4:CD8 T cell ratio in peripheral blood of PAH patients and controls. ....	57
Figure 2.7 Proportions of activated CD3 <sup>+</sup> T cells in peripheral blood of PAH patients and controls. ....	59
Figure 2.8 Proportions of activated CD4 <sup>+</sup> T cells in peripheral blood of PAH patients and controls. ....	60
Figure 2.9 Proportions of activated CD8 <sup>+</sup> T cells in peripheral blood of PAH patients and controls. ....	61
Figure 2.10 Proportions of CD4 <sup>+</sup> CD25 <sup>high</sup> Treg cells in peripheral blood of PAH patients and controls.....	63
Figure 2.11 Proportions of CD4 <sup>+</sup> CD25 <sup>high</sup> CD127 <sup>low</sup> Treg cells in peripheral blood of PAH patients and controls. ....	64
Figure 2.12 Proportions of activated CD4 <sup>+</sup> CD25 <sup>high</sup> Treg cells in peripheral blood of PAH patients and controls. ....	65
Figure 2.13 Proportions of activated CD4 <sup>+</sup> CD25 <sup>high</sup> CD127 <sup>low</sup> Treg cells in peripheral blood of PAH patients and controls.....	66
Figure 2.14 Proportion of B cells in peripheral blood of PAH patients and controls. ....	67
Figure 2.15 Proportions of activated B cells in peripheral blood of PAH patients and controls.....	68
Figure 2.16 Scatter plot showing spread of CD4 <sup>+</sup> T cell data in PAH patients and controls.....	69
Figure 2.17 Receiver operating characteristic curve to define optimum cut-off value for changes in the proportion of CD8 <sup>+</sup> T cells in the prediction of PAH.....	74
Figure 2.18 Proportions of CD4 <sup>+</sup> T cells in PAH patients at follow-up.....	77
Figure 2.19 Proportions of CD8 <sup>+</sup> T cells in PAH patients at follow-up.....	79

Figure 2.20 CD4:CD8 ratio in PAH patients at follow-up. ....	80
Figure 2.21 Proportions of CD4 <sup>+</sup> CD25 <sup>high</sup> Treg in PAH patients at follow-up.....	81
Figure 3.1 Representative gating hierarchy and dot plots templates used to define T cell subsets in blood and tissue samples. ....	98
Figure 3.2 Experimental design for the CD4 <sup>+</sup> T cell depletion study.....	104
Figure 3.3 Comparison of extent of muscularisation in paigen and chow fed animals from 1 week to 8 weeks after commencement of diets.....	109
Figure 3.4 Assessment of the percentage of muscularisation of pulmonary vessels in chow and paigen-fed animals.....	110
Figure 3.5 T cell subsets in peripheral blood of paigen and chow fed animals. ...	111
Figure 3.6 Proportions of CD4 <sup>+</sup> T cells in blood, spleen and lung tissue at 8 weeks in chow and paigen-fed ApoE <sup>-/-</sup> /IL-1R1 <sup>-/-</sup> mice. ....	113
Figure 3.7 Proportions of CD8 <sup>+</sup> T cells in blood, spleen and lung tissue at 8 weeks in chow and paigen-fed ApoE <sup>-/-</sup> /IL-1R1 <sup>-/-</sup> mice. ....	114
Figure 3.8 CD4:CD8 T cell ratio in blood, spleen and lung tissue at 8 weeks in chow and paigen-fed ApoE <sup>-/-</sup> /IL-1R1 <sup>-/-</sup> mice. ....	115
Figure 3.9 Proportions of CD4 <sup>+</sup> CD25 <sup>high</sup> Treg cells in blood, spleen and lung tissue at 8 weeks in chow and paigen-fed ApoE <sup>-/-</sup> /IL-1R1 <sup>-/-</sup> mice.....	116
Figure 3.10 Representative images of lung sections stained for CD4 <sup>+</sup> and CD8 <sup>+</sup> T cells from chow and paigen diet–fed mice at 8 weeks.....	118
Figure 3.11 Confirmation of CD4 <sup>+</sup> T cell depletion in peripheral blood of fat fed ApoE <sup>-/-</sup> /IL-1R1 <sup>-/-</sup> mice .....	120
Figure 3.12 Haemodynamic assessment of paigen-fed ApoE <sup>-/-</sup> /IL1R1 <sup>-/-</sup> mice given a CD4 <sup>+</sup> T cell depletion antibody or an IgG control.....	121
Figure 3.13 Analysis of number of remodelled vessels and degree of remodelling in lung tissue sections in CD4 depleted and IgG treated animals.....	123
Figure 3.14 Proportions of CD4 <sup>+</sup> T cells in blood, spleen or lung tissue of CD4 depleted animals and IgG treated controls.....	125
Figure 3.15 Proportions of CD8 <sup>+</sup> T cells in blood, spleen or lung tissue of CD4 depleted animals and IgG treated controls.....	126
Figure 3.16 CD4:CD8 T cell ratio in blood, spleen or lung tissue of CD4 depleted animals and IgG treated controls. ....	127
Figure 3.17 Proportions of CD4 <sup>+</sup> CD25 <sup>high</sup> Treg cells in blood, spleen or lung tissue of CD4 depleted animals and IgG treated controls.....	128
Figure 3.18 Representative images of CD4 and CD8 expression in the lung tissue of IgG treated and CD4 depletion antibody treated animals at 8 weeks after commencing paigen diet. ....	129

Figure 4.1 Standard curve for Hsp70 levels in human serum samples.....	151
Figure 4.2 Serum Hsp70 levels in the MCT rat and saline-treated controls.....	152
Figure 4.3 Hsp70 expression in lung tissue of fat fed ApoE <sup>-/-</sup> /IL1R1 <sup>-/-</sup> mice and chow fed controls.....	154
Figure 4.4 Hsp70 expression in lung tissue from paigen fed ApoE <sup>-/-</sup> /IL1R1 <sup>-/-</sup> mice after CD4 <sup>+</sup> T cell depletion. ....	155
Figure 4.5 Levels of Hsp70 protein and RNA expression in hypoxic and normoxic cell lysates. ....	157

# List of tables

Table 1.1 T lymphocyte cell subsets. ....	2
Table 1.2 T regulatory cell subsets. ....	4
Table 1.3 The most recent classification of pulmonary hypertension agreed upon at the WHO symposium in Dana Point, California. ....	10
Table 2.1 Pipetting scheme for Treg suppression assay .....	49
Table 2.2 Pulmonary arterial hypertension patient demographics. ....	53
Table 2.3 Correlation data between CD4 <sup>+</sup> T cells, CD8 <sup>+</sup> T cells, CD4 <sup>+</sup> CD25 <sup>high</sup> Treg cells and clinical parameters in IPAH patients.....	71
Table 2.4 Correlation data between CD4 <sup>+</sup> T cells, CD8 <sup>+</sup> T cells, CD4 <sup>+</sup> CD25 <sup>high</sup> Treg cells and clinical parameters in SSc-PAH patients. ....	72
Table 2.5 PAH specific drug therapy and shuttle walk test scores for all follow-up visits (IPAH and SSc-PAH patients).....	75

# Abbreviations

<b>ALK-1</b>	activin receptor-like kinase 1
<b>APC</b>	antigen presenting cell
<b>ApoE</b>	apolipoprotein E
<b>BMP</b>	bone morphogenetic protein
<b>BMPR2</b>	bone morphogenetic protein receptor type 2
<b>cAMP</b>	cyclic adenosine monophosphate
<b>CFSE</b>	carboxyfluorescein
<b>cGMP</b>	cyclic guanosine monophosphate
<b>CI</b>	cardiac index
<b>CO</b>	cardiac output
<b>con A</b>	concanavalin A
<b>cm<sup>2</sup></b>	square centimetre
<b>CRP</b>	C reactive protein
<b>CSA</b>	cross sectional area
<b>CTD</b>	connective tissue disease
<b>CTEPH</b>	chronic thromboembolic pulmonary hypertension
<b>CVBRU</b>	cardiovascular biomedical research unit
<b>DC</b>	dendritic cell
<b>Δ</b>	change
<b>ddH<sub>2</sub>O</b>	double distilled water
<b>dH<sub>2</sub>O</b>	distilled water
<b>DMSO</b>	dimethyl sulfoxide

<b>EC</b>	endothelial cell
<b>EDTA</b>	ethylenediaminetetraacetic acid
<b>EGFR</b>	epidermal growth factor receptor
<b>ELISA</b>	enzyme-linked immunosorbent assay
<b>eNOS</b>	endothelial nitric oxide synthase
<b>E-RA</b>	endothelin-1 receptor antagonist
<b>ET-1</b>	endothelin-1
<b>F</b>	french
<b>FEV1</b>	forced expiratory volume in 1 second
<b>Foxp3</b>	forkhead box P3
<b>FSC</b>	forward scatter
<b>FVC</b>	forced vital capacity
<b>g</b>	grams
<b>G</b>	guage
<b>H<sub>2</sub>O</b>	water
<b>HIF-1</b>	hypoxia-inducible factor 1
<b>HIV</b>	human immunodeficiency virus
<b>HR</b>	heart rate
<b>HRP</b>	horseradish peroxidase
<b>Hsp</b>	heat shock protein
<b>Hsp70</b>	heat shock protein 70
<b>ICAM-1</b>	intracellular adhesion molecule 1
<b>IFN<math>\gamma</math></b>	interferon gamma
<b>IgE</b>	Immunoglobulin E

<b>IgG</b>	Immunoglobulin G
<b>IL-1</b>	interleukin-1
<b>IL-1RA</b>	Interleukin-1 receptor antagonist
<b>“</b>	inch
<b>IPAH</b>	idiopathic pulmonary arterial hypertension
<b>Kg</b>	kilogram
<b>Kv</b>	voltage gated potassium channel
<b>L</b>	litre
<b>μL</b>	microlitre
<b>m</b>	meter
<b>M</b>	molar
<b>MAb</b>	monoclonal antibody
<b>MCT</b>	monocrotaline
<b>μg</b>	microgram
<b>μL</b>	microlitre
<b>mg</b>	milligram
<b>MIP-1α</b>	macrophage inflammatory protein 1 alpha
<b>mL</b>	millilitre
<b>mmHg</b>	millimetres of mercury
<b>mM</b>	millimolar
<b>mPAP</b>	mean pulmonary arterial pressure
<b>n</b>	number
<b>NADPH</b>	nicotinamide adenine dinucleotide phosphate-oxidase
<b>NFAT</b>	nuclear factor of activated T-cells

<b>NFκB</b>	Nuclear Factor-Kappa B
<b>ng</b>	nanogram
<b>NK cell</b>	natural killer cell
<b>nm</b>	nanometer
<b>NO</b>	nitric oxide
<b>P</b>	probability
<b>PAAT</b>	pulmonary artery acceleration time
<b>PA-EC</b>	pulmonary artery endothelial cell
<b>PAH</b>	pulmonary arterial hypertension
<b>PBMC</b>	peripheral blood mononuclear cell
<b>PBS</b>	phosphate buffered saline
<b>pg</b>	picogram
<b>PPARγ</b>	peroxisome proliferator-activated receptor gamma
<b>PH</b>	pulmonary hypertension
<b>PHA</b>	phytohaemagglutinin
<b>PVR</b>	pulmonary vascular resistance
<b>qPCR</b>	quantitative real-time polymerase chain reaction
<b>R</b>	pearson product-moment correlation coefficient
<b>RANTES</b>	regulated and normal T cell expressed and secreted
<b>RNA</b>	ribonucleic acid
<b>ROC</b>	receiver operating characteristic
<b>RPMI</b>	Roswell Park Memorial Institute
<b>RVH</b>	right ventricular hypertrophy
<b>RVSP</b>	right ventricular systolic pressure

<b>5-HT</b>	5-hydroxytryptamine (serotonin)
<b>SD</b>	standard deviation
<b>SEM</b>	standard error of the mean
<b>SERT</b>	serotonin transporter
<b>SLE</b>	systemic lupus erythematosus
<b>SMC</b>	smooth muscle cell
<b>SPVDU</b>	Sheffield pulmonary vascular disease unit
<b>SSC</b>	side scatter
<b>SSc</b>	scleroderma (system sclerosis)
<b>SSc-PAH</b>	systemic sclerosis-associated pulmonary arterial hypertension
<b>TGF-<math>\beta</math></b>	transforming growth factor beta
<b>TMB</b>	3,3',5,5'-Tetramethylbenzidine
<b>TNF<math>\alpha</math></b>	tumor necrosis factor-alpha
<b>Tph1</b>	tryptophan hydroxylase 1
<b>TRAIL</b>	Tumour Necrosis Factor (TNF)-Related Apoptosis-Inducing Ligand
<b>Treg</b>	T regulatory cell
<b>TRIS</b>	tris(hydroxymethyl)aminomethane
<b>TXA2</b>	thromboxane A2
<b>VCAM-1</b>	vascular cell adhesion protein 1
<b>VEGF</b>	vascular endothelial growth factor
<b>v/v</b>	volume to volume
<b>w/v</b>	weight to volume
<b>w/w</b>	weight to weight
<b>x g</b>	times gravity (also known as relative centrifugal force)

# **Chapter 1 General introduction**

## **1.1 Pulmonary circulation**

The cardiovascular system can be broadly divided into three parts: the pulmonary circulation, the systemic circulation and the coronary circulation. The coronary circulation is the circulation of blood in the blood vessels of the heart muscle, whilst the systemic circulation supplies the body with oxygenated blood from the heart, delivering deoxygenated blood back to the heart. In the pulmonary circulation, deoxygenated blood returning from the body enters the heart through the inferior and superior vena cavae and flows into the right atrium, then the right ventricle. The blood is then pumped out through the pulmonary artery through a complex network of dividing branches towards the capillaries in the lung, where gas exchange occurs. The oxygenated blood then leaves the capillaries via the pulmonary vein to re-enter the left atrium of the heart. Characteristics of a healthy pulmonary circulation include an network of highly compliant blood vessels which have low luminal pressure and high flow rates which encourage gas exchange (Harris, 1986).

## **1.2 T cell immunobiology**

T lymphocytes (T cells) are a subset of leukocytes that are involved in both pro- and anti-inflammatory immune responses. T cells can be distinguished from other lymphocyte subsets by the presence of a T cell receptor (TCR) on their cell surface which is involved in recognising antigens bound to major histocompatibility complex molecules (MHCs). Specific co-receptors including CD4 and CD8 found on the T cells along with accessory molecules, aid in the formation of a T cell receptor complex which transduces signals between the T cell and antigen presenting cell (APC).

T cells originate from haematopoietic stem cells in the bone marrow, but then populate the thymus where they mature and expand into immature thymocytes. A mechanism called central tolerance occurs in the thymus in which self-reactive T cells are removed via positive and negative selective processes. The remaining cells that have not been removed emerge as CD4<sup>+</sup>/CD8<sup>+</sup> cells (T cell precursors) and under the influence of certain transcription factors such as T-bet and cytokines such as IL-2, differentiate and proliferate into specific lineages of T cell (Table 1.1).

<b>Subset</b>	<b>Function</b>
CD4 <sup>+</sup> T cells	Can mature into effector, memory or Treg cells and are involved in Th1, Th2 and Th17 responses.
CD8 <sup>+</sup> T cells	Destroy virally infected cells and tumor cells via the secretion of perforin and granzymes, which cause apoptosis of target cells.
Regulatory T cells	Maintain immunological tolerance.
CD4 <sup>-</sup> CD8 <sup>-</sup> T cells	Pro- and anti-inflammatory properties and can protect against allograft rejection.
Memory T cells	Have previously encountered antigen and can rapidly proliferate and differentiate into effector T cells following antigen stimulation.

**Table 1.1 T lymphocyte cell subsets.**

*T cell subsets found within peripheral blood and their functions. CD= cluster of differentiation, Th= T helper type, Treg= T regulatory.*

CD8<sup>+</sup> T cells express the CD8 glycoprotein on their cell surface which can bind to MHC class 1 molecules on the surface of target cells. They can rapidly proliferate in response to IL-2 and destroy target cells via Fas and perforin dependent mechanisms, but do not require co-stimulatory signals unlike CD4<sup>+</sup> T cells (Broere *et al*, 2011). Memory T cells can be found in secondary lymphoid organs such as lymph nodes or spleen and can mount fast and effective responses to antigens that they have previously encountered. Memory T cells can rapidly proliferate and differentiate into effector T cells and typically express the cell surface protein CD45RO. These

cells can either be CD4<sup>+</sup> or CD8<sup>+</sup> and can be central or effector subtype (Sallusto *et al*, 2004). Double negative (CD4<sup>-</sup>CD8<sup>-</sup>) T cells are found in low numbers in the peripheral blood and do not express CD4 or CD8 glycoproteins. They are thought to have pro- and anti-inflammatory properties, producing both IL-4 and IL-17 and inducing immunoglobulin (Ig) and anti-DNA antibody production, however their exact function is still unknown (Alluno *et al*, 2012; Zlotnik *et al*, 1992).

The largest population of T cells are those defined by the expression of a protein named CD4 on their cell surface (CD4<sup>+</sup>). These cells become activated when presented with antigens via MHC class 2 molecules which are expressed on APCs. These cells (Th0) can then differentiate into many other cell types depending on the signals they receive. These include Th1, Th2, Th17 and Treg cells which all have different functions. Th0 cells differentiate into Th1 cells in the presence of IL-12 and IL-18 released from dendritic cells (DCs) and can then secrete IL-2 and IFN- $\gamma$  which act upon macrophages to enhance their killing ability and also encourage the proliferation of cytotoxic CD8<sup>+</sup> T cells (Mosmann and Sad, 2006). Th2 cells occur in the presence of IL-4 which can be released from B cells or DCs and they themselves can secrete IL-4, IL-5 and IL-10 and can act to enhance mast cell and eosinophil cell functions as well as promote B cell proliferation and antibody class switching (Constant and Bottomly, 1997). Th17 cells occur in the presence of TGF- $\beta$  and IL-6 and are involved in the recruitment, activation and migration of neutrophils as well as the production of IL-21 and IL-22 (Bettelli *et al*, 2007).

T lymphocytes have long been thought to be involved in both the initiation and resolution of disease and there has been much debate about the existence of T lymphocyte subpopulations which act as endogenous immunoregulators. A number of different immune Treg cell populations have been identified and can be classified into either naturally occurring (nTreg) or inducible T regulatory types (Tr1, Th3) cells (Scumpia *et al*, 2006). As well as this, T cell subsets including CD8<sup>+</sup> T cell suppressive cells,  $\gamma\delta$  T cells and natural killer T cells (NKT) all possess suppressive and regulatory functions (Boehmer, 2005; Miyara and Sakaguchi, 2007; Kabelitz, 1992) (Table 1.2).

<b>Subset</b>	<b>Function</b>	<b>Development</b>
nTreg	Immunosuppressive and tolerogenic responses (contact-dependent and independent mechanisms).	Thymus
Tr1	IL-10 mediated suppression and involved in mucosal immunity.	Periphery
Th3	TGF- $\beta$ mediated suppression and involved in mucosal immunity.	Periphery
NKT cell	Respond to atypical antigen presentation via CD1d molecule producing large amounts of cytokines (IL-4, IFN- $\gamma$ , GM-CSF).	Thymus
CD8 <sup>+</sup> T cell	IL-10 and TGF- $\beta$ mediated suppression.	Periphery
$\delta\gamma$ T cell	pro- and anti-inflammatory functions	periphery

**Table 1.2 T regulatory cell subsets.**

T regulatory cell subsets found centrally and in the periphery in humans, their function and location of development are also shown. NKT= natural killer T, nTreg= natural T regulatory cell, Th= helper type, CD= cluster of differentiation, IL= interleukin, IFN- $\gamma$ = interferon-gamma, GM-CSF= granulocyte-macrophage colony-stimulating factor and TGF- $\beta$ = transforming growth factor-beta.

CD8<sup>+</sup> suppressor T cells are found in the periphery and can produce several cytokines including IL-10 and TGF- $\beta$  in order to suppress both CD4<sup>+</sup> T cells and B cells (Filaci and Suci-Foca, 2002). They can also recognise Ig molecules, inhibit Th cell proliferation and suppress autoimmune responses (Liu *et al*, 1998; Hahn *et al*, 2005).

Tr1 cells are found in the gut and exert suppressive effects through contact-mediated independent mechanisms via the secretion of IL-10 and TGF- $\beta$ . They are thought to be involved in tolerance towards antigens and can suppress memory and naïve T cell responses (Roncarolo *et al*, 2006; Groux *et al*, 1997). Tr1 cells have also been shown to have cytotoxic functions (via the production of perforin and granzyme B) when induced by CD3/CD46 leading to the apoptosis of target cells (Grossman *et al*, 2004).

Th3 cells are also found in the gut and are generated from gut associated lymphoid tissue (GALT) in response to TGF- $\beta$ . These cells are primarily involved in the regulation of autoimmunity but have also been shown to aid IgA immune responses and can suppress Th1 and Th2 cell function and proliferation (Chen *et al*, 1994; Weiner, 2002).

Another T regulatory cell subset, the  $\gamma\delta$  T cell, is involved in recognising whole proteins instead of peptides presented via MHC molecules on APCs. They are thought to have characteristics of both innate and adaptive immunity and can have pro- and anti-inflammatory properties depending on the TCR that they express (Born *et al*, 2005; Zheng *et al*, 2013; Kuhl *et al*, 2009).

NKT cells are thought to also be involved in innate and adaptive immune responses and can produce cytokines and release cytotoxic molecules. They recognise glycolipid antigens presented by the CD1d molecule and can produce several cytokines including IL-4 and IFN- $\gamma$  (Godfrey *et al*, 2000). These cells also have the ability to indirectly sense infectious agents by responding to secreted cytokines from activated DCs (Tupin *et al*, 2007).

Finally, the most widely investigated group of T regulatory cells are the nTreg cells, which are a subpopulation of CD4<sup>+</sup> T cells that constitutively express high levels (<sup>+/bright/high</sup>) of the  $\alpha$ -chain of the IL-2 receptor (CD25). Treg cells represent 1–3% of CD4<sup>+</sup> T cells in normal humans and about 10% in rodents. The continuing controversy surrounding the presence of immunoregulatory T cells stems from the lack of reliable surface markers and inconclusive knowledge regarding their function and role within the immune response.

Sakaguchi *et al* were the first to describe the critical involvement of CD4<sup>+</sup>CD25<sup>high</sup> Treg cells in the maintenance of peripheral tolerance to self antigens (Sakaguchi *et al*, 1995). Depleted CD4<sup>+</sup> T cell suspensions were prepared from BALB/c *nu/+* mice lymph nodes and spleens. These mice carry the recessive nude gene on one chromosome and so have a normal thymus and immune system. CD25<sup>+</sup> T cells were depleted using a specific monoclonal antibody (mAb) from these cell preparations and these cells were then inoculated into BALB/c athymic nude (*nu/nu*) mice. All mice that

received the inoculation developed autoimmune diseases including thyroiditis and gastritis. This work demonstrated that a systemic autoimmune response occurs when CD4<sup>+</sup>CD25<sup>high</sup> Treg cells are removed within the first few days of birth and emphasised the importance of these cells in immunologic self-tolerance and the negative control of immune responses (Sakaguchi, 2004). Cumulatively, these studies show that the loss or absence of what are now termed Treg cells renders animals and human susceptible to serious disease.

Forkhead box protein 3 (Foxp3), a transcription factor that controls both CD4<sup>+</sup>CD25<sup>high</sup> Treg cell development and function, has been noted in mouse and human CD4<sup>+</sup>CD25<sup>high</sup> Treg cells (Hori *et al*, 2003). It has previously been demonstrated that Foxp3 is required for thymic development of Treg cells and that the expression of Foxp3 in naïve T cells provides a stimulus to convert them to Treg cells (Fontenot *et al*, 2003; Hori *et al*, 2003; Yagi *et al*, 2004). Foxp3 has also been shown to bind to DNA, localize to the nucleus and can act as a transcriptional repressor. It also antagonises nuclear factor of activated T-cells (NFAT) function by competing for DNA binding sites, inhibiting T cell development and proliferation (Schubert *et al*, 2001). Foxp3 is now thought to be a reliable intracellular marker of CD4<sup>+</sup>CD25<sup>high</sup> Treg cells.

### **1.2.1 Mechanisms of action of Treg cells**

There are several mechanisms by which Treg cells are thought to mediate a suppressive effect on other cells. Once activated, CD4<sup>+</sup>CD25<sup>high</sup> Treg cells suppress other T cells, NK cells and B cells, but can also affect the activation and function of monocytes, macrophages and dendritic cells (DCs) (Camara *et al*, 2003; Janssens *et al*, 2003; Taams *et al*, 2005; Ghiringhelli *et al*, 2006). CD4<sup>+</sup>CD25<sup>high</sup> Treg cells require T cell receptor stimulation to become activated and cytokines, including IL-2, to trigger their suppressive action (Thornton *et al*, 2004). *In vitro* studies into CD4<sup>+</sup>CD25<sup>high</sup> Treg suppressive activity using transwell experiments, have demonstrated that these cells can act on target cells in a cell-contact dependent manner (Wing

*et al*, 2006). CD4<sup>+</sup>CD25<sup>high</sup> Treg cells can also directly suppress effector T cells through molecules such as membrane transforming growth factor beta (TGF-β) or by killing effector cells via the release of the serine protease granzyme B (Grossman *et al*, 2004). They are also thought to act via the release of suppressive cytokines, such as IL-10, TGF-β and IL-35 (Chen *et al*, 2003). Finally, CD4<sup>+</sup>CD25<sup>high</sup> Treg cells can act as a “sink” to absorb surrounding IL-2 through their CD25 receptors (Thornton and Shevach, 1998). CD4<sup>+</sup>CD25<sup>high</sup> Treg cells can therefore compete with effector cells for IL-2, which is an essential growth factor for T cells (Figure 1.1).

Treg cells can be recruited into injured or inflamed tissue via their contact with endothelial derived intracellular adhesion molecule 1 (ICAM-1) and vascular cell adhesion molecule 1 (VCAM-1), which aid extravasation into the tissue from pulmonary vessels (Pribila *et al*, 2004). Endothelial contact with Treg cells is thought to not only activate Treg cells but initiate key anti-inflammatory and cardioprotective events to protect the endothelium from injury (Bedke *et al*, 2010). When activated by endothelial cells (ECs), Treg cells secrete IL-10 and TGF-β which can act as vasodilator by rescuing eNOS phosphorylation (Bhattacharyya *et al*, 2004). Treg secreted IL-10 can also reduce oxidative stress by inhibiting nicotinamide adenine dinucleotide phosphate-oxidase (NADPH) oxidase activity which produces reactive oxygen species under normal physiological conditions (Kassan *et al*, 2011). Treg cells can also interact with DCs (antigen-presenting cells), to cause tryptophan catabolism, leading to a reduction in T cell activation (Mellor and Munn, 1999; Terness *et al*, 2002; Fallarino *et al*, 2003). Hemeoxygenase-1, a stress-inducible protein, is produced by Treg cells, has anti-inflammatory properties and is mediated by inhibition of nuclear factor kappa B (NF-κB) activation (Gozzelino *et al*, 2010). This protein has also been shown to be protective in pulmonary arterial hypertension (PAH) (Christou *et al*, 2000). Treg cells have been shown to be protective in many cardiovascular diseases, including atherosclerosis and chronic heart failure, as they can modulate the effects of other immune cells (Mallat *et al*, 2005).

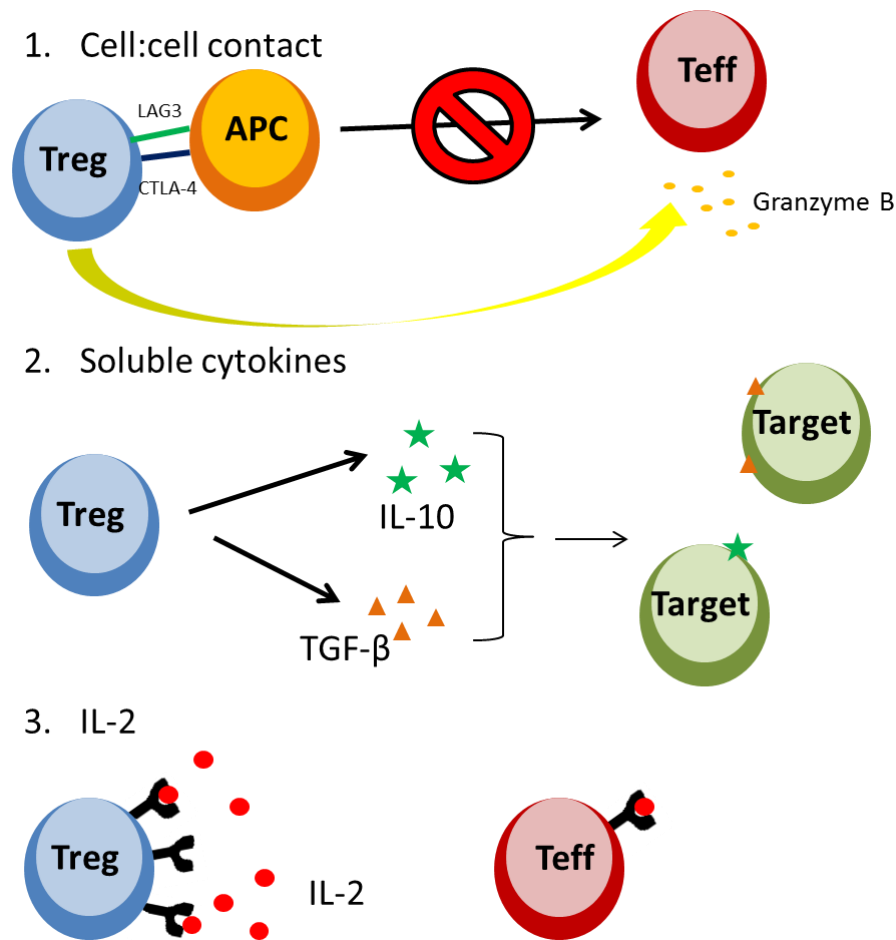


**Figure 1.1 T regulatory cell mechanisms of action**

1) Cell to cell contact (contact mediated) suppression. Treg cells can change the function of antigen presenting cells (APCs) via contact mediated suppression which can inhibit the proliferation of effector T cells. 2) Soluble cytokines released by Treg cells (IL-10 and TGF- $\beta$ ) can be released to inhibit the effects of target cells. 3) Treg cells can sink the excess IL-2 in the vicinity of T effector cells, inhibiting their function and proliferation (Thornton and Shevach, 1998; Nakamura et al, 2001; Joetham et al, 2007).

Defects in function or number of circulating Treg cells can upset the homeostatic balance of the immune system, and this is thought to propagate disease progression in many cardiovascular diseases (Mor et al, 2006; Ulrich et al, 2008; Tang et al, 2010; Wigren et al, 2012). Increased numbers of Treg cells have been noted in both the peripheral blood and pulmonary vessels of idiopathic pulmonary arterial hypertension (IPAH) patients, whilst in animal models of PAH, it has been demonstrated that

immune reconstitution with Treg cells, prior to vascular injury, can protect against the development and progression of PAH (Tamosiuniene *et al*, 2011). However, this work has only been undertaken in one subtype of PAH patients and few animal models of PAH, therefore, further work needs to be undertaken to address these issues.

## 1.3 Pulmonary hypertension

Pulmonary hypertension (PH) was first described in 1891 by Dr. Ernst von Romberg as an elevation in pulmonary blood pressure, leading to shortness of breath and dizziness (Romberg, 1891). PH is currently defined as a progressive increase in pulmonary vascular resistance (PVR), leading to right ventricular failure and death. Clinically, it is regarded as a mean pulmonary artery pressure (mPAP)  $\geq 25$  mmHg at rest as assessed by right heart catheterisation (Galie *et al*, 2009). This increase in pulmonary artery pressure can be caused by shunting of systemic blood, clots into the lung, vasoconstriction or vascular cell proliferation.

PH can be subdivided into several forms of the disease which include PAH, PH due to left heart disease, PH due to lung diseases and/or hypoxia, chronic thromboembolic disease (CTEPH) and PH with unclear and / or multifactorial mechanisms (Humbert, 2012). Each of these five groups of PH diseases has different causes and pathological features (Table 1.3). Haemodynamically, PH can also be defined as pre-capillary or post-capillary PH. Pre-capillary PH, defined as a mPAP  $\geq 25$  mmHg and a pulmonary wedge pressure of  $< 15$  mmHg, includes clinical groups 1, 3, 4 and 5 of the clinical classification system (Table 1.3) whilst post-capillary PH is defined as a mPAP  $\geq 25$  mmHg and a pulmonary wedge pressure of  $> 15$  mmHg and includes clinical group 2.

<b>1. Pulmonary arterial hypertension (PAH)</b>
<ul style="list-style-type: none"> <li><b>1.1 Idiopathic</b></li> <li>1.2 Heritable <ul style="list-style-type: none"> <li>1.2.1 BMPR2</li> <li>1.2.2 ALK1, endoglin (with or without hereditary haemorrhagic telangiectasia)</li> <li>1.2.3 Unknown</li> </ul> </li> <li>1.3 Drugs and toxins induced</li> <li>1.4 Associated with (APAH) <ul style="list-style-type: none"> <li><b>1.4.1 Connective tissue diseases</b></li> <li>1.4.2 HIV infection</li> <li>1.4.3 Portal hypertension</li> <li>1.4.4. Congenital heart disease</li> <li>1.4.5 Schistosomiasis</li> <li>1.4.6 Chronic haemolytic anaemia</li> </ul> </li> <li>1.5 Persistent pulmonary hypertension of the newborn</li> </ul>
<b>1' Pulmonary veno-occlusive disease and/or pulmonary capillary haemangiomatosis</b>
<b>2 Pulmonary hypertension due to left heart disease</b>
<ul style="list-style-type: none"> <li>2.1 Systolic dysfunction</li> <li>2.2 Diastolic dysfunction</li> <li>2.3 Valvular disease</li> </ul>
<b>3 Pulmonary hypertension due to lung diseases and/or hypoxia</b>
<ul style="list-style-type: none"> <li>3.1 Chronic obstructive pulmonary disease</li> <li>3.2 Interstitial lung disease</li> <li>3.3 Other pulmonary diseases with mixed restrictive and obstructive pattern</li> <li>3.4 Sleep-disordered breathing</li> <li>3.5 Alveolar hypoventilation disorders</li> <li>3.6 Chronic exposure to high altitude</li> <li>3.7 Development abnormalities</li> </ul>
<b>4 Chronic thromboembolic pulmonary hypertension</b>
<b>5 PH with unclear and/or multifactorial mechanisms</b>
<ul style="list-style-type: none"> <li>5.1 Haematological disorders: myeloproliferative disorders, splenectomy</li> <li>5.2 Systemic disorders: sarcoidosis, pulmonary Langerhans cell histiocytosis, lymphangioliomyomatosis, neurofibromatosis, vasculitis</li> <li>5.3 Metabolic disorders: glycogen storage disease, Gaucher disease, thyroid disorders</li> <li>5.4 Others: tumoural obstruction, fibrosing mediastinitis, chronic renal failure on dialysis</li> </ul>

**Table 1.3 The most recent classification of pulmonary hypertension agreed upon at the WHO symposium in Dana Point, California.**

*The five groups of pulmonary hypertension, including PAH, PH due to left heart disease, PH due to lung disease or hypoxia, chronic thromboembolic PH and PH with unclear and/or multifactorial origin. ALK-1 = activin receptor-like kinase 1 gene, APAH = associated pulmonary arterial hypertension, BMPR2 = bone morphogenetic protein receptor type 2, HIV = human immunodeficiency virus, PAH = pulmonary arterial hypertension. Subtypes focused on in this thesis are highlighted in red (Galie et al, 2009). Reproduced with the permission of Oxford University Press.*

## **1.4 Pulmonary arterial hypertension**

Group 1 of the Dana Point Classification (PAH) can be further divided into five subgroups. The first group, IPAH, previously called primary PH, is PAH with an unknown etiology, and is described further in Chapter 1.3 (Table 1.3, group 1.1). The second subgroup is hereditary PAH which including sporadic germline mutations in either bone morphogenetic protein receptor type 2 (BMPR2), activin-like kinase-1 (ALK-1), the glycoprotein endoglin and clinical familial cases with or without identified germline mutations (Table 1.3, group 1.2). The third subgroup of PAH consists of a group of patients diagnosed with PAH induced by drug and toxin use, such as amphetamines and the anorexigen (and serotonin reuptake inhibitor) dexfenfluramine (Table 1.3, group 1.3). Subgroup 4 includes conditions associated with PAH such as connective tissue disease, human immunodeficiency virus (HIV) infection and portal hypertension (Table 1.3, group 1.4). These conditions usually pre date the onset of PAH and can have similar clinical presentations to subgroup 1 (IPAH). This group is thought to account for approximately half of all PAH patient cases (Humbert *et al*, 2006; <http://www.ic.nhs.uk>, 2011). The final subgroup, group 5, includes persistent pulmonary hypertension of the newborn, which occurs due to failure of the pulmonary vasculature to relax at birth, resulting in hypoxemia (Table 1.3, group 1.5). For the purposes of this thesis, two PAH patient groups will be discussed further (IPAH and SSc-PAH).

### **1.4.1 Idiopathic pulmonary arterial hypertension**

IPAH is thought to occur at an incidence rate of 2.1 cases per million per year in the general population in the UK, with 32% of all PAH patients in the UK having IPAH (<http://www.ic.nhs.uk>, 2011; Hurdman *et al*, 2012). IPAH patients have a three-year survival rate of 63% with the usual cause of death being right ventricular failure as a result of chronic vasoconstriction and

vascular remodelling (Hurdman *et al*, 2012). IPAH is a vasculopathy consisting of a progressive narrowing and occlusion of small pulmonary arterioles. IPAH is defined as a persistent elevation of mPAP without a demonstrable cause and occurs more frequently in females (Humbert *et al*, 2006; Graham, 2011).

A pathological characteristic of IPAH, which occurs in 15% of all PAH patients, is the development of plexiform lesions. These arise as a result of proliferating ECs, neoangiogenesis and the accumulation of inflammatory progenitor cells, myofibroblasts and connective tissue elements such as elastin and collagen (Tuder *et al*, 1994). Plexiform lesions, most commonly found in IPAH patients, can be found at branching points of pulmonary arteries of less than 300µm in diameter and are often associated with concentric intimal obliteration of pulmonary vessels (Cool *et al*, 1997; Tuder, Lee, *et al*, 1998; Tuder, Radisavljevic, *et al*, 1998; Fishman, 2000). The plexiform lesion has been described by several groups as a dilated sac which has several channels that are separated by proliferating myofibroblasts and atypical ECs (Cool *et al*, 1999). Cool and colleagues used computerised 3D reconstructions of nine vessels in patient samples, as well as immunohistochemistry, to show that plexiform lesions are dynamic vascular structures that include ECs. Other groups have shown that ECs within plexiform lesions are highly proliferative and that altered survival of these cells contributes to the formation of these structures (Tuder *et al*, 1994; Lee *et al*, 1998; Sakao *et al*, 2005).

## **1.4.2 Pulmonary arterial hypertension secondary to connective tissue disease**

PAH is a well-documented complication of connective tissue diseases (CTD) such as mixed CTD and scleroderma (SSc). Symptoms and clinical presentation in CTD associated PAH is similar to that of IPAH patients, however there is a shorter survival time associated with this condition

(Mukerjee *et al*, 2003; Dorfmueller *et al*, 2007). SSc, particularly of the limited disease type, is the main CTD associated with PAH (Mathai and Hassoun, 2011; Hurdman *et al*, 2012). Patients with scleroderma associated PAH (SSc-PAH) have a three-year survival rate of 52% (Hurdman *et al*, 2012).

SSc is a systemic autoimmune disease associated with deposition of connective tissue in inappropriate places. It is characterised by the deposition of collagen in the skin, but also in other organs such as the kidneys, heart, lungs and stomach. Females appear more susceptible to this disease (4:1 ratio) and the peak onset is between 30-50 years (Gu *et al*, 2008). There are two main subgroups of SSc (limited and diffuse cutaneous), with the limited form being characterised by sclerotic plaques. Visceral involvement does not occur in this form of the disease and prognosis is better than in diffuse cutaneous-SSc (Simeon-Aznar *et al*, 2012). Raynaud's phenomenon can also be associated secondary to SSc development and is classed as the diffuse form of the disease (Geroulakos, 2011). Raynaud's phenomenon is a vasospasm of the arteries or arterioles causing a colour change after reperfusion. Raynaud's phenomenon secondary to SSc is a very severe condition and causes pain and digital ulceration due to ischemia (Guiducci *et al*, 2007). Vascular involvement in SSc has been shown to precede fibrosis and involves small vessels in which vascular remodelling is dysregulated (Kahaleh, 2008). Studies conducted on the vessel walls in these small arterioles show large gaps between ECs and a loss of integrity of the endothelial lining.

Immune dysregulation has long thought to be involved in the pathogenesis of SSc and several lines of research are currently being undertaken to assess whether this can be targeted with pharmacodynamic therapy. A randomised, double-blind, placebo-controlled, phase II multicentre clinical trial is currently being undertaken across America to determine the effect of Rituximab, a monoclonal antibody against CD20 (B cell marker) on the progression of SSc-PAH (<http://www.clinicaltrials.gov>, 2012).

## 1.5 Pathobiology of pulmonary arterial hypertension

PAH is a panvasculopathy, predominantly affecting the small pulmonary arteries (resistance arteries) and arterioles which regulate blood flow in the lung. In PAH, obstructions in the small pulmonary arteries caused by medial hypertrophy and concentric laminar intimal fibrosis cause complex changes such as EC dysfunction, inflammation, growth factor dysregulation and chronic vasoconstriction (Rabinovitch, 2008).

Studies in the 1960's and 1970's by Wagenvoort examined pulmonary arteries from patients with PH and described vasoconstriction and medial hypertrophy associated with intimal fibrosis and occasional plexiform lesions (Wagenvoort, 1960; Wagenvoort, 1970). Remodelling of the pulmonary arteries has subsequently been shown to result from the abnormal proliferation of vascular smooth muscle cells (SMC) as well as an increase in EC proliferation and dysfunction leading to medial hypertrophy, concentric intimal lesions and a thickened adventitia. This has also been confirmed in patients with hereditary PAH and in patients with BMPR2 mutations where intimal lesions were found to consist of ECs and myofibroblast cells (Cool *et al*, 1999; Atkinson *et al*, 2002). Chazova *et al* examined the structure of lung samples from patients with PAH and showed that all three layers (intima, media and adventitia) are involved in arterial remodelling (Chazova *et al*, 1995). Increased production of extracellular matrix, as well as elastin and collagen deposition lead to a gradual remodelling of the adventitial layer of the vessels (Hassoun, 2005). Fibrotic lesions in the intimal layer of the pulmonary arteries can also occur, leading to a thickening of the vessel wall which occurs due to the recruitment and proliferation of fibroblasts and myofibroblasts (Humbert, 2012).

EC dysregulation and dysfunction is a prominent feature of PAH, and has a considerable effect on the pulmonary vasculature and remodelling process. Under normal physiological conditions, the pulmonary endothelium regulates production of vasoactive mediators that control physical and

biochemical properties of pulmonary vessels that affect ability of the vessel to contract as well as cellular growth and proliferation. The endothelium maintains a low pressure environment, vascular tone and controls leukocyte trafficking (Young, 2012). In PAH, the endothelium of pulmonary vessels becomes injured which leads to apoptosis of usually quiescent cells. This encourages disruption of the pulmonary vascular intima leading to uncontrolled proliferation of underlying SMCs (Budhiraja *et al*, 2004). A dysfunctional endothelium also has a chronically impaired production of vasodilators and antiproliferative agents such as nitric oxide (NO) and prostacyclin and overexpresses vasoconstrictor and proliferative agents such as thromboxane A2 (TXA2) and endothelin-1 (ET-1) (Ozaki *et al*, 2001). It still remains unclear whether the imbalance of vasoconstrictive and vasodilatory substances is in response to vascular injury or a direct effect of EC dysfunction (Graham, 2011).

Prostacyclin, a metabolite of arachidonic acid, is produced by the endothelium and can act on SMCs to cause vasodilatation. Prostacyclin also inhibits vascular SMC proliferation, via the increase of intracellular cyclic adenosine monophosphate (cAMP) (Newby *et al*, 1992). Prostacyclin receptor knockout mice develop severe PAH and levels of prostacyclin have been shown to be decreased in PAH patients (Tuder *et al*, 1999; Hoshikawa *et al*, 2001). A reduced expression of endothelial nitric oxide synthase (eNOS) in the lungs of PAH patients has been shown to lead to decreased levels of NO and therefore decreased levels of cyclic guanosine monophosphate (cGMP) and increased vasoconstriction (Giaid and Saleh, 1995; Kim, 2011). PDE-5 within SMCs decreases levels of cGMP, having a similar effect to NO. PDE-5 activity has been shown to be increased in the lungs of hypoxic rats further suggesting a role for this molecule in PAH (Maclean *et al*, 1997).

Vasoconstrictive mediators such as ET-1, serotonin and TXA2, can also cause platelet aggregation and have mitogenic effects on smooth muscle cells (Hanasaki *et al*, 1990; Pakala *et al*, 1994; Ikeda *et al*, 1997). Vascular EC ET-1 levels have been shown to be increased in PAH and correlate with disease severity (Christman *et al*, 1992; Giaid *et al*, 1993; Rubens *et al*, 2001). TXA2 levels and receptor density within the right

ventricle have also been shown to be increased in PAH patients (Christman *et al*, 1992; Katugampola and Davenport, 2001).

Another important aspect of pulmonary vascular remodelling in PAH is SMC hyperplasia which leads to medial hypertrophy and luminal narrowing of distal vessels (Tajsic, 2011). Phenotypic changes occur within pulmonary artery SMCs in PAH, including a down regulation of functional voltage gated potassium channels that allow membrane depolarisation leading to vasoconstriction. This then leads to contraction and mitogenesis of these cells (Yuan *et al*, 1998). An increased serum IL-6 level, as noted in PAH patients, could also lead to increased migration of SMCs and the synthesis of IL-6 themselves (Humbert *et al*, 1995; Wang and Newman, 2003).

## **1.6 Mechanisms of pulmonary arterial hypertension pathogenesis**

Several mechanisms have been shown to contribute to the development and progression of PAH, however none can completely explain all aspects of its development. Although it is unclear whether a common molecular mechanism underlies the cause of PAH, several key pathways and molecules (e.g. BMPR2, inflammation, hypoxia, cytokines, shear stress), acting alone or in combination, have been proposed to play an important role in PAH pathogenesis (Tuder *et al*, 1994; Shimoda and Semenza, 2011).

### **1.6.1 Genetics**

Several genetic mutations have been shown to predispose PAH, the most widely studied of these are mutations leading to dysfunctional TGF- $\beta$  signalling. These will now be discussed in further detail.

### **1.6.1.1 Bone morphogenetic receptor 2 mutations**

Several groups have reported mutations in the *BMPR2* gene in 10-30% of patients with IPAH and > 75% of patients with hereditary PAH, but only 20% of affected family members succumb to the disease due to low penetrance of these mutations (Deng *et al*, 2000; Thomson *et al*, 2000; Austin, Phillips, *et al*, 2009). *BMPR2* is a type II serine / threonine kinase receptor, which is widely expressed in pulmonary vascular ECs and SMCs and is a crucial mediator in development and organogenesis, as noted by the fact that *BMPR2* knockout mice die during gastrulation (Beppu *et al*, 2000). In disease-free individuals, *BMPR2* is thought to be vascular protective as it regulates EC and SMC phenotypes (Majka *et al*, 2011). In ECs, *BMPR2* signalling promotes cell survival, whilst in SMCs it leads to inhibited proliferative responses and induces apoptosis (Zhang *et al*, 2003; Teichert-Kuliszewska *et al*, 2006).

Mutations in *BMPR2* lead to an impairment of intracellular signalling responses and apoptosis in ECs and SMCs (Lane *et al*, 2000). Morrell *et al* used <sup>3</sup>H-thymidine incorporation studies to demonstrate that pulmonary artery SMCs with *BMPR2* mutations are resistant to the growth inhibitory effects of BMPs and TGF- $\beta$ . They postulate that the disruption of TGF- $\beta$  signalling is a consequence of *BMPR2* mutations in IPAH patients (Morrell *et al*, 2001). This might help explain exuberant cellular proliferation and vascular obliteration seen in this disease.

### **1.6.1.2 Activin-receptor-like kinase 1 mutations**

Genetic studies have also shown mutations in another membrane bound receptor member of the TGF- $\beta$  receptor signalling superfamily protein, ALK-1. Mutations in the *ALK-1* gene, which encodes the TGF- $\beta$  receptor, have been reported in patients with hereditary hemorrhagic telangiectasia and PAH. Mutations of this type are less common than *BMPR2* mutations in PAH patients and can be due to missense, deletion and nonsense mutations (Trembath *et al*, 2001). Under normal conditions, ALK-1

is expressed in a limited number of cells including ECs and interacts with TGF- $\beta$ 1 and activins. It transduces TGF- $\beta$ 1 signals by phosphorylating Smad1 or Smad 5 (Oh *et al*, 2000; Lamouille *et al*, 2002).

### **1.6.1.3 Endoglin mutations**

Endoglin (also termed CD105) is a gene that encodes a TGF- $\beta$  receptor complex accessory protein that is found on chromosome 9 (Chaouat *et al*, 2004). It is permanently expressed on ECs and has been shown to interact with BMP-2 and BMP-7, which are involved in regulating TGF- $\beta$  signalling (Barbara *et al*, 1999). Endoglin is also involved in angiogenesis as well as the maintenance of vascular integrity (Ray *et al*, 2010). Mutations in endoglin can lead to hereditary haemorrhagic telangiectasia however an endoglin gene polymorphism has recently been found in SSc-PAH patients (McAllister *et al*, 1994; Wipff *et al*, 2007; Suzuki *et al*, 2012).

## **1.6.2 Voltage-gated potassium channels**

Potassium channels (Kv) are transmembrane-spanning proteins that regulate cell membrane potentials and calcium movement in and out of cells. The intracellular calcium levels influence the contractile and proliferative status of SMCs, which in turn affect vasodilatation and contraction.

Fawn hooded rats have an inherited platelet storage disorder and impairment of serotonin storage, making them susceptible to pulmonary hypertension (Bonnet *et al*, 2006). The Mitochondrial–Hypoxia Inducible Factor-1 $\alpha$ –Kv Channel Pathway becomes abnormally regulated in fawn hooded rats, which disrupts oxygen sensing (reducing hypoxic pulmonary vasoconstriction) and triggers the development of PAH (Bonnet *et al*, 2006). Similar abnormalities occur in human IPAH.

Mitochondrial abnormalities that disrupt the ROS-HIF-1 $\alpha$ -Kv1.5 O<sub>2</sub>-sensing pathway have recently been shown to be another contributing factor to the pathogenesis of PAH (Archer *et al*, 2008). This causes a reduction in

reactive oxygen species and an increase in hypoxia inducible factor 1 (HIF-1)  $\alpha$  activation. It has also been shown that decreased expression of the O<sub>2</sub>-sensitive K<sup>+</sup> channel (Kv1.5) in rats treated with chronic hypoxia, can lead to the progression on PAH (Michelakis *et al*, 2002). Post *et al* also noted that hypoxic conditions could inhibit whole cell K<sup>+</sup> currents in canine pulmonary artery SMCs which lead to vasoconstriction via membrane depolarisation and subsequent calcium entry (Post *et al*, 1992). Dichloroacetate, has been shown to increase oxidative phosphorylation within the mitochondria of SMCs, reversing both monocrotaline (MCT) and chronic hypoxia induced PAH in rats, providing evidence that this could be a potential therapeutic target in PAH patients (Michelakis *et al*, 2002; McMurtry *et al*, 2004).

### **1.6.3 Serotonin dysregulation**

Serotonin (5-HT) is a neurotransmitter that is synthesised in ECs through the action of tryptophan hydroxylase 1 (Tph1). It can then act upon 5-HT receptors to cause constriction and proliferation of pulmonary artery SMCs (Willers *et al*, 2006). 5-HT can also cause these effects in fibroblasts (Welsh *et al*, 2004).

The first suggestion that 5-HT may be involved in the pathogenesis of PAH was when there was an epidemic of clinical symptoms of PAH in patients taking appetite suppressant drugs (Aminorex and Dexfenfluramine), which inhibit 5-HT uptake in platelets (Gurtner, 1985). Plasma 5-HT levels have been shown to be increased in IPAH patients and it is suggested that 5-HT propagates the development of PAH both clinically and experimentally, via its ability to encourage vasoconstriction and remodelling of the pulmonary vasculature (Herve *et al*, 1990; Herve *et al*, 1995; Eddahibi *et al*, 1997; MacLean *et al*, 2000). ECs and SMCs from PAH patients also have an increased ability to produce 5-HT and proliferate in response to 5-HT than control cells (Eddahibi and Adnot, 2001; Willers *et al*, 2006). An increased expression of 5-HT receptors has also been confirmed in pulmonary arteries of PAH patients. Other studies suggest that PAH can be inhibited in mice deficient for 5-HT receptors, further emphasising their involvement in the pathogenesis of PAH (Launay *et al*, 2002).

An increased expression of the serotonin transporter (SERT) has also been reported in IPAH patients, whilst inhibition of this transporter in rats can prevent and even reverse PAH caused by MCT injection or hypoxia in mice (Eddahibi *et al*, 2001; Hironaka *et al*, 2003; Marcos *et al*, 2003; Guignabert *et al*, 2005).

The Tph1 gene was found to be increased in the lungs and pulmonary ECs from patients with IPAH and interestingly, a genetic deletion of this gene in mice has been shown to protect against hypoxia-induced PAH (Morecroft *et al*, 2007). The sex hormone, 17 $\beta$ -oestradiol, produced by the ovaries, has been shown to attenuate both hypoxic PAH and MCT induced PAH, via its effect on the 5-HT pathway (Lahm *et al*, 2012). 17 $\beta$ -oestradiol has also been shown to increase expression of Tph1 in human pulmonary artery SMCs from controls (White, Dempsey, *et al*, 2011).

There are several lines of evidence that converge to support the theory that serotonin dysregulation is involved in the pathogenesis of PAH. Firstly, the increased susceptibility of females for the disease and the fact that female mice overexpressing SERT exhibit PAH when induced by hypoxia, compared to males that remain unaffected (White, Dempsey, *et al*, 2011; White, Loughlin, *et al*, 2011). Only female SERT+ mice develop PAH whilst ovariectomy can completely abolish the development of PAH. Also, 17 $\beta$ -oestradiol has been shown to play a critical role in this process as its reintroduction into ovariectomized SERT+ mice re-established the disease state, further confirming a strong link between the female gender and serotonin responses (White, Dempsey, *et al*, 2011). Secondly, normal physiological 17 $\beta$ -oestradiol levels can increase the expression of cytochrome P450 1B1 (an oestrogen metabolising enzyme) and cause pulmonary artery SMCs to proliferate. 17 $\beta$ -oestradiol can also increase the expression of 5HT1B receptor, SERT and Tph1, which have all been shown to be involved in the pathogenesis of PAH (White, Dempsey, *et al*, 2011). Cytochrome P450 1B1 expression is increased in clinical and experimental PAH and has also been shown to be expressed at lower levels in females. Levels of this enzyme have also been shown to modify PAH disease progression. In cytochrome P450 1B1  $-/-$  mice, hypoxia induced PAH is attenuated whilst the administration of a cytochrome P450 1B1 inhibitor

(2,3',4,5'-tetramethoxystilbene) has been shown to limit hypoxia and hypoxia + sugen 5416 PAH development *in vivo* (Austin, Cogan, *et al*, 2009; White *et al*, 2012).

Finally, in the chronic hypoxic rat model of PAH, oral dehydroepiandrosterone treatment (an activator of calcium gated potassium channels) has been shown to prevent right ventricular hypertrophy (RVH) and pulmonary arterial vascular remodelling by opening large conductance calcium activated channels (Bonnet *et al*, 2003). Augmentation of these channels also leads to SMC repolarisation, leading to a protected PAH phenotype (Hampl *et al*, 2003). Taken together, these findings support the concept that the 5-HT pathway is involved in the pathogenesis of PAH.

#### **1.6.4 Plasma leptin and insulin resistance**

Leptin is an adipokine that regulates food intake and is released from adipose tissue enhancing metabolism. It acts on the hypothalamus to suppress appetite, but can also play a critical role in influencing innate and adaptive immune responses, as it has been shown to sustain low-grade inflammation which could lead to chronic disease. Leptin can induce T cell activation towards a Th1 response, including the production and release of IL-2 and other cytokines (Martin-Romero *et al*, 2000). Interestingly, a decrease in plasma leptin levels has also been shown to lead to an impaired immune response, and has been associated with increased incidences of coronary artery disease. In PAH, lower plasma leptin levels are associated with increased mortality (Lord *et al*, 1998; Ku *et al*, 2011; Tonelli *et al*, 2012). Recently, it was reported that IPAH and SSc-PAH patients have increased serum leptin levels, as well as an increased number and decreased function of circulating T cells expressing the leptin receptor. Huertas *et al* also confirmed that ECs from IPAH patients also synthesised more leptin and therefore suggested that this, in part, drives the pathogenesis of PAH (Huertas *et al*, 2012).

Regulation of leptin has been shown to be partly due to insulin, and insulin resistance has been shown to be associated with elevated plasma leptin levels (Saladin *et al*, 1995; Zimmet *et al*, 1998). Insulin resistance is

thought to be common in PAH, especially in female patients, and has been shown to be a risk factor in other cardiovascular diseases (Zamanian *et al*, 2009). Work undertaken by our laboratory confirms that ApoE deficient mice become insulin resistant on a high fat diet and are increasingly susceptible to PAH.

### **1.6.5 Other mediators**

Several other mediators have been shown to increase in PAH, such as ET-1, which has vasoconstrictive effects in blood vessels (Cacoub *et al*, 1997; Cacoub *et al*, 1997). Reduced bioavailability of endogenous NO has also been suggested to play a role in PAH (Giaid and Saleh, 1995).

Osteoprotegerin, a member of the tumor necrosis factor receptor superfamily, is a secreted glycoprotein expressed in heart and lung tissue that regulates pulmonary artery SMC proliferation and migration. It is modulated by BMPs, 5-HT and IL-1 and it has been found to be increased in serum and within lesions found in the lung tissue of PAH patients (Lawrie *et al*, 2008; Condliffe *et al*, 2012).

The cytokine, Tumor Necrosis Factor (TNF)-Related Apoptosis-Inducing Ligand (TRAIL) is a receptor for osteoprotegerin and has been shown to induce SMC proliferation and EC apoptosis *in vitro* (Corallini *et al*, 2008). TRAIL has also been found associated with pulmonary vascular lesions in both human and animal models of PAH further supporting the evidence that TRAIL has an important role in vascular biology. Recently, it has been reported that antibody blockade and genetic depletion of TRAIL in rodent models of PAH prevented the development of PAH (Hameed, Arnold, *et al*, 2011; Hameed, Chamberlain, *et al*, 2011). After recombinant TRAIL administration, PAH disease phenotype was restored, confirming that TRAIL is highly involved in the pathogenesis of PAH (Hameed *et al*, 2010; Hameed *et al*, In Press).

Osteopontin, also known as cytokine Eta-1, has also been suggested to play a role in PAH due to its ability to recruit macrophages and T cells to sites of inflammation and stimulate cytokine production within these cell types (Strom *et al*, 2004). It has also been suggested that this protein may

play a role in tissue repair and remodelling via its effects on vascular SMCs (Giachelli *et al*, 1998; Ashkar *et al*, 2000). Osteopontin levels are significantly elevated in the serum of IPAH patients and could be used as a biomarker in PAH (Lorenzen *et al*, 2011).

Iron deficiency is also frequently present in IPAH patients and is associated with disease severity and poor clinical outcome. Iron availability affects pulmonary haemodynamics by modifying mPAP and pulmonary vasoconstrictor responses to hypoxia (Ruiter *et al*, 2011). Oral iron therapy has been shown to be ineffective at restoring normal ferritin levels suggesting a problem with iron absorption in these patients. Interestingly, hepcidin, which regulates iron absorption and increases cellular iron storage, is raised in IPAH patients, impairing the body's ability to absorb iron from the gut (Rhodes *et al*, 2011).

Cytokine dysregulation is also a common feature in PAH, leading to an increase in pro-inflammatory cytokines, such as IL-1, IL-6 and fractalkine, within the serum of IPAH patients (Humbert *et al*, 1995; Balabanian *et al*, 2002). These inflammatory cytokines can then have important downstream effects in the inflammatory response to vessel remodelling, as discussed later in Chapter 1.6.6.

Taking all these mediators into consideration, it is highly likely that PAH has a multi-factoral pathobiology and it is unlikely that a single factor or gene mutation will explain all forms and cases of PAH.

## **1.6.6 Inflammatory mediators in pulmonary arterial hypertension**

Inflammation is thought to play an important role in the pathogenesis of PAH. Inflammatory cells, including macrophages, T and B lymphocytes, and DCs have been found associated with plexiform lesions in lung samples from patients with IPAH (Tuder *et al*, 1994; Balabanian *et al*, 2002). Recently, emphasis has been put on natural killer (NK) cell involvement in the pathogenesis of PAH. These cells are functionally impaired in IPAH patients, expressing decreased activation markers (NKp46, 2DL1/s1 and 3DL1) (Ormiston *et al*, 2012). NK cells bridge the gap between the innate

and adaptive immune system and their function is controlled by a balance between stimulatory and inhibitory signals that are delivered to the cell via receptor triggering (Smyth *et al*, 2005). A dysfunctional NK cell population could be a sign of an abnormal immune system and can lead to inappropriate immune processes (Sun *et al*, 2009).

T cells, B cells and macrophages are thought to produce and react to pro-inflammatory cytokines, such as IL-6 and tumor necrosis factor alpha (TNF- $\alpha$ ), that have been shown to be upregulated in the hypertensive pulmonary circulation and are thought to be linked to the structural remodelling which is seen in IPAH patients (Botney *et al*, 1994; Botney *et al*, 1994; Humbert *et al*, 1995; Fujita *et al*, 2001; Zaiman *et al*, 2008). More recently, Steiner *et al* described how IL-6 over-expression in transgenic mice caused PAH (Steiner *et al*, 2009). IL-1 is also a potent pro-inflammatory cytokine involved in immune responses and has been shown to play a key role in acute and chronic inflammatory and autoimmune disorders. IL-1 is secreted from monocytes, macrophages, neutrophils, vascular ECs and SMCs (Goodman *et al*, 1982; Libby, Ordovas, Auger, *et al*, 1986; Libby, Ordovas, Birinyi, *et al*, 1986; Warner *et al*, 1987; Lindemann *et al*, 1988; Loppnow *et al*, 1994). Previously published work has shown the importance of IL-1 in the response to vascular injury (Bevilacqua *et al*, 1985). Serum IL-1 levels have been found to be elevated in patients with PAH and it is proposed that this pro-inflammatory cytokine activates ECs, monocytes and T cells, and mediates SMC growth (Humbert *et al*, 1995). IL-1 receptor antagonist (IL-1RA) treatment can be used to reduce PAH in MCT treated rats and ApoE<sup>-/-</sup>/IL-1R1<sup>-/-</sup> mice, which further implicates IL-1 in the pathogenesis of PAH (Voelkel and Tudor, 1994; Lawrie *et al*, 2011). Increases in serum IL-2 have also been confirmed in IPAH, which correlate negatively with survival as IL-2 can promote T cell proliferation and activation augmenting inflammatory responses (Soon *et al*, 2010).

Elevated levels of macrophage inflammatory protein-1 $\alpha$  (MIP-1 $\alpha$ ) and increased P-selectin expression in patients with severe IPAH have also been reported (Humbert *et al*, 1995; Sakamaki *et al*, 2000). MCP-1, activates mononuclear cells and may play a role in the progression of PAH as anti-MCP-1 gene therapy can be used to inhibit vascular remodelling and

therefore MCT-induced PAH in rats (Ikeda *et al*, 2002). The severity of remodelling in PAH has also been shown to correlate with levels of serum IgE and IgG1, as well as the cytokines IL-5 and IL-4, and Fractalkine (an inflammatory chemokine) is also upregulated in patients with PAH (Balabanian *et al*, 2002). The chemokine regulated and normal T cell expressed and secreted (RANTES) can encourage cell recruitment in the lungs of patients with PAH and it has been reported that ECs are a primary source of RANTES (Dorfmueller *et al*, 2002).

As a key part of the immune system, it has been suggested that B cells may also be involved in the pathogenesis of PAH, as these cells have been found to be associated with other immune cells (macrophages and T cells) in plexiform lesions (Tuder *et al*, 1994). Ulrich *et al* also noted a change in the RNA expression profile of B cells in peripheral blood from IPAH patients, suggesting an increase in their activation when compared to healthy controls (Ulrich *et al*, 2008).

Bellotto *et al* were the first to suggest a link between anti-inflammatory therapy and improvements in the prognosis of patients with PAH (Bellotto *et al*, 1999). Other studies have also shown that the clinical status of patients with severe PAH associated with systemic lupus erythematosus (SLE) and mixed CTD also improved with immunosuppressant therapy (Morelli *et al*, 1993; Sanchez *et al*, 2006; Jais *et al*, 2008). Also, in MCT treated rats, dexamethasone, a corticosteroid and anti-inflammatory drug, has been shown to prevent and reverse PAH by improving haemodynamics and preventing pulmonary vascular remodelling. It is thought that this occurs via a reduction of inflammatory cells that express IL-6 and a reduction in the proliferative responses of SMCs (Price *et al*, 2011).

There is also a link between PAH and autoimmune diseases such as autoimmune thyroid disease, in which an autoimmune injury and an altered immunoregulatory response lead to the progression of PAH (Chu *et al*, 2002). Several studies have also noted auto-antibodies in the serum of PAH patients, including anti-phospholipid antibodies, anti-fibroblast antibodies, anti-centromere antibodies and anti-endothelial cell antibodies suggesting a dysfunctional immune phenotype (Luchi *et al*, 1992; Tamby *et al*, 2005; Tamby *et al*, 2006; Terrier *et al*, 2008). Anti-EC antibodies are thought to be

able to induce EC apoptosis and this is thought to initiate PAH disease progression.

Inflammatory cells are also thought to modify the expression of growth factors such as vascular endothelial growth factor (VEGF) and TGF $\beta$  within vascular cells (Shen *et al*, 1993; Tuder *et al*, 1994). These growth factors can then act on inflammatory cells in a similar manner to cytokines (Botney *et al*, 1994). Furthermore, inflammatory cells may provide the source of these growth factors, thereby providing a complex picture of how mediators and inflammatory cells interact within the disease setting of PAH.

These studies, taken together with the evidence of inflammatory cells being present in plexiform lesions of patients with PAH, as well as their altered functions and behaviour, further emphasises the relevance of inflammation in pathogenesis of PAH and its progression. Most of what is known about inflammatory processes and their involvement in the pathogenesis of PAH, is a result of work performed on animal models of PAH as human tissues or *in vivo* systems are generally unavailable to study the disease before death.

## **1.7 B and T cell involvement in the pathogenesis of pulmonary arterial hypertension**

Several lines of evidence suggest that lymphocytes are involved in the pathogenesis of PAH, with several research groups seeking to answer the question of whether specifically T cells contribute to the development of PAH or protect against it.

B cells are antibody producing adaptive immune cells that have been shown to be present surrounding plexiform lesions within the lung tissue of IPAH patients, along with several other inflammatory cells (Voelkel and Tuder, 1994). Also, as previously mentioned, the presence of auto-antibodies against cellular components within the serum of PAH patients also suggests a strong connection between B cells and PAH disease pathogenesis,

however only a limited number of studies have determined the proportions of B cells within the peripheral blood of PAH patients.

With regards to T cells, in several animal models of PAH, immune cells, specifically CD45<sup>+</sup> and CD3<sup>+</sup> T cells have been shown to be associated with vascular lesions within the lung of diseased animals. The localisation of these cells to the remodelled areas within the lung still does not explain whether they are there to either augment the progression of PAH or are increasing in number to protect the diseased vessels.

The presence of T cells in lung tissue sections taken from PAH patients has been investigated by several research groups (Voelkel and Tuder, 1995; Dorfmueller *et al*, 2002; Dorfmueller *et al*, 2003). These T cells are also accompanied by an increased number of DCs, monocytes and macrophages, suggesting that there is a strong inflammatory component to this disease (Tuder *et al*, 1994).

Other evidence to suggest that T cells are involved in PAH pathogenesis comes from studies in which athymic rats, lacking T lymphocytes, develop severe angioproliferative PAH after administration of the VEGFR2 inhibitor SU5416 given under normoxic conditions (Taraseviciene-Stewart *et al*, 2007). PAH also occurs in association with HIV infections, in which CD4<sup>+</sup> T cells are diminished. T cells would normally regulate the inflammatory response to vascular injury, but in this situation an over exuberant inflammatory response occurs. In other experiments using the above model of PAH, splenocytes from euthymic animals were injected into athymic animals, which protected the animals from the development of vascular lesions (Taraseviciene-Stewart *et al*, 2007; Ulrich *et al*, 2008). The MCT rat model of PAH has also been used to assess the effect that absence of CD4<sup>+</sup> T cells has on inflammatory response. However, Cuttica *et al* described how ablation of CD4<sup>+</sup> T cells protected against rising right ventricular pressures and RVH. When CD4<sup>+</sup> T cells were reintroduced into this model, it was noted that there was a markedly increased perivascular inflammation as well as vascular remodelling, increased right ventricular pressures and RVH after administration of MCT (Cuttica *et al*, 2011). It has also been shown that suppression of the adaptive immune system inhibits development of hypertension in experimental animal models. Systemic

hypertension was reduced to normal levels when an immunosuppressive treatment, mycophenolate mofetil, was given to genetically hypertensive rats (Rodriguez-Iturbe *et al*, 2001).

There have also been several recent reports detailing abnormal proportions of T cells in PAH patients. Ulrich *et al* studied T cell subsets in IPAH patient peripheral blood samples using flow cytometry and reported a decrease in the proportion of CD8<sup>+</sup> T cells and an increase in the proportion of CD4<sup>+</sup>CD25<sup>high</sup> Treg and Foxp3<sup>+</sup> Treg cells in peripheral blood (Ulrich *et al*, 2008). Austin *et al* also noted a higher proportion of CD4<sup>+</sup>CD25<sup>high</sup> Treg cells in patients with IPAH and further characterised the CD8<sup>+</sup> T cells within IPAH patients, revealing that there was a significant increase in effector-memory CD8<sup>+</sup> T cells (CD45RA<sup>+</sup> CCR7<sup>-</sup>). There was enhanced cytotoxic activity to peripheral antigens and a significant decrease in circulating naïve CD8<sup>+</sup> T cells (CD45RA<sup>+</sup> CCR7<sup>+</sup>) in patients with IPAH compared to controls (Austin *et al*, 2010). Lymphocyte profiles in PAH patients have also been studied by Soon *et al*, who reported elevated Treg cell subsets in patients with inheritable PAH with BMPR2 mutations, but not in CTEPH patients (Soon, 2008). It has been suggested that the increase in Treg cells could be necessary to suppress self-reactive T cells and that a dysfunctional immune system could contribute to the pathology of this disease. It is possible that the differences in prevalence of certain T cell subsets could be an indicator of the pathogenic role of these cells in PAH.

Austin *et al* also performed immunohistochemical analysis on IPAH patient lung tissue to identify T cell infiltration, and found increased numbers of CD3<sup>+</sup> and CD8<sup>+</sup> T cells in the peripheral lung of IPAH samples compared with controls (Austin *et al*, 2010). The functional ability of Treg cells from IPAH patients to suppress proliferation of T effector cells has also been assessed. Ulrich *et al* performed a co-culture assay to look at the functional status of CD4<sup>+</sup>CD25<sup>high</sup> Treg cells from IPAH patients, but found that it was the same in patients and controls. No other work has been performed on Treg suppressive capabilities in PAH patient peripheral blood samples to date. Other patient subgroups (SSc-PAH) have not been examined and only one assay has been used to determine the functional capacity of Treg cells

to inhibit T cell proliferation in IPAH patients (using a CyQuant proliferation kit) (Ulrich *et al*, 2008).

The patients included in these studies were all on drug treatments specifically for PAH, which may have affected lymphocyte number and function. Ulrich *et al* included only steroid-naïve patients in their analysis, however many IPAH patients included in their study were taking drugs used to treat PAH such as prostanoids, E-RAs and PDE-5 inhibitors, which could have altered their lymphocyte profile (Ulrich *et al*, 2008). In 2010, Austin *et al* performed a similar study, including IPAH patients receiving prostanoid therapy at the time of the study of lymphocyte profile in blood (Austin *et al*, 2010).

Despite these limitations to the aforementioned studies, these findings suggest that it is possible that CD4<sup>+</sup> T cell irregularities seen in patients may make patients susceptible to exaggerated vascular inflammation and vascular remodelling following vascular injury (Tamosiuniene and Nicolls, 2011).

### **1.7.1 T cells and their involvement in the pathogenesis of scleroderma**

The role of T cells in the pathogenesis of SSc is also relevant as these cells are thought to contribute to tissue damage due to production of soluble mediators such as IL-4, and IL-6 (Needleman *et al*, 1992). Studies on circulating T cell subsets in peripheral blood of patients with SSc are inconclusive, with studies reporting differing results. Inflammatory cell infiltration (including B cells, T cells and macrophages) can occur very early during the formation of lesions with skin lesions predominantly having CD4<sup>+</sup> T cell driven responses (Mavalia *et al*, 1997). These cells appear activated, exhibit oligoclonal expansion and are predominantly Th2 cells. Th2 T cells infiltrated skin lesions and produced IL-4, and the fibrosis seen in lesions can be prevented by anti-IL-4 treatment (Ong *et al*, 1998). Serum from SSc patients also had increased levels of Th2 cytokines (such as IL-4) (Needleman *et al*, 1992). An increase in the numbers of inflammatory cells infiltrating the skin in patients with SSc has been shown to correlate with skin

thickening and disease progression (Roumm *et al*, 1984). Drug therapies directed against activated T cells (cyclosporin A and tacrolimus) and a deficiency of CD4<sup>+</sup> T cells, have been shown to improve skin tightness in animal models (Wallace *et al*, 1994). This improvement has also been noted in SSc patients after they were treated with antilymphocyte globulin to remove T cells (Goronzy and Weyand, 1990).

Several groups have reported an increase in Treg cells (CD4<sup>+</sup>CD25<sup>+</sup> and CD25<sup>high</sup>Foxp3<sup>high</sup>CD127<sup>neg</sup> T cells) with diminished suppressive function in peripheral blood of SSc patients (Radstake *et al*, 2009). However, Antiga *et al* reported a decreased number of CD4<sup>+</sup>CD25<sup>bright</sup>Foxp3<sup>+</sup> Treg cells. Slobodin *et al* noted a correlation between CD4<sup>+</sup>CD25<sup>bright</sup>Foxp3<sup>+</sup> Treg cell numbers and disease severity and activity, suggesting a role for Treg cells in the pathogenesis of SSc. It was also suggested that this expansion of Treg cells in SSc appeared secondary to the expansion of activated CD4<sup>+</sup> T helper cells, as they were activated in the periphery to express Foxp3 and become active Treg cells (Slobodin *et al*, 2010).

Several other research groups have reported an increased ratio of CD4:CD8 T cells, due to a reduction in CD8<sup>+</sup> T cells in SSc patients (Barnett *et al*, 1989; Luzina *et al*, 2003; Antiga *et al*, 2010). Some researchers suggest that this reduction in CD8<sup>+</sup> T cells may be due to lymphocytotoxic antibodies or anti-lymphocyte antibody-blocking determinants in blood (Kessel *et al*, 2004). The reduction in CD8<sup>+</sup> T cells in peripheral blood of patients with SSc may also be due to tissue migration into the lungs, where they have been shown to increase in number and appear increasingly activated (Yurovsky *et al*, 1996).

Activated T cells (CD4<sup>+</sup> and CD8<sup>+</sup>) and elevated Th2 associated cytokines (IL-2, IL-4 and IL-6) have been found in peripheral blood of patients with SSc, further emphasising the involvement of abnormally activated T cells and immune responses in SSc (Freundlich and Jimenez, 1987; Gustafsson *et al*, 1990; Sakkas and Platsoucas, 2004).

## 1.8 Involvement of heat shock protein 70 in pulmonary arterial hypertension

Ritossa *et al* were the first to describe heat shock proteins (Hsp) when they inadvertently subjected *Drosophila melanogaster* larvae to an elevation in temperature and noticed that this induced the expression of new genes in the form of chromosomal puffs in salivary gland cells (Ritossa, 1962). Tissières *et al* later identified the products of these genes, to which the term 'heat shock proteins' was attributed (Tissières *et al*, 1974).

Hsps are a group of highly conserved proteins that are present in the cells of all organisms. They can be extracellularly localized or plasma membrane-bound and have been shown to be released into the extracellular compartment from a number of different cell types under a range of conditions, in which they have been shown to exhibit a number of pro- and anti-inflammatory properties. Hsps range in size from 10-150 kDa and they are classified into families on the basis of the molecular size; namely 110, 90, 70, 60 and 40 kDa. They are released from a variety of cells including vascular SMCs and tumour cells under stressful conditions (Ferrarini *et al*, 1992; Xu *et al*, 1997; Liao *et al*, 2000). Hsps have been shown to have several roles including molecular chaperones or proteases and can regulate intracellular protein folding (McLean *et al*, 2002). Hsp activity is regulated by HIF-1, a transcription factor involved in controlling genes concerned with promoting cell survival in low-oxygen conditions (Date *et al*, 2005). Pockley *et al* have shown Hsp70 can be detected in the serum of normal individuals, however it is up-regulated in response to stressful conditions such as heat, hypoxia or UV radiation, hence the name "stress protein" (Iwaki *et al*, 1993; Trautinger *et al*, 1996; Pockley *et al*, 1998).

Despite being thought of as a "danger signal" inducing pro-inflammatory immune responses, Hsp70 can also inhibit protein kinases and transcription factors, decreasing ICAM-1 expression on ECs and inhibiting leukocyte adhesion and cytokine production, acting in an anti-inflammatory

manner (House *et al*, 2001; Kohn *et al*, 2002; Nollen and Morimoto, 2002; Pratt and Toft, 2003). Recently, there has also been much interest in the cardioprotective role of Hsp70, as Hsp70 levels can be used to predict the development of atherosclerosis in subjects with established hypertension and it is proposed to modify the progression of disease (Pockley *et al*, 2003; Pockley *et al*, 2009). Pockley *et al* have demonstrated that elevated levels of circulating Hsp70 protect against the development of atherosclerosis in patients with established hypertension (Pockley *et al*, 2003). Vasopressin-induced hypertension has also been shown to increase Hsp70 mRNA induction in rat aorta (Xu *et al*, 1995; Pockley *et al*, 2002; Pockley *et al*, 2003).

Hsp70 over-expression can also protect cardiac cells against stimulated ischaemia or thermal stress and therefore, it is possible that Hsp70 may maintain or induce an anti-adhesive phenotype in the vascular endothelium, which would lead to an anti-inflammatory state (Brar *et al*, 1999; House *et al*, 2001).

Although these findings emphasise the importance of Hsps in protecting stressed endothelial and cardiac cells in systemic disease, the effect on pulmonary circulation / right ventricular failure is yet to be defined. At present there is limited information available regarding the relationship between Hsp70 expression and disease severity / disease pathogenesis in PAH patients.

In different disease states, Hsps can act in either a pro- or anti-inflammatory manner with Hsp70 and Hsp60 both inducing and inhibiting T cell proliferation and function (van Roon *et al*, 1997; Zanin-Zhorov *et al*, 2003; Zanin-Zhorov *et al*, 2006; Zanin-Zhorov *et al*, 2005). HSP60 signaling can activate TLRs (TLR2 and TLR4) via CD14, a co-receptor molecule expressed on the membrane of immune cells such as macrophages and T cells. The activation of these TLRs can then inhibit the activation (in activated T cells) of T-bet and Nuclear factor of activated T-cells (NFAT) via the TLR2 signaling pathway. This results in the depletion of TNF- $\alpha$ , IFN- $\gamma$  and IL-2 secretion, inhibiting Th1 cell differentiation.

However the suggestion that Hsps can have anti-inflammatory effects via interactions with Treg cell populations suggests that Hsp70 might

modulate the pathogenesis of PAH possibly via interactions with Treg cells (Pockley *et al*, 2003; Zanin-Zhorov *et al*, 2006; Borges *et al*, 2012).

## **1.9 Treatments of pulmonary arterial hypertension**

Although current treatments for PAH cannot completely cure the disease, they can help to prevent disease progression, prevent pulmonary artery thrombosis and relieve the symptoms of PAH by limiting vascular remodelling within the pulmonary arteries and improving oxygen supply. Treatments for PAH include anticoagulants, oxygen and diuretics for right heart failure as well as vasodilators including calcium-channel antagonists, endothelin-receptor antagonists (E-RA), phosphodiesterase type 5 inhibitors (PDE-5) and prostanoids (Rich *et al*, 1992; Quinn *et al*, 1998; Zhao *et al*, 2001).

E-RAs, such as Bosentan and Ambrisentan, inhibit vasoconstriction and the mitogenic effects of ET-1, causing vasodilatation. PDE-5 inhibitors, such as Sildenafil, are relatively selective pulmonary vasodilators via their ability to increase cyclic guanosine monophosphate (cGMP). Sildenafil also has anti-mitogenic properties, making this drug highly appealing to patients that are non-responsive to calcium channel blocker therapy. Prostanoids such as Epoprostenol (a synthetic prostacyclin), cause vasodilatation, platelet aggregation and have anti-proliferative properties on cultured vascular SMCs, suggesting they may have an effect on vessel remodelling (Rubin, 2002).

Combination therapy, using several combinations of the previously mentioned drugs, also shows promise, however the long term effects of this have not yet been confirmed (Hoepfer *et al*, 2004). Oxygen therapy and anti-coagulants such as warfarin are also used in combination with the previously mentioned drugs. New targets are emerging all the time regarding treatment of PAH, including rho kinase inhibitors, serotonin transporter inhibitors and regenerative therapy using bone marrow-derived endothelial-like progenitor

cells (Guignabert *et al*, 2005; Nagaoka *et al*, 2005; Zhao *et al*, 2005). These targets aim to have anti-proliferative and anti-remodelling effects as well as vasodilatory effects on SMCs (McLaughlin, 2011).

Despite advances in the understanding of PAH pathogenesis, at present there is still no cure for PAH except for a full lung transplantation, which only occurs in a few cases per year in the UK.

## **1.10 Aims and hypotheses**

The aim of this thesis was to determine the phenotypic profile of T cell populations in peripheral blood of patients with IPAH and SSc-PAH and compare these with controls. I aimed to use the fat fed ApoE<sup>-/-</sup>/IL1R1<sup>-/-</sup> mouse model of PAH to deduce the involvement of T cell subgroups in the progression of PAH disease and also aimed to determine the effect of T cell depletion had on the progression of PAH. I also aimed to determine Hsp70 levels in serum and lung samples to relate them to disease progression.

I hypothesised that patients within different PAH subgroups would exhibit an altered T cell profile in peripheral blood compared to corresponding controls. I also hypothesised that changes in circulating T cell subsets would correlate with disease progression and vascular remodelling in an animal model of PAH and that a reduced CD4<sup>+</sup> T cell subset may encourage the pathogenesis of PAH. I also hypothesised that changes in pulmonary vascular haemodynamics would cause EC stress and regulation of Hsp70.

# **Chapter 2 Characterising lymphocyte subpopulations in peripheral blood of patients with pulmonary arterial hypertension**

## **2.1 Introduction**

As previously discussed in chapter 1.7, T cells are thought to be involved in the pathogenesis of PAH. Despite this, only a limited number of studies detailing changes in proportions of T cell subsets in PAH patients have been performed. Previous studies are limited by patient cohorts that were already on PAH treatment and therefore the aim of this chapter was to analyse T cell subsets in treatment naïve PAH patients. Additionally, published literature in this field only encompasses IPAH patients and so patients with PAH associated with CTD, specifically SSc where T cells play an active role in disease progression, will be examined (Wallace *et al*, 1994).

## **2.2 Methods**

### **2.2.1 Ethics**

Ethical approval for this study was obtained from the Sheffield Local Research Ethics Committee (ref: 08 / H1308 / 193). Blood samples were taken after written informed consent was obtained from all participants in this study. Local Sheffield teaching hospital R and D approval for the Cardiovascular Biomedical Research Unit (CVBRU) tissue bank was also gained before the study was conducted (STH15222).

## 2.2.2 Patient Samples

All experiments were performed in Department of Cardiovascular Science Laboratories at the University of Sheffield, in collaboration with the National Institute for Health Research Cardiovascular Biomedical Research Unit (CVBRU) and the Sheffield Pulmonary Vascular Disease Unit (SPVDU). Blood was collected from patients attending the SPVDU with suspected PAH following written informed consent. Diagnosis was later confirmed at a consultant led management, diagnosis and treatment meeting. Patients with no PAH at right heart catheterisation, and healthy age and sex matched patients, were used as controls along with patients diagnosed with SSc alone. All enrolled patients met diagnostic criteria for IPAH and SSc-PAH in accordance with accepted international standards (Galie *et al*, 2009). This included a mean pulmonary arterial pressure (mPAP) of  $\geq 25$  mmHg with a pulmonary capillary wedge pressure of  $\leq 15$  mmHg, and exclusion of left ventricular dysfunction.

A total of 65 patients were recruited throughout the duration of this project, however only 13 SSc-PAH patients and 15 IPAH patients were included in this study. Data was excluded from patients with 1) sub-optimal peripheral blood mononuclear cell isolation and 2) a diagnosis after initial blood draw as “not IPAH” or “not SSc-PAH”.

A total of 16 healthy volunteers were recruited for this project with only one being excluded as it was later confirmed that they had taken anti-inflammatory medication before blood draw. A total of 9 SSc controls were also recruited, with one being excluded due to insufficient CD3<sup>+</sup> T cell events being recorded on analysis. SSc-no PAH patients were recruited from a rheumatology clinic as having no symptoms for PH or from the SPVDU as SSc patients referred with suspected PH who had a normal mean PAP at diagnostic right heart catheterisation. These patients were taking a range of medications including vasodilators, anti-inflammatories, proton pump inhibitors and pro-kinetic agents. Healthy control subjects were questioned about medical history and current drug therapies that they were undergoing prior to blood draw. To avoid changes in number and activation status of

circulating lymphocyte subsets due to drug therapies, healthy controls and SSc patients were included on the basis that they had not taken anti-inflammatory agents, anti-histamines or immune-suppressive therapies prior to blood donation nor had they any co-morbidities such as autoimmune or cardiovascular disease.

### **2.2.2.1 Lymphocyte subset staining in patient blood and controls**

Venepuncture was performed using a 21 G needle and 5 mL of blood was collected into lithium-heparin Vacutainer<sup>®</sup> (BD Biosciences, Oxford, UK). Isolation of peripheral blood mononuclear cells (PBMCs) was performed by density gradient centrifugation. Blood was diluted 1:1 with phosphate buffered saline (PBS) at room temperature and layered over an equal volume of density gradient medium LSM 1077 Lymphocyte. The preparation was centrifuged at 1200 x *g* for 20 minutes without a brake so as not to disrupt the layers generated during the centrifugation. Erythrocytes and dense granulocytes sedimented to leave a layer of PBMCs and platelets at the interface (Figure 2.1).

After isolation, PBMCs were counted using a haemocytometer and  $1 \times 10^6$  PBMCs placed into each of 4 tubes. These tubes were an unstained tube, an isotype control tube, a T cell and B cell staining tube and a Treg cell staining tube. Antibodies were used according to the manufacturer's instructions to stain the volume of blood or number of cells in each sample (see Appendix 1, section 3 for antibodies used). To each tube, 1  $\mu$ L normal mouse serum was added to prevent non-specific monoclonal antibody (mAb) binding. The samples were incubated at room temperature for 15 minutes. The T and B cell tube contained markers against CD3, CD4, CD8, CD19, CD45, CD25 and CD69 whilst the Treg tube contained markers against CD3, CD4, CD25, CD127, CD69 and Foxp3. Isotype controls were added to a separate tube to allow removal of non-specific binding when analysing data. An amine reactive live / dead viability dye was added to both staining tubes to use as a dead cell exclusion marker. The samples were incubated for 30 minutes at 4°C and washed in 1 mL PBS (300 x *g*, 5 minutes and 4°C).

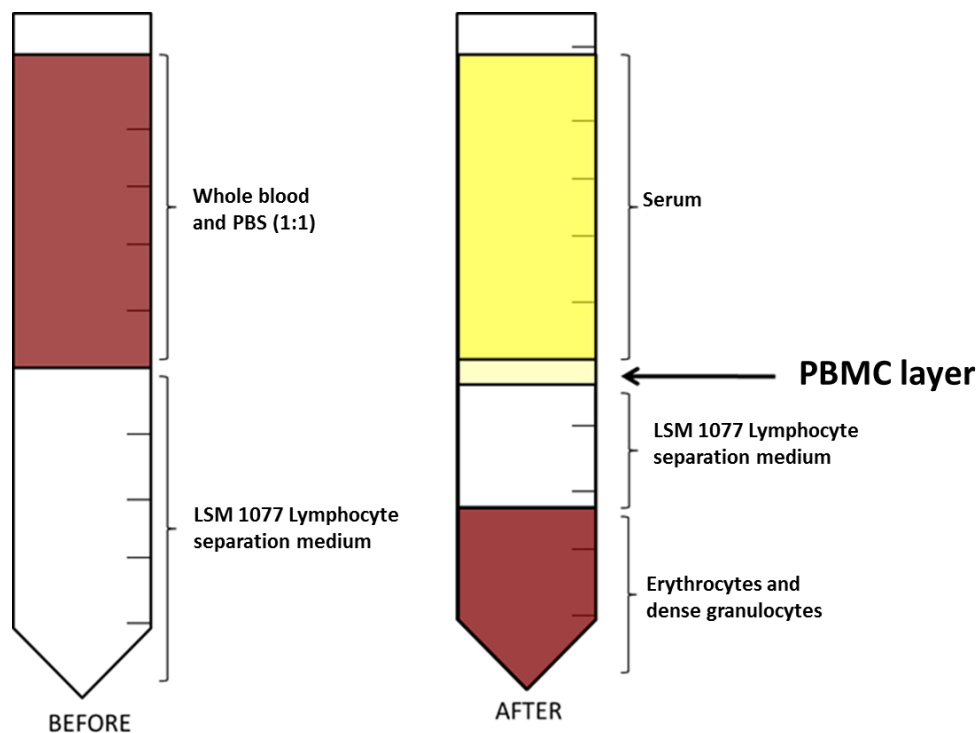


**Figure 2.1 Isolation of PBMCs from whole blood.**

*An illustration of the different layers before and after density gradient centrifugation using LSM 1077 Lymphocyte. Before centrifugation, the whole blood was added to an equal volume of PBS and gently placed on top of an equal volume of LSM 1077 Lymphocyte separation medium. After centrifugation, peripheral blood mononuclear cell (PBMC) collect at the interface between separated serum and LSM 1077 lymphocyte solution. Erythrocytes and dense granulocytes collect at the bottom of the tube. PBMCs can then be removed, washed and fluorescently conjugated antibodies used to detect different lymphocyte subsets.*

Intracellular Foxp3 staining was undertaken after staining for extracellular markers. The Foxp3 Fixation/Permeabilization Concentrate and Diluent kit from eBioscience were used. In brief, cells were incubated for 60 minutes at 4°C in the dark with freshly prepared fixation / permeabilization working solution. The cells were washed in 1 mL permeabilization buffer (300 x g, 5 minutes and 4°C) and 20 µL of anti-Foxp3 antibody added for 30 minutes, at 4°C in the dark. This was washed again before the cells were resuspended in 150 µL permeabilization buffer. Cells in all tubes were fixed

by adding 150  $\mu$ L 1X CELLFix™ and stored in the dark at 4°C to allow analysis the next day.

Lymphocytes were identified on the basis of their size and granularity, as represented by forward and side light scatter characteristics (FSC vs SSC respectively) and their expression of CD45. Multiparametric flow cytometry was performed on all samples using a BD™ LSRII flow cytometer (355 nm UV laser, 405 nm violet laser, 488 nm blue laser and a 633 nm red laser). All data were analysed using BD Biosciences FACSDIVA™ acquisition and data analysis software using the gating hierarchy and scatter plots / histograms shown in Figure 2.2 and Figure 2.3. Data on a minimum of 10,000 CD3<sup>+</sup> events (cells) in the lymphocyte gate were collected.

CD45 (a protein tyrosine phosphatase located in all leukocytes except erythrocytes and platelets) was used to distinguish lymphocytes and also to determine the proportion of B and T cells. To assess the number of B cells within the peripheral blood sample, CD19 (a marker of B cells) was used to distinguish B cells from T cells. T cell subsets were determined according to the expression of CD3 (part of the T cell receptor), CD4 (a glycoprotein expressed on the surface of T helper cells, monocytes, macrophages, and dendritic cells) or CD8 (a glycoprotein that serves as a co-receptor for the T cell receptor). Activated lymphocyte subsets were identified using the early activation marker, CD69.

As previously mentioned in Chapter 1.2, T regulatory cells (Treg cells) are important in balancing Th1 and Th2 responses, maintaining self-tolerance, and controlling autoimmunity.

The relative frequency of Treg cells ( $CD4^+CD25^{high}$ ,  $CD4^+CD25^{high}CD127^{low}$ ,  $CD4^+CD25^{high}Foxp3^+$  and  $CD4^+CD25^{high}CD127^{low}Foxp3^+$ ) were distinguished using markers against CD25 (the alpha chain of the IL-2 receptor), CD127 (interleukin-7 receptor- $\alpha$  chain) and Foxp3 (member of the forkhead box family of transcription factors). CD4 and CD25 are thought to identify Treg cells, however these cells could also include a subset of T cells that do not possess regulatory functions, as CD25 is also a T cell activation marker and can be expressed on T effector cells (Caruso *et al*, 1997). Therefore a combination of markers

including CD127 and Foxp3, as well as CD25, has been suggested to be a more robust method of identifying Treg cells (Banham *et al*, 2006; Su *et al*, 2012; Yu *et al*, 2012). CD127 has been shown to inversely correlate with Foxp3 expression in Treg cells and Foxp3 is thought to be involved in Treg cell function (mentioned previously in Chapter 1.2) (Banham, 2006; Liu *et al*, 2006; Hartigan-O'Connor *et al*, 2007). Current literature regarding markers used to identify and define Treg cells is conflicting; therefore, this study investigated the use of different combinations of mAbs for the identification of Treg cells.

To ensure the integrity of the experimental data and to correctly interpret multicolour flow cytometry data, it was necessary to employ a mechanism called colour compensation to take into account the inherent overlap of emission spectra from different fluorescent fluorophores. Each fluorescently conjugated mAb was incubated with anti-mouse IgG-coated compensation beads and the UV live dead stain incubated with ArC™ reactive beads. These were used to establish the degree of spectral overlap and compensate for it in analysis. FACSDIVA™ software was used to automatically calculate compensation using the fluorescent emission of mAb stained beads. This removed the spectral overlap which is caused by fluorescent emission of one fluorochrome “leaking” into the detection channel of another fluorochrome.

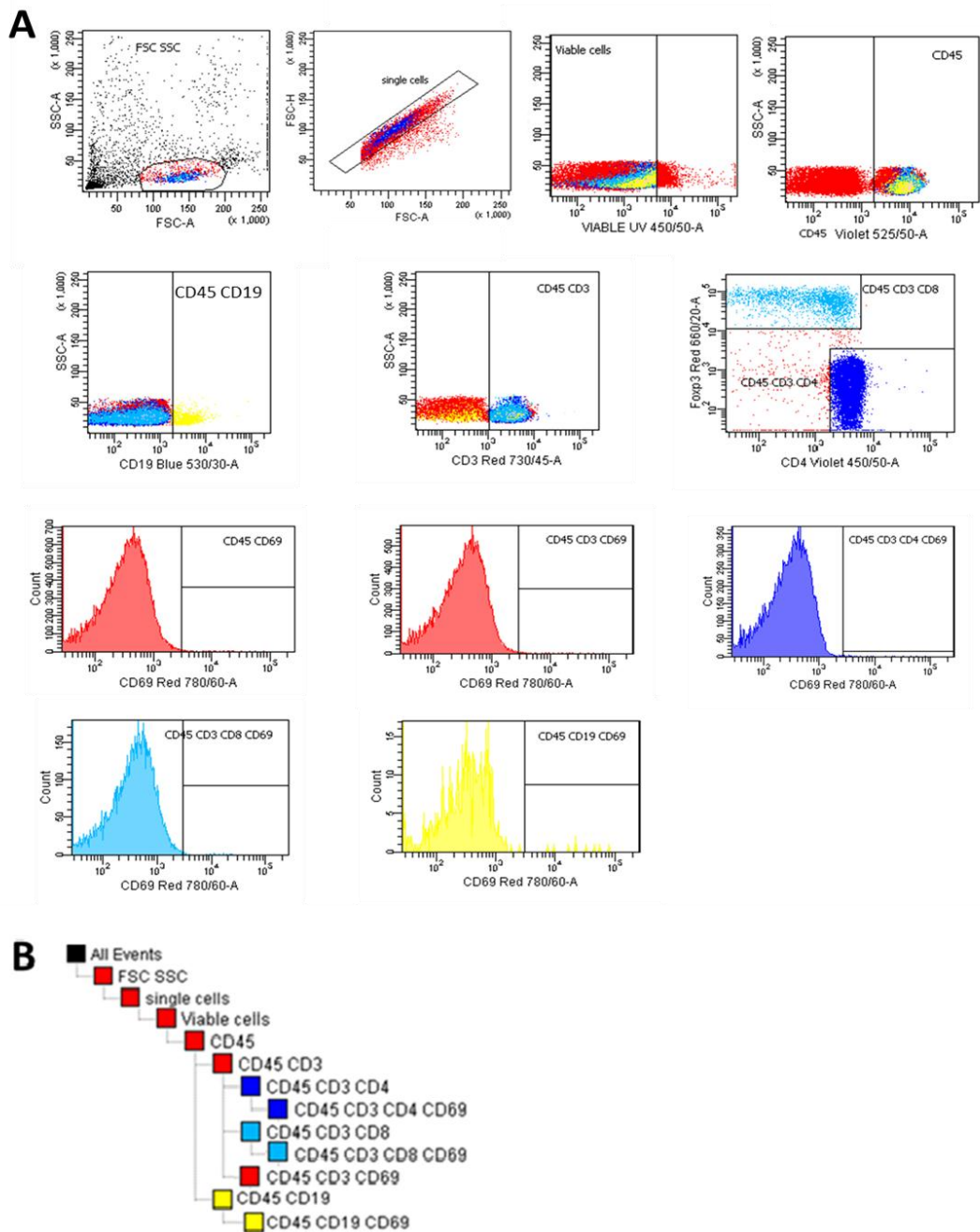


**Figure 2.2 Representative gating hierarchy template and acquisition plots used to define different lymphocyte subsets.**

A) Example dot plots and histograms depicting each gate in the gating hierarchy for T and B cells. B) The gating hierarchy used to distinguish T and B cell subsets as well as their activation status (CD69). Forward Scatter (FSC) and Side Scatter (SSC) were used to gate on the lymphocyte population before single cells and viable cells were selected for analysis. Laser detectors and marker are shown on  $x$  axis and count or SSC are shown on the  $y$  axis. Activation data are presented as a histogram whilst all other data are shown as scatter plots.

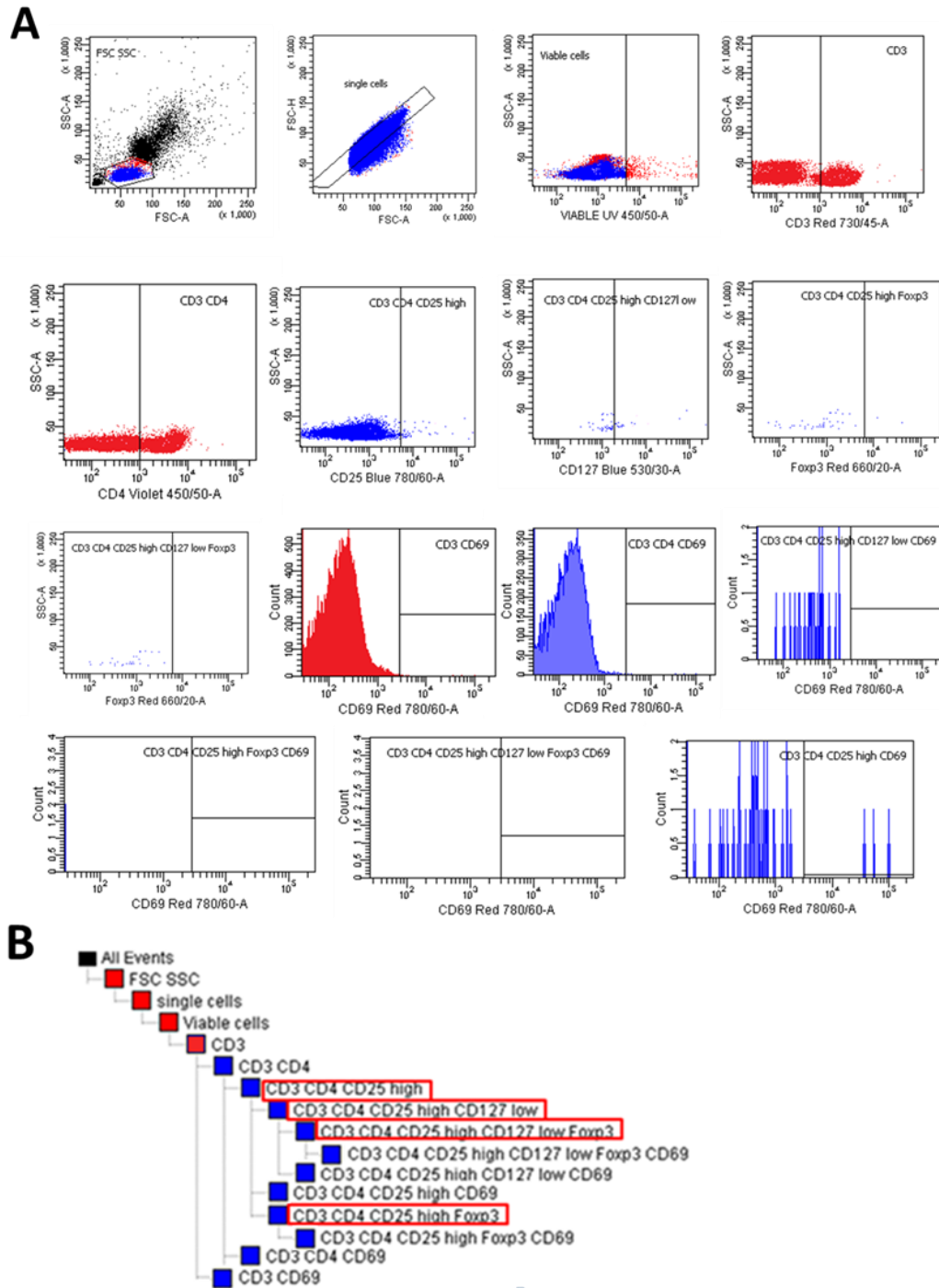


**Figure 2.3 Representative gating hierarchy template and acquisition plots used to define Treg cells.**

A) Example dot plots and histograms depicting each gate in the gating hierarchy for Treg cells. B) The gating hierarchy used to distinguish Treg cells and activation status (CD69). Forward Scatter (FSC) and Side Scatter (SSC) were used to gate on the lymphocyte population before single cells and viable cells were selected for analysis. Laser detectors and marker are shown on  $x$  axis and count or SSC are shown on the  $y$  axis. Activation data are presented as a histogram whilst all other data are shown as scatter plots.

### 2.2.3 Treg functional studies

A crucial component of our ability to resolve inflammatory responses involves the activation and activity of Treg cells. These cells have been shown to have a decreased suppressive function in inflammatory and autoimmune diseases such as multiple sclerosis and SSc, which explains how uncontrollable inflammatory processes dominate within these diseases (Venken *et al*, 2008; Radstake *et al*, 2009). Studies on suppressive capabilities of Treg cells from IPAH patients have revealed no differences between patients and controls, despite the increase in the proportion of Treg cells within the peripheral circulation (Ulrich *et al*, 2008).

Therefore this work aimed to define the suppressive capabilities of Treg cells from treatment naïve IPAH and SSc-PAH patients with regards to their ability to suppress the proliferation of T effector cells (also known as T responder cells). I hypothesised that despite being increased in number, these cells would show a decreased ability to regulate T effector cell proliferation, based on previously published literature in similar disease states (Radstake *et al*, 2009).

H<sup>3</sup>-thymidine (PerkinElmer, Buckinghamshire, UK) incorporation and CellTrace™ Violet (Invitrogen of Life Technologies Ltd, Paisley UK) incorporation were used to assess the capacity of Treg cells to suppress the proliferation of polyclonally activated T responder (Tresp) cells. Several commercial kits were available to isolate Treg cells (which also isolate T responder cells) and have been tested here to assess purity of isolated cells. As previously described, there are several cell surface markers which can be used to identify and isolate Treg cells, including CD127 and CD25 in immature Treg cells. Two commercially available Treg isolation kits were tested from STEMCELL technologies (STEMCELL Technologies, Grenoble, France) and Miltenyi Biotec (Miltenyi Biotec Ltd, Surrey, UK) to isolate Treg cells based on CD4<sup>+</sup> and CD25<sup>high</sup> expression (EasySep® Mouse CD4<sup>+</sup>CD25<sup>+</sup> Regulatory T Cell Isolation Kit and CD4<sup>+</sup>CD25<sup>+</sup> Regulatory T Cell Isolation Kit respectively). CD4<sup>+</sup>CD25<sup>+</sup>CD127<sup>dim/-</sup> Treg cell isolation was also undertaken using the CD4<sup>+</sup>CD25<sup>+</sup>CD127<sup>dim/-</sup> Regulatory T Cells Isolation Kit II from Miltenyi Biotec and the Complete Kit for Human

CD4<sup>+</sup>CD127<sup>low</sup>CD25<sup>+</sup> Regulatory T Cells from STEMCELL Technologies. The protocols for these separation techniques are described below.

### **2.2.3.1 EasySep® Mouse CD4<sup>+</sup>CD25<sup>+</sup> Regulatory T Cell Isolation Kit**

After informed consent was provided, 50 mL of whole blood was taken from healthy volunteers into BD Vacutainer® Blood Collection Tube using a 21 gauge needle. To isolate CD4<sup>+</sup> T cells from whole blood, 2.5 mL of RosetteSep® Human CD4<sup>+</sup> T cell Enrichment Cocktail (STEMCELL Technologies, Grenoble, France) was added to whole blood and incubated at room temperature for 20 minutes. The sample was diluted with an equal volume of PBS + 2% v/v foetal calf serum (FCS, 52.5 mL) and mixed gently. The diluted sample was layered over 15 mL density medium (RosetteSep® DM-L) and centrifuged at 1200 x g at room temperature for 20 minutes with the brake off. The enriched cells were removed from the density medium:plasma interface and washed twice in PBS + 2% v/v FCS. This involved adding 10 mL PBS + 2% FCS centrifuging at 1200 x g for 5 minutes at room temperature and aspirating the supernatant.

After isolating CD4<sup>+</sup> T cells, it was possible to isolate CD25<sup>+</sup> T cells using the human CD25 positive selection kit. CD25 positive T cell isolation was undertaken by transferring 500 µL of the pre-enriched CD4<sup>+</sup> T cells into a 5 mL polystyrene tube. 25 µL EasySep® positive selection cocktail was added to the cell suspension, mixed well and incubated at room temperature for 15 minutes. The EasySep® Magnetic Nanoparticles were resuspended and 25 µL added to the cells. This was mixed well and incubated at room temperature for 10 minutes. The cell suspension was brought to a total volume of 2.5 mL by adding Memorial Institute medium 1640 (RPMI) (Sigma Aldrich, Dorset, UK) with 2% v/v FCS and left to stand for 5 minutes. The cells were mixed thoroughly and the tube placed into "The Big Easy" EasySep® Magnet. The magnet was picked up and in one continuous movement, the tube and magnet inverted to pour off the supernatant fraction. The magnetically labelled cells remained inside the tube, held by the

magnetic field. The magnet and tube were returned to the upright position and the tube removed. 2.5 mL RPMI medium + 2% v/v FCS was added to the cells and mixed well. The tube was placed back into the magnet, left to rest for 5 minutes and the supernatant poured off again. This process was repeated twice more for a total of four 5-minute separations.

The advantages of using the STEMCELL kits are that it is possible to save time by isolating cells directly from whole blood, rather than undertaking a PBMC preparation before isolating T cells. Also, the STEMCELL kits use magnets rather than columns to isolate the cells and there are also less wash steps involved, which decreases the amount of time it takes to isolate the Treg cells.

### **2.2.3.2 CD4<sup>+</sup>CD25<sup>+</sup> Regulatory T cell Isolation Kit**

After informed consent was provided, 50 mL of whole blood was taken from healthy volunteers into BD Vacutainer® Blood Collection Tubes using a 21 gauge needle. To isolate CD4<sup>+</sup>CD25<sup>+</sup> Treg cells from whole blood using the Miltenyi Biotec CD4<sup>+</sup>CD25<sup>+</sup> Regulatory T Cell Isolation Kit, the PMBCs had to firstly be isolated (Chapter 2.2.2.1). The PMBCs were counted using a haemocytometer, centrifuged at 300 x g for 10 minutes and the supernatant removed. The cells were resuspended in RPMI medium + 2% v/v FCS to get a 2.5x10<sup>7</sup> / mL suspension. 10 µL of CD4<sup>+</sup> T Cell Biotin-Antibody Cocktail was added per 1x10<sup>7</sup> total cells. This was mixed well and incubated at 4°C for 10 minutes. 20 µL Anti-Biotin MicroBeads were added per 1x10<sup>7</sup> total cells. This was mixed well and incubated for 15 minutes at 4°C. The cells were washed in 1.5 mL per 1x10<sup>7</sup> total cells by centrifugation for 10 minutes at 300 x g. The supernatant was then removed and the cells resuspended in 500 µL buffer.

To deplete the non-CD4<sup>+</sup> cells, an LD column was prepared by rinsing with 2 mL PBS + 2% FCS and placed in the magnetic field of a MACS separator before the cell suspension was added. The unlabelled cells (CD4<sup>+</sup> T cells) were passed through the column and the column was then washed again with 2 mL buffer and the unlabelled cells collected. The cell

suspension was centrifuged for 10 minutes at 300 x g, before the supernatant was removed and the cell pellet resuspended in 90 µL of PBS + 2% v/v FCS. 10 µL CD25 Microbeads were then added to the cell suspension (scaled up accordingly if more than  $1 \times 10^7$  total cells were used) and left to incubate for 15 minutes in the dark at 4°C. 1.5 mL of PBS + 2% v/v FCS was added to the cells, before they were centrifuged at 300 x g for 10 minutes to wash them. The CD4<sup>+</sup>CD25<sup>+</sup> Treg cells were positively selected by applying the cell suspension to a pre-prepared MS column. The column was placed in the magnetic field of a MACS separator and was prepared by adding 500 µL PBS + 2% v/v FCS before the cell suspension was applied. The flow through was collected (CD4<sup>+</sup> Tresp cells) and the column washed 3 times with 500 µL PBS + 2% v/v FCS. The column was removed from the separator, and placed in a collection tube before 1 mL PBS + 2% v/v FCS was then pipetted onto the column and the column immediately flushed out using the plunger to collect the magnetically labelled cells (CD4<sup>+</sup>CD25<sup>+</sup> Treg cells). This step was repeated twice more to increase the purity of the Treg population.

### **2.2.3.3 CD4<sup>+</sup>CD25<sup>+</sup>CD127<sup>dim/-</sup> Regulatory T Cells Isolation Kit II**

The isolation of CD4<sup>+</sup>CD25<sup>+</sup>CD127<sup>dim/-</sup> Treg cells from whole blood using the Miltenyi Biotec CD4<sup>+</sup>CD25<sup>+</sup> Regulatory T Cell Isolation Kit employs the same basic technique as previously described in the CD4<sup>+</sup>CD25<sup>+</sup> Regulatory T Cell Isolation kit from Miltenyi Biotec, however for the depletion of non-CD4<sup>+</sup> cells a different cocktail of biotin conjugated antibodies is used. The resultant Treg cell population is CD4<sup>+</sup>CD25<sup>+</sup>CD127<sup>dim/-</sup> rather than CD4<sup>+</sup>CD25<sup>+</sup>.

#### **2.2.3.4 Complete Kit for Human CD4<sup>+</sup>CD127<sup>low</sup>CD25<sup>+</sup> Regulatory T Cells**

The isolation of CD4<sup>+</sup>CD25<sup>+</sup>CD127<sup>low</sup> Treg cells was undertaken in the same manner that CD4<sup>+</sup>CD25<sup>+</sup> Treg cells were isolated using the EasySep® Mouse CD4<sup>+</sup>CD25<sup>+</sup> Regulatory T Cell Isolation Kit from STEMCELL Technologies, however instead of using the RosetteSep® Human CD4<sup>+</sup> T cell enrichment cocktail, the RosetteSep® Human CD4<sup>+</sup>CD127<sup>low</sup> Regulatory T Cell Pre-enrichment cocktail was added.

#### **2.2.3.5 Assessment of purity of T regulatory and T responder cell populations**

The purity of the Tresp and Treg cell populations isolated using the above approaches was measured using flow cytometry to determine which kit would be most reliable when setting up the Treg suppression assay. Purity of Treg cell populations (CD4<sup>+</sup>CD25<sup>high</sup>) was calculated as a percentage of the parent CD4<sup>+</sup> T cell population. Purity of Tresp cells (CD4<sup>+</sup>CD25<sup>-</sup>) was also assessed as a percentage of the parent CD4<sup>+</sup> T cell population. Purity of Tresp cells isolated in each kit was < 95% which meant that either kit could be used to isolate this T cell subset. However, Treg cell purity differed between the kits. The Miltenyi Biotec CD4<sup>+</sup>CD25<sup>+</sup> Treg cell isolation kit provided a 64% pure Treg cell population, whereas the CD4<sup>+</sup>CD25<sup>+</sup>CD127<sup>-</sup> Treg cell isolation kit from Miltenyi Biotec produced a 76.4% pure Treg cell population. The STEMCELL Technologies CD4<sup>+</sup>CD25<sup>+</sup> Treg isolation kit gave a 77% pure Treg cell population, whilst the CD4<sup>+</sup>CD25<sup>+</sup>CD127<sup>-</sup> Treg cell isolation kit from STEMCELL Technologies provided a Treg cell population that was 90% pure. Therefore the STEMCELL kit was used to isolate Tresp and Treg cells for subsequent Treg suppression assays.

### 2.2.3.6 Treg cell suppression assays

Treg cell function was assessed via the ability of this population to inhibit the proliferative responses of Tresp cells to a polyclonal stimulus (Treg suppression inspector beads). These beads (anti-biotin MACSiBead particles coated with biotinylated CD2, CD3, and CD28 antibodies) were added to co-cultures of different ratios of Tresp and Treg cells to induce Tresp cell proliferation. In culture, Tregs alone are hypoproliferative (anergic) whereas Tresp cells alone show a proliferative response, which can be measured.

The Treg suppression assay was set up using 50 mL peripheral blood taken from healthy volunteers. The STEMCELL Technologies CD4<sup>+</sup>CD127<sup>low</sup>CD25<sup>+</sup> Treg isolation kit was used to isolate Treg cells and Tresp cells to perform this assay, as this proved to produce the purest populations of Tresp and Treg cells. Treg cells and Tresp cells were isolated, as previously described, under sterile conditions. The number of both Treg cells and Tresp cells was determined to ensure there were enough to run the assay ( $9 \times 10^5$  Tresp cells and  $6 \times 10^5$  Treg cells needed to run assay in triplicate). Cell suspensions were washed and resuspended in RPMI with 2% v/v FCS at  $5 \times 10^5$  cells / mL. The appropriate volumes of both Tresp and Treg cells and Treg suppression inspector beads were transferred to a 96 well culture plate (Table 2.1).

The wells were filled to a total volume of 210  $\mu$ L with RPMI + 2% v/v FCS before incubating the plate at 37°C and 5–7% v/v CO<sub>2</sub> for 4 – 5 days. To measure proliferation using H<sup>3</sup>-thymidine, 1 $\mu$ Ci of H<sup>3</sup>-thymidine was added to each well and incubated at the same conditions described previously, for a further 16 hours. The cells were washed and harvested using a cell harvester (Skatron instruments, Suffolk, UK). H<sup>3</sup>-thymidine incorporation was measured for 10 minutes using a scintillation counter (Beckman coulter, High Wycombe, UK). H<sup>3</sup>-thymidine is incorporated into new strands of DNA during mitotic cell division, and the radioactivity of the sample is measured using a scintillation counter. Only proliferating cells incorporate H<sup>3</sup>-thymidine, so this method measures DNA synthesis and can be used to quantify proliferation rates.

Ratio Tresp cells: Treg cells	Tresp cells ( $5 \times 10^5$ cells / mL)	Treg cells ( $5 \times 10^5$ cells / mL)	Treg Suppression Inspector ( $1 \times 10^7$ MACSiBead particles / mL)	Culture medium (RPMI + 2% v/v FCS)
1:0	100 $\mu$ L	-	5 $\mu$ L	105 $\mu$ L
0:1	-	100 $\mu$ L	5 $\mu$ L	105 $\mu$ L
1:1	100 $\mu$ L	100 $\mu$ L	10 $\mu$ L	-
2:1	100 $\mu$ L	50 $\mu$ L	7.5 $\mu$ L	53 $\mu$ L
4:1	100 $\mu$ L	25 $\mu$ L	6.5 $\mu$ L	79 $\mu$ L
8:1	100 $\mu$ L	12.5 $\mu$ L	6.0 $\mu$ L	92 $\mu$ L
Control 1:0	100 $\mu$ L	-	-	110 $\mu$ L
Control 0:1	-	100 $\mu$ L	-	110 $\mu$ L

Total Volume	600 $\mu$ L	387.5 $\mu$ L	40 $\mu$ L	654 $\mu$ L
Total volume for 1 assay (triplicates)	1800 $\mu$ L	1200 $\mu$ L	120 $\mu$ L	2 mL

**Table 2.1 Pipetting scheme for Treg suppression assay**

*Treg and Tresp cells were co-cultured in different ratios (column 1) with or without Treg suppression inspector beads to provide a polyclonal stimulus for Tresp cell proliferation (column 4). Culture medium was also added before incubation (column 5). Total volumes for all components and for an assay in triplicate are shown in grey boxes. Data is kindly reproduced with permission of Miltenyi Biotec (Miltenyi Biotec Ltd, Surrey, UK).*

CellTrace™ Violet (Invitrogen of Life Technologies Ltd, Paisley, UK) was also used to detect Treg cell suppressive capabilities. CellTrace™ Violet diffuses into cells (in this case, T responder cells) and is cleaved by intracellular esterases creating a fluorescent compound which can bind to intracellular amines producing a fluorescent signal. Treg cell function can be determined by the ability of these cells to suppress the proliferation of Tresp cells, as measured on the basis of a decline in the fluorescence of proliferating cells. CellTrace™ Violet was prepared according to the manufacturer's instructions (see Appendix 1, section 1) and incubated with Tresp cells for 20 minutes, at 37°C and protected from light. Unbound dye was then quenched, before the cells were added to the 96 well culture plate,

as previously described in the Treg suppression assay. Proliferation was assessed using flow cytometry (LSRII flow cytometer, violet 450 / 50 nm filter), with each violet peak representing a successive generation of Tresp cells proliferating in response to the Treg suppression inspector beads. Cells that were not proliferating remained to the right of the histogram at the brightest violet peak. With each cell division the intensity of the signal was reduced and the mean fluorescent index decreased.

Numerous problems were encountered in performing this assay including an insufficient number of isolated Treg cells, proliferation of control populations and low purity of isolated Treg cell populations. Other groups have also noted problems in conducting Treg cell suppression assays due to small numbers of isolated Treg cells, suggesting that this is a major drawback of studying regulatory activity of Treg cells *in vitro* (Smolders *et al*, 2009). If patient consent could be gained for a larger volume of blood to be donated (150 - 200 mL), a higher number of Treg cells could be isolated and the assay performed in triplicate to produce more reliable results. Purity of the isolated Treg cell population was also an issue as only a 90% pure population could be obtained. This meant that Tresp cells could be found within the Treg cell population, which could have affected the results of the assay. If a larger volume of blood can be used in future experiments, Treg and Tresp cells could be obtained via fluorescence activated cell sorting rather than via the methods used here. For cell sorting, several antibodies can be used to detect Treg cells (CD4, CD25 and CD127) and the resulting populations would be of a higher purity level.

The functionality of Treg cells could be assessed using other methods including measuring the release of mediators (IL-10 and TGF- $\beta$ ) and measuring activation of cells themselves, via the expression of activation markers such as CD69 (Lindsey *et al*, 2007). These methods, such as ELISPOT and flow cytometry, can provide an alternative way of quantifying Treg cell function. To measure proliferative responses of T responder cells to different ratios of Treg cell, other methods could be used such as flow cytometry to stain for T cell specific markers (CD4 and CD25) and the use of counting beads to determine exact cell numbers. However, this would require a larger volume of peripheral blood to isolate Tresp and Treg cells, a factor

which has limited some studies mentioned in this thesis. Other stimulatory methods could also be tested and used to conduct the proliferation assay, including concanavalin A (conA), or phytohaemagglutinin (PHA) stimulation (Trickett and Kwan, 2003).

## **2.2.4 Statistical Analysis**

Proportional cell data were expressed as box and whisker plots showing minimum and maximum values. GraphPad Prism version 5.00 for Windows (GraphPad Software, San Diego, California USA, [www.graphpad.com](http://www.graphpad.com)) was used for statistical analysis. To account for any non-normal data distributions, and for consistency of analysis, statistical significance was evaluated using nonparametric statistical techniques. Differences between two groups were compared using a two-tailed, Mann-Whitney test whilst differences between multiple groups were compared using a Kruskal-Wallis test using Dunn's post hoc test to compare all pairs of data. Both tests had 95% confidence intervals. A P value < 0.05 was considered statistically significant in all tests.

## **2.3 Results**

### **2.3.1 Patient demographics**

A total of 28 PAH patients were recruited and included in these studies including 13 SSc-PAH and 15 IPAH patients. The mean age of SSc-PAH patients was 66 years whilst for IPAH patients it was 58 years. This compared to a mean age of 60 in the healthy control group and 62 in the SSc-no PAH control group. Of the 13 SSc-PAH patients recruited, 8 were female whilst for the 15 IPAH patients, 9 were female. There was also a bias towards limited SSc-PAH patients compared to diffuse cutaneous SSc-PAH patients. Clinical parameters were assessed in patient groups at visit 1 to

confirm PAH diagnosis. The full patient demographics are described in Table 2.2.

There was a significantly higher mPAP in IPAH patients compared to SSc-PAH patients ( $55.86 \pm 12.31$  mmHg vs  $37.40 \pm 14.52$  mmHg,  $n=13-15$ ,  $P=0.007$ ). There was also a higher pulmonary vascular resistance (PVR) in IPAH patients compared to SSc-PAH patients ( $847.60 \pm 366.80$  dynes/cm<sup>5</sup> vs  $492.00 \pm 436.90$  dynes/cm<sup>5</sup>,  $n=13-15$ ,  $P=0.02$ ). There was no significant difference in Cardiac Output (CO) or Cardiac Index (CI) between the groups.

The SSc-PAH patients showed a significantly lower forced expiratory volume compared to IPAH patients ( $1.10 \pm 1.06$  vs  $2.12 \pm 0.69$ ,  $n=13-15$ ,  $P=0.03$ ), whilst FEV1 / FVC ratio did not significantly change between the two PAH patient groups. There was also no significant difference in shuttle walk test between groups. The shuttle walk test is a measure of the functional capacity of the patient and requires the patient to walk between two cones to a set of auditory beeps played on a CD with increasing speed. The patient walks for as long as possible until they become too breathless or can no longer keep up with the beeps, at which point their shuttle walk test score is calculated as the number of shuttles between cones (each shuttle represents 10 metres).

	Healthy	SSc-no PAH	SSc-PAH	IPAH	Statistical Analysis
<b>n</b>	15	8	13	15	N/A
<b>Age</b>	60 ± 3	62 ± 8	66 ± 8	58 ± 16	N/S
<b>Sex</b>	8F 6M	7F 1M	8F 5M	9F 6M	N/A
<b>Phenotype</b>	N/A	7 ltd,1 diff	12 ltd, 1 diff	N/A	N/A
<b>mPAP (mmHg)</b>	N/A	N/A	37.40 ± 14.52	55.86 ± 2.31	**
<b>CO (L/min)</b>	N/A	N/A	5.65 ± 1.79	4.55 ± 1.54	N/S
<b>PVR (dynes/cm<sup>5</sup>)</b>	N/A	N/A	492.00 ± 436.90	847.60 ± 366.80	*
<b>FEV1 actual (L)</b>	N/A	N/A	1.10 ± 1.06	2.12 ± 0.69	*
<b>FEV1 / FVC actual</b>	N/A	N/A	0.43 ± 0.39	0.68 ± 0.09	N/S
<b>Shuttle walk test (m)</b>	N/A	N/A	238.00 ± 173.30	192.70 ± 156.10	N/S
<b>CI</b>	N/A	N/A	2.85 ± 0.78	2.63 ± 0.78	N/S
<b>HR (bpm)</b>	N/A	N/A	76.56 ± 13.57	79.67 ± 18.21	N/S

**Table 2.2 Pulmonary arterial hypertension patient demographics.**

*n* number (*n*), age, sex, phenotype of disease, mean pulmonary artery pressure (mPAP) measured in millimetre of mercury (mmHg), cardiac output (CO) measured in litres per minute (L/min), pulmonary vascular resistance (PVR) measured in dynes/cm<sup>5</sup>, forced expiratory volume in one second (FEV1) measured in litres (L), forced vital capacity (FVC), shuttle walk test, cardiac index (CI) and heart rate (HR) measured in beats per minute (bpm) are shown for healthy, SSc-no PAH controls and IPAH and SSc-PAH patients. Male (M) and female (F) participants as well as the phenotype of their disease, limited (ltd) or diffuse cutaneous (diff) are shown. Data depicted as mean ± SD. Patient groups compared using a two tailed Mann Whitney test whilst patient and control groups were compared using a Kruskal Wallis Test with Dunn's post hoc test. A 95% confidence interval was used where  $P < 0.05$  is considered significant (\*). Not applicable (N/A) applied where statistical analysis was not undertaken and N/S where statistical analyses were not significant.

## **2.3.2 T cell subsets in patient and control peripheral blood samples**

To determine lymphocyte subpopulations within the circulation, lymphocytes were isolated from peripheral blood, analysed using flow cytometry and T and B cell subgroups detected. Patients with IPAH and SSc-PAH, as well as healthy controls and SSc alone without evidence of PAH, were enrolled on the study. Changes in proportions of different T cell subsets were determined in each study group after gating around the total lymphocyte population and collecting 10,000 CD3<sup>+</sup> T cell events. Proportions of CD4<sup>+</sup> T cells, CD8<sup>+</sup> T cells and a CD4:CD8 T cell ratio, a numerical value used clinically, were calculated for each study group.

### **2.3.2.1 CD4<sup>+</sup> T cell subset**

There was no change in the proportion of circulating CD4<sup>+</sup> T cells (as a percentage of total CD3<sup>+</sup> T cells) in the peripheral blood of PAH patient groups when compared to both control groups (Figure 2.4, A). To determine if there was a change in the proportion of CD4<sup>+</sup> T cells in the individual patient groups, the group was split into IPAH and SSc-PAH patients and compared to their relevant controls (Figure 2.4, B and C). There was however, still no difference in the proportion of CD4<sup>+</sup> T cells between groups.

There was also no change in total lymphocyte counts in whole blood, as noted from clinical data in either IPAH or SSc-PAH patients when compared to control samples.

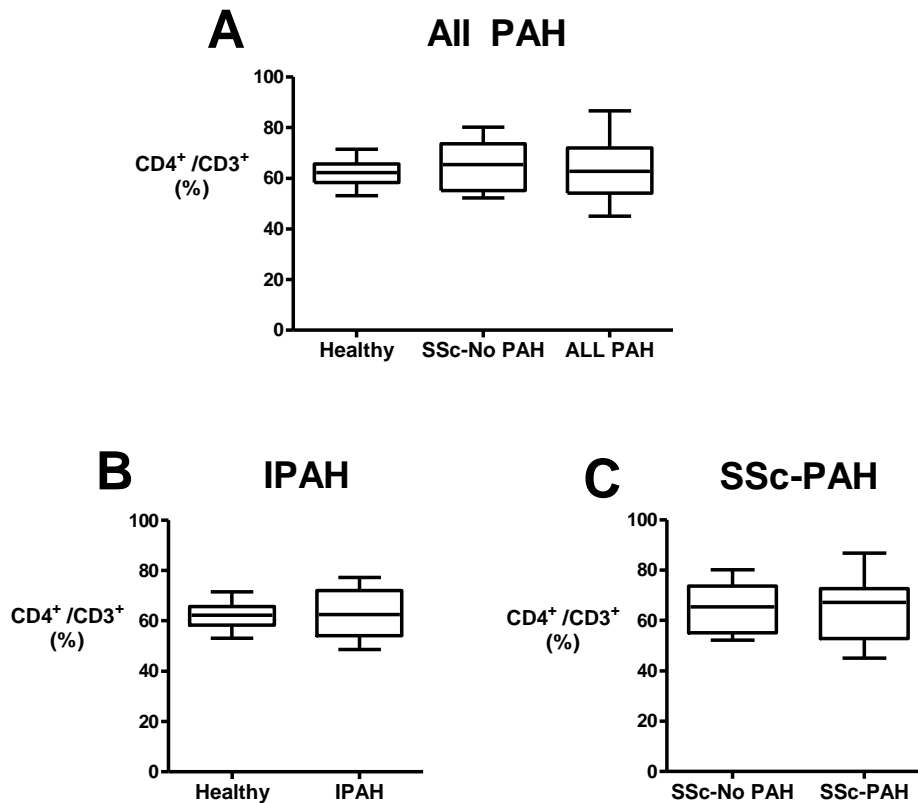


**Figure 2.4 Proportions of CD4<sup>+</sup> helper T cells in peripheral blood of PAH patients and controls.**

A) CD4<sup>+</sup> T cells in all PAH patients. B) CD4<sup>+</sup> T cells in healthy controls and IPAH patients. C) CD4<sup>+</sup> T cells in Scleroderma controls (SSc-no PAH) and SSc-PAH patients. Data are shown as a percentage of total CD3<sup>+</sup> T cells. Data analysed by a Kruskal Wallis Test with Dunn's post hoc test or by a two tailed Mann Whitney test. A 95% confidence interval was used where  $P < 0.05$  is considered significant (\*). All Box and whisker plots depict median with minimum to maximum values in each study group. IPAH patients  $n=15$ , SSc-PAH patients  $n=12$ , healthy controls  $n=15$ , SSc no-PAH controls  $n=8$ .

### 2.3.2.2 CD8<sup>+</sup> T cell subset

Analysis of the proportion of CD8<sup>+</sup> T cells showed a trend for a lower T cell population in the PAH patient population (Figure 2.5, A). To determine if this was common across both groups or specific to IPAH or SSc-PAH the

data were further broken down into these groups only and compared with corresponding controls (Figure 2.5, B and C). In IPAH patients, there was no difference in proportions of CD8<sup>+</sup> T cells, when compared to healthy controls (Figure 2.5, B). However, the proportion of CD8<sup>+</sup> T cells in SSc-PAH patients was significantly lower than in SSc-no PAH controls (18.10 ± 8.14% vs 30.40 ± 9.14%, n=7-12, P=0.009) (Figure 2.5 C).

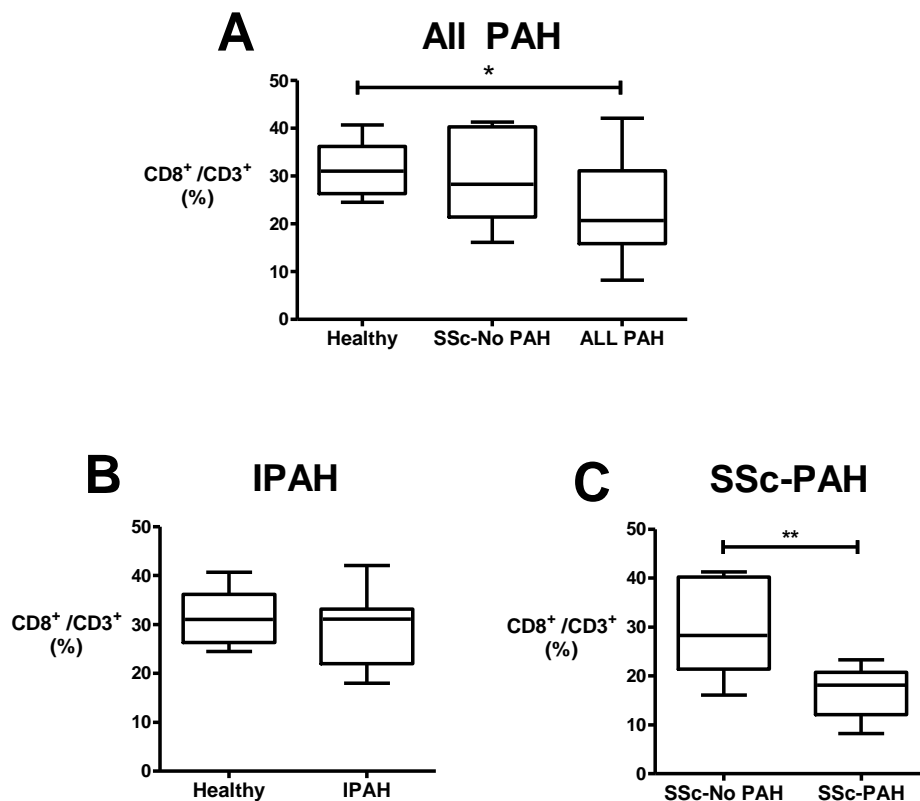


**Figure 2.5 Proportions of CD8<sup>+</sup> cytotoxic T cells in peripheral blood of PAH patients and controls.**

A) CD8<sup>+</sup> T cells in all PAH patients. B) CD8<sup>+</sup> T cells in healthy controls and IPAH patients. C) CD8<sup>+</sup> T cells in scleroderma controls (SSc-no PAH) and SSc-PAH patients. Data are shown as a percentage of total CD3<sup>+</sup> T cells. Data analysed by a Kruskal Wallis Test with Dunn's post hoc test or by a two tailed Mann Whitney test. A 95% confidence interval was used where P < 0.05 (\*) and P < 0.001 (\*\*) are considered significant. All Box and whisker plots depict median with minimum to maximum values in each study group. IPAH patients n=15, SSc-PAH patients n=12, healthy controls n=15, SSc no-PAH controls n=7.

### 2.3.2.3 CD4:CD8 T cell ratio

There was no difference in the CD4:CD8 T cell ratio when all PAH patients were compared to both control groups (Figure 2.6, A). However, due to the decrease in the proportion of CD8<sup>+</sup> T cells, there was a corresponding significantly higher CD4:CD8 ratio in SSc-PAH patients compared to SSc-no PAH controls ( $3.52 \pm 2.28$  vs  $1.90 \pm 1.46$ ,  $n=7-11$ ,  $P=0.018$ ) (Figure 2.6, C). There was no difference in the CD4:CD8 T cell ratio in IPAH patients when compared to healthy controls noted in this study (Figure 2.6, B).

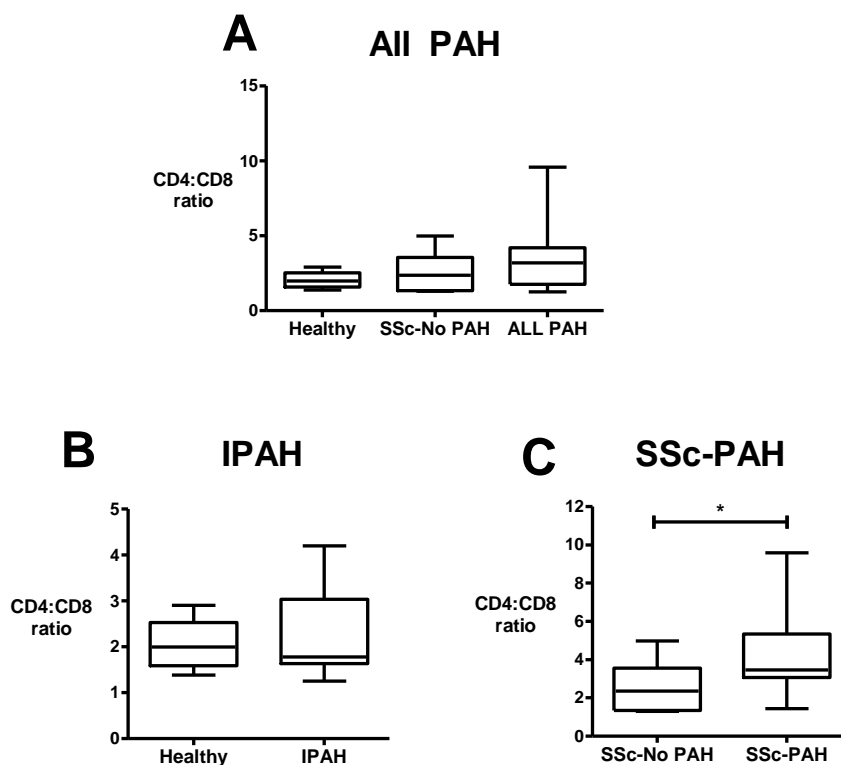


**Figure 2.6 CD4:CD8 T cell ratio in peripheral blood of PAH patients and controls.**

A) CD4:CD8 ratio in all PAH patients. B) CD4:CD8 ratio in healthy controls and IPAH patients. C) CD4:CD8 ratio in scleroderma controls and SSc-PAH patients. Data analysed by a Kruskal Wallis Test with Dunn's post hoc test or by a two tailed Mann Whitney test. A 95% confidence interval was used where  $P < 0.05$  is considered significant (\*). All Box and whisker plots depict median with minimum to maximum values in each study group. IPAH patients  $n=13$ , SSc-PAH patients  $n=11$ , healthy controls  $n=15$ , SSc no-PAH controls  $n=7$ .

### **2.3.3 Activation status of T cell subsets in patient and control peripheral blood samples**

I next sought to determine if there were any changes in lymphocyte activation by examining the expression of CD69, an early activation marker of lymphocytes.

#### **2.3.3.1 Activation status of CD3<sup>+</sup> T cells**

The proportion of activated (CD69<sup>+</sup>) CD3<sup>+</sup> T cells was not significantly different across both control groups and both patient groups (Figure 2.7, A). This was also the case when IPAH patients were compared to healthy controls, and SSc-PAH patients were compared to SSc-no PAH controls (Figure 2.7, B and C). There was a greater degree of variation in the proportion of activated CD3<sup>+</sup> T cells between patients within both the IPAH subgroup (0.004% to 2.5%) and SSc-PAH group (0% to 4.97%), which may have masked changes in these patient subsets. Previous studies have not identified the activation status of circulating T cells within SSc-PAH and IPAH patients, therefore further studies need to be undertaken to give a greater degree of confidence in this work.

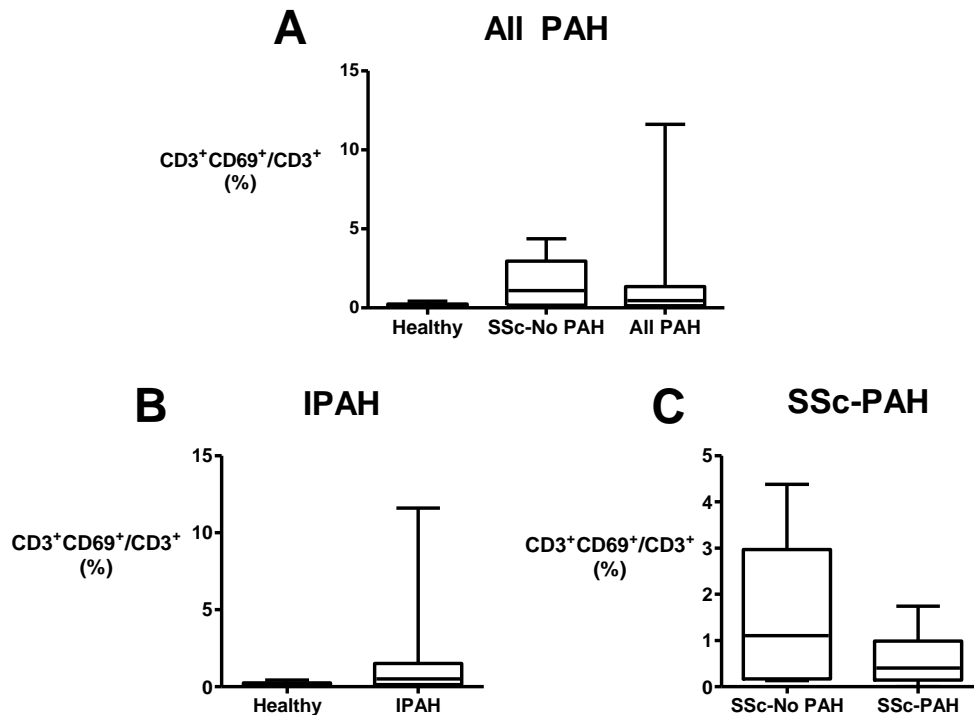


**Figure 2.7 Proportions of activated  $CD3^+$  T cells in peripheral blood of PAH patients and controls.**

A)  $CD3^+CD69^+$  T cells in all PAH patients. B)  $CD3^+CD69^+$  T cells in IPAH patients and healthy controls. C)  $CD3^+CD69^+$  T cells in SSc-no PAH and SSc-PAH patients. All data presented as a proportion of total  $CD3^+$  T cell population. Data analysed by a Kruskal Wallis Test with Dunn's post hoc test or by a two tailed Mann Whitney test. A 95% confidence interval was used where  $P < 0.05$  is considered significant (\*). All Box and whisker plots depict median with minimum to maximum values in each study group. IPAH patients  $n=15$ , SSc-PAH patients  $n=13$ , healthy controls  $n=14$ , SSc no-PAH controls  $n=7$ .

### 2.3.3.2 Activation status of $CD4^+$ T cells

In all PAH patients there was no difference in the proportion of activated  $CD4^+$  T cells in comparison to healthy controls or SSc-no PAH patient controls (Figure 2.8, A). To confirm that one patient group was not masking a change in another group, these data were further split into IPAH and SSc-PAH patient groups and compared to corresponding controls. Again,

there was no difference in the proportion of activated CD4<sup>+</sup> T cells between IPAH patients and healthy controls, or between SSc-PAH patients and SSc-no PAH controls (Figure 2.8, B and C).

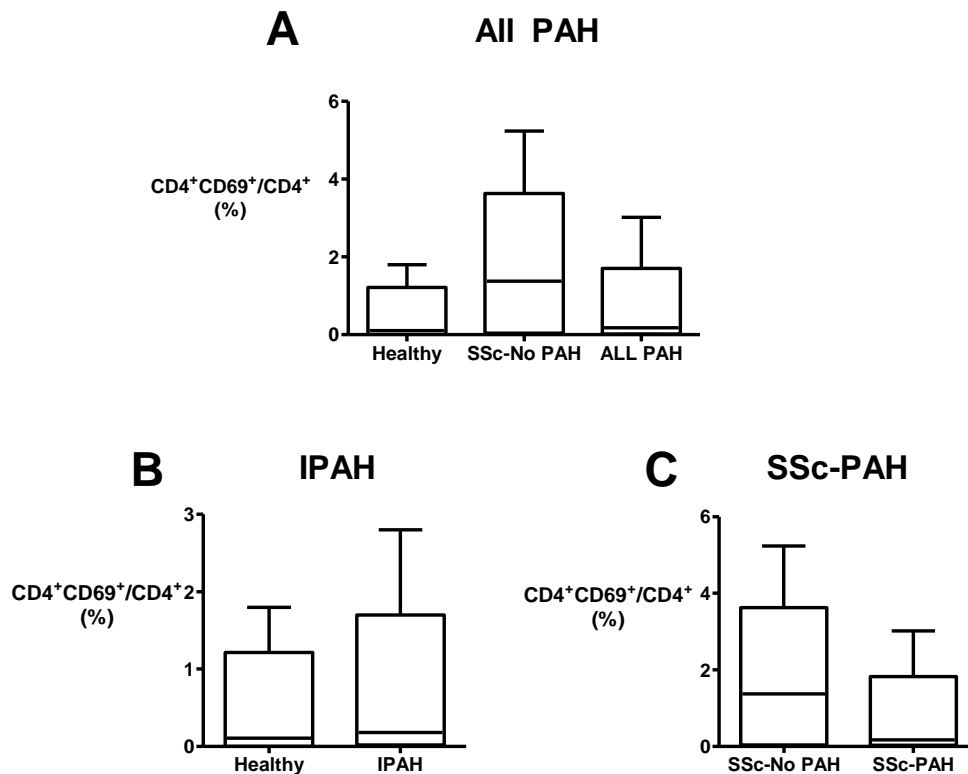


**Figure 2.8 Proportions of activated CD4<sup>+</sup> T cells in peripheral blood of PAH patients and controls.**

A) CD4<sup>+</sup>CD69<sup>+</sup> T cells in all PAH patients. B) CD4<sup>+</sup>CD69<sup>+</sup> T cells in IPAH patients and healthy controls. C) CD4<sup>+</sup>CD69<sup>+</sup> T cells in SSc-no PAH and SSc-PAH patients. All data presented as a proportion of the total CD4<sup>+</sup> T cell population. Data analysed by a Kruskal Wallis Test with Dunn's post hoc test or by a two tailed Mann Whitney test. A 95% confidence interval was used where  $P < 0.05$  is considered significant (\*). All Box and whisker plots depict median with minimum to maximum values in each study group. IPAH patients  $n=15$ , SSc-PAH patients  $n=12$ , healthy controls  $n=15$ , SSc no-PAH controls  $n=7$ .

### 2.3.3.3 Activation status of CD8<sup>+</sup> T cells

There was no difference in the proportion of activated CD8<sup>+</sup> T cells in PAH patients compared to controls (Figure 2.9, A) or after considering IPAH (Figure 2.9, B) and SSc-PAH groups separately (Figure 2.9, C).

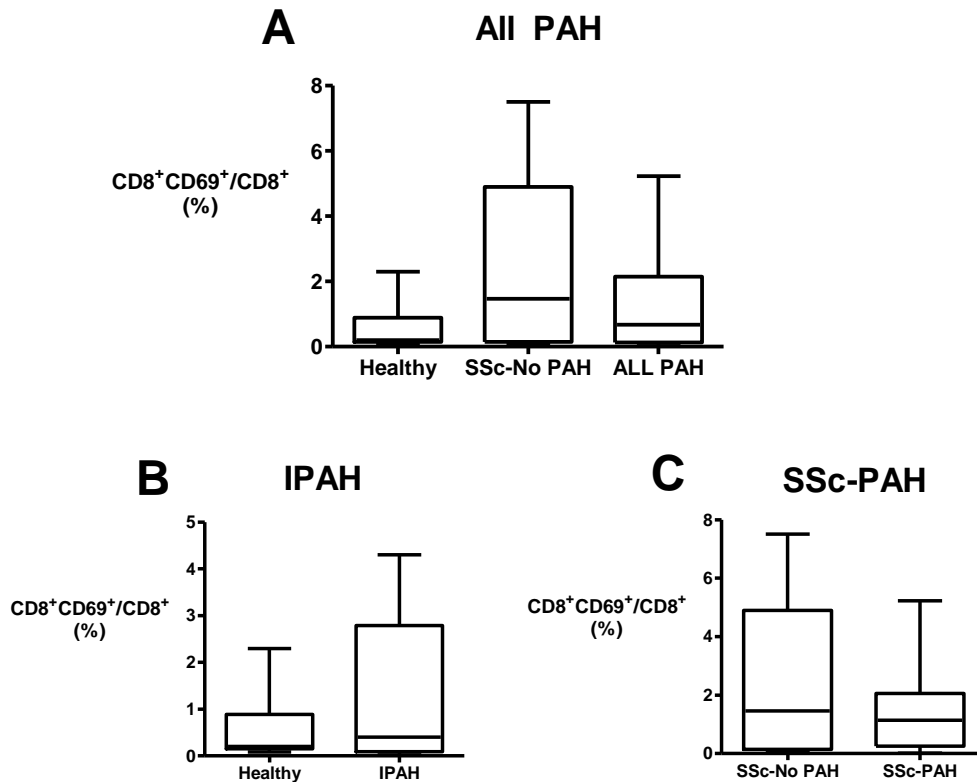


**Figure 2.9 Proportions of activated CD8<sup>+</sup> T cells in peripheral blood of PAH patients and controls.**

A) CD8<sup>+</sup>CD69<sup>+</sup> T cells in all PAH patients. B) CD8<sup>+</sup>CD69<sup>+</sup> T cells in IPAH patients and healthy controls. C) CD8<sup>+</sup>CD69<sup>+</sup> T cells in SSc-no PAH and SSc-PAH patients. Data are shown as a percentage of total CD8<sup>+</sup> T cells. Data analysed by a Kruskal Wallis Test with Dunn's post hoc test or by a two tailed Mann Whitney test. A 95% confidence interval was used where  $P < 0.05$  is considered significant (\*). All Box and whisker plots depict median with minimum to maximum values in each study group. IPAH patients  $n=13$ , SSc-PAH patients  $n=12$ , healthy controls  $n=15$ , SSc no-PAH controls  $n=7$ .

### 2.3.4 T regulatory cells and their activation status in patient and control peripheral blood samples

Another T cell subset thought to be crucial in the resolution of an immune response is the Treg cell (Fehervari and Sakaguchi, 2004). Therefore, proportions and activation status of this cell type were analysed within patient and control groups. For this study, Treg cells were characterised based upon the expression of cell surface markers (CD3, CD4, CD25, and CD127) and intracellular expression of Foxp3. CD25 is the  $\alpha$ -chain of the IL-2 receptor and CD127 is the  $\alpha$ -chain of the IL-7 receptor. CD4<sup>+</sup>CD25<sup>+</sup>CD127<sup>low/-</sup> Treg cells express Foxp3, with CD127 expression on Treg cells being inversely proportional to Foxp3 expression, therefore a combination of these markers was used (Liu *et al*, 2006; Shen *et al*, 2009).

Data shown are CD4<sup>+</sup>CD25<sup>high</sup> and CD4<sup>+</sup>CD25<sup>high</sup>CD127<sup>low</sup>, as Foxp3 event counts were too low. Therefore the analysis using the combination of CD25, CD127 and Foxp3 are not shown here (CD4<sup>+</sup>CD25<sup>high</sup> Foxp3<sup>+</sup> and CD4<sup>+</sup>CD25<sup>high</sup>CD127<sup>low</sup> Foxp3<sup>+</sup>). From this point forward in this thesis only two combinations of markers will be used to define a Treg cell (CD4<sup>+</sup>CD25<sup>high</sup> and CD4<sup>+</sup>CD25<sup>high</sup>CD127<sup>low</sup>).

When defined as CD4<sup>+</sup>CD25<sup>high</sup>, proportions of Treg cells in all PAH patients were no different in comparison to controls (Figure 2.10, A). When broken down into separate patient groups, this observation was also noted in IPAH patients, with no change in proportions of CD4<sup>+</sup>CD25<sup>high</sup> Treg cells compared to healthy controls and in SSc-PAH patients compared to SSc-no PAH controls (Figure 2.10, B and C).

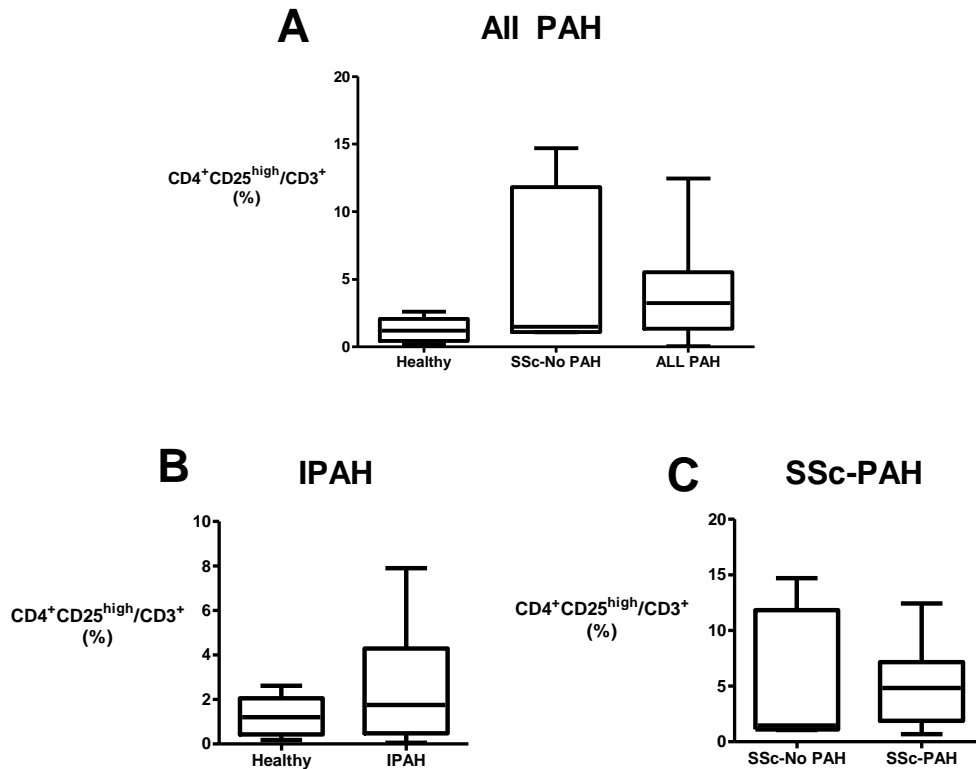


**Figure 2.10 Proportions of  $CD4^+CD25^{high}$  Treg cells in peripheral blood of PAH patients and controls.**

A)  $CD4^+CD25^{high}$  Treg cells in all PAH patients. B)  $CD4^+CD25^{high}$  Treg cells in healthy controls and IPAH patients. C)  $CD4^+CD25^{high}$  Treg cells in scleroderma controls (SSc-no PAH) and SSc-PAH patients. Data are shown as a percentage of total  $CD3^+$  T cells. Data analysed by a Kruskal Wallis Test with Dunn's post hoc test or by a two tailed Mann Whitney test. A 95% confidence interval was used where  $P < 0.05$  is considered significant (\*). All Box and whisker plots depict median with minimum to maximum values in each study group. IPAH patients  $n=15$ , SSc-PAH patients  $n=12$ , healthy controls  $n=13$ , SSc no-PAH controls  $n=7$ .

When defined as  $CD4^+CD25^{high}CD127^{low}$ , proportions of Treg cells are not different between all PAH patients and controls (Figure 2.11, A). This is also true when IPAH patients are compared to healthy controls (Figure 2.11, B) and SSc-no PAH are compared to SSc-PAH patients (Figure 2.11, C).

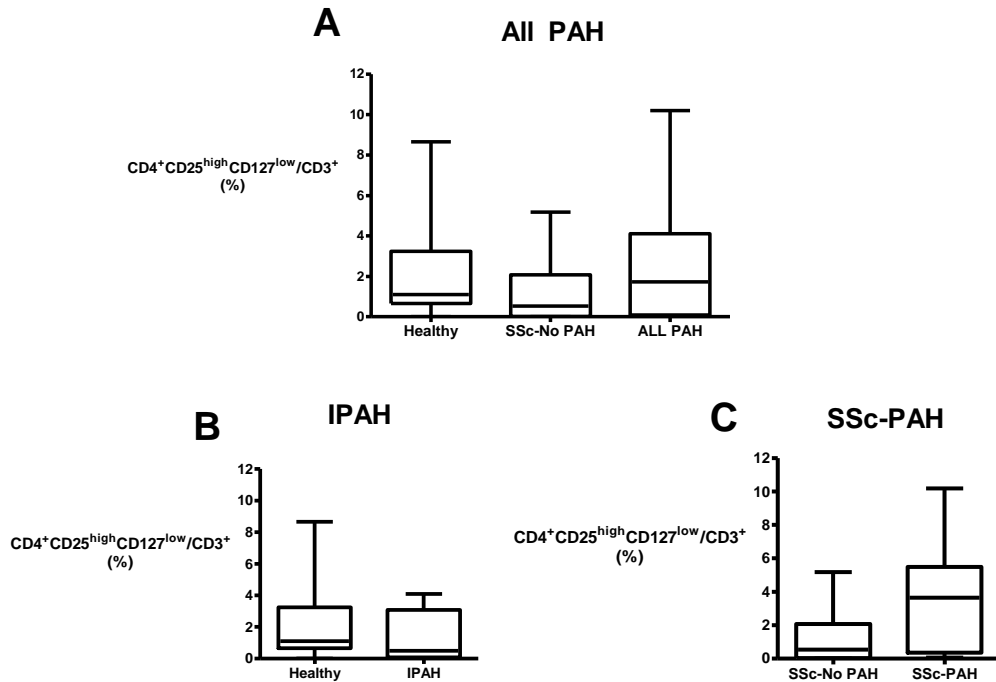


**Figure 2.11 Proportions of  $CD4^+CD25^{high}CD127^{low}$  Treg cells in peripheral blood of PAH patients and controls.**

A)  $CD4^+CD25^{high}CD127^{low}$  Treg cells in all PAH patients. B)  $CD4^+CD25^{high}CD127^{low}$  Treg cells in healthy controls and IPAH patients. C)  $CD4^+CD25^{high}CD127^{low}$  Treg cells in scleroderma controls and SSc-PAH patients. Data are shown as a percentage of total  $CD3^+$  T cells. Data analysed by a Kruskal Wallis Test with Dunn's post hoc test or by a two tailed Mann Whitney test. A 95% confidence interval was used where  $P < 0.05$  is considered significant (\*). All Box and whisker plots depict median with minimum to maximum values in each study group. IPAH patients  $n=15$ , SSc-PAH patients  $n=10$ , healthy controls  $n=13$ , SSc no-PAH controls  $n=8$ .

As there was no difference in the proportion of Treg cells in either patient group, I next looked to determine whether there was any change in the activation status of Treg cells. Using  $CD4^+CD25^{high}$  as the first combination to describe Treg cells, there appears to be no change in the proportion of activated  $CD4^+CD25^{high}$  cells in PAH patients compared to controls (Figure 2.12, A). There was still no difference between patient and control groups when they were compared separately to their corresponding controls (Figure 2.12, B and C), however there was a greater spread of data

in the SSc-PAH patient group compared to SSc-no PAH controls (Figure 2.12, C).

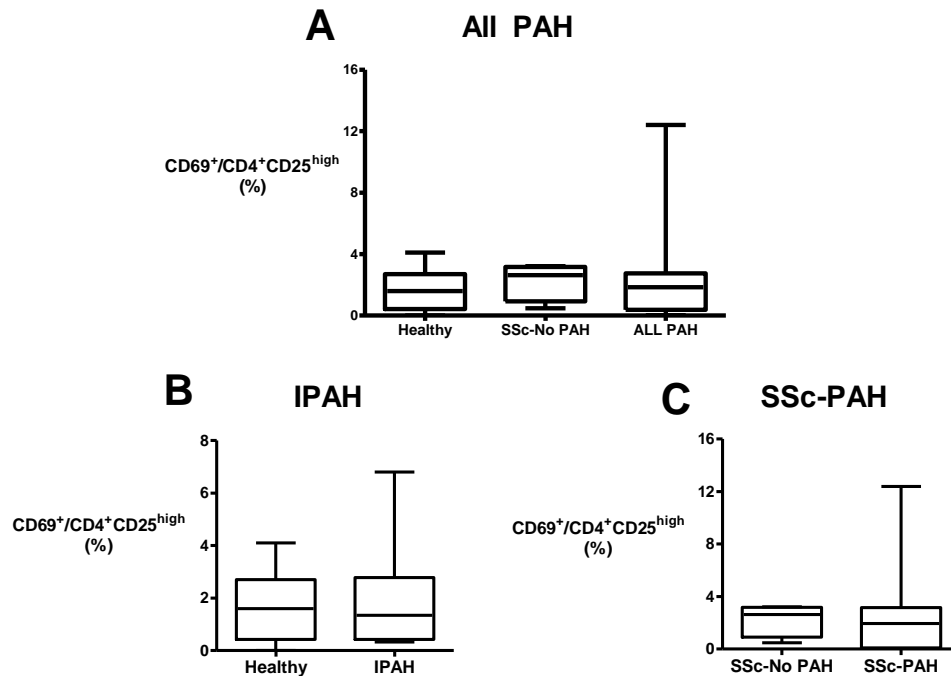


**Figure 2.12 Proportions of activated  $CD4^+CD25^{high}$  Treg cells in peripheral blood of PAH patients and controls.**

A) Activated  $CD4^+CD25^{high}$  Treg cells in all PAH patients ( $CD69^+$ ). B) Activated  $CD4^+CD25^{high}$  Treg cells in healthy controls and IPAH patients. C) Activated  $CD4^+CD25^{high}$  Treg cells in scleroderma controls (SSc-no PAH) and SSc-PAH patients. Data are shown as a percentage of total Treg cell population ( $CD4^+CD25^{high}$ ). Data analysed by a Kruskal Wallis Test with Dunn's post hoc test or by a two tailed Mann Whitney test. A 95% confidence interval was used where  $P < 0.05$  is considered significant (\*). All Box and whisker plots depict median with minimum to maximum values in each study group. IPAH patients  $n=12$ , SSc-PAH patients  $n=10$ , healthy controls  $n=13$ , SSc no-PAH controls  $n=5$ .

When Treg cells were defined as  $CD4^+CD25^{high}CD127^{low}$ , there was no difference in the activation of  $CD4^+CD25^{high}CD127^{low}$  Treg cells between patient and controls (Figure 2.13, A). The patient groups were also split into IPAH and SSc-PAH patients to compare with corresponding patient controls. This analysis revealed that in IPAH and SSc-PAH patients, there was no

change in activation of  $CD4^+CD25^{high}CD127^{low}$  Treg cells between the patient groups compared to their corresponding controls (Figure 2.13, B and C).

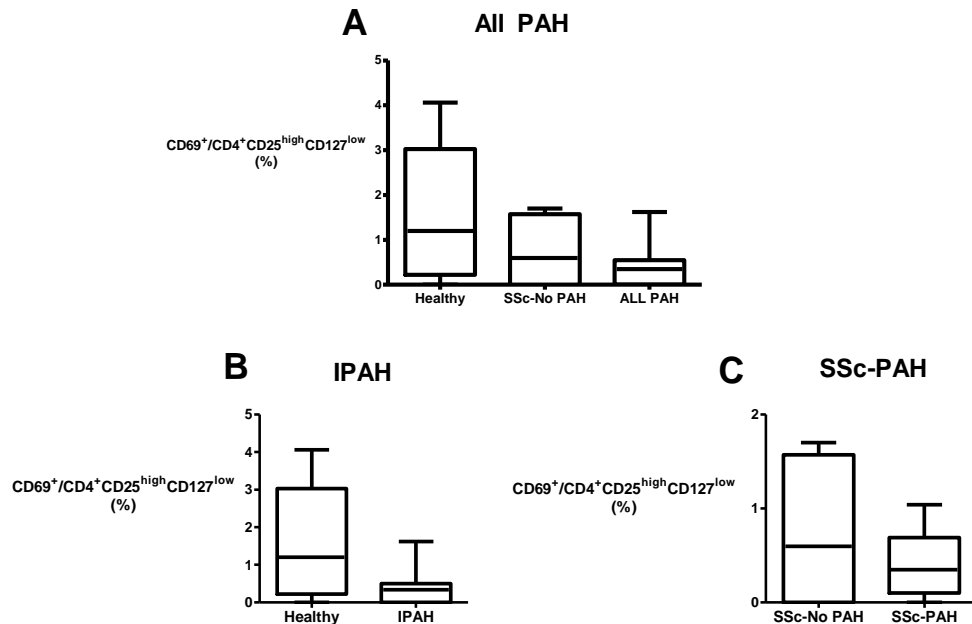


**Figure 2.13 Proportions of activated  $CD4^+CD25^{high}CD127^{low}$  Treg cells in peripheral blood of PAH patients and controls.**

A) Activated  $CD4^+CD25^{high}CD127^{low}$  Treg cells in all PAH patients. B) Activated  $CD4^+CD25^{high}CD127^{low}$  Treg cells in healthy controls and IPAH patients. C) Activated  $CD4^+CD25^{high}CD127^{low}$  Treg cells in scleroderma controls and SSc-PAH patients. Data are shown as a percentage of total Treg cell population ( $CD4^+CD25^{high}CD127^{low}$ ). Data analysed by a Kruskal Wallis Test with Dunn's post hoc test or by a two tailed Mann Whitney test. A 95% confidence interval was used where  $P < 0.05$  is considered significant (\*). All Box and whisker plots depict median with minimum to maximum values in each study group. IPAH patients  $n=10$ , SSc-PAH patients  $n=7$ , healthy controls  $n=12$ , SSc no-PAH controls  $n=5$ .

### 2.3.5 B cells and their activation status in patient and control peripheral blood samples

Another major lymphocyte subset was B cells, which are involved in producing antibodies within the humoral immune response. To gain a greater understanding of abnormalities in immune cell subsets within PAH patients,

the proportion of B cells and their activation status were considered next. The proportion of B cells (CD19<sup>+</sup>) as a percentage of total CD45<sup>+</sup> leukocytes was measured in each patient and control sample, along with the activation status, as shown by expression of CD69.

There was no difference in the proportions of B cells (CD45<sup>+</sup>CD19<sup>+</sup>) between patient and control groups (Figure 2.14, A). There was also no difference in either IPAH patients (Figure 2.14, B) or SSc-PAH patients (Figure 2.14, C) when compared to corresponding controls. There was, however, a trend for a higher proportion of B cells in SSc-no PAH patients compared to healthy controls ( $9.95 \pm 3.06$  vs  $6.40 \pm 2.43$ ,  $n=4-10$ ,  $P=0.07$ ) (Figure 2.14, A).

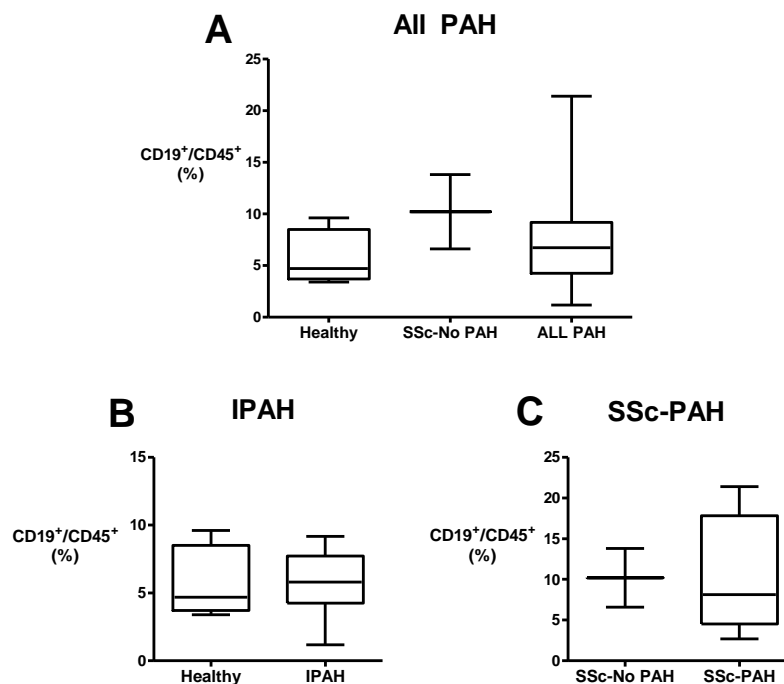


**Figure 2.14 Proportion of B cells in peripheral blood of PAH patients and controls.**

A) Proportion of B cells (CD19<sup>+</sup>) in all PAH patients. B) Proportion of B cells in IPAH patients. C) Proportion of B cells in SSc-PAH patients. Data expressed as a proportion of CD45<sup>+</sup> cells. Data analysed by a Kruskal Wallis Test with Dunn's post hoc test or by a two tailed Mann Whitney test. A 95% confidence interval was used where  $P < 0.05$  is considered significant (\*). All Box and whisker plots depict median with minimum to maximum values in each study group. IPAH patients  $n=11$ , SSc-PAH patients  $n=9$ , healthy controls  $n=10$ , SSc no-PAH controls  $n=4$ .

CD69 expression was used to investigate changes in the activation status of B cells within patient and control samples. The proportion of activated B cells was similar in control groups and all PAH patients (Figure 2.15, A). There was also no change in the proportion of B cells when all PAH patients were split into IPAH patients and SSc-PAH groups and compared to their corresponding controls (Figure 2.15, B and C). There was a large range of activated B cells in all SSc-PAH patients and healthy volunteers, as shown by the large minimum and maximum data bars. Further work to increase the sample population of these cohorts would allow for more accurate conclusions to be drawn about the changes in activation status of B cells within these subsets.

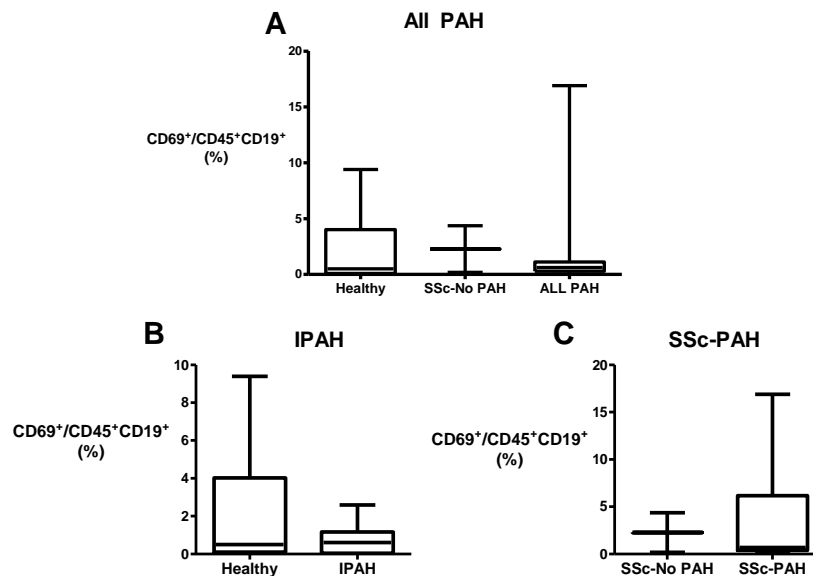


**Figure 2.15 Proportions of activated B cells in peripheral blood of PAH patients and controls.**

A) Proportion of activated B cells ( $CD19^+CD69^+$ ) in all PAH patients. B) Proportion of activated B cells in IPAH patients. C) Proportion of activated B cells in SSc-PAH patients. Activation status of B cells expressed as a  $CD69^+$  cells as a proportion of  $CD45^+CD19^+$  cells. Data analysed by a Kruskal Wallis Test with Dunn's post hoc test or by a two tailed Mann Whitney test. A 95% confidence interval was used where  $P < 0.05$  is considered significant (\*). All Box and whisker plots depict median with minimum to maximum values in each study group. IPAH patients  $n=10$ , SSc-PAH patients  $n=9$ , healthy controls  $n=10$ , SSc no-PAH controls  $n=4$ .

## 2.3.6 Correlations between clinical data and T cell subsets

After initial analysis of proportional CD4<sup>+</sup> T cell data in patients and controls, it was evident that although there was no overall change in the mean of each data set, there was an increase in the spread of data in the patient groups compared to their corresponding controls (Figure 2.16).

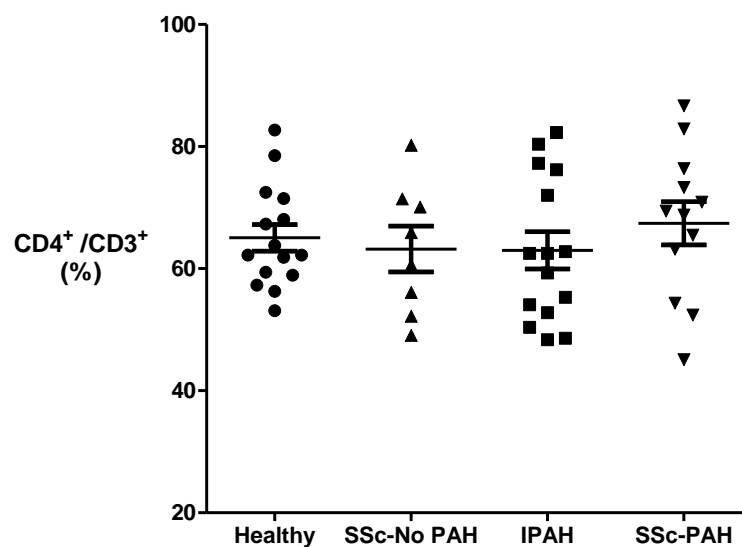


**Figure 2.16 Scatter plot showing spread of CD4<sup>+</sup> T cell data in PAH patients and controls.**

*IPAH and SSc-PAH patient groups are shown along with SSc-no PAH and healthy control groups. Data are shown as a percentage of total CD3<sup>+</sup> T cells. Error bars depict mean  $\pm$  SEM. n=8-15 per patient group.*

Therefore to determine whether or not this change in the range of data within the CD4<sup>+</sup> T cell subset correlated with disease severity I compared clinical data from both SSc-PAH and IPAH patients against the proportion of CD4<sup>+</sup> T cells in each patient blood sample. A correlation of the proportion of CD8<sup>+</sup> T cells and CD4<sup>+</sup>CD25<sup>high</sup> Treg cells and clinical parameters was also made. Clinical phenotyping was undertaken at visit 1 before PAH specific treatment was administered. An R and P value were calculated for each pair

of data using a two tailed, non-parametric (Spearman) correlation test with a 95% confidence level. Pairs of data that had a P value < 0.05 were considered significant.

There is a significant negative correlation between CD4<sup>+</sup> T cells and the shuttle walk test (R=-0.54 and P=0.04) in IPAH patients, however no significant correlations were noted between CD8<sup>+</sup> T cells, CD4<sup>+</sup>CD25<sup>high</sup> Treg cells and other clinical parameters (Table 2.3). I also noted a significant negative correlation between CD4<sup>+</sup> T cells and cardiac index (CI) (R=-0.7 and P=0.03) in SSc-PAH patients, however no significant correlations were seen between CD8<sup>+</sup> T cells, CD4<sup>+</sup> CD25<sup>high</sup> Treg cells and other clinical parameters (Table 2.4). These data suggest that proportions of CD4<sup>+</sup> T cells are inversely proportional to clinical markers of disease progression such as CI and shuttle walk test in PAH patients and could be used in the future in diagnosis or prognosis in PAH patients.

Comparison		R value	P value
eGFR	vs CD4 <sup>+</sup> T cells	0.14	0.80
	vs CD8 <sup>+</sup> T cells	0.63	0.42
	vs CD4 <sup>+</sup> CD25 <sup>high</sup> Treg cells	0.64	0.18
CRP	vs CD4 <sup>+</sup> T cells	0.14	0.64
	vs CD8 <sup>+</sup> T cells	0.06	0.86
	vs CD4 <sup>+</sup> CD25 <sup>high</sup> Treg cells	-0.03	0.93
FEV1	vs CD4 <sup>+</sup> T cells	0.00	0.99
	vs CD8 <sup>+</sup> T cells	0.22	0.50
	vs CD4 <sup>+</sup> CD25 <sup>high</sup> Treg cells	-0.02	-0.95
FEV1/FVC ratio	vs CD4 <sup>+</sup> T cells	-0.14	0.64
	vs CD8 <sup>+</sup> T cells	0.26	0.42
	vs CD4 <sup>+</sup> CD25 <sup>high</sup> Treg cells	-0.47	0.09
Shuttle	<b>vs CD4<sup>+</sup> T cells</b>	<b>-0.54</b>	<b>0.04</b>
	vs CD8 <sup>+</sup> T cells	0.30	0.32
	vs CD4 <sup>+</sup> CD25 <sup>high</sup> Treg cells	0.06	0.83
HR	vs CD4 <sup>+</sup> T cells	0.15	0.59
	vs CD8 <sup>+</sup> T cells	-0.22	0.47
	vs CD4 <sup>+</sup> CD25 <sup>high</sup> Treg cells	-0.22	0.44
mPAP	vs CD4 <sup>+</sup> T cells	0.05	0.85
	vs CD8 <sup>+</sup> T cells	-0.31	0.30
	vs CD4 <sup>+</sup> CD25 <sup>high</sup> Treg cells	-0.06	0.84
CO	vs CD4 <sup>+</sup> T cells	0.28	0.32
	vs CD8 <sup>+</sup> T cells	-0.48	0.10
	vs CD4 <sup>+</sup> CD25 <sup>high</sup> Treg cells	0.25	0.37
PVR	vs CD4 <sup>+</sup> T cells	-0.26	0.34
	vs CD8 <sup>+</sup> T cells	0.30	0.32
	vs CD4 <sup>+</sup> CD25 <sup>high</sup> Treg cells	-0.23	0.42
CI	vs CD4 <sup>+</sup> T cells	0.03	0.92
	vs CD8 <sup>+</sup> T cells	-0.28	0.35
	vs CD4 <sup>+</sup> CD25 <sup>high</sup> Treg cells	0.26	0.34

**Table 2.3 Correlation data between CD4<sup>+</sup> T cells, CD8<sup>+</sup> T cells, CD4<sup>+</sup>CD25<sup>high</sup> Treg cells and clinical parameters in IPAH patients.**

*R and P values are shown. Estimated glomerular filtration rate (eGFR), C reactive protein (CRP), Forced expiratory volume in one second (FEV1), forced vital capacity (FVC), shuttle walk test (shuttle), heart rate, (HR), mean pulmonary artery pressure (mPAP), cardiac output (CO), pulmonary vascular resistance (PVR) and cardiac index (CI) are shown. n=15 and significant data shown in bold (P< 0.05).*

Comparison		R value	P value
eGFR	vs CD4 <sup>+</sup> T cells	-0.10	0.95
	vs CD8 <sup>+</sup> T cells	0.30	0.63
	vs CD4 <sup>+</sup> CD25 <sup>high</sup> Treg cells	-0.40	0.52
CRP	vs CD4 <sup>+</sup> T cells	-0.37	0.50
	vs CD8 <sup>+</sup> T cells	0.66	0.18
	vs CD4 <sup>+</sup> CD25 <sup>high</sup> Treg cells	-0.31	0.56
FEV1	vs CD4 <sup>+</sup> T cells	0.03	1.00
	vs CD8 <sup>+</sup> T cells	-0.01	0.96
	vs CD4 <sup>+</sup> CD25 <sup>high</sup> Treg cells	0.00	1.00
FEV1/FVC ratio	vs CD4 <sup>+</sup> T cells	0.15	0.80
	vs CD8 <sup>+</sup> T cells	0.13	0.78
	vs CD4 <sup>+</sup> CD25 <sup>high</sup> Treg cells	-0.23	0.65
Shuttle	vs CD4 <sup>+</sup> T cells	0.43	0.25
	vs CD8 <sup>+</sup> T cells	-0.62	0.09
	vs CD4 <sup>+</sup> CD25 <sup>high</sup> Treg cells	0.30	0.44
HR	vs CD4 <sup>+</sup> T cells	-0.03	0.95
	vs CD8 <sup>+</sup> T cells	-0.28	0.46
	vs CD4 <sup>+</sup> CD25 <sup>high</sup> Treg cells	-0.02	0.98
mPAP	vs CD4 <sup>+</sup> T cells	0.10	0.79
	vs CD8 <sup>+</sup> T cells	0.22	0.54
	vs CD4 <sup>+</sup> CD25 <sup>high</sup> Treg cells	-0.35	0.31
CO	vs CD4 <sup>+</sup> T cells	-0.35	0.33
	vs CD8 <sup>+</sup> T cells	-0.32	0.37
	vs CD4 <sup>+</sup> CD25 <sup>high</sup> Treg cells	0.50	0.14
PVR	vs CD4 <sup>+</sup> T cells	0.22	0.54
	vs CD8 <sup>+</sup> T cells	0.20	0.58
	vs CD4 <sup>+</sup> CD25 <sup>high</sup> Treg cells	-0.55	0.10
CI	<b>vs CD4<sup>+</sup> T cells</b>	<b>-0.70</b>	<b>0.03</b>
	vs CD8 <sup>+</sup> T cells	-0.04	0.92
	vs CD4 <sup>+</sup> CD25 <sup>high</sup> Treg cells	0.21	0.44

**Table 2.4 Correlation data between CD4<sup>+</sup> T cells, CD8<sup>+</sup> T cells, CD4<sup>+</sup>CD25<sup>high</sup> Treg cells and clinical parameters in SSc-PAH patients.**

*R and P values are shown. Estimated glomerular filtration rate (eGFR), C reactive protein (CRP), Forced expiratory volume in one second (FEV1), forced vital capacity (FVC), shuttle walk test (shuttle), heart rate, (HR), mean pulmonary artery pressure (mPAP), cardiac output (CO), pulmonary vascular resistance (PVR) and cardiac index (CI) are shown. n=12 and significant data shown in bold (P< 0.05).*

## 2.3.7 Patient survival analysis

As proportions of CD4<sup>+</sup> T cells were shown to be inversely proportional to clinical markers of disease progression, I next sought to determine whether proportions of T cell subsets could be used to predict survival in PAH patients.

Receiver-operating characteristics curves (ROC) and Kaplan-Meier survival analyses were performed using proportions of CD4<sup>+</sup> T cells, CD8<sup>+</sup> T cells or CD4<sup>+</sup>CD25<sup>high</sup> Treg cells. Firstly, ROC curves were constructed for IPAH, SSc-PAH, SSc-no PAH patients and healthy controls using proportional data on CD4<sup>+</sup>, CD8<sup>+</sup> and Treg cell subsets.

GraphPad Prism software was used to undertake ROC curve analyses in which proportions of each T cell subset from each patient subgroup (IPAH and SSc-PAH) were compared against their corresponding controls. A confidence interval of 95% was used and the results reported as a percentage. A combination of percentage sensitivity and percentage specificity that gave the highest likelihood ratio (the most confidence that a negative result is a true negative and that a positive result is a true positive) was selected. After performing a ROC analysis, a value of 83.33% sensitivity and 85.71% specificity for SSc-PAH patients and controls was chosen with a cut-off value of 22% for CD8<sup>+</sup> T cells (P= 0.008) (Figure 2.17). I had intended to use these results to perform a Kaplan-Meier survival analysis; however there were insufficient clinical events in the SSc-PAH patient group to undertake this analysis.

The analysis of CD4<sup>+</sup> T cells and CD4<sup>+</sup>CD25<sup>high</sup> Treg cells in SSc-PAH and all T cell subsets and IPAH patients revealed no significant differences.

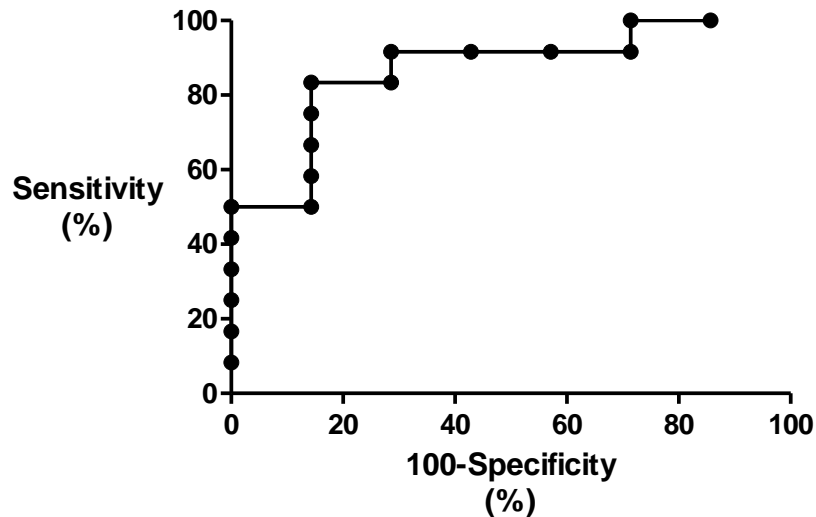


**Figure 2.17 Receiver operating characteristic curve to define optimum cut-off value for changes in the proportion of CD8<sup>+</sup> T cells in the prediction of PAH.**  
*Data shown are for SSc-PAH patients.*

### **2.3.8 Lymphocyte subset analysis in patients undergoing PAH treatment**

At the SPVDU patients return for follow-up visits after commencing a PAH specific therapy to be assessed for disease progression and the efficacy of the treatment plan. As these samples were available, I next sought to determine whether there was any change in the lymphocyte subsets previously discussed after commencing PAH specific treatment and whether they related to a marker of disease progression, the shuttle walk test, and the cut-off value from the ROC curve previously mentioned.

Of the 29 confirmed PAH patients from whom I had collected data regarding lymphocyte subsets (15 IPAH and 13 SSc-PAH), further data were collected from 5 of these patients (4 IPAH and 1 SSc-PAH) at follow-up over a period of 3 years. Data could not be collected from all patients for several reasons, including a lack of consent, death or due to the recent recruitment of the patient, as follow-up visits occurred on average every 6 months.

Patients were diagnosed at visit 1 after which they were started on a course of PAH treatment applicable to their disease state and progression.

Blood samples were collected from these patients at subsequent follow-up visits and data compared to previous treatment-naïve data collected at visit 1. Table 2.5 depicts PAH specific drug, time between visits and shuttle walk test results for all visit 1s and follow-ups (IPAH and SSc-PAH patients).

Of the 5 follow-up patients recruited two were taking Bosentan or Ambrisentan (both E-RAs) throughout the duration of their treatment whilst two were taking Sildenafil (PDE-5 inhibitor). One patient was prescribed both Bosentan and Sildenafil. Of the 5 patients, 3 increased their shuttle walk test scores, 1 did not change from visit 1 to follow-up and the other had a decreased shuttle walk test score.

Patient ID and PAH subtype	Treatment At visit 1	Treatment At follow-up visit	Shuttle walk test at visit 1 (m)	Shuttle walk test (m) at follow-up visit (m)	Time between visits (months)	Δ shuttle walk test (m)
276, SSc-PAH	Bosentan	Bosentan	80	180	10	+100 #
90, IPAH	Bosentan	Ambrisentan	130	210	23	+80 #
353, IPAH	Bosentan Sildenafil	Bosentan Sildenafil	420	260	5	-160
380, IPAH	Sildenafil	Sildenafil	30	30	8	0
442, IPAH	Sildenafil	Sildenafil	360	370	7	+10

**Table 2.5 PAH specific drug therapy and shuttle walk test scores for all follow-up visits (IPAH and SSc-PAH patients).**

*Patients 276, 90, 353, 380 and 442 were recruited upon return to the clinic for blood cell analysis using flow cytometry. The PAH-specific treatment taking at each visit and the time between visits (months) is shown. Shuttle walk test results at both visit 1 and follow-up (metres) and the change between these (Δ shuttle walk test) in metres is also shown. A change in walking distance of more than 50 m is clinically significant (#) (Rasekaba et al, 2009). Ambrisentan and bosentan are both E-RAs whilst sildenafil is a PDE-5 inhibitor.*

Analysis of how different treatment regimes affected T cell subsets at return visits was assessed by grouping patients according to which PAH-specific drug treatment they were taking at visit 1, and not the disease

subtype (IPAH or SSc-PAH). As the sample population of each treatment group was so small, it is difficult to draw definitive conclusions from the data, however the data were still analysed.

Proportions of CD4<sup>+</sup> T cells did not appear to follow any trend in patients taking E-RAs (Figure 2.18, A). If these data are further divided into patient subtypes, the SSc-PAH patient taking an E-RA showed a decrease in the proportion of circulating CD4<sup>+</sup> T cells at follow-up. The two patients taking PDE-5 inhibitors showed a decrease in their proportions of CD4<sup>+</sup> T cells at follow-up (Figure 2.18, B). Patient 353, the only patient on both an E-RA and a PDE-5 inhibitor showed a trend for an increase in CD4<sup>+</sup> T cells from visit 1 to follow-up (plotted on both graphs, Figure 2.18, A and B).

Interestingly, both patients only taking E-RAs had a significant improvement in their shuttle walk test results, whereas the proportion of circulating CD4<sup>+</sup> T cells appeared to be returning to those that were present in healthy controls (62.20% as a proportion of total CD3<sup>+</sup> T cells). Patients given PDE-5 inhibitors exhibited no improvement in their shuttle walk test scores. The patient given both drugs (patient 535) had a decreased shuttle walk test result at follow-up visit, but had an improved CD4<sup>+</sup> T cell compartment.

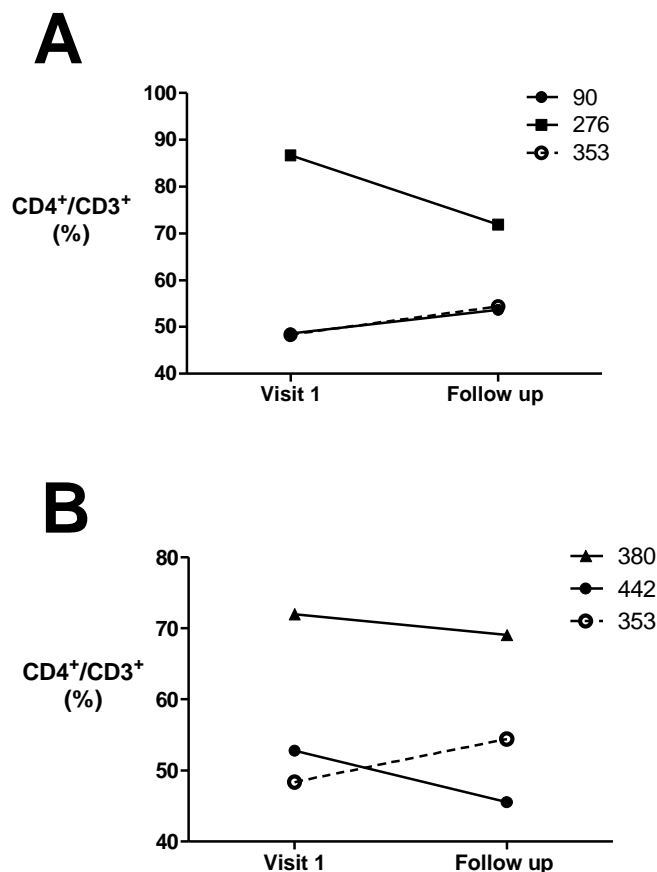


**Figure 2.18 Proportions of CD4<sup>+</sup> T cells in PAH patients at follow-up.**

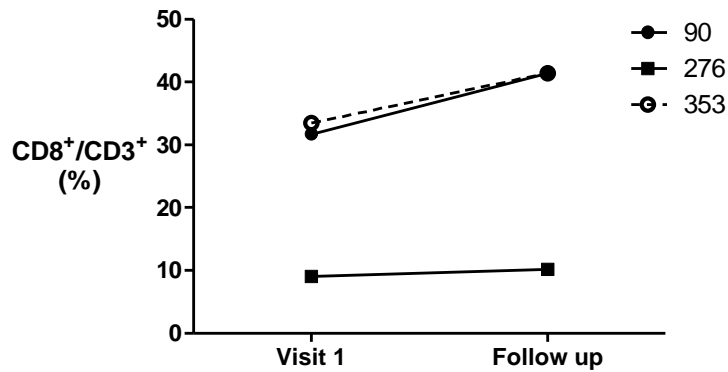
A) CD4<sup>+</sup> T cells as a proportion of total CD3<sup>+</sup> T cells in patients taking endothelin-1 receptor antagonists B) CD4<sup>+</sup> T cells as a proportion of total CD3<sup>+</sup> T cells in patients taking PDE-5 inhibitors. Patient 353, taking an endothelin-1 receptor antagonist and a PDE-5 inhibitor, is shown on both treatment graphs. Data shown are from visits 1 and follow-up. n=3.

Proportions of CD8<sup>+</sup> T cells in patients taking E-RAs showed a communal increase in the proportion of CD8<sup>+</sup> T cells in response to these drugs in both IPAH and SSc-PAH patients (276, 90, 353) (Figure 2.19, A). Patient 276 (SSc-PAH) remained within the cut off value determined from the ROC curve in Chapter 2.3.7 (22%), despite a significant increase in the distance walked in the shuttle walk test (+100 m). An increase in distance walked was also noted in patient 90 at the follow-up visit as well as an increase in the proportion of CD8<sup>+</sup> T cells in the blood. Patients taking PDE-5 inhibitors exhibited a decrease in the proportion of CD8<sup>+</sup> T cells at follow-up,

with one IPAH patient (442) showing a decreased proportion of CD8<sup>+</sup> T cells below the 22% cut off value determined from the ROC curve (determined using data from SSc-PAH patients) (Figure 2.19, B). Patient 353, taking both medications showed an increase in the proportion of circulating CD8<sup>+</sup> T cells in response to both medications, however their shuttle walk test score decreased significantly between visits (Figure 2.19, A and B).

Taking these two sets of data together to create CD4:CD8 T cell ratio figures, there appears to be no communal trend in patients taking E-RAs, however, patient 276 had an improved shuttle walk test result at follow-up, matched by a reduced CD4:CD8 T cell ratio towards a healthy level (1.9). It would be interesting to note whether the walk distance continues to increase with further E-RA treatment at a future follow-up visit. Patients 442 and 353 that were given PDE-5 inhibitors showed no change in the CD4:CD8 T cell ratio, however patient 380 showed an increased CD4:CD8 T cell ratio (Figure 2.20 A and B). There were mixed changes in shuttle walk test results at follow-up visits within this treatment group.

# A



# B

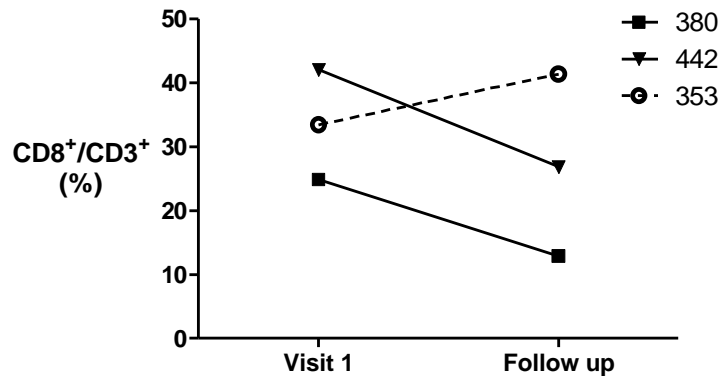


**Figure 2.19 Proportions of CD8<sup>+</sup> T cells in PAH patients at follow-up.**

A) CD8<sup>+</sup> T cells as a proportion of total CD3<sup>+</sup> T cells in patients taking endothelin-1 receptor antagonists B) CD8<sup>+</sup> T cells as a proportion of total CD3<sup>+</sup> T cells in patients taking PDE-5 inhibitors. Patient 353, taking an endothelin-1 receptor antagonist and a PDE-5 inhibitor, is shown on both treatment graphs. Data shown are from visits 1, 2 and 3. n=3.

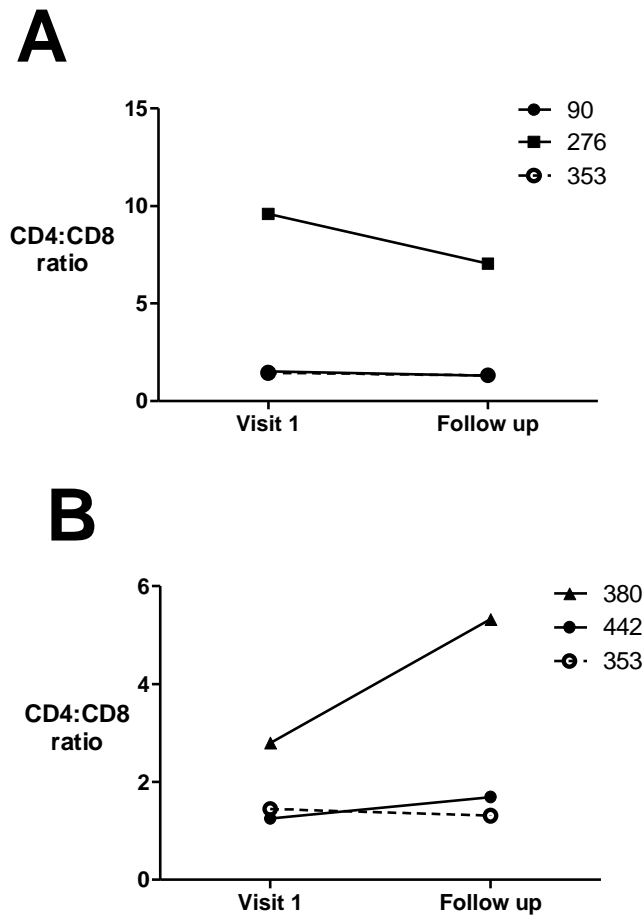


**Figure 2.20 CD4:CD8 ratio in PAH patients at follow-up.**

A) CD4<sup>+</sup> T cells as a proportion of total CD3<sup>+</sup> T cells in patients taking endothelin-1 receptor antagonists B) CD4<sup>+</sup> T cells as a proportion of total CD3<sup>+</sup> T cells in patients taking PDE-5 inhibitors. Patient 353, taking an endothelin-1 receptor antagonist and a PDE-5 inhibitor, is shown on both treatment graphs. Data shown are from visits 1 and follow-up. n=3.

A subgroup of T cells important in the resolution of immune response are Treg cells. These cells were defined here as CD4<sup>+</sup>CD25<sup>high</sup>, as differences in proportional data noted previously in section 2.3.4, demonstrated no change in results if either combination of markers is used to define them. In patients taking E-RAs, there was a decrease in proportions of Treg cells in all patients, whilst patients taking PDE-5 inhibitors exhibited no communal group change (one increased and the other decreased, Figure 2.21, A and B). PDE-5 inhibitors had a mixed effect on proportions of Treg

cells in patient 442 and 380, with patient 442 showing no significant change in the proportions of Treg cells and patient 380 showing an increase in the proportions of Treg cells. However, the two patients with no change or a decrease in their shuttle walk test result at follow-up visit showed an increase in the proportion of circulating Treg cells, compared to patient 442 who had a modest increase in their shuttle walk test result (+10 m) and had no change in the proportion of circulating Treg cells (Figure 2.21, B). Patient 353, taking both medications showed an increase in the proportion of circulating  $CD4^+CD25^{high}$  Treg cells in response to both medications, closely resembling the response noted in patient 380 (Figure 2.21, A and B).

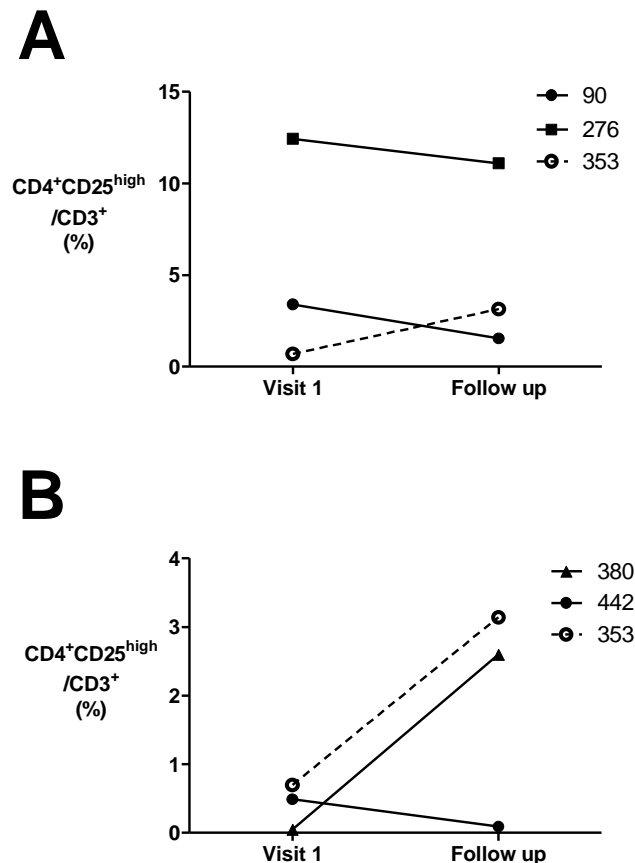


**Figure 2.21 Proportions of  $CD4^+CD25^{high}$  Treg in PAH patients at follow-up.**

A)  $CD4^+$  T cells as a proportion of total  $CD3^+$  T cells in patients taking endothelin-1 receptor antagonists B)  $CD4^+$  T cells as a proportion of total  $CD3^+$  T cells in patients taking PDE-5 inhibitors. Patient 353, taking an endothelin-1 receptor antagonist and a PDE-5 inhibitor, is shown on both treatment graphs. Data shown are from visits 1 and follow-up.  $n=3$ .

As previously noted, the small number of patients recruited at follow-up visits, makes it difficult to draw definitive conclusions from this preliminary data and further work needs to be undertaken to gain a greater understanding of the effect of different PAH treatment options on proportions of lymphocyte subsets, however these data may prove to be highly interesting.

## **2.4 Discussion**

The main aim of the work presented in this chapter was to determine the phenotypic profile of T cell populations in peripheral blood of treatment-naïve IPAH and SSc-PAH patients. Data regarding correlations between clinical parameters and T cell subsets were also collected and comparisons made between T cell subsets, treatment plans and changes in shuttle walk test compared at follow-up visits in patients that had begun PAH specific treatment. Treg cell functional assays were also undertaken in healthy volunteers with a view to determining abnormal functional responses of Treg cells in PAH patients at a later date.

### **2.4 1 Clinical peripheral lymphocyte subset analysis**

Clinical studies performed to evaluate abnormalities in T cell subsets in PAH patients are limited and report conflicting results regarding the proportions of some subsets of T cell, therefore further work has been undertaken to determine definitive trends (Soon, 2008; Ulrich *et al*, 2008; Austin *et al*, 2010). Previous studies all had one major limitation in that consenting patients had already been diagnosed with PAH and had commenced PAH specific treatments, which could have affected proportions of T cell subsets within the peripheral circulation. Therefore, it was important to establish a view of T cell subset abnormalities at baseline, in treatment-

naïve PAH patients. My study is believed to be the first published analysis of T cell subsets in peripheral blood of treatment-naïve IPAH and SSc-PAH patients.

Data published in this thesis suggest that treatment-naïve SSc-PAH patients have a significantly smaller proportion of CD8<sup>+</sup> T cells than SSc-no PAH controls. One explanation as to why CD8<sup>+</sup> T cell proportions are decreased in SSc-PAH patients (and noted in IPAH in previously published literature, but not in my results), could be that the Treg cell population could be acting as an “IL-2 sink” (previously described in Chapter 1.2.1). This reduction in pro-inflammatory cytokine could have a negative impact on Th1 (CD8<sup>+</sup> T cell) proliferation (McNally *et al*, 2011). Increased IL-6 serum levels have been noted in PAH patients, however the source of IL-6 increase is unclear. Dodge *et al* recently confirmed that IL-6 from DCs can inhibit Th1 responses in the mucosal lung environment (Dodge *et al*, 2003). A similar response may be occurring in the pulmonary circulation in PAH, however further studies need to be undertaken to define the source of the increase in serum IL-6. It is also important to note that in previous studies in SSc-no PAH patients, proportions of CD8<sup>+</sup> T cells were reduced in peripheral blood and showed an increased apoptotic phenotype (Kessel *et al*, 2004).

Daley *et al* have suggested that PAH is a Th2 mediated disease (CD4<sup>+</sup> T cells are the prominent cell type), as the deletion of CD4<sup>+</sup> T cells from mice stimulated with aspergillus antigen challenge or depletion of IL-13 prevented pulmonary arterial muscularisation (Daley *et al*, 2008). This is in contrast to Song *et al*, who propose that in BMPR2<sup>+/-</sup> mice treated with MCT and adenovirus expressing 5-lipoxygenase, showed an increased expression of MCP-1- $\alpha$  in lung tissue which could be driving a Th1 driven immune response (Song *et al*, 2008). The marked difference in T cell subset dominance (Th1 or Th2 driven) in both these models of PAH suggests that different initiating factors used to induce PAH produce different effects on T cell subsets. A Th2 dominant phenotype has previously been noted in SSc-no PAH patients, further emphasising the importance of this subgroup of T cells in SSc-PAH patients (Boin *et al*, 2008).

A decrease in CD8<sup>+</sup> T cells has previously been noted in IPAH patients compared to healthy controls, however another study refutes this

finding and concurs with work undertaken in this thesis; confirming no change in CD8<sup>+</sup> T cell populations in IPAH patients (Ulrich *et al*, 2008; Austin *et al*, 2010). One explanation for this disparity in findings could be that patients recruited onto these studies were undergoing treatment for PAH. Prostanoids are shown to inhibit T cell proliferation, while PDE-5 inhibitors have been shown to increase proliferation and activation of tumour infiltrating CD8<sup>+</sup> T cells further demonstrating the mixed effects that PAH specific treatments have on T cell populations (Lee *et al*, 2005; Serafini *et al*, 2006). SSc-PAH patients recruited in this study were on average slightly older and with a wider age range compared to the IPAH patients studied by Austin *et al*, where no change in CD8<sup>+</sup> T cell numbers in IPAH patient peripheral blood was noted. There have been published reports suggesting that T cell subsets (CD4<sup>+</sup>, CD8<sup>+</sup> and Treg cells) decrease until the age of 30 and then remain constant until 70 years of age, after which point they decrease further (Utsuyama *et al*, 1992). Ulrich *et al* also noted a decreased proportion of CD8<sup>+</sup> T cell in IPAH patient peripheral blood, and this was in patients with an average age of 51 years, which is similar to those enrolled in this study. Further investigation into whether age is a factor in these studies needs to be carried out, and if possible, younger SSc-PAH and IPAH patients need to be recruited and their results compared to those of older PAH patients to confirm that age does not affect T cell subsets in PAH patients.

No change in activation status of T cells (CD4<sup>+</sup> or CD8<sup>+</sup>) in either patient group compared to corresponding controls was noted in my study. In IPAH patients there was an increased spread of data regarding CD4<sup>+</sup> T cell activation compared to healthy controls; however this was not statistically significant. Further studies using an increased number of data sets will allow for more definitive conclusions to be drawn. The addition of other T cell activation markers such as CD30, HLA-DR and CD40L will allow for comparisons to be made between previously published literature and this work (Caruso *et al*, 1997).

In my study, a combination of markers was used to define Treg cells using flow cytometry. However, due to low event numbers, Foxp3 was not used as the data were unreliable. Therefore only CD4<sup>+</sup>CD25<sup>high</sup> and CD4<sup>+</sup>CD25<sup>high</sup>CD127<sup>low</sup> were used to define Treg cells. Proportions of Treg

cells ( $CD4^+CD25^{high}$  and  $CD4^+CD25^{high}CD127^{low}$ ) were no different between patients groups and corresponding controls in my study, however an increase in the proportion of circulating Treg cells has previously been described by both Austin *et al* and Ulrich *et al* in IPAH patients compared to healthy controls (Ulrich *et al*, 2008; Austin *et al*, 2010). As previously mentioned, these differences could be due to the age, sex and disease state of the patient, or their PAH specific therapy.

There was also no change in activation status of Treg cells in either patient group, however there was a greater spread of data within the SSc-PAH group compared to both control groups. This could reflect the severity of the disease in patients or possibly differences in age and sex as SSc-PAH is a relatively heterogeneous disease. Previous data gained from work performed on Treg cells from SSc-no PAH patients are conflicting. When limited and diffuse cutaneous patients are grouped together, it was noted that there was an increased proportion of Treg cells and a lower expression of the activation marker CD69 in peripheral blood of SSc-no PAH patients compared to healthy controls (Giovannetti *et al*, 2010; Slobodin *et al*, 2010; Mathian *et al*, 2012). However, in a study undertaken in diffuse cutaneous SSc-no PAH patients only, a decreased proportion of Treg cells was noted in peripheral blood (Papp *et al*, 2011). These studies further confirm the complexity of interpreting results from studies on patients with this disease and suggest that grouping of patients into different disease subtypes is important when analysing data.

I found no significant change in the proportion of  $CD4^+$  T cells in peripheral blood of IPAH patients, which has previously been noted by other studies in IPAH patients undergoing PAH specific treatment (Ulrich *et al*, 2008). I also noted no change in the proportion of  $CD4^+$  T cells in peripheral blood of SSc-PAH patients compared to SSc-no PAH controls. There was, however, an increased range of data in SSc-PAH and IPAH patients, making me question the possibility of using  $CD4^+$  T cells to predict disease severity and patient survival. If proven, these clinical measurements could provide a quick and reliable test of disease progression.

The proportion of circulating B cells in peripheral blood was also analysed, however there was no change between both patient groups and

their corresponding controls. The spread of data in both the IPAH patient group and the SSc-PAH patient group was larger than the control group and there was also a large spread of data regarding activation of B cells in all patient groups and healthy controls. This increase in the spread of data suggests that the proportion and activation of B cells is variable within patients and controls.

The choice of control groups for PAH research is a controversial issue, as each subset of PAH patients requires a different control. For IPAH patient controls, healthy volunteers are used to compare against patient samples. However it has been suggested that a more accurate control group for immune system studies in PAH would be patients with heart failure without co-morbidities such as angina or stroke, as this would provide a relevant clinical group without an inflammatory component. For SSc-PAH, the relevant control group is SSc-no PAH. However this could be further divided into limited and diffuse cutaneous SSc to determine whether the response seen is a result of SSc disease progression.

## **2.4.2 Correlation of clinical parameters with proportions of CD4<sup>+</sup> T cells in pulmonary arterial hypertension patients**

Correlations between disease progression and clinical biochemical parameters such as CRP levels have been noted in CTEPH patients (Quarck *et al*, 2009), however correlations between changes in T cell subsets and clinical parameters measured at baseline have not been undertaken before in PAH patients. These data could prove highly useful in clinical diagnosis and monitoring of PAH progression as well as having potential to be used as a prognostic biomarker in clinical PAH.

Work performed for this thesis confirmed that there was a significant negative correlation between the proportion of CD4<sup>+</sup> T cells and Cardiac Index (CI) in treatment-naïve SSc-PAH patients. This suggests that as the

heart's performance decreases, the CD4<sup>+</sup> T cell population increases. In treatment-naïve IPAH patients there was a significant negative correlation between CD4<sup>+</sup> T cells and the shuttle walk test. Both of these correlations could be used in future to predict the progression of PAH disease. Proportions of CD8<sup>+</sup> T cells may also be used as a prognostic indicator in PAH. A Kaplan-Meier survival analysis could not be performed due to low death event numbers in SSc-PAH patients. Future analysis of CD8<sup>+</sup> T cells proportions and survival data with increased patient numbers may provide evidence that CD8<sup>+</sup> T cell proportions can predict survival.

To exclude the possibility that these results are not a chance finding by looking for many associations, a second, completely separate cohort of patients could be studied and compared against the first cohort analysed in this thesis.

### **2.4.3 Treatments of pulmonary arterial hypertension and their effect on T cell subsets proportions**

There is little evidence regarding the effects that PAH specific treatments, such as Bosentan and Sildenafil, have on healthy T cell populations and those in IPAH and SSc-PAH patients. This study area merits further investigation into how T cell subset changes can affect disease progression and whether manipulation of T cell subsets can be used as a viable treatment option. A low number of study participants and a varied time between visit 1 and follow-up visits made it hard to draw definitive statistical conclusions from preliminary work performed for this thesis. Neither treatment option has beneficial effects to modify proportions of CD8<sup>+</sup> T cells or CD4<sup>+</sup>CD25<sup>high</sup> Treg cells to a “normal” level suggesting that, as proportions of CD8<sup>+</sup> T cells are abnormally regulated in SSc-PAH patients, a more directed therapy to improve proportions of CD8<sup>+</sup> T cells is needed.

E-RAs are an effective treatment option for PAH patients as they inhibit vasoconstriction within the pulmonary vessels. The effect that E-RAs

have on T cell subsets however, is under-investigated. Stimulation of ET-1 receptors has been shown to provoke an increase in T cell number and their recruitment to inflammatory sites, whilst E-RAs reduce T cell recruitment to sites of injury including the lungs (Fujitani *et al*, 1997; Sampaio *et al*, 2000; Zarpelon *et al*, 2012). ET-1 also acts through ET-1B receptors on ECs, to produce eNOS, which converts L-arginine into NO. NO production has been shown to inhibit IL-2 signalling in Th1 cells, leading to anergy of these cells (Bauer *et al*, 1997). In addition, SSc-PAH patients taking Bosentan for 12 months have been shown to exhibit reduced serum levels of ICAM-1, VCAM-1, P-selectin and platelet endothelial cell adhesion molecule 1 (PECAM-1), whilst T cells expressing lymphocyte function-associated antigen 1 (LFA-1) returned to normal levels from an increased level at baseline. These data suggest that Bosentan can regulate T cell / EC interactions and can inhibit T cell recruitment (Iannone *et al*, 2008).

PDE-5 inhibitors such as Sildenafil are also a common choice in PAH treatment. Sildenafil has been shown to increase cGMP levels in T cells resulting in an increase in number and activation state of tumor-infiltrating CD8<sup>+</sup> T cells. However, it has been shown not to have an effect on the proportion of CD4<sup>+</sup> T cells, including Treg cells (CD4<sup>+</sup>Foxp3<sup>+</sup>) in cancer patients (Serafini *et al*, 2006). PDE inhibitors such as Rolipram have also been implicated in the resolution of inflammatory responses via their ability to inhibit IL-2 production in T cells (Robicsek *et al*, 1991; Gantner *et al*, 1998; Claveau *et al*, 2004). IL-4 and IL-5 production in Th2 cells has also been shown to be inhibited by PDE-4 inhibitors and non-selective PDE inhibitors such as Ibudilast can change the cytokine profile towards a Th2 phenotype (Crocker *et al*, 1996; Feng *et al*, 2004). These studies suggest that PDE inhibitors may have an effect on the number and function of T cell subsets in other disease settings, however, the effect that PDE-5 specifically has on T cell subsets in PAH remains unclear and further analyses need to be undertaken to determine their effects.

Taken together, the results from my studies suggest that E-RAs may regulate production and activation of T cell subsets as a therapy for PAH. However, a more specific use of immunosuppressant therapies to regulate T cell subsets in conjunction with this treatment may be needed. Indeed, in

patients with SSc, Iloprost and low dose cyclosporine A have already been shown to improve patient skin fibrosis and reduce IL-6 levels, however side effects of cyclosporine A use are of concern and this drug combination does not address the rebalancing of T cell subsets that are abnormal in PAH patients (Filaci *et al*, 1999). In SSc patients, Bosentan has been shown to reduce levels of IL-2, IL-6, IL-8 and IFN- $\gamma$ , whilst Sildenafil has been shown to reduce IL-1 $\beta$ , IL-2, IFN- $\gamma$  and TNF- $\alpha$  serum levels in a mouse model of multiple sclerosis. These results suggest that PAH specific treatments are capable of influencing the cytokine milieu towards a Th2 phenotype (CD4<sup>+</sup> T cell dominant), which could protect against disease and promote the resolution of inflammatory processes (Bellisai *et al*, 2011; Nunes *et al*, 2012).

Data will continue to be collected by the pulmonary vascular research group at Sheffield University, as it is anticipated that an increase in information regarding T cell subsets and treatments will provide a greater understanding of how these specific drugs are affecting the T cell populations and how they could be manipulated to aid prevention of disease progression in PAH.

## **2.4.4 Limitations leading to future work**

Despite the novel findings presented in this thesis, this work has limitations mainly due to the low patient numbers. To gain a larger statistical population, more time is required to investigate a larger number of patients.

### **2.4.4.1 Patient cohorts**

Despite the large patient cohort recruited throughout the duration of the project, only around half could be used in this study. Sub-optimal PBMC isolation, diagnosis of “not PAH” after initial blood draw and a low CD3<sup>+</sup> T cell event count for successful flow cytometric analysis were problems that limited numbers. Some patients that were initially thought to have IPAH or SSc-PAH were subsequently diagnosed as having another subset of PH (class 2-5 of Dana point classification) and were also not used in this study. Thus, recruitment of a sufficient number of patients to identify changes in T

cell subsets between patients and controls was challenging. However, as the study progressed, more accurate phenotyping of patients and analysis of T cell subsets by flow cytometric analysis occurred, leading to a more reliable set of results and a higher number of patients being recruited to the study.

Patients returning to the SPVDU after visit 1 were also recruited for follow-up analysis of how PAH specific drug treatment was affecting proportions of T cell subsets within peripheral blood. Unfortunately these return visits were often irregular and variability made patient comparison difficult. Despite this, changes appeared to be occurring in T cell populations in PAH patients on PAH specific therapy, therefore this work needs further validation. A longer time period to collect samples will enable more analyses to be undertaken. This work is continuing within the pulmonary vascular disease group at Sheffield University.

Unfortunately, end stage lung tissue was not available from IPAH or SSc-PAH patients following death, as post mortem tissue is currently unavailable in Sheffield. Lung tissue sections would allow analysis of infiltrating T cell subsets such as CD4<sup>+</sup>, CD8<sup>+</sup> and Treg cells as well as their activation status. These data could then be compared with peripheral blood samples to further elucidate the reason for changes in circulating peripheral T cell subsets noted previously in this thesis. Even though studies into CD4<sup>+</sup> and CD8<sup>+</sup> T cell proportions within IPAH patient tissue have been carried out, this is not the case for SSc-PAH and analysis of infiltrating Treg cells has not been performed in either disease group.

#### **2.4.4.2 Foxp3 expression in T regulatory cells**

Levels of Foxp3 expression in CD4<sup>+</sup>CD25<sup>high</sup> Treg cells could not be detected in peripheral blood samples, as event numbers detected by flow cytometry were extremely low. A possible explanation could be that the levels of Foxp3 were too low to detect, and / or that the transient expression of Foxp3 was being overlooked at the time of analysis.

The validity of Foxp3 as a marker of Treg cells is still questionable. Some researchers believe that it is a highly valuable marker of functional Treg cells, whilst others have noted an upregulation of Foxp3 in human

activated non-regulatory CD4<sup>+</sup> T cells and CD8<sup>+</sup> regulatory T cells, thereby making it less reliable as a definitive marker of Treg cells (Banham *et al*, 2006; Liu *et al*, 2006; Joosten *et al*, 2007; Wang *et al*, 2007). Previous studies have also shown that Foxp3 is not expressed on IL-10 secreting Treg cell populations and Treg cells can also downregulate their expression of Foxp3, losing their suppressor functions (Vieira *et al*, 2004).

## 2.4.5 Concluding remarks

The work undertaken in this thesis confirmed a significant decrease in the proportion of circulating CD8<sup>+</sup> T cells in SSc-PAH patients, but failed to show an increase in the proportion of circulating CD4<sup>+</sup>CD25<sup>high</sup>Treg cells, as previously described by Austin *et al* and Ulrich *et al* in IPAH patients undergoing PAH therapy (Ulrich *et al*, 2008; Austin *et al*, 2010). This work further confirms the importance of determining changes in lymphocyte subsets in treatment-naïve patients, to determine the effect that the disease, and not the treatments, have on circulating T cell populations.

A negative correlation between proportions of circulating CD4<sup>+</sup> T cells and clinical parameters, including CI and the shuttle walk test, was observed in PAH patients. This suggested that with further studies, the proportion of circulating CD4<sup>+</sup> T cells has potential to be used as a valuable diagnostic or prognostic biomarker in both IPAH and SSc-PAH patients (Pendergrass *et al*, 2010).

# Chapter 3 ApoE<sup>-/-</sup>/IL-1R1<sup>-/-</sup> high fat diet model of pulmonary arterial hypertension

## 3.1 Introduction

Animal disease models offer a valuable insight into the progression of a disease rather than an end stage analysis of the disease state, which can be gained from patient samples at death. These models also allow for the detection of transient changes in factors affecting disease progression and biomarkers. Despite differences in onset of the disease, most models converge on the same endpoints of pulmonary vascular remodelling, an increase in mPAP and right ventricular failure. Although these models closely resemble human disease, no single model can completely recapitulate it.

Determining whether alterations in T cell profiles occur at the same time, prior to, or after changes in pulmonary circulation requires the use of animal models of PAH. It is also uncertain whether inflammation itself causes PAH or if inflammation occurs as a result of PAH. It could be possible that both of these situations occur together (Tamosiuniene and Nicolls, 2011).

Several models of PAH providing evidence for T cell involvement in the pathogenesis of PAH have been published. Studies have used immunohistochemistry to show CD3<sup>+</sup> and CD45<sup>+</sup> T cell localisation to lesions within the pulmonary vasculature in these models (Marsboom *et al*, 2008; Song *et al*, 2008; Steiner *et al*, 2009; Summer *et al*, 2009; Cuttica *et al*, 2011). The presence of these cells could be either as a consequence of the disease (attempting to resolve inflammatory processes) or in a causative role (instigating an inflammatory response).

Work undertaken by Tarasviciene-Stewart *et al* using an athymic nude rat model of PAH (in which the animals were given a vascular endothelial growth factor receptor blocker to induce PAH), has led to the

discovery that the absence of T cells enhances vascular remodelling, whilst replenishing this subset of lymphocytes prevents vascular remodelling (Taraseviciene-Stewart *et al*, 2007). In a more recent publication by this group, immune reconstitution using CD4<sup>+</sup> or CD4<sup>+</sup>CD25<sup>high</sup> T regulatory cells, was shown to lead to attenuated development of PAH (Tamosiuniene *et al*, 2011). These data, along with other reports, suggest a strong link between changes in T cell subset proportions and the progression of PAH, thereby providing an interesting area for further investigation.

Apolipoprotein E (ApoE) is a plasma glycoprotein involved in cholesterol metabolism due to its ability to transport cholesterol and other lipids among various cells in the body. It is a constituent of all lipoproteins except low-density lipoproteins and is synthesised in the liver, brain, spleen and kidney, but has recently been shown to be produced by monocytes and macrophages in blood vessels (Meir and Leitersdorf, 2004). In SMCs, BMP-2 signalling is peroxisome proliferator-activated receptor gamma (PPAR $\gamma$ ) and ApoE dependent and produces antiproliferative effects on SMCs. Mice with a deletion of PPAR $\gamma$  in SMCs spontaneously develop PAH (Hansmann *et al*, 2008). ApoE is also thought to have anti-inflammatory properties as it can suppress type 1, pro-inflammatory responses by inhibiting lymphocyte proliferation (Kelly *et al*, 1994; Ali *et al*, 2005). ApoE also protects against the development of atherosclerosis as ApoE<sup>-/-</sup> mice develop spontaneous hypercholesterolemia and atherosclerotic lesions (which can be exacerbated by an atherogenic diet), similar to those seen in the human condition (Bellosta *et al*, 1995; Thorngate *et al*, 2000).

IL-1 has also been implicated in the pathogenesis of atherosclerosis via its ability to induce SMC proliferation and act as a co-stimulatory signal for T cell activation (Moyer *et al*, 1991; Hansson, 2001). IL-1 is a pro-inflammatory cytokine released by a variety of cells including SMCs, ECs and mononuclear phagocytes and a link between increased serum levels of IL-1 and disease progression in PAH patients has been observed (Hogquist *et al*, 1991; Humbert *et al*, 1995; Imai *et al*, 2000; Clarke *et al*, 2009). Chronic treatment with human IL-1RA has been shown to reduce PAH and RVH in the MCT model of PAH and reduce PAH development in fat-fed ApoE<sup>-/-</sup> mice

further suggesting a role of IL-1 in the pathogenesis of PAH (Voelkel and Tuder, 1994; Lawrie *et al*, 2011).

Because of a previous interest in atherosclerosis, our laboratory had access to mice deficient in IL-1R1 and ApoE. A cross was made between these two strains, which revealed the surprising finding that ApoE<sup>-/-</sup>/IL-1R1<sup>-/-</sup> mice acquired reduced atherosclerosis, but developed a severe form of PAH (RVSP average 75 mmHg) when fed on a high fat diet (paigen diet). A more severe form of distal pulmonary vascular remodelling was noted in these mice compared to ApoE<sup>-/-</sup> mice (Lawrie *et al*, 2011). In this model there is an exaggerated PAH phenotype despite reduced atherosclerosis and this is thought to be due to an alternatively primed IL-1R1 transcript expressed within the lungs, but not the aorta of these mice. This allows intact IL-1 signalling within the lung and pulmonary vasculature. Increased serum cytokine levels (IL-6 and IL-1 $\beta$ ) have also been noted in this model along with an increase in perivascular inflammatory cell infiltrates. Taken together, these findings make this model an interesting tool to study the involvement of inflammation in the pathogenesis of PAH. Immunohistochemical analysis revealed complex lesions and perivascular CD3<sup>+</sup> T cells in the lungs of these mice. This model is therefore phenotypically relevant to studying the inflammatory processes involved in the development of these vascular lesions and the progression of PAH and provides a novel model of PAH development.

Whilst work undertaken in the athymic rat treated with Sugren 5416 has noted inflammatory cell infiltration of tissue surrounding pulmonary vessels preceding an increase in right ventricular pressure by several days (Tamosiuniene *et al*, 2011), a timecourse of the disease aimed at identifying the exact point at which this increase in T cells occurs within the peripheral circulation and lung tissue has not been undertaken. Therefore, work described in this chapter aimed to characterise T cell subsets in chow and fat-fed ApoE<sup>-/-</sup>/IL1R1<sup>-/-</sup> animals along a timecourse, as well as in CD4<sup>+</sup> T cell depleted ApoE<sup>-/-</sup>/IL1R1<sup>-/-</sup> animals, and relate changes in T cell subsets to vessel remodelling within the pulmonary arteries. It also determined whether changes in proportions of T cell subsets occur as a cause or consequence of disease progression. I hypothesised that an increase in the proportion of

circulating T cells would occur as disease progressed. I also hypothesised that with the deletion of CD4<sup>+</sup> T cells, disease phenotype would worsen due to the removal of protective Treg cells within the CD4<sup>+</sup> T subset.

## 3.2 Methods

All experimental procedures were approved by the University of Sheffield Ethics Committee and conformed to Home Office regulations under the Animals Scientific Procedures Act (1986). Work was carried out under project licence PPL 40 / 3517. ApoE<sup>-/-</sup>/IL1R1<sup>-/-</sup> mice were generated at JAX labs by cross breeding ApoE<sup>-/-</sup> (JAX 2052) with IL-1R1<sup>-/-</sup> (JAX 3245) mice (Maine, USA) (Chamberlain *et al*, 2006; Chamberlain *et al*, 2009). All mice were on a C57 / BL6 background and housed in a controlled environment with a 12 hour light / dark cycle at 22°C and a constant air pressure. Littermates were housed together with a maximum of 5 animals per cage, with all cages being provided with environmental enrichment.

### 3.2.1 ApoE<sup>-/-</sup>/IL-1R1<sup>-/-</sup> timecourse study

Forty 10 week old male ApoE<sup>-/-</sup>/IL1R1<sup>-/-</sup> mice were fed on either paigen diet (18.5% fat, 0.9% cholesterol, 0.5% cholate, 0.259% sodium) or chow diet (4.3% fat, 0.02% cholesterol) *ad libitum* (n=5-6 per group) for 1, 2, 4, 6 or 8 weeks. Paigen diet was supplied by Special Diet Services (Braintree, Essex, UK) and chow diet was supplied by Harlan Global Diets (Madison, USA) (Appendix 1, section 4). Time points of 1, 2, 4, 6 and 8 weeks were selected for both chow and paigen-fed mice. At each time point, peripheral blood and lung tissue were collected and weight measurements (to the nearest 0.1g) were taken (week 0 and at each time point before sacrifice).

Extensive phenotyping of this animal model was not carried out to maximise the opportunity to optimise a flow cytometry protocol to stain small amounts of blood from mice. Assessment of disease was assessed by

quantifying the degree of pulmonary vascular remodelling on processed lung sections.

### **3.2.1.1 Cardiac puncture**

Cardiac puncture was performed to collect peripheral blood samples, as this provided the largest volume of blood for flow cytometry analysis. Around 1 mL blood was collected via cardiac puncture for flow cytometry. Cardiac puncture was performed on anaesthetised animals after loss of the pedal reflex. The animal was placed on a pre-heated mat (37°C) on its back. The heart was palpated before a 20 G needle, attached to a syringe, was inserted at a 25° angle, slightly left of and under the sternum. The needle was directed towards the animal's head. Blood was drawn up into the syringe from the heart until between 600-1000 µL blood had been collected. The blood was then transferred into a BD Vacutainer® Blood Collection Tube and placed on ice to maintain cellular integrity.

### **3.2.1.2 Lung and splenic tissue preparation**

To detect changes in proportions of T cells present in splenic tissue and the migration of these cells into the lung tissue, the right lung and spleen were also removed for immune cell analysis (at week 8 time point only). These were both passed through separate 100 µm cell strainers (BD Biosciences, Oxford, UK) into 500 µL of 0.15% w/v Collagenase A (Roche, Welwyn Garden City, UK) and PBS respectively. Collagenase A was used to dissociate lung tissue and liberate immune cells to be analysed using flow cytometry. Lung tissue was allowed to incubate with collagenase A for 1 hour at 37°C in a water bath before being washed in PBS and processed for flow cytometric analysis. Lung tissue was also incubated with 500 µL of 1X GIBCO® Hank's Balanced Salt Solution which was used as a negative control, to rule out the possibility of non-tissue derived cells from the blood in the lung affecting the results. T cell proportions were compared using flow cytometry prior to the use of Collagenase A in these animal studies.

### 3.2.1.3 Flow cytometric analysis of T cell subsets in blood and tissue samples

Detection of changes in T cell subsets in peripheral blood and liberated cell suspensions was performed using flow cytometric analysis. Blood and dissociated tissue samples were split into 3 equal amounts and placed in separately labelled epindorfs labelled “unstained”, “isotype controls” and “stained”. Cell suspensions were stained according to the manufacturer’s instructions using the panel of fluorescently conjugated antibodies and isotype controls shown in Appendix 1, section 3. In brief, cell suspensions were incubated with the required amount of fluorescently conjugated antibodies against CD3, CD4, CD8, CD25 and a UV live / dead marker, for 30 minutes at 4°C in the dark, before the cells were washed at 300 x g for 5 minutes at 4°C in cell staining buffer (PBS + 10% v/v FCS).

In studies of T cell subsets in mouse models of PAH, antibodies raised against CD4 and CD25 were used to define Treg cells. In mice, all CD4<sup>+</sup> and CD25<sup>high</sup> cells are regulatory T cells, whilst in humans this is not the case, as CD25<sup>high</sup> cells are not all Treg cells (Taams *et al*, 2001; Su *et al*, 2012). Therefore, additional Treg cell markers were used to define Treg cells in human studies.

The cells were then resuspended in 100 µL cell staining buffer and incubated with 4 mL 1X red blood cell lysis solution (Miltenyi Biotec, Surrey, UK) for 20 minutes at room temperature in the dark. The cells were then washed in cell staining buffer as previously described and the cells resuspended in 20 µL cell staining buffer before 150 µL 1X CELLFix™ was added (BD Biosciences, Oxford, UK). Samples were stored at 4°C to allow for analysis at a later date (within 4 days).

Lymphocytes were identified on the basis of their size and granularity using a forward and side light scatter plot with dead cells excluded from the analysis using the UV live / dead dye. Data on a minimum of 10,000 CD3<sup>+</sup> events was collected for each sample in the lymphocyte gate and FACSDIVA™ software was used for analysis. The gating strategy and example scatter plots used to analyse the samples are shown in Figure 3.1. Compensation was undertaken using anti-rat IgG-coated compensation

beads (BD Biosciences, Oxford) and ARC™ reactive beads (Invitrogen of Life Technologies Ltd, Paisley UK) as previously mentioned in Chapter 2.2.2.1. FACSDIVA™ software was used to automatically set up and apply the compensation.

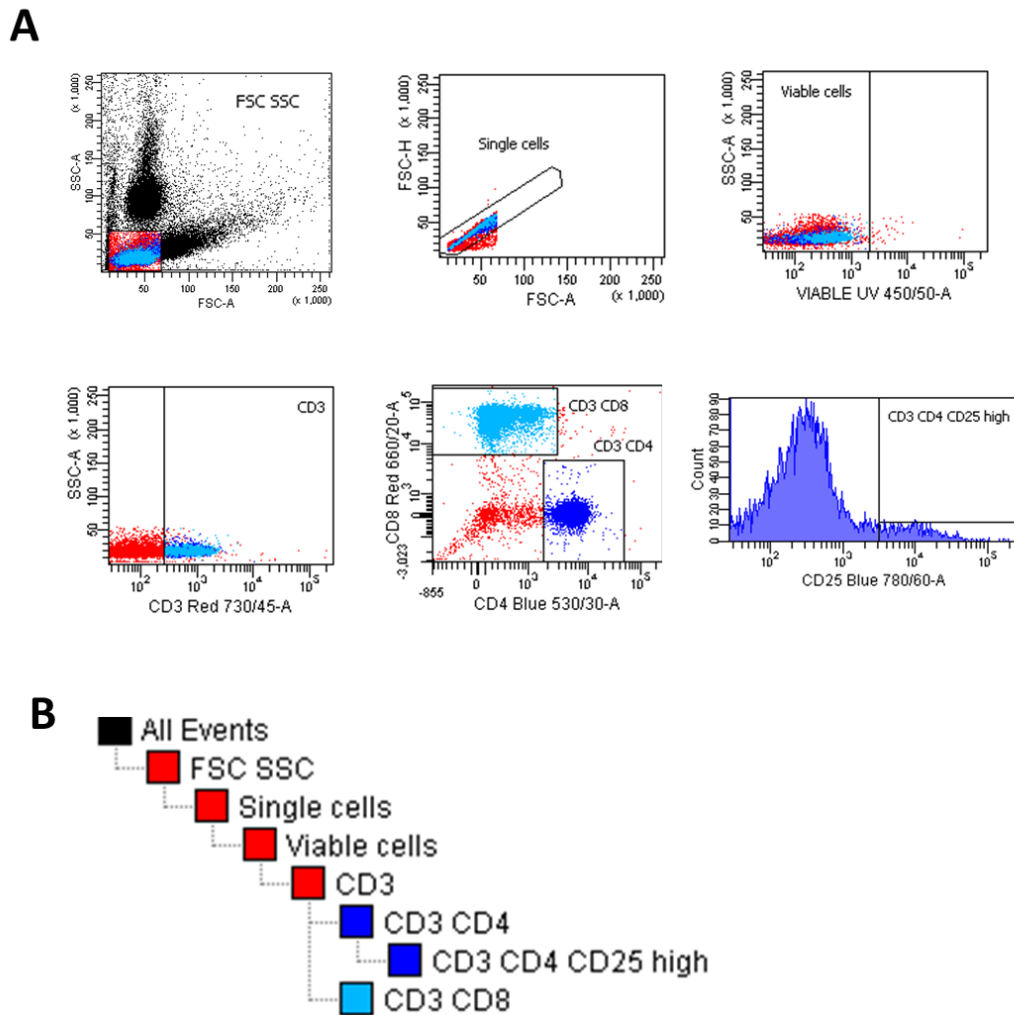


**Figure 3.1 Representative gating hierarchy and dot plots templates used to define T cell subsets in blood and tissue samples.**

A) Representative dot plots showing T cell populations. B) Representative gating hierarchy. Forward scatter (FSC) and side scatter (SSC) cells gated on, then doublet cells removed to leave single cells. Viable cells were then gated on and a gate placed around CD3<sup>+</sup> T cells. T cell subsets including CD4<sup>+</sup>, CD8<sup>+</sup> and CD4<sup>+</sup>CD25<sup>high</sup> were then gated on.

### **3.2.1.4 Tissue preparation for analysis by immunohistochemistry**

The abdominal aorta was exposed and cut to allow blood to drain. A transverse incision was made below the diaphragm from one side of the animal to the other, exposing the liver and stomach. A vertical abdominal incision was then made to expose the lower abdominal contents. Using small forceps, the zyphoid process was lifted and a hole was made in the diaphragm below the sternum. The right and left sides of the chest wall were then cut free and the chest wall removed. A saline-filled syringe was inserted into the right ventricle and saline injected slowly to flush the lung of blood. A mid-line incision was made in the neck to expose the trachea thereby enabling it to be cut. The heart and lungs were removed en bloc and the spleen removed from the abdominal cavity.

Blood was flushed out of the body by dissection of the lower aorta and the left lung was inflated using a 10 mL syringe attached to a 20 G needle. This was then filled with 10 mL water and attached to a small length of tubing inserted into the trachea. To inflate the lung, a tie was made around the trachea and tube to ensure water retention. The water was then injected slowly into the lung to inflate it. The lung and heart were then placed in a falcon tube containing 10 mL formalin for 24 hours to fix the tissue. After 24 hours, the left lung was removed and processed as below.

Lung and splenic tissue was embedded and cut according to sample size and type (lungs into 4 pieces, spleens embedded whole). Tissue was sandwiched between 2 sheets of Whatman Grade 1 filter paper then placed inside a plastic cassette. Cassettes were then placed in a large beaker filled with 50% v/v ethanol, covered and left to dehydrate for 1 hour. The 50% v/v ethanol was removed and replaced with 70% v/v ethanol for 1 hour before again being replaced by 90% v/v ethanol for 1 hour. Two 100% v/v ethanol dehydration steps were then performed for 1 hour each before the cassettes were put into a mix of 50:50 xylene:ethanol mix for 1 hour. The cassettes were removed, placed in xylene for two 1 hour periods and placed into pots of molten wax at 60°C for 1 hour.

After 1 hour in molten wax, the cassettes were removed from the pots and the tissue block recovered. The flat side of the cut tissue was placed flat-side down into clear plastic moulds before molten wax was used to fill the mould and the cassette lid placed on top. This was repeated for all samples and the moulds left to set overnight before sections were cut.

For sectioning, wax blocks were pressed from the moulds and placed on ice for at least 1 hour, prior to cutting with a Leica RM2135 microtome (Leica Microsystems, Wetzlar, Germany). All vessels were cut to 5  $\mu$ m thickness and floated out on a water bath, heated to 35°C, to flatten the sections. Sections were mounted on Polysine™ glass slides.

### **3.2.1.5 Immunohistochemical analysis**

Lung sections were stained with antibodies against CD8, CD4, CD25, smooth muscle actin (SMA) and vessel elastin to assess marker expression within the lungs taken from both chow and paigen fed ApoE<sup>-/-</sup>/IL1R1<sup>-/-</sup> mice. This involved de-waxing the slides in 100% v/v xylene for 10 minutes before re-hydrating them through graded ethanol to water (100% v/v ethanol; 100% v/v ethanol, 90% v/v ethanol, 70% v/v ethanol, 50% v/v ethanol each for 2 minutes). Endogenous peroxidases were then blocked with 3% hydrogen peroxide for 10 minutes before being rinsed in water. The slides were incubated in 1% w/v milk buffer (Marvel, available in supermarket stores) for 30 minutes at room temperature to stop non-specific binding of the secondary antibody. Excess milk buffer was removed by tilting the slide and blotting the drained liquid before the primary antibody was added for 1 hour at room temperature in a humidity chamber (see Appendix 1, section 5 for all antibodies and clone numbers used in immunohistochemical analyses). The slides were washed 3 times in PBS before being incubated with the secondary antibody for 30 minutes at room temperature in the humidity chamber. The slides were washed a further 3 times in PBS and incubated for 30 minutes with Vectastain Elite ABC kit working reagent (see Appendix 1, section 5), washed and then incubated with DAB substrate for 5 minutes before being rinsed in water. The slides were counterstained using Carazzi's Haematoxylin for 1 minute then washed in water. The slides were finally

dehydrated through graded alcohols 50% v/v ethanol, 70% v/v ethanol, 90% v/v ethanol, 100% v/v ethanol; 100% v/v ethanol each for 2 minutes) to 100% v/v xylene, before being mounted using DPX mountant (see Appendix 1, section 5).

For some stains it was necessary to use an antigen retrieval step before incubating sections with the primary antibody. Antigen retrieval is a method that can be used to break up protein cross-links formed when tissues are processed by formalin fixation. This allows hidden antigenic sites to become available for antibodies to bind to. Several heat mediated antigen retrieval methods were used for a variety of different staining procedures (see Appendix 1, section 5). The antigen retrieval step was undertaken after incubation with hydrogen peroxide and before the milk buffer step. Citrate buffer, TRIS / EDTA or EDTA (see Appendix 1, section 5) were heated in a heat proof container in a water bath to 95°C before slides were added for 20 minutes (10 minutes for EDTA). After this time, the heat proof container was removed from the water bath and left to cool to room temperature for a further 20 minutes. The slides were then rinsed once in PBS.

For Millers Elastin staining, slides were re-hydrated in 100% v/v xylene for 10 minutes before passing through 100%, 90% and 70% v/v ethanol for 2 minutes each, then in water for 2 minutes. The sections were oxidised with potassium permanganate for 3 minutes. The slides were rinsed in water then bleached with oxalic acid and rinsed in water again. The nuclei were stained with Carazzi's haematoxylin for 2 minutes before the tissue was differentiated by incubating with acid alcohol for a few seconds (see Appendix 1, section 5). The slides were "blued" with hot running water before being stained with alcian blue pH 2.5 for 5 minutes. The slides were rinsed in water followed by 95% v/v industrial methylated spirits before Miller's Elastin stain was added for 30 minutes. After rinsing in water, the slides were put in 95% v/v IMS briefly before being rinsed in water. Curtis' Modified van Gieson was added to the slides for 6 minutes before they were dehydrated back through 70%, 90% and 100% v/v ethanol then 100% v/v xylene. The slides were mounted using DPX mountant and left to dry for 24 hours.

Stained slides were analysed using a camera mounted to a light microscope utilising NIS-elements software version 3.0 (Nikon, Badhoevedorp, The Netherlands).

### **3.2.1.6 Analysis of Vessel Remodelling**

To determine the effect that paigen diet had on the process of remodelling within pulmonary arteries, two techniques were used to assess and quantify the amount of remodelling. This included analysing the media and cross-sectional area of vessels to give a ratio of the number of affected vessels and also the degree to which they were affected, by classifying each vessel as fully occluded, partly occluded and not occluded. These analyses were performed on SMA and Millers Elastin stained sections using NIS-elements software. For both analyses, the pulmonary arteries were categorised based on their external diameter and divided into 3 groups: small pulmonary arterioles with a diameter of  $<50\ \mu\text{m}$ , medium pulmonary arteries with a range in diameter from 51 to  $100\ \mu\text{m}$ , and large pulmonary arteries with a diameter greater than  $100\ \mu\text{m}$ . For SMA analysis, the degree of muscularisation was calculated as the area of the media divided by the cross-sectional area of the whole artery (media / CSA). A well characterised method for analysing the percentage of muscularised vessels within tissue was used which included measuring alcian blue elastic van Gieson staining. 6 views of lung sections and the pulmonary arteries were categorised as occluded (slit-like, or no lumen remaining), muscularised (crescent, or complete rings of muscle), or nonmuscular (no apparent muscle) and counted (Schermuly, 05; Lawrie *et al*, 2011).

### 3.2.2 CD4<sup>+</sup> T cell depletion model

To determine the effect that depletion of CD4<sup>+</sup> T cells had on disease progression, an antibody against this cell subset was administered to fat-fed ApoE<sup>-/-</sup>/IL1R1<sup>-/-</sup> mice for 4 weeks and then the mice left to develop PAH on paigen diet. The haemodynamic assessment of disease progression was then compared to IgG treated control mice fed with paigen diet for 8 weeks. The protective effect that these cells had on the disease phenotype was also assessed, as the removal of this cell subset also removed Treg cells involved in inflammatory response resolution. This study also provided information regarding the question of whether CD4<sup>+</sup> T cells were found in the lung as a cause or consequence of the disease.

Twelve 10-13 week old male ApoE<sup>-/-</sup>/IL1R1<sup>-/-</sup> mice were fed paigen diet for 8 weeks. Mice were ear clipped to identify individual mice within a cage. Weight measurements (to the nearest 0.1g) were taken at week 0 and week 8. Intraperitoneal injections of either LEAF purified anti-mouse CD4 antibody or purified rat IgG control (see Appendix 1, section 4) both at a dose of 0.5 mg / mouse, were given once weekly, for 4 weeks from the commencement of paigen diet. Six animals were assigned to each treatment group (Figure 3.2). Before mice were sacrificed (after 8 weeks of feeding on paigen diet), echocardiography and cardiac catheterisation were undertaken to assess the haemodynamic changes between the two groups. Data gained from this would later be used to compare changes in T cell profiles to corresponding changes within the pulmonary circulation.

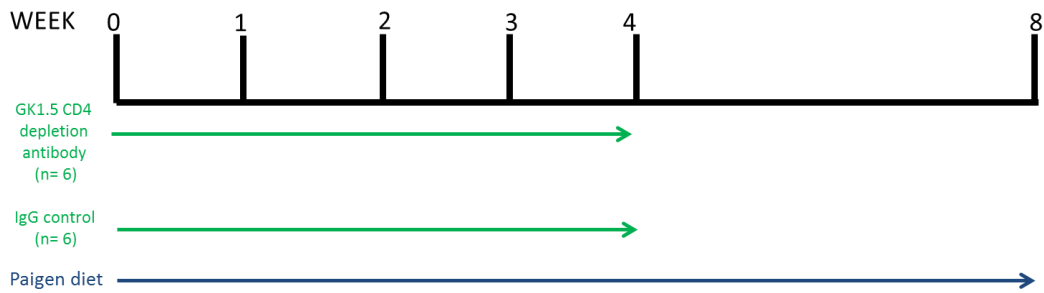


**Figure 3.2 Experimental design for the CD4<sup>+</sup> T cell depletion study.**

An 8 week timecourse was set up to study the progression of PAH in IgG treated controls and CD4 antibody treated animals fed on paigen diet. 12 ApoE<sup>-/-</sup>/IL1R1<sup>-/-</sup> mice were split into two groups (6 in each group) and given 0.5 mg / mouse / week dose of GK1.5 CD4 depletion antibody or IgG control for 4 weeks. After this time the mice continued to be fed on paigen diet for a further 4 weeks before being sacrificed, echocardiography and cardiac catheterisation carried out and organs and tissues removed.

### 3.2.2.1 Echocardiography

To gain a greater understanding of the changes in size and shape of the heart, echocardiography was performed using the Vevo 770 system (Visual Sonics, Toronto, Canada) using an RMV707B scan head. Data collection was undertaken by Dr Abdul Hameed, Ms Nadine Arnold and Dr Alan Lawire and data analyses by myself. Anaesthetised animals were placed on a heated platform and covered to minimise heat loss and rectal temperature, heart rate, and respiratory rate recorded continuously throughout the study. Anaesthesia was induced and maintained using isoflurane through oxygen (5% v/v Isoflurane, 2 L / minute oxygen), maintaining heart rates at around 450 to 500 beats per minute, whenever possible. The mice were depilated and preheated ultrasound gel was applied (Aquasonics 100 Gel; Parker Labs, Inc., Fairfield, NJ). From the right parasternal long axis view, right ventricle free wall parameters were determined using M-mode.

Standard parameters of the left ventricle were measured using 2-dimensional, M-mode and Doppler pulse wave in the short axis view at the level of the papillary muscles. Analysis was performed offline using the

accompanying software (Vevo 770, V3.0; Visual Sonics). Measurements were taken during the relevant phase of the cardiac cycle that did not coincide with inspiration artefact.

### **3.2.2.2 Cardiac catheterisation**

To measure the haemodynamic alterations that are a consequence of disease, left and right ventricular catheterisation were performed using a closed chest method. The right ventricle was assessed via the right external jugular vein and the left ventricle via the right internal carotid artery under isoflurane-induced anaesthesia.

The Millar catheter was placed in a beaker of saline for 20 minutes prior to calibration. The pedal reflex was then checked before the neck fur was wetted with ethanol. Fine scissors were used to make an incision to the right of midline from the neck to the clavicle to expose the external jugular vein. Fine curved forceps were used to dissect the tissue around the vein. The vein was then isolated and a 4.0 suture passed underneath it to ligate the vein distal to the heart. A second suture was placed around the vein and loosely tied proximally to the heart (ready to tie around the catheter once inserted). Tension was then placed on the distal suture with forceps so that the vein was stretched before a 25 G 5/8" needle (bent at a 90° angle) was inserted into the vein and the catheter inserted simultaneously.

After the catheter was inserted the suture was loosely tied off to prevent bleeding. The catheter was then advanced into the right ventricle. Systemic pressures were recorded by pulling the catheter back and using the proximal suture to tie off the vein. CO data was derived using a pressure volume catheter and the CI was normalised by body weight.

Data were collected from the right ventricle using a Millar ultra-miniature pressure-volume PVR-1030 1F catheter (Millar Instruments Inc, Houston, TX, USA) and from the left ventricle using a Millar ultra-miniature pressure-volume PVR-1045 1F catheter, coupled to a Millar MPVS 400 and a PowerLab Client data acquisition system version 7 (AD Instruments, Oxford, UK) and recorded using Lab chart Pro software (version 6.0, for

Microsoft windows, AD Instruments, Oxfordshire, UK). Pressure volume analysis was performed using PVANv2.3 (Millar Instruments Inc, Houston, USA).

### **3.2.2.3 Blood and tissue sample collection, preparation and analysis**

As previously described, peripheral blood samples were collected via cardiac puncture, and lung and splenic tissue collected and prepared for flow cytometric analysis. Tissue sections were prepared for immunohistochemical and immunocytochemical analysis of vessel remodelling and T cell marker expression (see Chapter 3.2.1.1 - 3.2.1.6 for collection, preparation and analysis of samples).

### **3.2.2.4 CD4<sup>+</sup> T cell depletion confirmation**

To confirm that CD4<sup>+</sup> T cells had been efficiently depleted, blood was taken from 6 randomly selected mice (3 on IgG control and 3 on CD4-depletion antibody) and stained using fluorescently conjugated antibodies against CD3, CD4 and CD8 at week 5 (1 week after cessation of administering the anti-CD4 antibody). Before being analysed by flow cytometry, 100 µL of blood was taken via a 20G needle from the tail vein into a BD Vacutainer® Blood Collection Tube. Blood was stained for 30 minutes as previously described in Chapter 3.2.1.3 and then red blood cells lysed. Antibodies were used in accordance with manufacturer's guidelines and a tube containing relevant isotype controls was also set up.

## **3.2.3 Statistical analysis**

A non-Gaussian distribution was assumed for all data. A two-way ANOVA with Bonferroni post hoc test was performed to compare data from treatment groups along a timecourse. A two-tailed Mann-Whitney U test with

95% confidence intervals was used, where appropriate, to compare pairs of data. A P value of < 0.05 was considered significant.

## **3.3 Results**

### **3.3.1 ApoE<sup>-/-</sup>/IL-1R1<sup>-/-</sup> timecourse**

Analysis of T cell subsets in peripheral blood from PAH patients revealed changes in several subsets. To determine whether these changes occur before, during, or later in the progression of vessel remodelling, an animal model of PAH was used, as patient samples only refer to end stage disease states. The ApoE<sup>-/-</sup>/IL-1R1<sup>-/-</sup> mouse model of PAH is a highly inflammatory based model of PAH, providing a relevant tool for the analysis of T cell subsets within blood and tissues.

Changes in haemodynamics, vessel remodelling and T cell subsets in peripheral blood, were assessed in animals after 1, 2, 4, 6 and 8 weeks on either chow or paigen diet.

#### **3.3.1.1 Haemodynamic and vessel remodelling analysis**

Disease progression was assessed using several parameters including body weight and measurements of vessel remodelling including the number of vessels affected and the degree of remodelling. Body weight was assessed at every time point (week 1 to 8) and no change in weight between animals fed on chow or paigen was noted at any time point.

The degree of muscularisation was measured using the area of the media divided by the cross-sectional area (CSA) of the whole artery (media / CSA). The medial / CSA of small pulmonary arteries and arterioles (<50 µm) in paigen-fed animals was increased significantly at week 6 compared to chow-fed controls ( $0.11 \pm 0.04$  vs  $0.40 \pm 0.05$ , n=4-5, P=0.0001) and also at week 8 ( $0.11 \pm 0.05$  vs  $0.37 \pm 0.04$ , n=4, P=0.0001) (Figure 3.3, A). There

was also an increase in media / CSA from week 2 onwards in paigen-fed animals, however these differences were not significant until week 6.

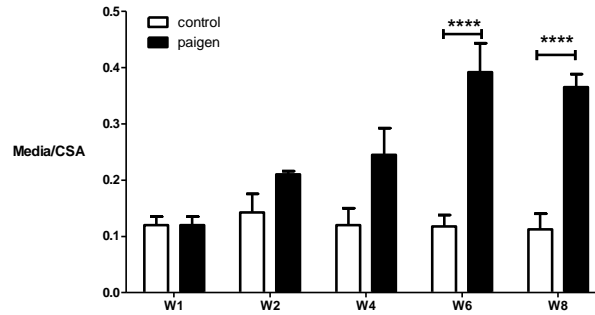
An increased media / CSA was also noted in medium sized vessels (50-100  $\mu\text{m}$ ) in paigen-fed animals at week 8 ( $0.06 \pm 0.005$  vs  $0.17 \pm 0.05$ ,  $n=4-5$ ,  $P=0.0001$ ). Again, a gradual increase in the media / CSA of vessels was noted in paigen-fed animals from week 1, however when compared to chow fed controls, there was no significant difference until week 8 (Figure 3.3, B).

An increase in media / CSA was also seen in large vessels ( $>100$   $\mu\text{m}$ ) at week 6 ( $0.04 \pm 0.04$  vs  $0.19 \pm 0.06$ ,  $n=4-5$ ,  $P < 0.01$ ) and at week 8 ( $0.06 \pm 0.005$  vs  $0.17 \pm 0.05$ ,  $n=4-5$ ,  $P < 0.001$ ) in paigen-fed animals compared to chow fed controls (Figure 3.3, C).

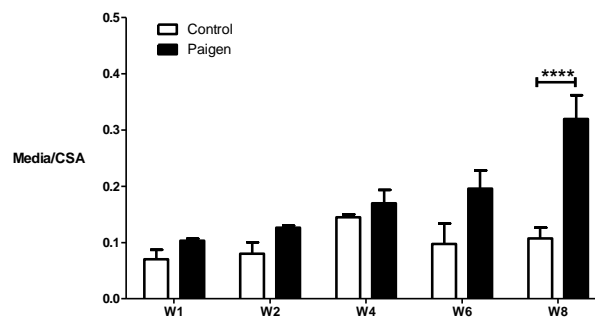
Taken together, these data suggest that an increased degree of muscularisation is occurring in pulmonary vessels of all sizes after commencement of the paigen diet in  $\text{ApoE}^{-/-}/\text{IL-1R1}^{-/-}$  mice. These data are comparable with previously published data regarding paigen feeding in the  $\text{ApoE}^{-/-}/\text{IL-1R1}^{-/-}$  mouse (Lawrie *et al*, 2011).

The proportion of muscularised vessels as a percentage of total vessels was calculated based on the number of affected pulmonary arteries divided by the total number of arteries multiplied by 100 in elastin van Gieson stained lung tissue sections. There is a trend for an increase in the percentage of muscularisation in all vessel sizes from week 6 onwards in paigen-fed animals compared to chow-fed controls (Figure 3.4, A-C). At week 8, the percentage of muscularisation increased in large vessels ( $>100$   $\mu\text{m}$ ) in paigen-fed animals compared to chow fed controls ( $12.45 \pm 5.71$  vs  $50.00 \pm 28.88$ ,  $n=4-5$ ,  $P < 0.05$ ) (Figure 3.4, C).

### A <50 $\mu$ m



### B 51-100 $\mu$ m



### C >100 $\mu$ m

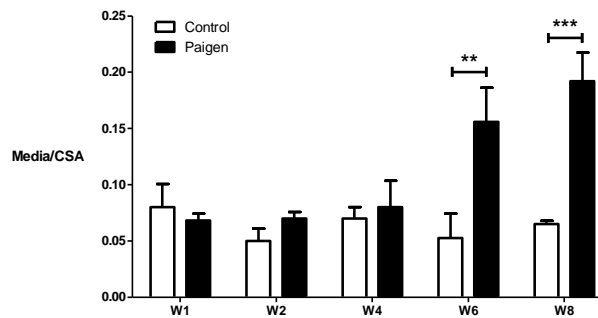


**Figure 3.3 Comparison of extent of muscularisation in paigen and chow fed animals from 1 week to 8 weeks after commencement of diets.**

Extent of muscularisation measured as media/cross sectional area (Media/CSA), was measured in chow fed (clear bars) and paigen-fed (black bars) mice at 1, 2, 4, 6, and 8 weeks (W1-8) after staining for smooth muscle actin and vessel size quantified using immunohistochemistry A) <50  $\mu$ m vessels, B) 51-100  $\mu$ m vessels and C) >100  $\mu$ m vessels.  $n=2-5$ . Error bars depict mean  $\pm$  SEM. Data analysed using a two-way ANOVA with Bonferroni post hoc test.  $P < 0.05$  was considered significant (\*).

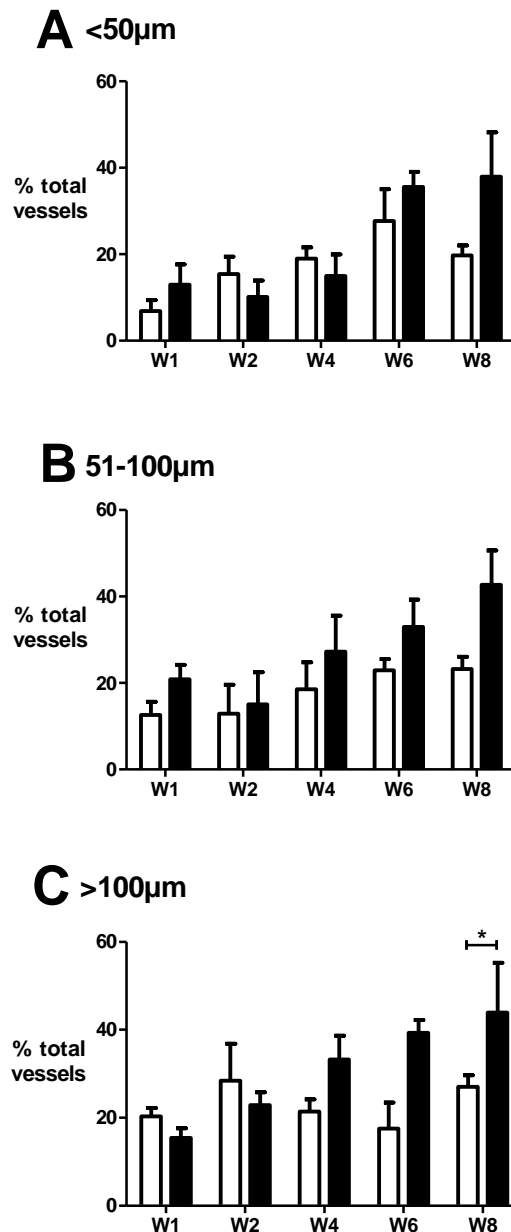


**Figure 3.4 Assessment of the percentage of muscularisation of pulmonary vessels in chow and paigen-fed animals.**

Vessel analysis using alcian blue elastin van Gieson staining on tissue sections taken from animals fed paigen or chow diet for 8 weeks. A) <50 µm vessel analysis B) 51-100 µm vessel analysis C) >100 µm vessel analysis. In all graphs the clear bar represents chow fed animals and the black bar represents paigen-fed animals. Data show % muscularised vessels. Error bars represent mean  $\pm$  SEM,  $n=3-5$  per group. Data analysed using a two-way ANOVA with Bonferroni post hoc test.  $P < 0.05$  considered significant.

### 3.3.1.2 Circulating T cell subset analysis

The aim of this chapter was not only to identify changes in haemodynamic parameters and vessel remodelling between chow and paigen fed animals, but also to relate these changes to alterations in T cell subsets throughout a timecourse of PAH progression. To do this, an analysis of circulating T cell subsets was conducted using peripheral blood samples taken via cardiac puncture at week 1 to 8.

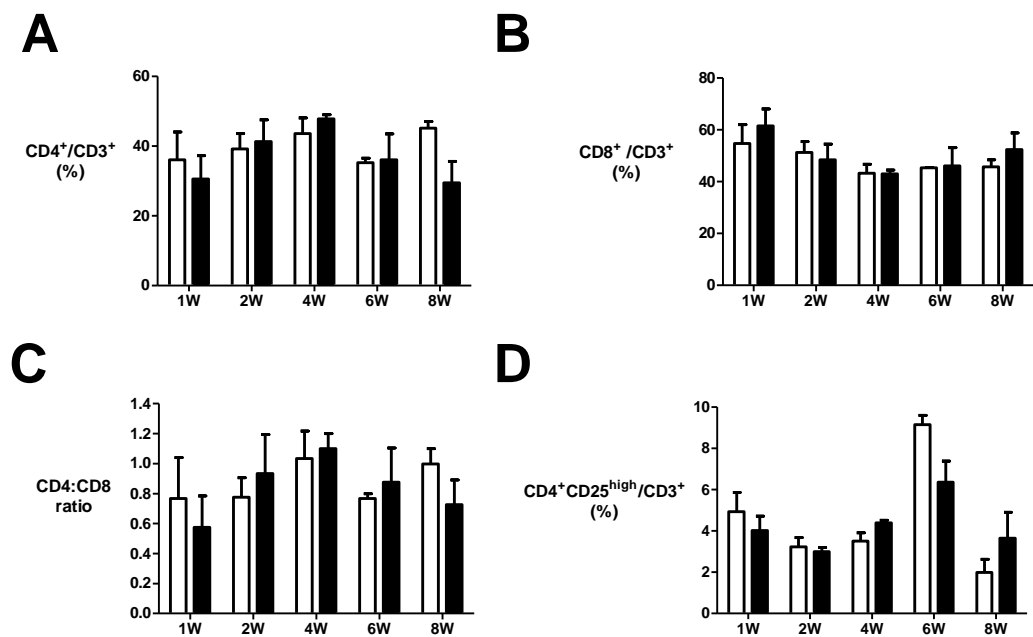


**Figure 3.5 T cell subsets in peripheral blood of paigen and chow fed animals.** Peripheral blood was stained for T cell subsets and data are shown as a proportion of CD3<sup>+</sup> T cells. A) Proportion of CD4<sup>+</sup> T cells B) Proportion of CD8<sup>+</sup> T cells C) CD4:8 ratio D) Proportion of Treg (CD4<sup>+</sup>CD25<sup>high</sup>) cells. Time points of week 1, 2, 4, 6 and 8 are shown along the X axis. n=2-4 and error bars depict mean ± SEM. White bars depict chow fed animals and black bars represent paigen-fed animals. Data analysed using a two-way ANOVA with Bonferroni post hoc test. No results were significant.

These data are non-conclusive for any obvious significant changes in any T cell subset at any time point in paigen fed mice compared to chow fed controls (Figure 3.5, A to D). Interestingly, there was a significant increase in Treg cells (CD4<sup>+</sup>CD25<sup>high</sup>) in chow fed controls at week 6 compared to paigen fed animals, however this is unexplainable (Figure 3.5, D).

I also investigated whether there was a modified recruitment of T cell subsets into lung tissue, as well as changes in T cell proportions within the spleen. Proportions of CD4<sup>+</sup> T cells, CD8<sup>+</sup> T cells and CD4<sup>+</sup>CD25<sup>high</sup> Treg cells were assessed at week 8 in blood as well as spleen and lung tissue. Lung tissue was digested by incubating the tissue with collagenase A, as previously described in chapter 3.2.1.2, to dissociate the tissue and liberate immune cells. The tissue from both lung and spleen were then passed through cell strainers to remove cells for flow cytometric analysis.

Although not significant, there was a trend for a decrease in CD4<sup>+</sup> T cells (as a proportion of total CD3<sup>+</sup> T cells) in blood of paigen-fed ApoE<sup>-/-</sup>/IL-1R1<sup>-/-</sup> mice at week 8 (27.75 ± 12.30% vs 45.65 ± 3.94%, n=4/group, P=0.11). No significant changes in CD4<sup>+</sup> T cell populations were noted in spleen or lung tissue (Figure 3.6).

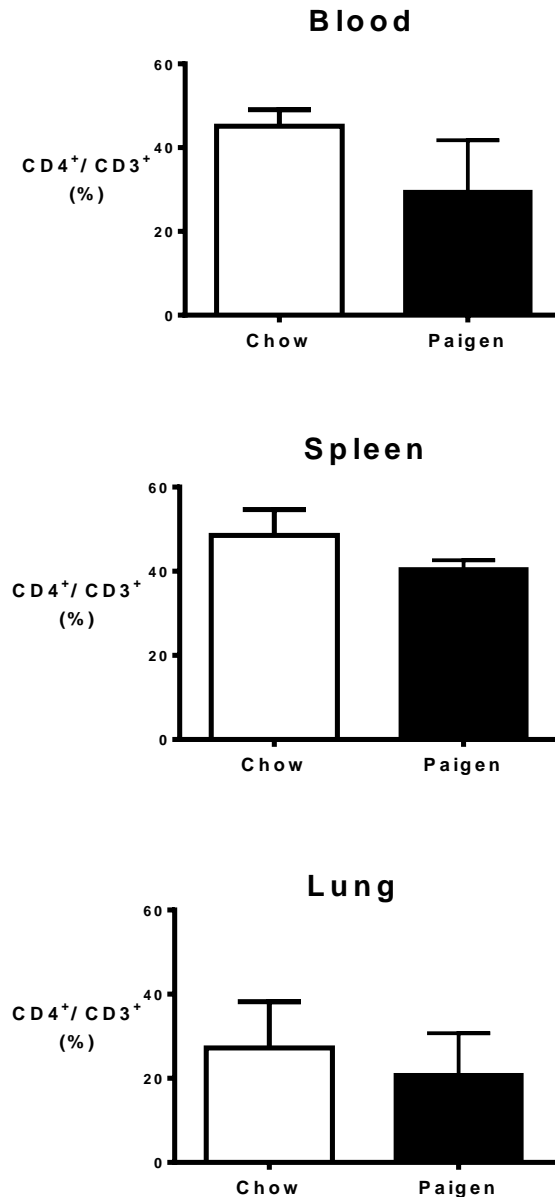


**Figure 3.6 Proportions of CD4<sup>+</sup> T cells in blood, spleen and lung tissue at 8 weeks in chow and paigen-fed ApoE<sup>-/-</sup>/IL-1R1<sup>-/-</sup> mice.**

Error bars show mean  $\pm$  SD and n=4/group. A Mann-Whitney U test with 95% confidence intervals was carried out on all data with a P value of < 0.05 considered significant (\*).

There was a tendency for increased proportions of CD8<sup>+</sup> T cells in the lung tissue in paigen-fed mice at week 8 compared to chow fed controls (36.35  $\pm$  5.57% vs 22.35  $\pm$  8.01%, n=4/group, P=0.057), however their proportions did not change in blood or splenic tissue (Figure 3.7).

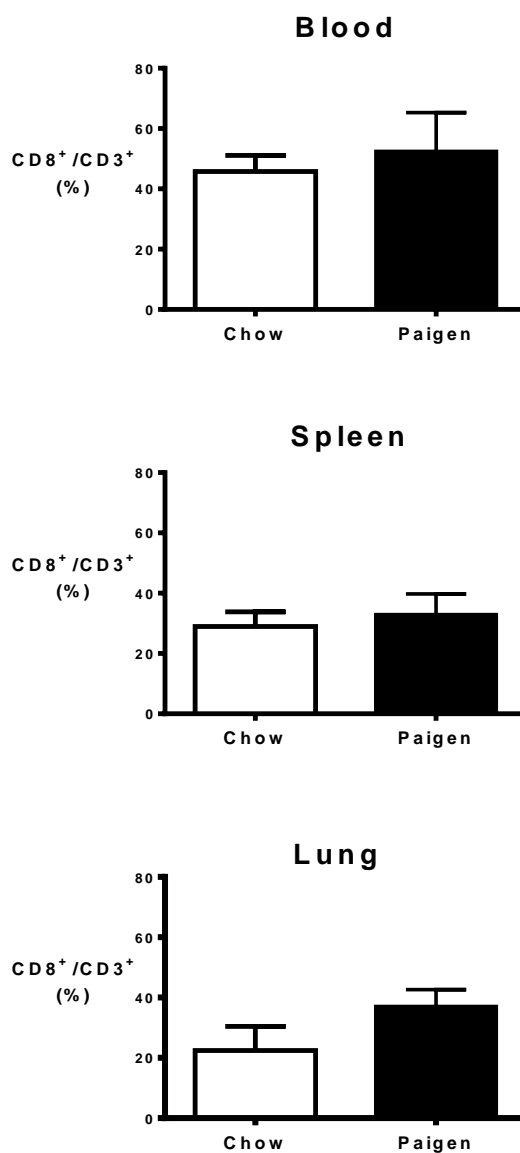


**Figure 3.7 Proportions of CD8<sup>+</sup> T cells in blood, spleen and lung tissue at 8 weeks in chow and paigen-fed ApoE<sup>-/-</sup>/IL-1R1<sup>-/-</sup> mice.**

Error bars show mean  $\pm$  SD and n=4/group. A Mann-Whitney U test with 95% confidence intervals was carried out on all data with a P value of < 0.05 considered significant (\*).

There was a significant decrease in CD4:CD8 T cell ratio in the blood of paigen-fed animals compared to chow fed controls ( $0.52 \pm 0.15\%$  vs  $0.93 \pm 0.20\%$ , n=4/group, P=0.02). There was also a tendency for a decrease in

CD4:CD8 T cell ratio in paigen-fed animals in lung and splenic tissue; however these results were not significant (Figure 3.8).

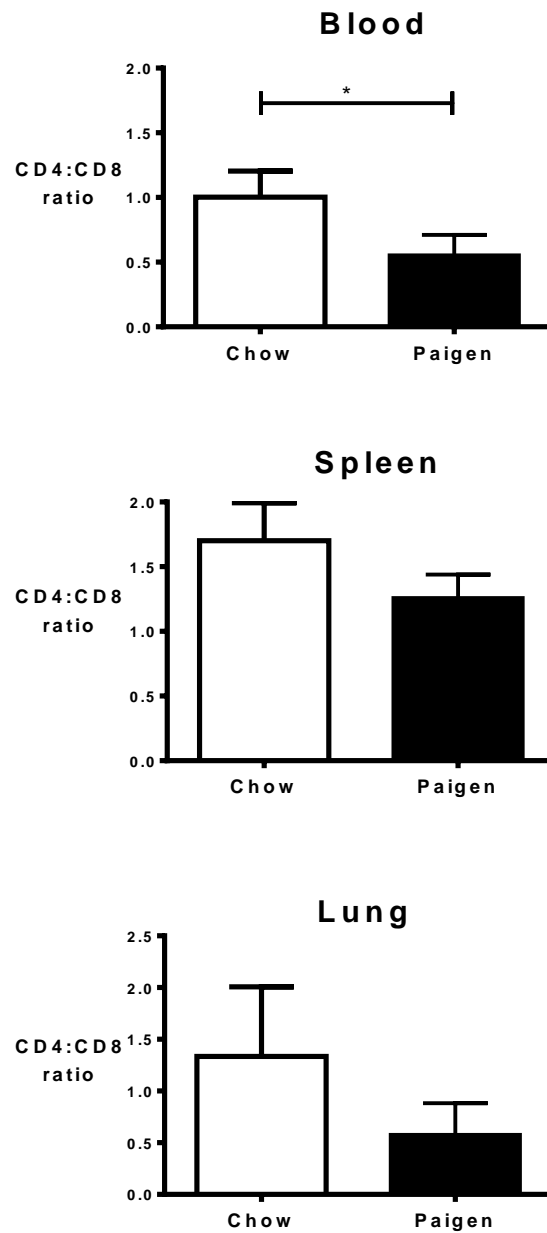


**Figure 3.8 CD4:CD8 T cell ratio in blood, spleen and lung tissue at 8 weeks in chow and paigen-fed ApoE-/-/IL-1R1-/- mice.**

*Error bars show mean  $\pm$  SD and n=4/group. A Mann-Whitney U test with 95% confidence intervals was carried out on all data with a P value of < 0.05 considered significant (\*).*

There were no differences in the proportion of CD4<sup>+</sup>CD25<sup>high</sup> Treg cells in paigen-fed animals in the blood, spleen or lung tissue compared to chow fed controls (Figure, 3.9).

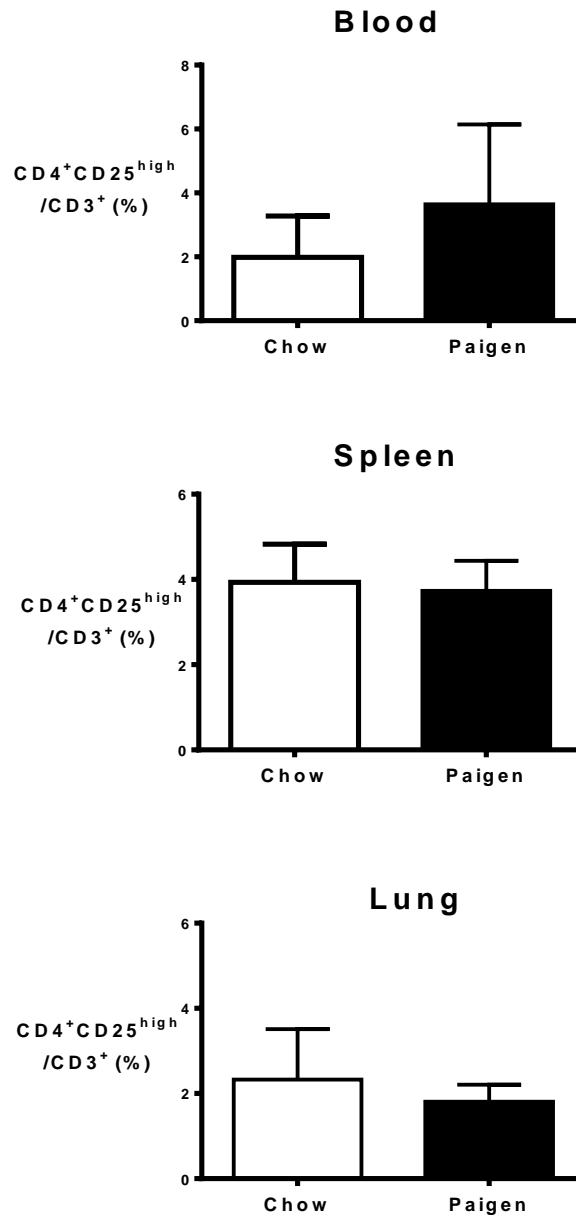


**Figure 3.9 Proportions of CD4<sup>+</sup>CD25<sup>high</sup> Treg cells in blood, spleen and lung tissue at 8 weeks in chow and paigen-fed ApoE<sup>-/-</sup>/IL-1R1<sup>-/-</sup> mice.**

Error bars show mean  $\pm$  SD and n=4/group. A Mann-Whitney U test with 95% confidence intervals was carried out on all data with a P value of < 0.05 considered significant (\*).

Taken together these data suggest there is a tendency for a decrease in CD4<sup>+</sup> T cells in peripheral blood of paigen-fed animals at week 8, however Treg cells appear to be protected from this effect and their proportions do not decrease. There is a tendency for an increase in the proportions of CD8<sup>+</sup> T cells in the lung of paigen-fed animals, suggesting a recruitment of these cells to the tissue, however neither of these observations are statistically significant.

### **3.3.1.3 Cell marker expression within lung tissue**

After noting a change in the proportions of T cell subsets within blood, spleen and lung tissue using flow cytometric analysis, a further analysis of T cell populations within lung tissue was undertaken using immunohistochemistry. To confirm the changes in proportions of T cell subsets, previously noted in lung tissue (Chapter 3.3.1.2), immunocytochemical analyses were performed on random formalin-fixed, paraffin embedded, 5 µm thick sections of lung tissue taken from chow and paigen-fed ApoE<sup>-/-</sup>/Il-1R1<sup>-/-</sup> animals at each time point. Antibodies against CD4, CD8 and CD25 T cells were incubated with tissue sections for 1 hour before being analysed (see Appendix 1, section 5 for antibody specifics and clone numbers).

An increase in perivascular CD4<sup>+</sup> T cells was noted in paigen-fed animals at week 8 compared to chow fed controls (Figure 3.10). Minimal staining for CD8<sup>+</sup> T cells in paigen-fed animals was noted at 8 weeks compared to chow fed controls. An increased amount of CD4<sup>+</sup> and CD8<sup>+</sup> T cell staining was also noted throughout the lung tissue of paigen-fed animals at 8 weeks. CD25 staining could not be detected in either chow or paigen-fed animals at week 8.

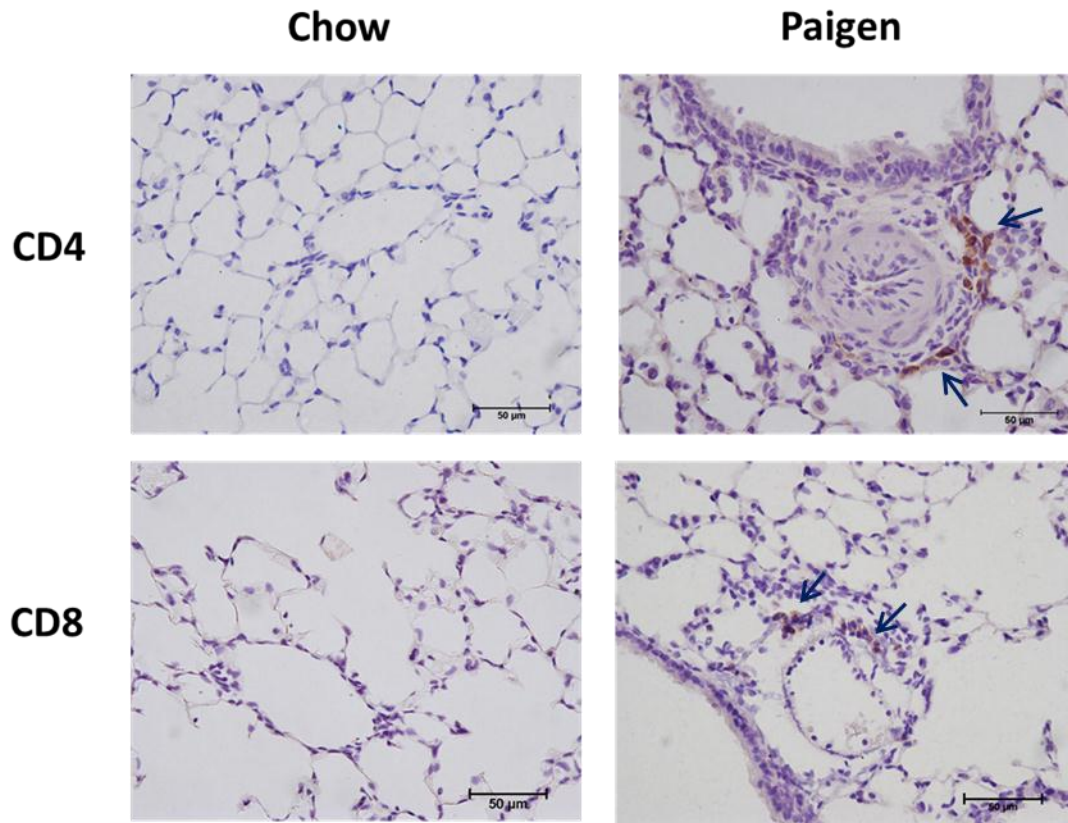


**Figure 3.10 Representative images of lung sections stained for CD4<sup>+</sup> and CD8<sup>+</sup> T cells from chow and paigen diet-fed mice at 8 weeks.**

Sections were immunostained for CD4 and CD8 markers in chow and paigen-fed animals. Images taken at X400 magnification. Arrows depict staining. Scale bar =50 µm.

As previously noted in chapter 4.3.1.2, there is a tendency for a decrease in proportions of CD4<sup>+</sup> T cells in peripheral blood of paigen-fed animals at week 8, but there is no change in the proportion of CD4<sup>+</sup> T cells in lung and splenic tissue, as confirmed by flow cytometric analysis. However, an increase in CD4<sup>+</sup> T cells was noted in immunohistochemical analysis of lung tissue sections taken from paigen-fed mice at 8 weeks. CD8<sup>+</sup> T cells appear to be recruited to the lung tissue of paigen-fed animals at week 8 (as noted in both flow cytometry and histochemical analysis).

### **3.3.2 Depletion model**

There was a tendency for a decreased proportion of CD4<sup>+</sup> T cells in the blood of paigen fed animals, so I next sought to determine whether changes in the proportions of CD4<sup>+</sup> T cells in blood and lungs were due to the disease itself or were an effect of the disease. I therefore depleted this subset within the same model, to confirm whether CD4<sup>+</sup> T cells propagated or abrogated disease progression.

#### **3.3.2.1 Confirmation of CD4<sup>+</sup> T cells depletion**

Confirmation of CD4<sup>+</sup> T cells depletion was undertaken using flow cytometry on peripheral blood from 3 randomly selected IgG controls and 3 CD4 depleted mice at 5 weeks after commencement of paigen diet (1 week after finishing the 4 week antibody treatment or IgG control).

CD4<sup>+</sup> T cells were sufficiently depleted in antibody treated animals when compared to IgG controls (Figure 3.11). Of note, was the difference in proportions of both CD4<sup>+</sup> and CD8<sup>+</sup> T cells between animals within the IgG treatment group. CD4<sup>+</sup> T cells ranged from 6.8% to 27.1% and CD8<sup>+</sup> T cells from 12.5% to 41.8% in this control group. Proportions of both CD4<sup>+</sup> and CD8<sup>+</sup> T cells were low in mouse AL642, which may have been due to an increase in CD4<sup>-</sup>CD8<sup>-</sup> cells.

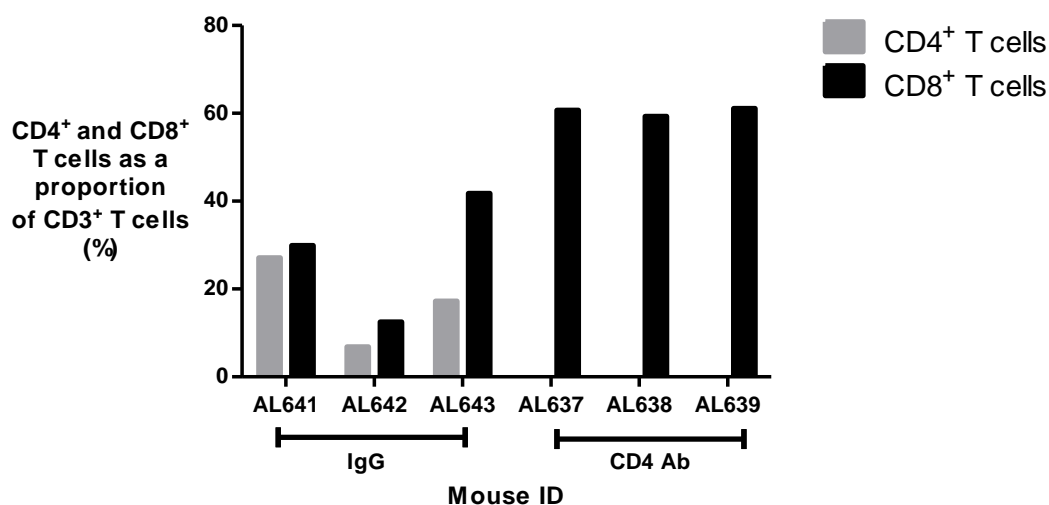


**Figure 3.11 Confirmation of CD4<sup>+</sup> T cell depletion in peripheral blood of fat fed ApoE<sup>-/-</sup>/IL-1R1<sup>-/-</sup> mice**

Confirmation of depletion was undertaken at week 5 (1 week after ceasing either CD4 antibody or IgG control). 3 IgG control and 3 CD4 Ab treated mice were selected at random to check that the CD4 depletion antibody had taken effect. Anti-CD3 AF700, Anti-CD4 PB and anti-CD8 APC antibodies were used to detect CD3<sup>+</sup>, CD4<sup>+</sup> and CD8<sup>+</sup> T cells. Data are expressed as CD4<sup>+</sup> (grey) and CD8<sup>+</sup> (black) populations as a proportion of the total number of CD3<sup>+</sup> T cells. IgG treated controls are shown on the left and CD4 depletion antibody treated animals (CD4 Ab) are shown on the right of the graph.

### 3.3.2.2 Haemodynamic and vessel remodelling analysis

To detect changes in haemodynamics, echocardiography and cardiac catheterisation were undertaken at 8 weeks in both CD4 depleted animals and IgG treated controls. There was no difference in the weights of CD4 depleted and IgG control animals at week 0 and week 8.

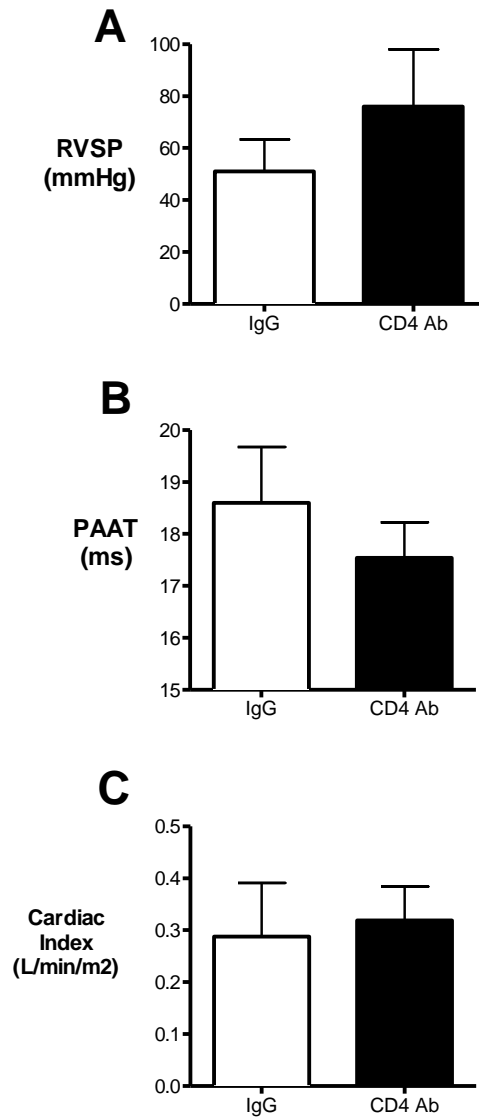


**Figure 3.12 Haemodynamic assessment of paigen-fed ApoE<sup>-/-</sup>/IL1R1<sup>-/-</sup> mice given a CD4<sup>+</sup> T cell depletion antibody or an IgG control.**

A) Right ventricular systolic pressure (mmHg). B) Pulmonary artery acceleration time (PAAT) (ms). C) Cardiac Index (L/min/m<sup>2</sup>). RVSP measurements were made using closed chest cardiac pressure volume catheterisation, whilst a pressure volume catheter was used to assess cardiac output which was then used to derive a value of CI. PAAT measurements were taken using Vevo 770 echocardiography equipment. Error bars represent mean  $\pm$  SD and n=4/group. A Mann-Whitney U test with 95% confidence intervals was carried out on all data.  $P < 0.05$  considered significant (\*).

There was a trend for an increase in RVSP in CD4 depleted animals compared to IgG controls (57.47 mmHg vs 44.66 mmHg, n=4, P=0.3) (Figure 3.12, A). There was no change in CI in CD4 depleted animals compared to IgG treated controls at week 8 (Figure 3.12, C). Doppler ultrasound assessment of pulmonary artery acceleration time (PAAT), showed a trend for a decrease in CD4 depleted mice compared to IgG treated animals (Figure 3.12, B). These data (RVSP, PAAT and CI) are comparable with previously published data concerning the fat-fed ApoE<sup>-/-</sup>/IL-1R1<sup>-/-</sup> mouse model of PAH (Lawrie *et al*, 2011).

To determine the effect that CD4<sup>+</sup> T cell depletion had on the remodelling process within the lungs of fat-fed ApoE<sup>-/-</sup>/IL-1R1<sup>-/-</sup> mice, two analyses were carried out on lung tissue sections taken from both IgG treated and CD4 depletion antibody treated animals. This included assessing the degree of muscularisation of the pulmonary arteries and arterioles and determining the percentage of total vessels that were muscularised.

There was a trend for increased media / CSA, as explained in Chapter 3.2.1.6, in CD4 depleted animals in all vessel sizes compared to IgG controls, however this was not significant (Figure 3.13, A). This suggests that there is an increased degree of muscularisation within the vessels of CD4 depleted animals, however this effect is minimal. Elastin van Gieson staining was used to assess remodelling in pulmonary vessels, providing a measurement of the percentage of vessels that were muscularised. There was a trend for an increase in the percentage of muscularised vessels in lung sections from CD4 depletion antibody treated animals in small vessels (<50 µm) compared to IgG treated controls (Figure 4.13, B). The percentage of muscularised medium and large vessels (51-100 µm and >100 µm) were no different between groups. Taken together, these data suggest that there are a greater number of muscularised vessels that have a greater degree of muscularisation in CD4 depleted animals, illustrating a slightly more severe disease PAH phenotype in these animals.

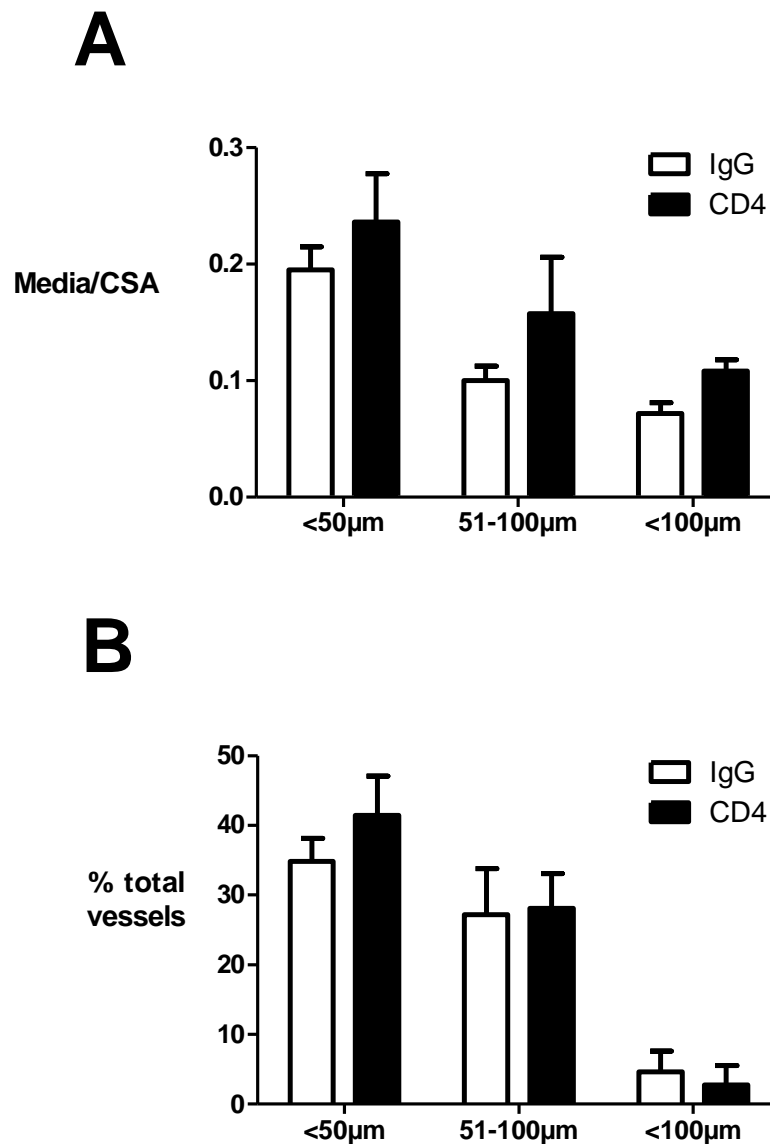


**Figure 3.13 Analysis of number of remodelled vessels and degree of remodelling in lung tissue sections in CD4 depleted and IgG treated animals.** Vessels were split into three different sized groups (<50 µm, 50-100 µm and >100 µm) as well as those animals treated with IgG control (clear bars) and CD4 depletion antibody (black bars). A) Media / CSA (cross sectional area) ratio is shown for each vessel size. B) Analysis of degree of remodelling in each vessel size. Data shown are from muscularised vessels. Error bars represent mean  $\pm$  SEM,  $n=5-6$  per group. Data analysed using a two-way ANOVA with Bonferroni post hoc test.  $P < 0.05$  was considered significant (\*).

### 3.3.2.3 T cell subset analysis in blood and tissue samples

Changes in T cell subsets in CD4 depleted animals were assessed by flow cytometry facilitating analyses regarding T cells and disease progression at 8 weeks after beginning paigen-fed diet. T cell subsets (CD4<sup>+</sup>, CD8<sup>+</sup> and CD4<sup>+</sup>CD25<sup>high</sup>) in peripheral blood, spleen and lung tissue of CD4 depleted and IgG control animals were analysed using flow cytometry after 8 weeks on paigen diet. A comparison of T cell subsets within the circulation and within tissue was then determined.

The proportion of CD4<sup>+</sup> T cells in splenic and lung tissue was significantly lower in CD4 depleted animals compared to IgG controls (16.85 ± 7.89% vs 56.20 ± 10.41%, n=4, P=0.02 and 0.31 ± 0.48% vs 2.10 ± 0.64%, n=4, P=0.05). There was a trend for a decrease in the proportion of CD4<sup>+</sup> T cells (as a percentage of total CD3<sup>+</sup> T cells) within blood at week 8; however this was not significant (Figure 3.14). CD4<sup>+</sup> T cell depletion had been confirmed at week 5 in CD4 Ab treated animals, however the CD4<sup>+</sup> T cell subset appeared to be recovering from transient depletion in blood, spleen and lung at week 8, as the proportion of CD4<sup>+</sup> T cells in the circulation and tissue was returning to normal levels.

The CD4:CD8 T cell ratio was significantly lower in CD4 depleted animals in blood (0.27 ± 0.04 vs 0.73 ± 0.42, n=4, P=0.02) lung (2.10 ± 0.64 vs 0.31 ± 0.48, n=4, P=0.05), and splenic tissue (0.25 ± 0.17 vs 2.15 ± 0.60, n=4, P=0.02) at week 8, which correlates with previously shown data regarding an increased proportion of CD8<sup>+</sup> T cells (Figure 3.15) and decreased proportion of CD4<sup>+</sup> T cells (Figure 3.14).

Proportions of Treg (CD4<sup>+</sup>CD25<sup>high</sup>) cells remained at similar levels in IgG and CD4 depletion treated animals in blood, spleen and lung tissue at week 8 (Figure 3.17). There is a large spread of data within the IgG control group in both blood and lung tissue, and therefore a larger sample size is needed to note any definitive changes in proportions of Treg cells within these environments.

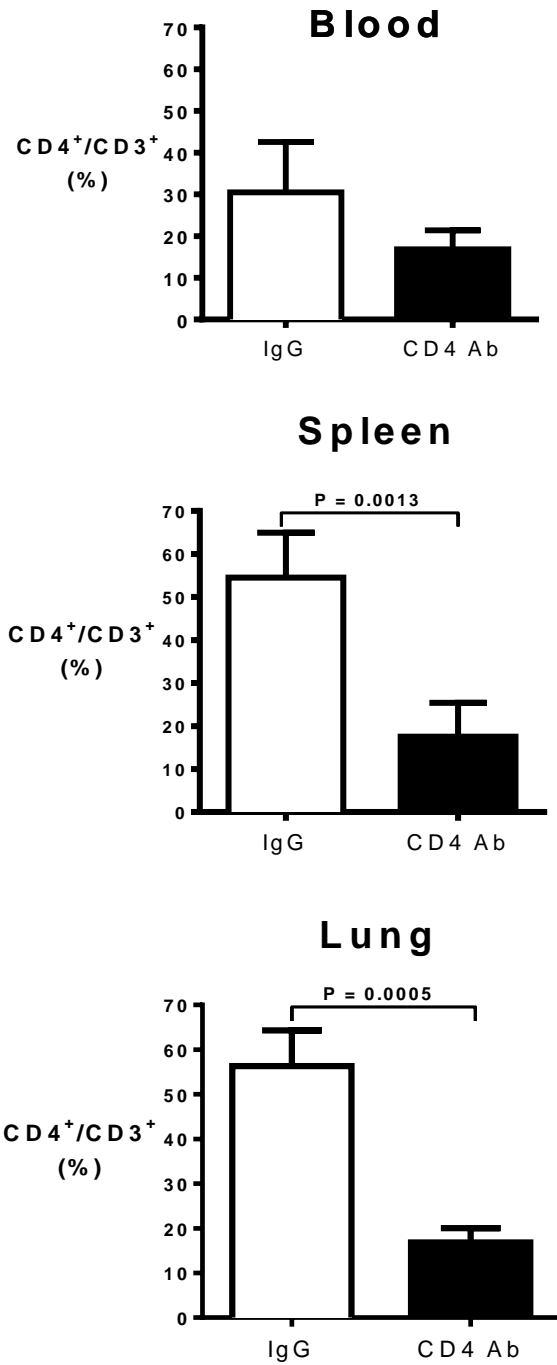


**Figure 3.14 Proportions of CD4+ T cells in blood, spleen or lung tissue of CD4 depleted animals and IgG treated controls.**

Data from IgG controls (IgG), clear bars, and CD4 Ab treated animals (CD4 Ab), black bars are shown. CD4<sup>+</sup> T cells are expressed as a proportion of the total CD3<sup>+</sup> T cell population. Error bars represent mean  $\pm$  SD, n=4/group. A Mann-Whitney U test with 95% confidence intervals was carried out on all data with a P value of < 0.05 considered significant (\*).

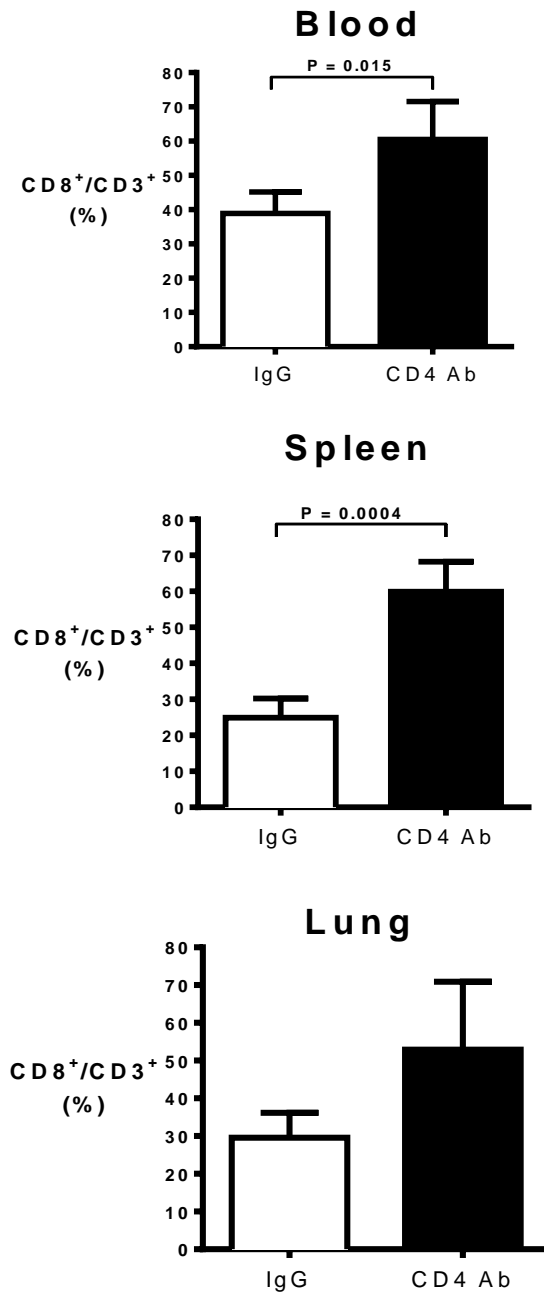


**Figure 3.15 Proportions of CD8+ T cells in blood, spleen or lung tissue of CD4 depleted animals and IgG treated controls.**

Data from IgG controls (IgG), clear bars, and CD4 Ab treated animals (CD4 Ab), black bars are shown. CD8<sup>+</sup> T cells are expressed as a proportion of the total CD3<sup>+</sup> T cell population. Error bars represent mean  $\pm$  SD, n=3-4/group. A Mann-Whitney U test with 95% confidence intervals was carried out on all data with a P value of < 0.05 considered significant (\*).

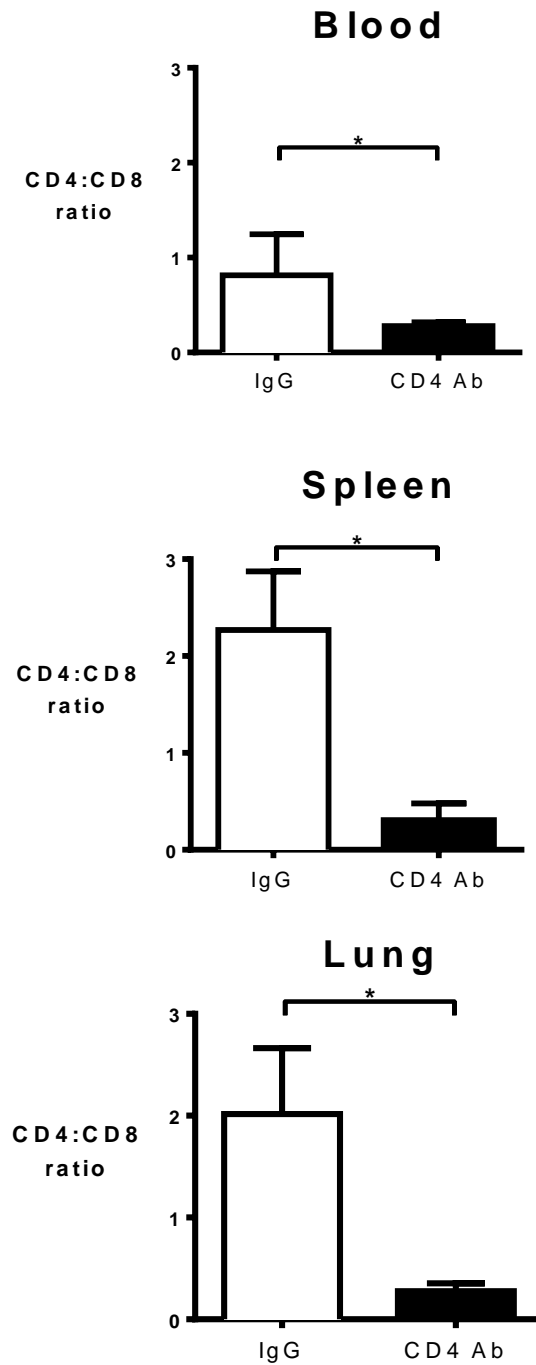


**Figure 3.16 CD4:CD8 T cell ratio in blood, spleen or lung tissue of CD4 depleted animals and IgG treated controls.**

Data from IgG controls (IgG), clear bars, and CD4 Ab treated animals (CD4 Ab), black bars are shown. Error bars represent mean  $\pm$  SD,  $n=4$ /group. A Mann-Whitney U test with 95% confidence intervals was carried out on all data with a P value of < 0.05 considered significant (\*).

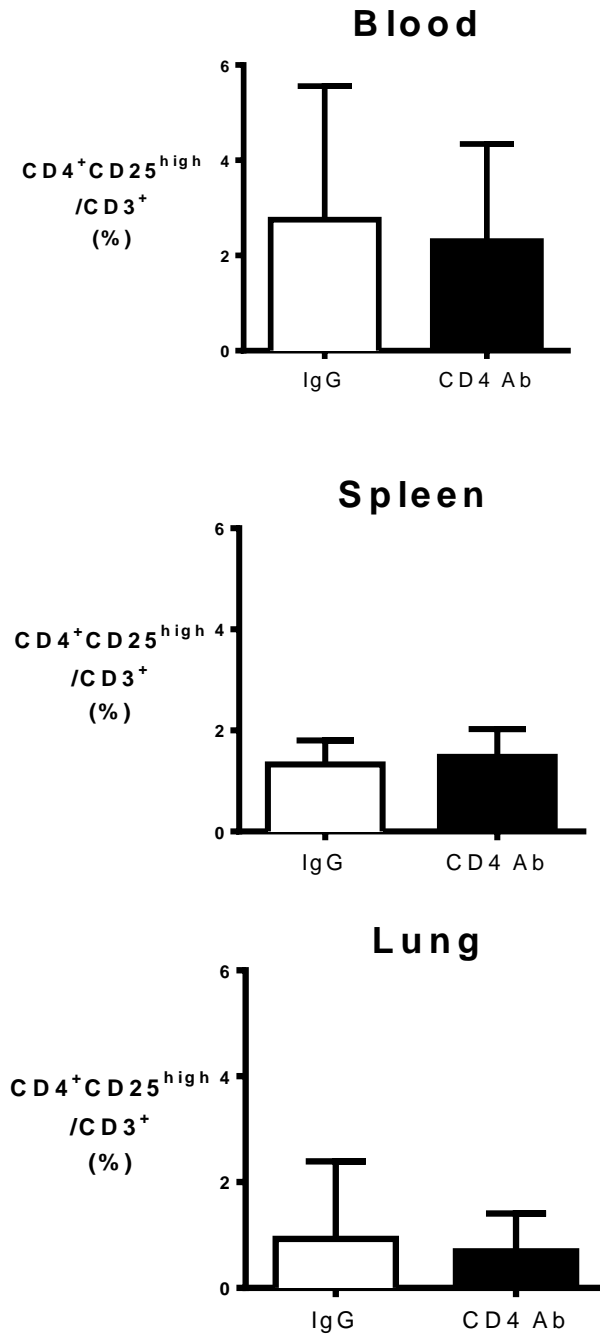


**Figure 3.17 Proportions of CD4<sup>+</sup>CD25<sup>high</sup> Treg cells in blood, spleen or lung tissue of CD4 depleted animals and IgG treated controls.**

Data from IgG controls (IgG), clear bars, and CD4 Ab treated animals (CD4 Ab), black bars are shown. CD4<sup>+</sup> CD25<sup>high</sup> Treg cells are expressed as a proportion of the total CD3<sup>+</sup> T cell population. Error bars represent mean  $\pm$  SD, n=4/group. A Mann-Whitney U test with 95% confidence intervals was carried out on all data with a P value of < 0.05 considered significant (\*).

### 3.3.2.4 Cell marker expression within lung tissue

To assess T cell infiltration into lung tissue, immunohistochemical analyses were performed on random formalin-fixed, paraffin embedded 5  $\mu\text{m}$  thick sections of lung tissue taken from IgG and CD4 depletion antibody treated animals at 8 weeks after beginning paigen-fed diet. These images were then compared with data collected by flow cytometric analysis on lung tissue samples mentioned previously in Chapter 3.3.2.3.

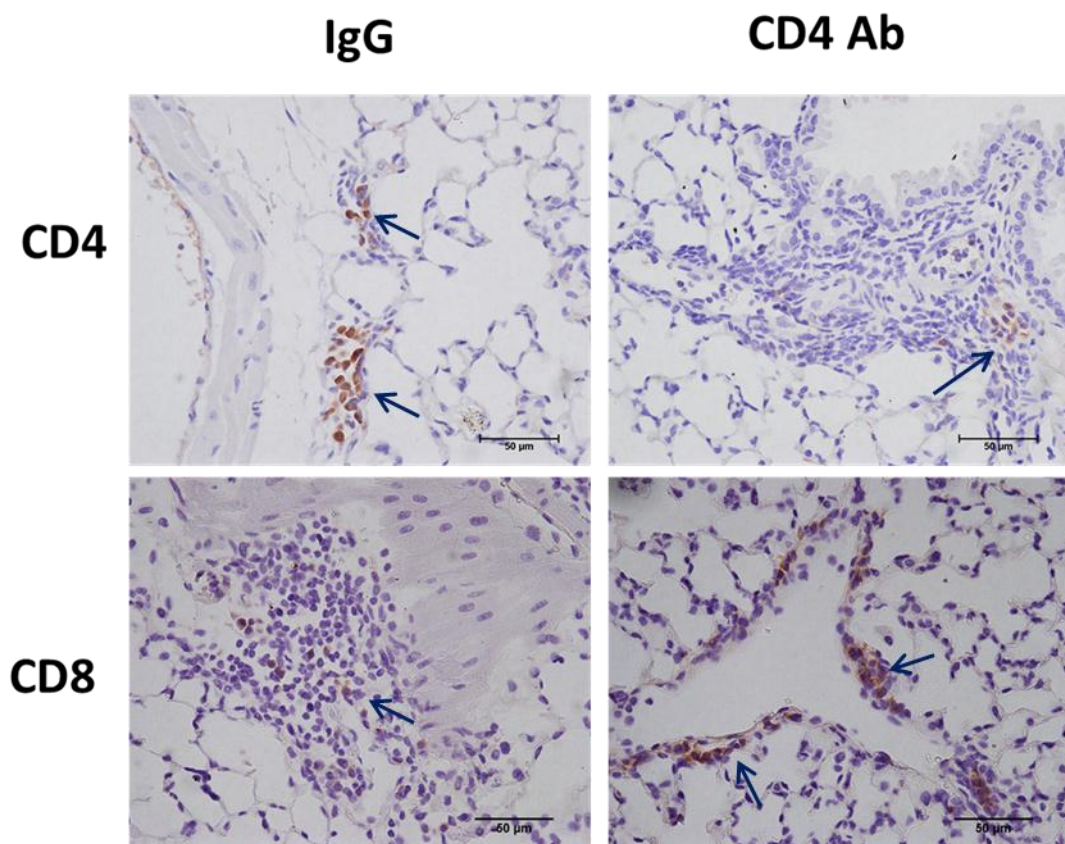


**Figure 3.18 Representative images of CD4 and CD8 expression in the lung tissue of IgG treated and CD4 depletion antibody treated animals at 8 weeks after commencing paigen diet.**

*IgG and CD4 depletion antibody (CD4 Ab) treated animals shown. Images taken at X400 magnification. Arrows depict staining. Scale bar =50  $\mu\text{m}$ .*

The number of CD4<sup>+</sup> T cells decreased in CD4 depleted animals compared to IgG controls within lung tissue (Figure 3.18). Staining for CD4 was still evident around vessels but was reduced compared to IgG controls where perivascular CD4<sup>+</sup> T cells were evident. The number of CD8<sup>+</sup> T cells increased in lung tissue of CD4 depleted animals compared to IgG controls and associated vessels. These images correlated with data collected via flow cytometric analysis of lung tissue regarding a decrease in CD4<sup>+</sup> T cells and an increase in CD8<sup>+</sup> T cells. There was no staining for CD25 present in either CD4 Ab treated animals or IgG treated controls. This was as expected, as previous work undertaken in Chapter 3.3.1.3 also revealed no CD25 staining at 8 weeks in paigen-fed animals.

## **3.4 Discussion**

Human samples can only provide information regarding end stage disease states. Therefore animal models, such as the fat fed ApoE<sup>-/-</sup>/IL-1R1<sup>-/-</sup> mouse model of PAH, can be utilised to determine changes in T cell subsets and other biomarkers along a timecourse of the disease. This allows a comparison of T cell subsets at different stages of disease progression with vessel remodelling and changes in haemodynamics. Although changes in T cell subsets within the peripheral circulation and lung tissue of PAH patients has been noted in Chapter 2.3.2 and in previously published literature, it is unclear whether these changes occur as a cause or consequence of the disease (Tuder *et al*, 1994; Dorfmueller *et al*, 2002; Dorfmueller *et al*, 2003; Ulrich *et al*, 2008; Austin *et al*, 2010).

### **3.4.1 ApoE<sup>-/-</sup>/IL-1R1<sup>-/-</sup> Timecourse**

A timecourse of PAH was set up using the fat-fed ApoE<sup>-/-</sup>/IL1R1<sup>-/-</sup> mouse model of PAH to study changes in T cell subset proportions and relate these changes to disease progression (as assessed by haemodynamic parameters and vessel remodelling analysis). This was to

determine whether changes in T cell subsets were as a cause or consequence of the disease.

In this study no significant changes were noted in any T cell subset (CD4<sup>+</sup>, CD8<sup>+</sup> or CD4<sup>+</sup>CD25<sup>high</sup>) at any time point, between chow fed and paigen fed animals. Confirmation of disease progression was obtained via vessel remodelling analysis and was noted to be increased at week 6 and 8. This result was unexpected as an increased number of lung tissue infiltrating CD4<sup>+</sup> T cells has been noted in a previously published study at 1 week after endothelial cell injury caused by MCT in Rag1<sup>-/-</sup> mice (Cuttica *et al*, 2011). Differences in results noted could be due to the way in which PAH was initiated and the fact that B cells were also not present in the animals included in the study undertaken by Cuttica *et al*.

When the 8 week time point was analysed in more detail changes in T cell populations in the lung and splenic tissue as well as in the blood were noted. There was a tendency for a decreased proportion of CD4<sup>+</sup> T cells in peripheral blood of paigen fed animals compared to chow fed controls, however this was not observed in splenic and lung tissue. A tendency for an increase in the proportion of CD8<sup>+</sup> T cells was noted within lung tissue of paigen fed animals at 8 weeks compared to chow fed controls. An increased number of CD8<sup>+</sup> T cells were also noted in immunohistological analysis of lung tissue sections from these animals, further confirming the increased infiltration of CD8<sup>+</sup> T cells into the remodelling lung tissue. An increased number of tissue infiltrating CD8<sup>+</sup> T cells has previously been observed in IPAH end-stage lung tissue and it is suspected that a decreased proportion of CD8<sup>+</sup> T cells in peripheral blood could be due to their migration to lung tissue (Ulrich *et al*, 2008; Austin *et al*, 2010). Despite this observation in human IPAH samples in previous studies, a decrease in of CD8<sup>+</sup> T cells was not noted in this model at 8 weeks. Proportions of Treg cells did not change between groups at week 8 in blood, lung tissue or splenic tissue.

Unfortunately, no firm conclusions can be drawn from these data, but this study reminds us how difficult it is to compare clinical disease with animal models. The complexity of the disease and undertaking this work also makes studying disease progression and mechanisms of disease difficult. It was anticipated that T cell subsets may change in accordance with disease

progression, as infiltrating T cells have been found to precede EC injury and vascular remodelling in the rat MCT model of PAH, however this was not noted in this diet induced model of PAH (Cuttica *et al*, 2011). These differences may be due to in the induction of disease or could be due to the two different animals (rats vs mice) used to investigate the disease.

### **3.4.2 CD4 depletion model**

As a tendency for a decreased proportion of circulating CD4<sup>+</sup> T cells was noted in the blood of paigen fed animals at week 8, and considering previous studies in rat and mouse models of PAH suggested a protective effect of CD4<sup>+</sup> T cells, a depletion model was set up to determine the effect that depletion of CD4<sup>+</sup> T cells had on PAH disease progression.

CD4 depleted animals exhibited a significant elevation in RVSP (57.47 ± 54.00 mmHg compared to 44.66 ± 27.50 mmHg in IgG treated controls) and a corresponding decrease in PAAT, confirming that CD4 depleted animals have a more severe disease phenotype. An increase in number of affected pulmonary vessels and the amount of muscularisation within them was also noted in CD4 depleted animals, further confirming increased vessel remodelling and disease progression.

Proportions of CD4<sup>+</sup> T cells was significantly reduced in the lungs and spleen of CD4 depleted animals compared to controls, but there was only a trend for a decrease in CD4<sup>+</sup> T cells in the blood of these animals. This could be because, after 4 weeks of being on the diet alone without the antibody treatment, the CD4<sup>+</sup> T cell compartment is being restored in the blood. Proportions of CD8<sup>+</sup> T cells, as predicted in the CD4 depleted animals, were significantly increased in blood, lung and splenic tissue, due to the decreased proportion of CD4<sup>+</sup> T cells. In future work, the addition of counting beads to determine actual cell number will allow for a more detailed view of whether the number of CD8<sup>+</sup> T cells changes in these animals. Interestingly, there was no change in the proportion of Treg cells in the blood, lung or splenic tissue of CD4 depleted animals compared to IgG treated controls. This could be because the Treg cells are being protected from depletion.

However, the reason for this and the mechanism behind this response is currently unknown.

Previous studies in animal models of PAH have suggested a role for T cells in both protecting against PAH and propagating its progression. In athymic rat models of PAH, the induction of PAH using Sugen 5416 with and without hypoxia as well as in MCT treatment, has shown T cells to be protective. This was due to the fact that when CD4<sup>+</sup> T cells were reconstituted after initial injury, perivascular injury associated with endothelial cell apoptosis and vascular remodelling was reduced. CD4<sup>+</sup>CD25<sup>high</sup> Treg cells also showed the same response (Miyata *et al*, 2000; Taraseviciene-Stewart *et al*, 2005; Taraseviciene-Stewart *et al*, 2007; Tamosiuniene *et al*, 2011). In euthymic animals, where T and B cell subsets are intact, a depletion of CD4<sup>+</sup> T cells also increased the animals' susceptibility to developing PAH.

Despite these studies suggesting a protective role for T cells in the development of PAH, RAG-1<sup>-/-</sup> mice which are devoid of T and B cells, when given angiotensin II infusion, desoxycorticosterone acetate or MCT, showed a decreased hypertensive response and less vascular remodelling. Adoptive transfer of T cells restored the hypertensive phenotype (Guzik *et al*, 2007; Cuttica *et al*, 2011). These studies in RAG-1<sup>-/-</sup> mice suggest that in these models of PAH, T cells propagate disease progression rather than protect against vascular remodelling.

The role that T cells play in each experimental model of PAH seems to be different and makes it difficult to choose an appropriate and reliable animal model to study inflammatory mechanisms in PAH. Despite this, T cells do appear to be important in PAH disease progression, whether it be in a positive or negative way, and therefore warrant further investigation.

### 3.4.3 Concluding remarks

Collectively, these animal studies suggest that T cell subsets are not abnormally regulated over time during the progression of PAH disease in the fat-fed ApoE<sup>-/-</sup>/IL1R1<sup>-/-</sup> and that depletion of CD4<sup>+</sup> T cells propagates disease progression. This has been noted in another experimental model of PAH in which athymic nude rats developed PAH under normoxic conditions due to the absence of T cells and MCT treatment (Miyata *et al*, 2000; Taraseviciene-Stewart *et al*, 2007). These data together with previously published data, support the theory that T cells, specifically CD4<sup>+</sup> T cells, are involved in protecting against disease progression, and it is thought that this may be due to the Treg cell subset within this T cell compartment (Tamosiuniene *et al*, 2011).

Following further investigation, the clinical relevance of this work might enable T cell targeted therapy to be undertaken to restore the T cell subset regulatory effect and allow for the control of disease progression.

# Chapter 4 Heat shock protein 70 expression in pulmonary arterial hypertension

## 4.1 Introduction

A major molecular mechanism underpinning the progression of PAH disease is the dysfunction of endothelial processes. This may occur as a result of several sources of injury: hypoxia, shear stress or inflammation. Dysfunction of the EC layer can upset the balance between vasoconstriction and vasodilation, which can then initiate other downstream processes such as increased endothelial permeability and indirectly, the generation of cytokines (Davignon and Ganz, 2004). In PAH, altered EC proliferation results in the formation of plexiform lesions, a common pathological feature in clinical PAH (Tuder *et al*, 1994; Cool *et al*, 1999). Decreased production of endothelial vasoactive mediators such as NO and prostacyclin also leads to exuberant SMC growth and eventually structural remodelling of the pulmonary arteries (McLaughlin and McGoon, 2006). The stress placed on these ECs may cause them to produce and secrete stress proteins in an attempt to protect the endothelium from necrosis and apoptosis (Wang *et al*, 1995).

Hsps are a group of extremely conserved proteins that are present in intracellular compartments of all organisms. They can also be present in the extracellular milieu or associated with the plasma membrane. Hsps have been shown to be released by a number of different cell types including renal tubular cells (due to oxidative stress), monocytes (due to heat shock), PBMCs (due to heat shock), vascular SMCs (due to mechanical force stress), T cells (due to glucocorticosteroid-induced stress) and ECs (due to heat shock and oxidative stress) (Jornot *et al*, 1991; Wang *et al*, 1995; Fukuda *et al*, 1996; Poccia *et al*, 1996; Bachelet *et al*, 1998; Xu *et al*, 2000;

Hunter-Lavin *et al*, 2004). This occurs under a range of conditions, in which they have been shown to exhibit a number of pro- and anti-inflammatory properties including inducing the production of IL-6 in ECs, SMCs and macrophages. Hsps have also been shown to enhance the function of regulatory T cell populations, inhibit acute allograft rejection and temper inflammatory responses and it has also been suggested that self-Hsp70 itself, can induce Treg expansion and activation by increasing levels of IL-10 (Stordeur and Goldman, 1998; Borges *et al*, 2012).

As well as pro- and anti-inflammatory properties, Hsps also have been shown to have cardio-protective roles. Initially, this was shown in the cardiac cell line, H9c2 derived from rat heart, which were protected against thermal or ischaemic stress because they over-expressed Hsp70 (Mestril *et al*, 1994; Heads *et al*, 1995). This protective effect was also seen in primary rat cardiac myocyte cultures transfected to over-express Hsp70 and in coronary ECs over-expressing Hsp70 (Cumming *et al*, 1996; Suzuki *et al*, 1998). The expression of cardio-protective Hsps such as Hsp70 in response to inducers of stress, such as heavy metal ions or protease inhibitors, is thought to protect the stressed endothelium by modulating leukocyte–endothelial interactions, reducing the number of adherent leukocytes and their migration through the vessel wall (Chen *et al*, 1996; Lynes *et al*, 2007). *In vitro* assays have also been undertaken, confirming that Hsp60 can activate immune cells such as Treg cells via activation of Toll-like receptor 2, enhancing their suppressive capabilities (van Roon *et al*, 1997; Zanin-Zhorov *et al*, 2003; Zanin-Zhorov *et al*, 2006). In 1993, Johnson and Tytell noted that Hsp70 protected the viability of stressed aortic SMCs *in vitro* via cell surface contact rather than internalisation (Johnson and Tytell, 1993).

The cardioprotective and anti-inflammatory nature of Hsp70 also make it an interesting and suitable protein target to investigate within the field of hypertensive disease. Several studies have been undertaken in this field. The first showed elevated Hsp70 levels in patients with peripheral vascular and renal vascular disease whilst Pockley *et al* noted elevated anti-Hsp70 and anti-Hsp65 antibody levels in patients with hypertension (Wright *et al*, 2000; Pockley *et al*, 2002). Elevated Hsp70 levels have also been linked to a reduced incidence of cardiovascular disease in patients with established

hypertension, further suggesting a link between circulating Hsp70 levels and cardioprotection (Pockley *et al*, 2003). There is however, no data regarding circulating levels of Hsp70 in serum or expressed Hsp70 within ECs in patients with PAH (IPAH or SSc-PAH). This is also true for experimental models of PAH. This research would allow for the differentiation between expressed and secreted Hsp70 being involved in the pathogenesis of PAH and allow for analysis into whether disease progression alters circulating and expressed Hsp70 levels.

Therefore, the aim of this work was to determine levels of circulating Hsp70 in clinical serum samples as well as the expression pattern of circulating and expressed Hsp70 in serum and lung tissue using a rat and mouse model of PAH. Depletion of CD4<sup>+</sup> T cells was also undertaken to determine the role of these cells in the pathogenesis of PAH. I aimed to ascertain whether Hsp70 expression was driven by the disease, by determining the expression of Hsp70 within the lung tissue in IgG treated and CD4<sup>+</sup> T cell depleted paigen fed animals. The influence that hypoxia (stress) has on Hsp70 expression in cultured pulmonary artery endothelial cells (PA-ECs) was also studied *in vitro*. This work was undertaken to identify how Hsp70 levels relate to disease progression. Based on published literature, I hypothesised that changes in pulmonary haemodynamics would cause endothelial stress and regulation of Hsp70 which would cause an increase in the production and release of Hsp70 from ECs within the pulmonary vessels (Jornot *et al*, 1991; Suzuki *et al*, 1998; Pockley *et al*, 2003; Luo *et al*, 2007; Pockley *et al*, 2009).

## **4.2 Methods**

Several *in vitro* methods were used to determine expression levels and localisation of Hsp70 both in murine models of PAH and in clinical samples. These are detailed below along with a brief explanation as to why they were chosen.

### **4.2.1 Serum Hsp70 levels in Pulmonary Arterial Hypertension**

As previously mentioned, elevated Hsp70 levels are associated with a reduced incidence of cardiovascular disease in patients with established hypertension, however to date, circulating Hsp70 levels in serum have not been analysed in IPAH or SSc-PAH patients (Pockley *et al*, 2003). This work therefore aimed to determine Hsp70 levels in the serum of IPAH, SSc-PAH patients and healthy controls using the Hsp70 high sensitivity EIA kit which has been validated for the measurement of Hsp70 in serum and plasma (ENZO Life Sciences, Exeter, UK).

Serum samples were analysed according to the manufacturer's instructions and the assay contents from the Hsp70 high sensitivity EIA kit (see Appendix 1, section 1). Before starting the assay, the wash buffer was prepared by adding 50 mL of the supplied wash buffer concentrate to 950 mL of deionised water. This was kept at room temperature during the assay. A standard curve ranging from 0.2 ng / mL to 125 ng / mL was set up using the Hsp70 intermediate standard and assay buffer supplied in the kit. The Hsp70 intermediate standard was prepared by adding 395  $\mu$ L assay buffer to 5  $\mu$ L of the 10  $\mu$ g / mL recombinant human Hsp70. A serial dilution was then made to produce standards of 12.5, 6.25, 3.13, 1.56, 0.78, 0.39 and 0.2 ng / mL. All samples and standards were kept on ice during the assay. The samples were diluted 1 in 2 with assay buffer to remove matrix interference in the assay. 100  $\mu$ L of serum samples and standards were added to an ELISA microtiter plate pre-coated with a mouse monoclonal antibody specific

to Hsp70 (clone number LK1.1). Standards were run in duplicate while samples were run once due to the availability of a limited volume of sample from each patient. 100  $\mu$ L of assay buffer was also added to the control well. The plate was sealed then incubated for 2 hours at room temperature. The plate was washed by adding 400  $\mu$ L of assay wash buffer, emptying the contents of the wells and repeating these two steps twice more. All traces of wash buffer were removed after the third wash by firmly tapping the plate onto a paper towel. This left the bound Hsp70 on the plate. 100  $\mu$ L of rabbit polyclonal antibody specific to Hsp70 was then added which bound to the captured Hsp70 on the plate. The plate was sealed and incubated for 1 hour at room temperature then washed as previously described. 100  $\mu$ L of horseradish peroxidase (HRP) conjugate solution (goat anti-rabbit IgG conjugated to HRP) was added to each well except the control well, to bind to the previous antibody. The plate was covered and incubated for 1 hour at room temperature, then washed as before to remove excess HRP conjugate solution. 100  $\mu$ L of 3,3',5,5'-Tetramethylbenzidine (TMB) substrate was added to each well except the control to generate a detectable blue colour. The plate was then covered and incubated for 30 minutes at room temperature before 100  $\mu$ L of stop solution was added to stop the substrate reaction. After zeroing the microplate reader against the substrate blank control well, the optical density (resultant yellow colour) was read at 450 nm. The amount of signal is directly proportional to the level of Hsp70 in each sample. The plate was also read at an irrelevant wavelength and the readings subtracted from this reading to remove cross-plate variation in optical properties. Data was analysed with a 4-parameter logistic curve fit using GraphPad Prism version 5.00 for Windows. Unknown sample values were quantified against this standard curve. The sensitivity was determined by interpolation at 2 standard deviations above the mean signal at background (0 ng / mL). The inter-assay coefficient of variation was 12.8% to 19.1% and the intra-assay coefficient of variation was 3.9% to 11.4% for this kit.

## 4.2.2 Hsp70 levels in rat monocrotaline serum

An animal model of PAH was also set up to identify changes in serum Hsp70 levels in relation to disease progression. The rat MCT model of PAH is a well characterised model of PAH. MCT, when given to rats causes tissue damage in the lung, including cellular infiltration into the interstitium, endothelial injury and thickening of the medial wall of small pulmonary arteries which gives rise to PAH (Ghodsfi and Will, 1981; Reindel and Roth, 1991; Roth and Reindel, 1991; Miyata *et al*, 2000). It is thought to be the most aggressive form of PAH in any animal model and works by directly damaging the vascular endothelium and eventually leads to lethal PAH (Dumitrascu *et al*, 2008; Stenmark *et al*, 2009). The samples used in this study were archived serum samples that had been generated in a previous study undertaken by Dr Abdul Hameed and stored at -80°C for <6 months (Hameed *et al*, 2009). For the induction of PAH, male Sprague Dawley rats (Charles River, UK) were given a single subcutaneous injection of MCT (Sigma Aldrich, Dorset, UK) at a dose of 60mg / kg. Serum samples were collected on day 2,7,14, 21 and 28 post MCT injection and analysed for circulating Hsp70 levels.

Based on previously published literature, I hypothesised that levels of serum Hsp70 would increase in MCT treated rats as vascular remodelling became evident (Pockley *et al*, 2003). The Hsp70 high sensitivity EIA kit was used to analyse serum samples from a time course (2, 7, 14, 21, 28 days after MCT administration, n=4 / group) of samples from a MCT model of PAH. Serum samples were diluted 1 in 4 using assay buffer supplied with the kit to remove matrix interference. This dilution was chosen after a pilot study was performed on several dilutions of the same rat serum sample to determine which dilution fell within the range of the kit. All reagents were supplied with the kit, which was used according to the manufacturer's instructions, as previously mentioned in Chapter 4.2.1.

### **4.2.3 Hsp70 expression in lung tissue from animal models of pulmonary arterial hypertension**

Intracellular expressed Hsp70 levels were also analysed in lung tissue of MCT treated animals and compared against IgG control animals. This was to determine whether circulating Hsp70 levels (analysed in serum samples derived from clotted blood samples) correlated with tissue expressed Hsp70 levels. There is little evidence to show that stressed ECs produce Hsp70 in response to heat shock or ischaemic stress, however their production of other Hsps is well documented (Jornot *et al*, 1991; Li *et al*, 1992; Xu *et al*, 1994; Wang *et al*, 1995; Piotrowicz *et al*, 1997; Pfister *et al*, 2005). Despite this, it is possible that ECs express Hsp70 in response to stress and therefore this matter needed to be evaluated further.

As increased intracellular levels of Hsp70 have also been noted in patients with end stage vascular disease, I hypothesised that Hsp70 levels in the lung tissue would be increased in MCT treated animals as the disease progressed (Wright *et al*, 2000).

Immunohistochemistry using a mouse mAb against Hsp70 (clone number C92F3A-5), was used to assess Hsp70 expression within the lung tissue of MCT treated and saline treated animals at different time points after MCT injection. Paraffin embedded lung sections (kindly obtained from Dr Abdul Hameed) were analysed as previously described in Chapter 3.2.1.4 and 3.2.1.5. A citrate buffer antigen retrieval step was used and a biotinylated goat anti-mouse IgG secondary antibody was used to detect the primary antibody (Appendix 1, section 5). Stained slides were analysed using a camera mounted on a light microscope utilising NIS-elements software version 3.0.

A second experimental model of PAH, the fat fed ApoE<sup>-/-</sup>/IL1R1<sup>-/-</sup> mouse model (previously described in Chapter 3.2.1) was also used to further confirm that disease progression has an effect on Hsp70 expression within the lung tissue of diseased animals. Depletion of CD4<sup>+</sup> T cells, thought

to propagate disease progression within fat fed ApoE<sup>-/-</sup>/IL1R1<sup>-/-</sup> mice was also thought to alter Hsp70 expression in tissues, as the disease was predicted to be more severe, and therefore there would be more remodelling (Taraseviciene-Stewart *et al*, 2007). It was considered that an increase in vascular remodelling would lead to an increase in Hsp70 tissue expression levels, as several cell types involved in this vascular remodelling process (SMCs and ECs) have been shown to express Hsp70 in response to stress (Jornot *et al*, 1991; Xu *et al*, 1997; Liao *et al*, 2000).

The primary Hsp70 antibody used to detect Hsp70 using immunohistochemistry techniques had no manufacturer recommended dilution, so several were tried to optimise staining within mouse lung tissue (1 in 50, 1 in 100, 1 in 200, and 1 in 500) including antigen retrieval with citrate buffer to strengthen the staining signal (see Appendix 1, section 5). A negative control of PBS with secondary antibody was used with all optimisation protocols. After optimisation of the staining procedure, Hsp70 expression was assessed using a 1 in 500 dilution (diluted in PBS) of a monoclonal anti-mouse Hsp70 primary antibody (clone number C92F3A-5) and incubated for 1 hour at room temperature. A biotinylated monoclonal goat anti-mouse secondary antibody was used to detect the primary antibody at a 1 in 200 dilution in PBS. This was incubated for 30 minutes at room temperature. An antigen retrieval step, using citrate buffer (see Appendix 1, section 5) was carried out for 20 minutes before blocking non-specific binding of the primary antibody with 1% w/v milk buffer. Vectastain Elite ABC working reagent was then added and DAB substrate (3, 3'-diaminobenzidine) used to detect colour formation and Carazzi's Haematoxylin was used to stain the nuclei of cells. Sections were analysed and images captured using a camera mounted on a light microscope and NIS-elements software.

#### **4.2.4 Influence of hypoxia on Hsp70 expression by cultured pulmonary artery endothelial cells**

Hypoxia, the impaired oxygen supply to tissues, can affect ECs lining vessels in a variety of ways, including altering the transcription of certain genes and changing vascular tone (Mehta *et al*, 1988). This occurs via the upregulation and release of inflammatory mediators and growth factors in an effort to initiate processes such as angiogenesis (Faller, 1999; Michiels *et al*, 2000). Under hypoxic conditions, ECs can change their metabolic states and produce reactive oxygen species in an attempt to undertake anaerobic glycolysis (Paternotte *et al*, 2008). The long term effects of a hypoxic environment on ECs can be irreversible remodelling of the vasculature and SMC proliferation (Faller, 1999). Chronic hypoxia is also thought to increase eNOS production of NO via glutathione oxidation, which can lead to an increase in Hsp production (Kim *et al*, 1997; Shipp *et al*, 2012).

In PAH, the impact that hypoxia has on vessel remodelling is unclear, however it is thought that hypoxic conditions could lead to increased SMC proliferation and extracellular matrix deposition. The cellular changes that occur due to hypoxia are also noted in end-stage PAH patients, thereby further emphasising the importance of hypoxia in the development of PAH (Chan and Loscalzo, 2008). However, little is known about how EC Hsp70 expression relates to disease progression, and whether as previously stated, Hsp70 is involved in cardioprotection (Pockley *et al*, 2003).

Therefore, to determine the effect of hypoxia on the Hsp70 expression profile in ECs, an *in vitro* method using cultured PA-ECs was established and Hsp70 protein and RNA expression assessed. The aim of these experiments was to assess the expression of intracellular and secreted Hsp70 in cell lysate and supernatant samples taken from cultured PA-ECs under hypoxic and normoxic conditions. I therefore hypothesised that Hsp70 expression and release would increase in hypoxic conditions on PA-ECs.

#### **4.2.4.1 Pulmonary artery endothelial cell culture**

PA-ECs (Cascade Biologics of Life Technologies Ltd, Paisley, UK) were thawed from frozen stocks (stored at  $-150^{\circ}\text{C}$ ) and resuspended in M200 complete culture medium. Cells were grown in  $75\text{ cm}^2$  culture flasks in a humidified  $37^{\circ}\text{C}$  incubator with 5% v/v  $\text{CO}_2$  and passaged as they reached 80-90% confluence (approximately every 7 days) using Trypsin-EDTA (0.05% v/v trypsin and 0.5 mM EDTA). Cells were maintained in M200 complete growth medium supplemented with 10% v/v FCS, 1% w/v penicillin and 1% w/v streptomycin.

#### **4.2.4.2 Hypoxic cell culture and sample collection**

For hypoxic studies, PA-ECs were cultured in M200 complete growth medium before being removed from the flask and transferred to M199 media (2% v/v FCS in complete growth medium) (see Appendix 1, section 2) to align all cells to the same point in the cell cycle before inducing Hsp70 expression in hypoxic conditions. Hsp expression has been shown to be upregulated in S phase of the cell cycle in HeLa cells, and so to avoid inaccurate results due to cell-cycle specific expression of Hsp70, the cells were aligned to the same point (Milarski and Morimoto, 1986).

PA-ECs were cultured under normoxic (21% v/v  $\text{O}_2$  and 5% v/v  $\text{CO}_2$ ) and hypoxic (1% v/v  $\text{O}_2$  and 5% v/v  $\text{CO}_2$ ) conditions in M199 media in order to mimic the physiological conditions of the pulmonary endothelium in PAH (hypoxic environment within the remodelling vessels). A range of different passage numbers (3-8) were used to ensure that the response seen was not due to the age of the cells.

Two 6-well flat bottomed plates were coated with collagen before being rinsed in PBS three times for each time point. For collagen coating, 2 mL collagen stock (see Appendix 1, section 2) was added to each well on the 6-well plate. This was left to incubate for 1 hour at room temperature before being removed and the plate washed 3 times with sterile PBS. PA-ECs were

seeded onto the 6-well plate at  $12 \times 10^4$  cells / mL with 2 mL of M199 media in each well. Plates were then placed in either a hypoxic (Ruskinn, Bridgend, UK) or normoxic incubator (Sanyo, Loughborough, UK) for 6, 12, 24, 48 or 72 hours.

At these time points, the plates were collected from the incubators and the supernatants removed and stored at  $-80^\circ\text{C}$  in cryovials. The plates were then washed with PBS on ice three times to remove any traces of supernatant. All traces of PBS were removed by firmly tapping the plates onto paper towels before 200  $\mu\text{L}$  of boiling lysis buffer (see Appendix 1, section 2) was added to each well to form a layer across the whole surface for 5 minutes. A cell scraper was used to detach all the cells and the lysate was then transferred to a 1.5 mL microfuge tube, before being boiled for another 5 minutes at  $100^\circ\text{C}$ . The lysate samples were each split into two, centrifuged at  $12000 \times g$  for 10 minutes at  $4^\circ\text{C}$ , the supernatant removed and the cell pellets stored at  $-80^\circ\text{C}$ . One lysate sample was then used in a protein assay and Hsp70 singleplex multibead kit whilst the other was used to extract RNA and protein using an AllPrep RNA/Protein Kit.

#### **4.2.4.3 Quantification of Hsp70 in cell lysate and supernatant samples**

At a later date, a protein assay was undertaken to detect levels of total protein in 1 sample of each cell lysate (BioRad DC protein assay, Hertfordshire, UK). This protein assay was chosen as it could be used with the detergent in the lysis buffer without complications. This was performed according to the manufacturer's instructions. Briefly, working reagent A was prepared by adding 20  $\mu\text{L}$  of reagent S (surfactant solution) to 1 mL of reagent A (alkaline copper tartrate solution). Protein standards were prepared with a range of 0.2 mg / mL to 1.5 mg / mL using the Protein standard I provided (1.5 mg / mL). This was originally a lyophilised preparation, which was rehydrated in 20 mL  $\text{dH}_2\text{O}$ . Protein standards included 1.5, 0.75, 0.5 and 0.2 mg / mL. 5  $\mu\text{L}$  of standards and samples were pipetted in duplicate onto a clean, dry microtitre plate. 25  $\mu\text{L}$  of working

reagent A was added to each well. This binds protein to a coloured chelate complex with cupric ions ( $\text{Cu}^{2+}$ ) in an alkaline environment with tartrate solution. 200  $\mu\text{L}$  reagent B (Folin reagent) was then added to each well. The plate was then left for 15 minutes at room temperature. In this part of the reaction, folin is reduced producing a blue colour which can be measured. The optical density was read at 750 nm. The plate was also read at an irrelevant wavelength and the readings subtracted from this reading to remove cross-plate variation in optical properties. Data were analysed with a 4-parameter logistic curve fit using GraphPad Prism version 5.00 for Windows. Data gained from the protein assay were then used to normalise the protein samples which were diluted appropriately with PBS to a concentration of 300  $\mu\text{g} / \text{mL}$  (as this was the lowest total protein amount previously determined).

The supernatant samples were defrosted to room temperature and were concentrated using a centrifugal protocol using Amicon Ultra-2 3K devices (originally Millipore Corporation, Massachusetts, USA) according to the manufacturer's instructions. A previous pilot study undertaken by myself had shown that Hsp70 levels in unconcentrated supernatant samples were below the detection limit of the Hsp70 singleplex multibead kit, and therefore they were concentrated for future assays. Briefly, this involved inserting the Amicon Ultra-2 devices into filtrate collection tubes. The supernatant samples were then added to the devices and covered with collection tubes. These were pushed firmly onto the devices and the filter devices placed into a swinging bucket rotor centrifuge for 60 minutes at 3000 x g. The device was removed from the centrifuge, and the Amicon Ultra-2 devices separated from the filtrate collection tubes. The Amicon Ultra-2 filter devices were then inverted and placed back in the centrifuge to spin for 2 minutes 3000 x g to transfer the sample from the devices to the collection tubes. After concentration, the samples were stored at  $-80^{\circ}\text{C}$ .

The stored lysate and supernatant samples were analysed using the Hsp70 singleplex multibead kit to assess Hsp70 expression. Samples were defrosted and kept on ice before use. They were run either neat (supernatant samples) or at a concentration of 300  $\mu\text{g} / \text{mL}$  (lysate samples). All reagents were supplied with the kit and the assay was performed according to the

manufacturer's instructions. For reagent preparation, working HSP/Chaperone Multibead Buffer (termed wash buffer from now onwards) was prepared by adding 2 mL HSP/Chaperone Multibead Buffer solution to 18 mL water. Working Hsp70 capture beads were prepared to a working 1X stock by adding 60  $\mu$ L of stock Hsp70 capture beads to 1440  $\mu$ L of assay buffer. Working strep-PE conjugate was also made to a 1X stock by adding 120  $\mu$ L strep-PE conjugate stock to 2880  $\mu$ L assay buffer. Working Hsp antibody was made to a 1X stock by adding 120  $\mu$ L Hsp antibody stock to 2880  $\mu$ L assay buffer. Standards were prepared by adding 1250  $\mu$ L assay buffer to the defrosted standard cocktail vial, before vortexing briefly and being left at room temperature for 5 minutes. The vial was then vortexed briefly again and was ready for use. Standards ranging from 1.37 to 1000 ng / mL were prepared including 1000 ng / mL, 333.3 ng / mL, 111.1 ng / mL, 37.04 ng / mL, 12.35 ng / mL, 4.17 ng / mL and 1.37 ng / mL. 25  $\mu$ L of each sample and standard were pipetted into labelled 17 x 100 mm polypropylene test tubes. Standards were run in duplicate whilst samples were run once as sample volume was limited.

25  $\mu$ L of chaperone buffer was added to two additional tubes labelled "standard 0" and "setup tube". 25  $\mu$ L of working Hsp70 capture beads was added to each tube including all standards and the setup tube. The tubes were covered with foil and incubated for 1 hour at room temperature. The tubes were then washed 3 times by adding 500  $\mu$ L working wash buffer per tube, centrifuging at 200 x g for 5 minutes and aspirating the supernatant. This was repeated another 2 times to give a total of 3 washes. 50  $\mu$ L working Hsp70 antibody reagent was then added to every tube. The tubes were covered with foil and incubated at room temperature for an hour before being washed 3 times with working wash buffer as previously mentioned. 50  $\mu$ L working strep-PE conjugate was added to every tube and covered with foil before incubating at room temperature for 30 minutes. The tubes were all washed 3 times as previously described and 250  $\mu$ L working wash buffer added to each tube before the samples were analysed on an LSRII flow cytometer (BD Biosciences, Oxford, UK). The setup tube was used to detect the Hsp70 capture beads which were gated around in a forward and side scatter plot. A stopping gate of 1000 events was set up and a threshold of

5000 was used to remove cell debris. Data obtained were collected as median fluorescent intensity and analysed with a 4-parameter logistic curve fit using GraphPad Prism version 5.00 for Windows, so that sample concentrations of Hsp70 could be read as ng / mL. Unknown samples were quantified against this standard curve. The sensitivity was determined by interpolation at 2 standard deviations above the mean signal at background (0 ng / mL). The inter-assay coefficient of variation was 5.9% to 16.6% and the intra-assay coefficient of variation was 3.1% to 6.2% for this kit.

#### **4.2.4.4 Quantification of Hsp70 in isolated RNA samples**

A second set of cell lysate samples were used to purify and remove total protein and RNA. Levels of Hsp70 within RNA samples were measured whilst the protein samples were used by myself in another study measuring Hsp60 levels; however this work is not included in this thesis. RNA and protein were collected using the AllPrep RNA/Protein Kit according to the manufacturer's instructions.

The Protein Cleanup spin columns were vortexed gently to resuspend the resin before the caps were loosened a quarter turn. The bottom closures were then snapped off and the columns placed in 2 mL collection tubes that had been supplied. These were then centrifuged for 3 minutes at 750 x *g*. The Protein Cleanup spin columns were then equilibrated by adding 500  $\mu$ L PBS, vortexing gently and centrifuging for 3 minutes at 750 x *g*. The Protein spin columns were then transferred to clean microcentrifuge tubes. Cell lysate samples collected previously in Chapter 4.2.4.2 were defrosted and kept on ice. They were then homogenised by pipetting up and down several times before being pipetted into AllPrep spin columns in 2 mL collection tubes. These were then centrifuged for 1 min at 7000 x *g*. At that point, the AllPrep spin columns contained the bound RNA and the flow through contained the total protein. The flow through (containing total protein) was then added dropwise onto the centre of the slanted gel bed in Protein

Cleanup spin columns. These were centrifuged for 3 minutes at 240 x *g*. The Protein Cleanup spin columns were then removed from the microcentrifuge tubes. The flow through solution contained purified total protein which was stored at -80°C.

AllPrep spin columns were then placed in new 2 mL collection tubes and 350 µL Buffer RLT added to each. The columns were centrifuged for 1 minute at 7000 x *g*. 350 µL of 70% v/v ethanol was added to the flow throughs and mixed. 700 µL of each sample was then added to separate RNeasy spin columns which had been placed in 2 mL collection tubes. The lids were closed and the columns spun for 1 minute at 7000 x *g*. The flow throughs were discarded and 700 µL Buffer RW1 was added to each RNeasy spin column. The lids were closed and the columns spun for 30 seconds at 7000 x *g*. The flow throughs were discarded and 500 µL Buffer RPE was added to each RNeasy spin column. The lids were closed again and the columns spun for 30 seconds at 7000 x *g* to wash the spin column membranes. The flow throughs were discarded and this step was repeated. The RNeasy spin columns were then centrifuged for 1 minute at full speed to remove residual wash buffer, then placed in new 1.5 mL collection tubes and 40 µL of RNase-free water was added directly to each spin column membrane. The lids were closed and the columns centrifuged for 1 minute at 7000 x *g* to elute the RNA. The RNA samples were used immediately to transcribe cDNA for use in a real-time PCR reaction.

For reverse transcription of RNA to cDNA, 1 µL of all RNA samples was analysed on the Thermo Scientific NanoDrop™ 1000 Spectrophotometer (Thermo Fisher Scientific, Hemel Hempstead, UK) to calculate RNA concentration. Briefly this involved adding 1 µL of RNA onto the lower measurement pedestal, closing the sampling arm to initiate a spectral measurement and the operating software on the computer collecting measurements. Results were used to calculate the volume of each sample needed to run 2 µg RNA in a RT-PCR reaction.

The high capacity cDNA reverse transcription kit (Applied Biosystems of Life Technologies Ltd, Paisley, UK) was used to convert 2 µg RNA into cDNA. This involved adding 10 µL 2X RT master mix to each tube of a PCR microtube and cap strip (Sigma-Aldrich, Dorset, UK). To make the master

mix, 2  $\mu\text{L}$  10X RT buffer was added to 0.8  $\mu\text{L}$  25X dNTPs, 2  $\mu\text{L}$  10X reverse transcriptase random primers, 1  $\mu\text{L}$  MultiScribe™ reverse transcriptase, 1  $\mu\text{L}$  RNase inhibitor and 3.2  $\mu\text{L}$  nuclease free water. The volume of RNA sample required was made up to 10  $\mu\text{L}$  with sterile  $\text{H}_2\text{O}$  and the samples were added to each tube of the PCR microtube and cap strip. The master mix was incubated for 1 hour at 37°C and then 95°C for 5 minutes in a PCR machine (G-storm, East Sussex, UK) as these parameters had been used previously within the laboratory.

The resulting cDNA samples were used for real-time PCR amplification of Hsp70. For this, 15  $\mu\text{L}$  cDNA was added to 52.5  $\mu\text{L}$  RNase free water. An RT negative sample was also added to 52.5  $\mu\text{L}$  RNase free water. The cDNA negative control contained just 67.5  $\mu\text{L}$  RNase free water. For the primer control, 25  $\mu\text{L}$  of each primer was added in separate tubes to 250  $\mu\text{L}$  of the TaqMan Gene Expression Master Mix (master mix). The master mix contains AmpliTaq Gold® DNA Polymerase, UP (Ultra Pure), Uracil-DNA glycosylase, dNTPs with dUTP, ROX™ Passive Reference and Optimised buffer components. The primers for Hsp70 and ATP3 (as a control) (both from Applied Biosystems Biosystems of Life Technologies Ltd, Paisley, UK) were used in this assay. A total of 5.5  $\mu\text{L}$  of each primer was then added to 4.5  $\mu\text{L}$  of diluted cDNA in duplicate on the microplate. The plate was covered with a MicroAmp™ Optical Adhesive Film and analysed on a 7900HT Real-Time PCR system (Applied Biosystems of Life Technologies Ltd, Paisley, UK). For the reaction the thermal cycling conditions were set to a UDG Incubation step of 2 minutes at 50°C, followed by a step for enzyme activation for 10 minutes at 95°C finally followed by a PCR step for 40 cycles in which a denaturing step (15 seconds at 95°C) and an annealing and elongation step (1 minute at 60°C) occur. Sequence Detection System (SDS) version 2.3 software was used to automatically calculate the baseline and threshold for the amplification curves and Relative quantification (delta, delta CT) for the Hsp70 gene was determined using GraphPad Prism.  $\Delta\text{CT}$  was calculated as the difference in CT values between Hsp70 and ATP5B and Hsp70 was normalised against ATP5B.

## 4.3 Results

### 4.3.1 Circulating Hsp70 levels in pulmonary arterial hypertension

Analysis of Hsp70 levels in serum samples taken from IPAH and SSc-PAH patients and healthy controls was undertaken using the Hsp70 high sensitivity EIA kit; however Hsp70 serum levels in patients and controls were below the detection limit (0.2 ng / mL). The standard curve for this experiment is shown below (Figure 4.1). In future tests, concentrating the human serum samples before running the Hsp70 high sensitivity EIA kit would provide more reliable results, as the resulting data points would fall within the linear range of the standard curve.

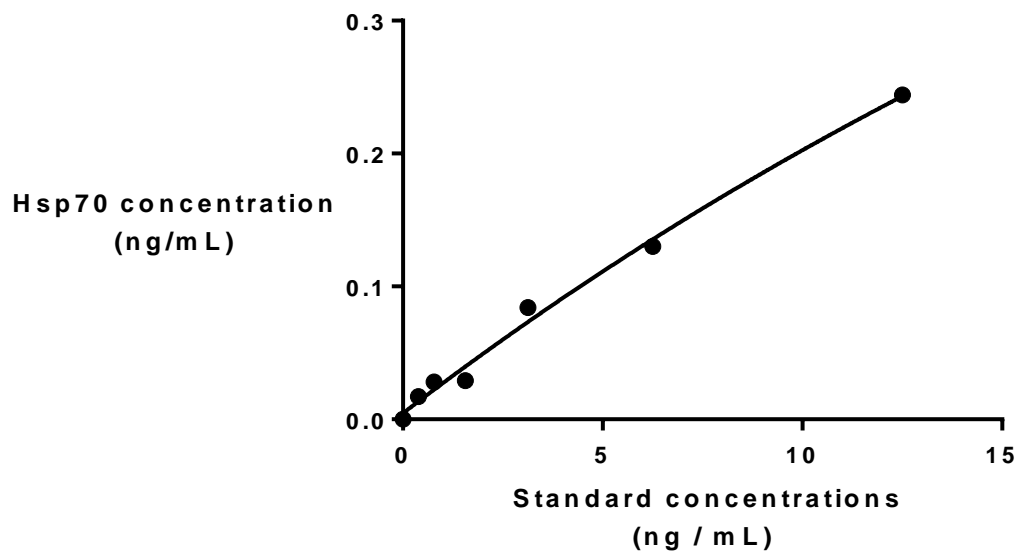


**Figure 4.1 Standard curve for Hsp70 levels in human serum samples.**

Standard curve produced using the Hsp70 high sensitivity EIA kit. Standards of 12.5, 6.25, 3.13, 1.56, 0.78, 0.39 and 0.2 ng / mL were setup.

### 4.3.2 Hsp70 levels in rat serum

As Hsp70 serum levels in patient samples could not be detected using the available kit, circulating Hsp70 levels in serum from the rat MCT model of PAH were assessed to determine whether Hsp70 levels changed with disease progression.

There was a failure of an increase in levels of circulating Hsp70 in MCT treated animals at day 14 compared to saline controls ( $3703 \pm 2596.0$  pg / mL vs  $2007 \pm 475.6$  pg / mL respectively,  $n=4$ /group,  $P=0.01$ ) (Figure 4.2).

Unfortunately serum samples from the fat fed ApoE<sup>-/-</sup>/IL1R1<sup>-/-</sup> mouse model of PAH were not available due to a limited blood sample size collected, however tissue was available for both the MCT rat model and the fat fed ApoE<sup>-/-</sup>/IL1R1<sup>-/-</sup> mouse model of PAH, and these were used to investigate the expression and localisation of Hsp70 within the lung tissue.

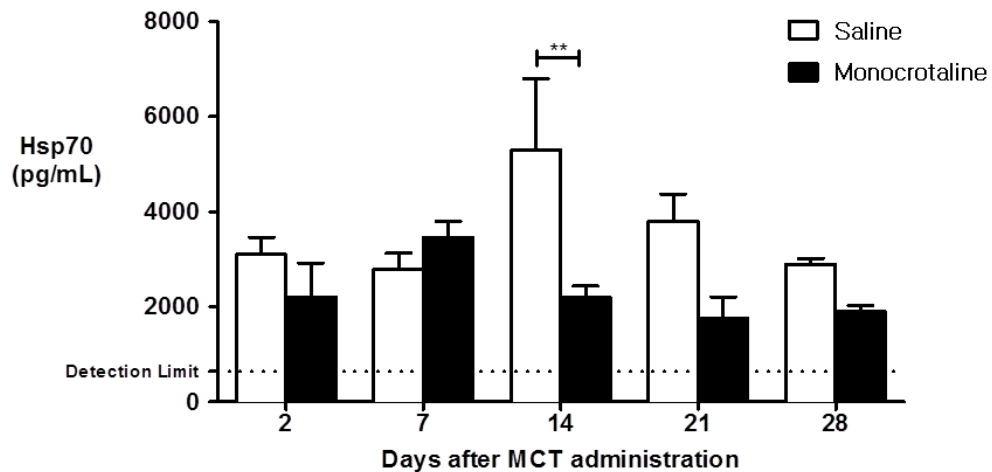


**Figure 4.2 Serum Hsp70 levels in the MCT rat and saline-treated controls.**

Saline (white bars) and MCT treated (black bars) animals at time points of 2, 7, 14, 21 and 28 days.  $n=4$  per group and data as  $\pm$  SEM is shown. Detection limit set to lowest standard  $\pm 2$  SD (640 pg / mL). Data at each time point were analysed using a two-way ANOVA with a Bonferroni post hoc test where  $P < 0.05$  is considered statistically significant (\*).

### **4.3.3 Hsp70 expression in the lungs of rat and mouse models of pulmonary arterial hypertension**

After identifying a decrease in circulating Hsp70 within the serum of MCT treated rats at 14 days post injection, I next examined the localisation and distribution of Hsp70 within the lung tissue in the MCT rat model of PAH and the fat fed ApoE<sup>-/-</sup>/IL1R1<sup>-/-</sup> mouse model of PAH. This was to determine whether circulating levels of Hsp70 correlated with tissue expressed Hsp70 within the lung, as this is the main site of vascular remodelling in PAH. The process of vascular remodelling is thought to induce stress protein expression due to the stressful nature of the environment (hypoxia, sheer stress and inflammation). I hypothesised that Hsp70 expression would correlate with disease severity. Immunohistochemistry to detect Hsp70 protein expression was performed on paraffin embedded lung sections taken from both MCT and saline-treated animals at 2, 7, 14, 21 and 28 days post injection as well as fat fed ApoE<sup>-/-</sup>/IL1R1<sup>-/-</sup> mice at weeks 1 to 8. No Hsp70 expression was noted in either MCT or saline treated animals.

A second animal model of PAH (fat fed ApoE<sup>-/-</sup>/IL1R1<sup>-/-</sup> mouse) was therefore studied for changes in Hsp70 expression within diseased tissue, as the disease developed. Hsp70 was detected in a much larger number of perivascular inflammatory cells at all time points in fat fed ApoE<sup>-/-</sup>/IL1R1<sup>-/-</sup> mice compared to chow fed controls (Figure 4.3). Inflammatory cell infiltration into the lung tissue is more markedly apparent in this model which corresponds to the areas of high Hsp70 expression, suggesting that perivascular inflammatory cells are the source of the Hsp70, not the endothelium itself. In future work, it would be of interest to determine the exact identity of these cells that are expressing Hsp70 using a dual staining immunohistochemistry protocol.

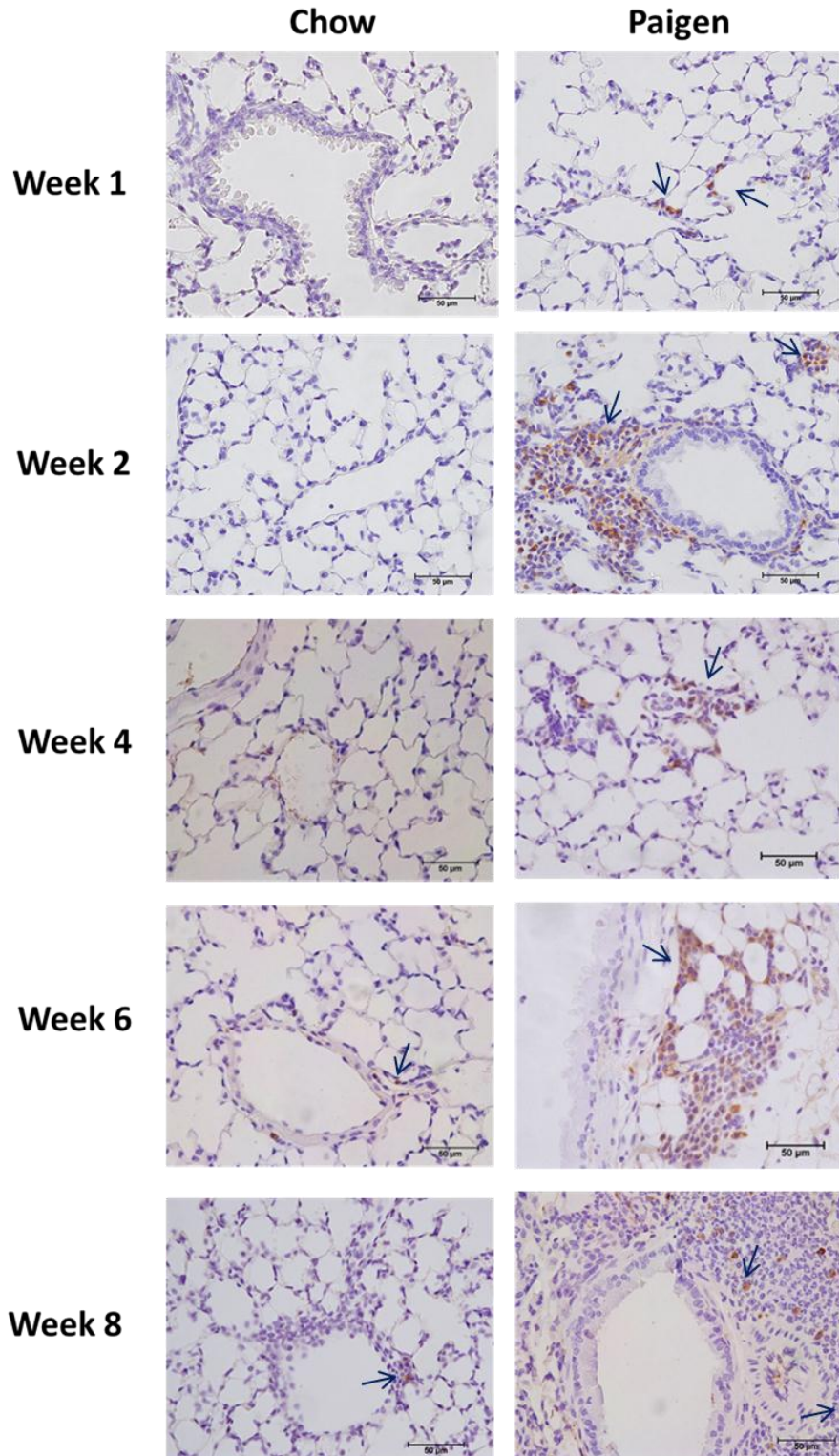


**Figure 4.3 Hsp70 expression in lung tissue of fat fed ApoE<sup>-/-</sup>/IL1R1<sup>-/-</sup> mice and chow fed controls.**

Representative images of Hsp70 expression at weeks 1 to 8 after commencing paigen or chow fed diet in ApoE<sup>-/-</sup>/IL1R1<sup>-/-</sup> mice. All images taken at 400X magnification.

CD4<sup>+</sup> T cells are thought to be involved in the pathogenesis of PAH and have been found associated with plexiform lesions within the lung tissue of IPAH patients (Tuder *et al*, 1994). However, it is still unknown whether they are functioning to regulate the disease or propagate its progression. Therefore, to study the role of these cells within PAH, CD4<sup>+</sup> T cells were depleted in the paigen fed ApoE<sup>-/-</sup>/IL1R1<sup>-/-</sup> mouse of PAH and disease progression assessed.

I aimed to determine whether Hsp70 expression was driven by the disease, by determining the expression of Hsp70 within the lung tissue in IgG treated and CD4 depleted paigen fed animals. I hypothesised that due to the infiltration of Hsp70-expressing inflammatory cells into the lung tissue of remodelling vessels noted previously in the paigen fed ApoE<sup>-/-</sup>/IL1R1<sup>-/-</sup> mouse of PAH, that removal of CD4<sup>+</sup> T cells may affect Hsp70 expression in lung tissue of CD4 depleted animals.

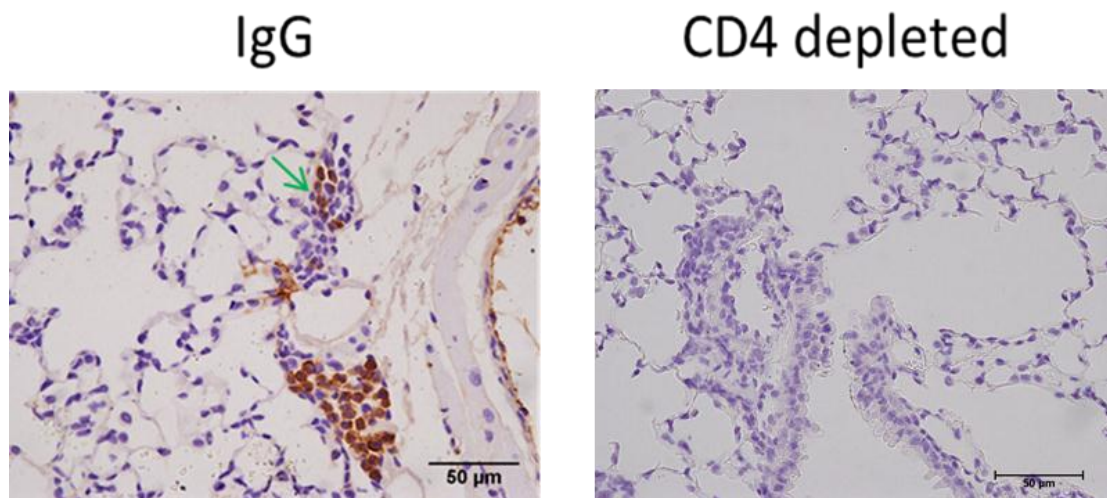


**Figure 4.4 Hsp70 expression in lung tissue from paigen fed ApoE<sup>-/-</sup>/IL1R1<sup>-/-</sup> mice after CD4<sup>+</sup> T cell depletion.**

*Green arrows show location of Hsp70 staining specific to inflammatory cells. Images taken at X400 magnification.*

Depleting CD4<sup>+</sup> T cells rendered these animals more susceptible to PAH, as proven by an increase in RVSP and an increased number of remodelled vessels (Chapter 3.3.2.2). Hsp70 expression in CD4 depleted animals was markedly reduced, suggesting that as there were inflammatory cells expressing Hsp70 in IgG treated controls, that CD4<sup>+</sup> T cells may be the source of the Hsp70 in these animals (Figure 4.4). Depleting CD4<sup>+</sup> T cells had no effect on the expression of Hsp70 on ECs as Hsp70 was again not noted in ECs.

#### **4.3.4 Effect of hypoxia on cultured pulmonary artery endothelial cell Hsp70 expression**

Hypoxia is thought to be involved in the development of PAH via its effects on SMC proliferation and vessel remodelling, however little is known about its effects on EC expression of Hsps. Therefore, to determine the effect of hypoxia on Hsp70 expression in ECs, an *in vitro* method using PA-ECs was established and Hsp70 protein and RNA expression assessed.

In cell lysate samples, levels of Hsp70 protein did not significantly change when compared to normoxic samples. Hsp70 levels in lysates from normoxic and hypoxic cells increased throughout the time course, but were comparable in each condition (Figure 4.5, A).

Quantitative real time-PCR was also used to quantify levels of Hsp70 gene expression in cell lysate samples taken from PA-ECs cultured in either hypoxic or normoxic conditions at several time points. Data were normalised to ATP5B gene content and are shown in Figure 4.5, B.

There is a significant decrease in the relative expression of Hsp70 in hypoxic lysates compared to normoxic lysates at 6 hours ( $2.26 \pm 0.36$  vs  $13.78 \pm 3.58$ ,  $n=2-3$ ,  $P=0.02$ ), however, relative expression levels of Hsp70 remain low in both normoxic and hypoxic conditions at 24 and 48 hour time points.

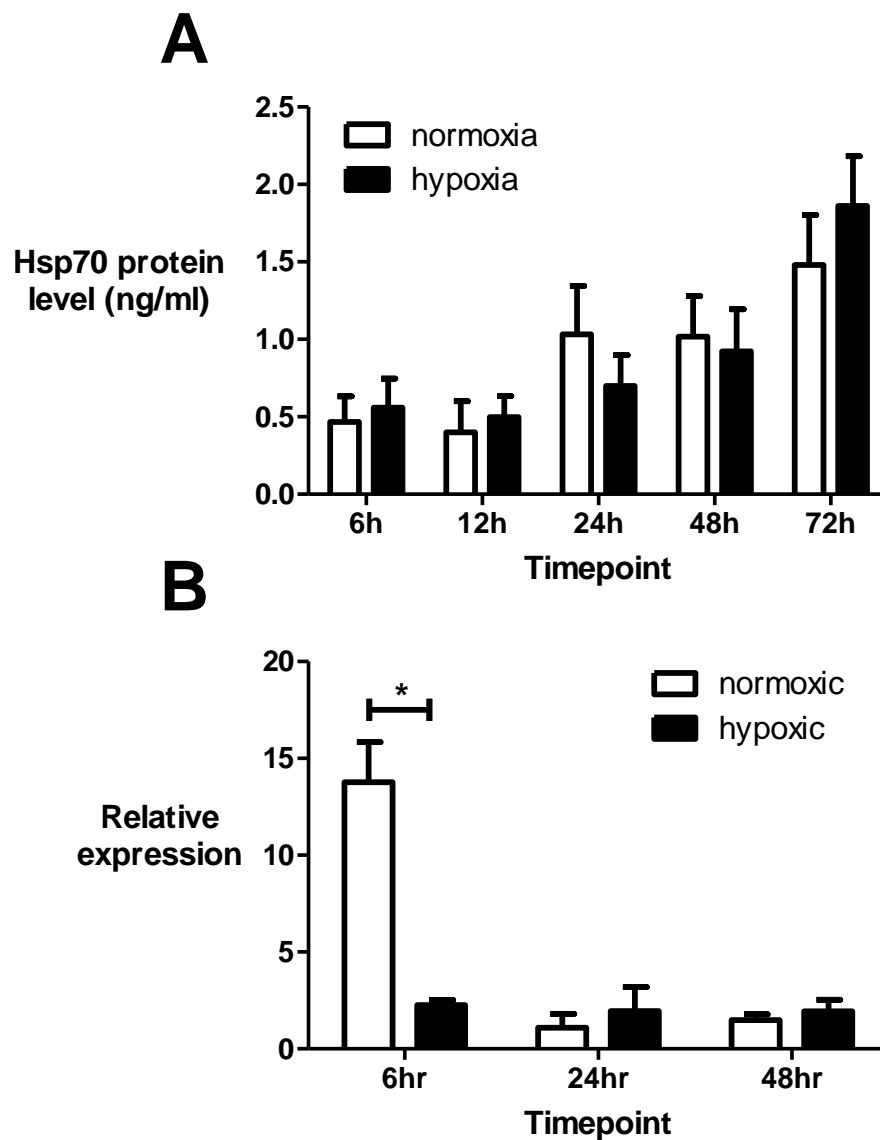


**Figure 4.5 Levels of Hsp70 protein and RNA expression in hypoxic and normoxic cell lysates.**

Normoxic groups are shown as clear bars and hypoxic groups as black bars. Data as  $\pm$  SEM are shown. A) Hsp70 levels in cell lysates from cultured PA-ECs in normoxic and hypoxic conditions for 6 - 72 hours,  $n=3-10$ . B) Relative expression of Hsp70 RNA at 6 - 48 hours in normoxic and hypoxic cell lysates,  $n=2-3$ . Data at each time point were analysed using a two-way ANOVA with a Bonferroni post hoc test where  $P < 0.05$  is considered statistically significant (\*).

## 4.4 Discussion

Previous studies undertaken by Pockley *et al* have demonstrated that elevated Hsp70 levels correlate with a reduced incidence of cardiovascular disease in patients with established hypertension, however little is known about the cardioprotective effects of Hsp70, especially within the setting of PAH (Pockley *et al*, 2003). Little evidence also exists on whether ECs express Hsp70 in response to heat shock or ischaemic stress and to what extent this expression protects the stressed endothelium from necrosis and apoptosis (Wang *et al*, 1995; Zhu *et al*, 1996; Amrani *et al*, 1998; Luo *et al*, 2007).

Therefore, the aim of this work was to determine levels of circulating Hsp70 in clinical end stage disease serum samples as well as the expression pattern of circulating and expressed Hsp70 in serum and lung tissue in animal models of PAH. The effect that altered disease progression had on expression of Hsp70 in endothelial and inflammatory cells was also assessed in a CD4 depletion model to determine whether Hsp70 expression was driven by the disease. The influence of hypoxia on EC Hsp70 expression was also assessed *in vitro* to determine how Hsp70 levels relate to disease progression. Immunohistochemistry was also undertaken on mouse and rat lung tissue from animal models of PAH to determine cellular location of Hsp70 expression along a time course of the disease. This work aimed to address these gaps in knowledge surrounding Hsp70 and its expression in PAH patients and experimental models.

Circulating levels of Hsp70 were below the detection limit of the kit used in serum samples from healthy controls and PAH patients. In future, either the serum needs to be concentrated before use, a Western blot used to quantify Hsp70 protein levels or a more sensitive ELISA may need to be used in order to quantify Hsp70 in serum from PAH patients. This is the only commercial kit available to detect Hsp70 in human plasma and serum samples, and has been used by several groups to detect circulating Hsp70 levels in a variety of conditions. In one study undertaken in healthy volunteers and patients with chronic fatigue syndrome, levels of circulating

Hsp70 between 0.9 and 1.5 ng / mL were recorded (Jammes *et al*, 2009). Similar levels have also been reported in patients with hepatic stenosis, after coronary bypass and in resting healthy individuals (Dybdahl *et al*, 2002; Fortes and Whitham, 2009; Tarantino *et al*, 2012). The detection limit of the kit is 0.09 ng / mL as stated by the supplier, and the first points on the standard curve fall within the range of the results noted in the studies mentioned above, suggesting that a more sensitive means of Hsp70 detection is needed in these samples.

After inconclusive studies using serum samples from human end-stage disease, an experimental time course of disease was undertaken to detect changes in serum Hsp70 levels and Hsp70 expression in lung tissue and relate this to human disease progression. In experimental PAH models, serum Hsp70 levels decreased in MCT treated rats from day 14. This is interesting as previous work undertaken in this model describes vascular remodelling and right ventricular hypertrophy as being evident at day 21 post MCT injection (Roth *et al*, 1981; Le Pavec *et al*, 2009). Levels of circulating Hsp70 remain lower in serum from MCT treated animals compared to saline-treated controls from day 14 to 28 post MCT injection.

Work undertaken in patients with cardiovascular diseases such as coronary artery disease and carotid atherosclerosis also correlate with data gained from my study, in that low circulating Hsp70 levels are more common in patients compared to controls (Zhu *et al*, 2003; Martin-Ventura *et al*, 2007). This is also the case in patients with atherosclerosis associated with essential hypertension, where an increased intima-media thickness was less prevalent in patients with a high serum level of Hsp70 (Pockley *et al*, 2003). Taken together, data from the MCT model of PAH and from previous human studies, suggest that Hsp70 may protect against or modify the progression of cardiovascular disease, and that a dysregulation or reduced level of circulating Hsp70 could be prognostic of a poor response to prevent disease progression (Pockley and Frostegard, 2005).

Hsp70 expression was not noted in the lung tissue of either MCT or saline treated rats. Hsp70 expression detection using this clone (C92F3A-5) has been undertaken before in other tissues and cell lines, however there is little evidence to suggest that it has been used to determine Hsp70

expression levels in paraffin-embedded rat lung sections (Mestril *et al*, 1994). Further investigations using alternative antibodies and clones could help to identify Hsp70 expression in rat lung tissue in the MCT timecourse in the future.

An increased expression of Hsp70 was noted across the whole of the timecourse undertaken in paigen ApoE<sup>-/-</sup>/IL1R1<sup>-/-</sup> mice compared to chow fed controls. Disease progression can be noted at week 6 and 8 in paigen fed animals, as noted by an increase in vessel remodelling. In these animals, Hsp70 expression is noted after 1 week of beginning the diet suggesting that the diet may be causing the increased expression of Hsp70, not the remodelling process. However this has not been confirmed and literature regarding this subject is sparse.

After depletion of CD4<sup>+</sup> T cells, PAH disease progression worsened, as defined by increased RVSP and vessel remodelling. In these animals, levels of Hsp70 seen within the lung tissue decreased, suggesting that CD4<sup>+</sup> T cells may be the source of Hsp70 expression within the lung, further supporting a role for T cells in PAH. Further investigations need to take place to determine the identity of the Hsp70 expressing cells.

The original hypothesis of this element of the study was that changes in pulmonary haemodynamics would cause endothelial stress, which in turn would cause an increased production and release of Hsp70 from ECs within the pulmonary vessels. Interestingly, no EC specific staining for Hsp70 was noted at any point in experimental animal models. Limited evidence exists confirming the ability of ECs to express Hsp70 in response to stress, however Hsp70 EC expression has been noted in *in vitro* hypoxic studies (Chapter 4.3.4) (Jornot *et al*, 1991; Wang *et al*, 1995; Suzuki *et al*, 1998).

There could be several explanations as to why Hsp70 expression was noted in EC *in vitro* hypoxic studies, but not in immunohistochemistry from *in vivo* MCT or the fat fed ApoE<sup>-/-</sup>/IL1R1<sup>-/-</sup> mouse model lung samples of PAH. Firstly, *in vitro* hypoxia is a very different environment to MCT and diet induced PAH *in vivo*. Therefore differences could have occurred due to the way in which the PAH phenotype was induced or the fact that *in vivo* and *in vitro* conditions are not always similar. Both MCT and paigen diet have been shown to have an effect on EC function, and therefore possibly Hsp

production; however, the mechanisms by which they exert these effects remain unclear (Wilson *et al*, 1992; Thomas *et al*, 1998; Reilly *et al*, 2006). Another difference between these studies was the time in which the assays were undertaken. The hypoxic experiments were short exposures to hypoxic stress (6 to 72 hours) whereas MCT and diet induced PAH are chronic stressors, lasting 1-2 months. This could mean that EC expression of Hsp70 could have been missed in immunohistochemical staining as transient Hsp70 expression has been noted in other cells (Jaattela *et al*, 1992; Sanz *et al*, 1997; Ammon-Treiber *et al*, 2004).

To determine the effect of hypoxia, a known contributing factor in PAH, on EC production of Hsp70, an *in vitro* culture model using PA-ECs was set up to determine levels of PA-EC-expressed and secreted protein and RNA expression in PA-EC cells of Hsp70 at different time points of hypoxic exposure. Unfortunately, the release of Hsp70 could not be analysed in supernatant samples, as levels of Hsp70 released by PA-ECs during a 6 - 72 hour incubation in hypoxic conditions was below the detection limit of the kit available at the time. Using a higher number of seeded PA-ECs in the incubation stage of this assay could overcome this issue in the future.

Hsp70 levels in normoxic and hypoxic cell lysates increased throughout the timecourse, but were comparable in each condition. Hsp70 levels have been shown to increase in HeLa cells at the S phase of the cell cycle (RNA replication stage) (Milarski and Morimoto, 1986). As there are more cells present at 72 hours (due to proliferation) compared to 6 hours in culture (in both normoxic and hypoxic conditions) it is possible that the rise in Hsp70 noted is due to an increased number of proliferating cells. There was however, no difference between normoxic and hypoxic cell Hsp70 protein expression in cell lysate samples at any time point. This is interesting, as previous studies have noted that human microvascular ECs (HMEC-1 cell line) and bovine ECs can adapt to hypoxic conditions by producing ATP independently of oxygen. They have been shown to convert glucose to lactate via anaerobic glycolysis and Hsp70 expression levels mimic those seen under normal physiological conditions (Graven *et al*, 1993; Oehler *et al*, 2000). Although the precise reason why this adaptation occurs is unclear, it is thought that ECs are well adapted to low levels of oxygen in the

vasculature compared to other cell types, and can cope better with hypoxic conditions.

An unexpected and unexplainable increase in Hsp70 RNA expression was noted in normoxic cell lysates at 6 hours compared to hypoxia treated PA-ECs. After this time point relative expression of Hsp70 remained low in both normoxic and hypoxic conditions at 24 and 48 hour time points. As previously mentioned this could be due to an adaptive response of ECs to the hypoxic environment.

In conclusion, these studies showed a decrease in serum Hsp70 levels in the MCT rat model of PAH from week 14 as PAH progression was noted to occur. Hsp70 expression in perivascular inflammatory cells within lung tissue sections from fat fed ApoE<sup>-/-</sup>/IL1R1<sup>-/-</sup> mice was increased compared to chow fed controls, however it is unclear whether this is an effect of the method in which PAH was induced (paigen diet) or a consequence of PAH itself. Further investigations into Hsp70 expression in lung tissue sections from other disease models of PAH may help to answer this question. In cultured PA-ECs subjected to hypoxia there was no change in RNA or PA-EC expression levels of Hsp70 protein at any time point from 6 - 72 hours compared to normoxic controls. These data confirm that cultured PA-ECs can express Hsp70 in both normoxic and hypoxic conditions, however hypoxic insult does not increase Hsp70 levels in these cells compared to normoxic controls. Despite seeing a decrease in Hsp70 serum levels in MCT treated rats, further work needs to be undertaken to 1) determine Hsp70 serum levels in PAH patients and 2) determine whether this protein can be used as a biomarker of PAH in the future.

## Chapter 5 General Discussion

PAH is a life threatening condition which is caused by the gradual occlusion of pulmonary vessels due to vasoconstriction, vessel remodelling, *in situ* thrombosis and inflammation. This restricts blood flow and increases pressures within these vessels, leading to increased strain on the heart, RVH, right ventricular failure and death. Many factors are thought to be involved in the pathogenesis of PAH, including inflammatory processes.

Several sources suggest that T cells of the adaptive immune system are particularly involved in this process. Firstly, T cells have been found associated with vascular lesions in IPAH patient lung tissue (Tuder *et al*, 1994). Secondly, several experimental models have shown that T cells protect against the progression of experimental PAH disease (Miyata *et al*, 2000; Taraseviciene-Stewart *et al*, 2005; Taraseviciene-Stewart *et al*, 2007), whilst immunosuppressive therapy has been shown to prevent experimental PAH and limit clinical PAH disease progression (Morelli *et al*, 1993; Bellotto *et al*, 1999; Rodriguez-Iturbe *et al*, 2001; Sanchez *et al*, 2006; Jais *et al*, 2008; Price *et al*, 2011). In human studies, alterations in T cell subsets have been noted in the peripheral blood and lung tissue of IPAH patients undergoing PAH specific treatment, further suggesting that a dysfunctional T cell compartment may be involved in PAH pathogenesis (Ulrich *et al*, 2008; Austin *et al*, 2010). However, it is still unknown whether these changes in T cell populations are a cause or an effect of the disease. In experimental models of PAH, inflammation has been shown to precede vascular remodelling, however, literature on this subject is limited and so further work needs to be undertaken to clarify this issue (Cuttica *et al*, 2011).

Hsp expression has been shown to be protective against stresses such as hypoxia and shear stress in several cell types, including SMCs and monocytes (Guzik *et al*, 1999; Xu *et al*, 2000). Hsp70 is a member of the stress protein family and its expression can be upregulated on all cells under stressful conditions such as heat shock or hypoxia. There is little evidence however, that ECs produce Hsp70 in response to hypoxia or oxidative stresses and Hsp70 serum levels have not been determined in IPAH and

SSc-PAH to date. Decreased levels of serum Hsp70 have been shown to correlate with increased risk of carotid atherosclerosis in patients with established hypertension, suggesting a cardioprotective role of Hsp70 in patients with hypertensive disease (Pockley *et al*, 2003).

Therefore work undertaken in this thesis aimed to elucidate the role of T cells in the pathogenesis of PAH in patients with PAH and animal models, as well as determine expression levels of Hsp70 and Hsp70 serum levels in PAH patients and animal models. How changes in proportions of T cell subsets, changes in Hsp70 expression and serum levels correlate with disease progression, were also assessed.

Previous studies have attempted to determine proportions of circulating lymphocytes in IPAH patients, but were limited by patient cohorts that were already on PAH treatment. Work was therefore undertaken to analyse T and B cell subsets in treatment-naïve PAH patients (SSc-PAH and IPAH). It was hypothesised that patients in different PAH subgroups would exhibit an altered T cell profile in peripheral blood. Multicolour flow cytometry was used to determine T cell (CD4 / 8 / 25 / 127) and B cell (CD19) subset profiles in peripheral blood of incident cases of IPAH and SSc-PAH, whilst CD69 (an early activation marker found on lymphocytes) was used to detect T and B cell activation.

The main finding of this work was that the relative frequency of CD8<sup>+</sup> cytotoxic T cells in treatment-naïve patients with SSc-PAH was significantly decreased compared to their corresponding controls. No change in the relative frequency of CD8<sup>+</sup> T cells was noted in IPAH patients, which conflicts with previously published data from Ulrich *et al*, who noted a diminished proportion of CD8<sup>+</sup> T cells in the peripheral blood of IPAH patients undergoing PAH treatment (Ulrich *et al*, 2008). Differences noted between studies may be due to the cohort of patients analysed or the PAH specific treatments they were taking (discussed previously in Chapter 2.4.1). Further work could assess the function of this decreased subset of T cells, as this could provide information regarding their decreased proportions in PAH patients and their role within disease pathogenesis. No significant changes in other T or B cell lymphocyte subsets or their activation status were noted in either patient group in this study.

Correlation analyses between clinical parameters and proportions of T cell subsets highlighted a negative correlation between CD4<sup>+</sup> T cells and CI in SSc-PAH patients and CD4<sup>+</sup> T cells and the shuttle walk test in IPAH patients. Further analysis of proportions of CD4<sup>+</sup> T cells within the circulation of PAH patients could predict disease progression, or even diagnosis, in the future.

Follow-up blood sample analysis in returning patients after administration of PAH specific treatment, suggested that E-RA could return the proportion of circulating CD4<sup>+</sup> T cells to “normal” levels and improve a patient’s exercise capacity compared to PDE-5 inhibitors. It was noted that neither treatment had beneficial effects on the modification of proportions of CD8<sup>+</sup> T cells or CD4<sup>+</sup>CD25<sup>high</sup> Treg cells to a “healthier” level. Further work needs to be undertaken in order to increase the study number and the validity of these statements. Studies have shown that PAH specific therapies including Sildenafil and Prostaglandin I<sub>2</sub> analogs, can modify T cell responses in other disease settings such as asthma, by suppressing DC activation and T cell stimulatory function and reducing their recruitment into the airways (Jaffar *et al*, 2007; Zhou *et al*, 2007; Wang *et al*, 2009). These studies suggest that T cell activation and migration can be modulated by these therapies, however literature regarding this topic is scarce and further work needs to be done to identify the exact effects that each therapy has on the proportion of circulating T cell subsets and their activation status. In future, it may be beneficial to prescribe therapies to PAH patients to restore the balance between Th1 and Th2 cells.

Human samples only provide information regarding end stage disease states, therefore animal models, such as the fat fed ApoE<sup>-/-</sup>/II-1R1<sup>-/-</sup> mouse model of PAH, are utilised to determine factors involved in the pathogenesis of PAH. Although changes in T cell subsets within peripheral circulation and lung tissue of PAH patients has been noted in Chapter 2.3.1 and in previously published literature, it is unclear whether these changes occur as a cause or consequence of the disease (Tuder *et al*, 1994; Dorfmueller *et al*, 2002; Dorfmueller *et al*, 2003; Ulrich *et al*, 2008; Austin *et al*, 2010). It was hypothesised that these changes in T cell subsets would correlate with disease progression and vessel remodelling. To elucidate cause or effect of

changes in T cell frequency, I examined a time course of the paigen diet-fed ApoE<sup>-/-</sup>/IL-1R1<sup>-/-</sup> mouse model of PAH. In this model there was no difference in circulating T cell subsets whilst disease progression was confirmed by analysis of vessel remodelling. This was unexpected as a decreased proportion of circulating CD8<sup>+</sup> T cells had been noted in the blood of SSc-PAH patients previously in Chapter 2.3.1. This further emphasises the difficulties faced when using animal models to mimic human disease and the complexity of these experiments.

The effect of CD4<sup>+</sup> T cell depletion was also assessed in the paigen diet-fed ApoE<sup>-/-</sup>/IL-1R1<sup>-/-</sup> mice as these cells were thought to propagate disease progression. It was noted that CD4<sup>+</sup> T cells are protective as their removal using a depletion antibody increased RVSP and vessel remodelling in CD4 depleted animals. This could be due to the lack of Treg cells, found within the CD4<sup>+</sup> T cell compartment, as previous studies in other models have noted Treg cells can protect against Sugden 5416 initiated PAH in rats (Tamosiuniene *et al*, 2011). Therefore, a depletion of CD4<sup>+</sup> T cells propagates disease progression in the fat-fed ApoE<sup>-/-</sup>/IL-1R1<sup>-/-</sup> mouse model of PAH, as shown by an increase in RVSP and increased vascular remodelling.

To determine the effect that disease progression has on Hsp70 levels in clinical and experimental serum samples, Hsp70 expression within lung tissue and *in vitro* EC Hsp70 expression in animal models of disease, several techniques were used. These included, ELISA, immunohistochemistry, qPCR and Hsp70 Singleplex Multibead™ kit. Hsp70 was undetectable in clinical serum samples in IPAH and SSc-PAH patients, however in experimental models, a decreased serum level of Hsp70 was noted in monocrotaline treated rats, which coincided with vascular remodelling. Hsp70 expression in perivascular inflammatory cells within lung tissue of fat-fed ApoE<sup>-/-</sup>/IL-1R1<sup>-/-</sup> mice also increased along a timecourse of disease progression. There was also no difference noted in Hsp70 RNA and protein expression in cultured ECs exposed to hypoxic and normoxic conditions. These data suggest a protected phenotype ECs which may be adapting to hypoxic conditions (Oehler *et al*, 2000). Limitations regarding the detection limit of currently available Hsp70 serum and plasma detection kits currently

hinders research in this area. Further work needs to be undertaken to quantify Hsp70 serum levels in PAH patients, possibly via the use of Western blots, whilst serum Hsp70 analysis could be undertaken in the fat-fed ApoE<sup>-/-</sup>/IL-1R1<sup>-/-</sup> mouse model of PAH to relate changes of Hsp70 within lung tissue in inflammatory cells to circulating serum Hsp70 levels.

Taken together, these findings suggest that subtypes of PAH are associated with distinct T cell profiles, perhaps reflecting the different aetiologies. Alterations in circulating CD8<sup>+</sup> T cells suggest a dysfunctional immune system which could contribute to disease pathogenesis. In experimental models, the depletion of CD4<sup>+</sup> cells was found to propagate disease progression, whereas Hsp70 levels were found to decrease in the serum of MCT treated rats but increase within inflammatory cells infiltrating the remodelled lung tissue in paigen diet-fed ApoE<sup>-/-</sup>/IL-1R1<sup>-/-</sup> mice. Further work to elucidate the exact role that T cells play in the pathogenesis of PAH needs to be undertaken, however these data suggest that circulating levels of CD4<sup>+</sup> and CD8<sup>+</sup> T cells could be used in the diagnosis of PAH and as a prognostic marker in PAH patients in the future (Pendergrass *et al*, 2010).

In the future, further work could be undertaken to increase the sample population of patients being studied. Along with this, ethical approval to obtain a greater volume of blood could also be sought to continue the work regarding Treg cell function. Further work to analyse a greater number of subpopulations of T and B cells within the peripheral blood of PAH patients and controls could also be undertaken. A second cohort of patients could also be used to compare with the first set to confirm previous findings. Other models of PAH could also be used to assess T cell responses *in vitro* along a timecourse of the disease as well as assessing the involvement of Hsp70 in the pathogenesis of the disease.

There is growing evidence of the importance of lymphocytes (B and T cells) in the resolution of disease pathogenesis in PAH. Firstly, immune reconstituted Treg cells have been shown to prevent early inflammation and attenuate PAH development in athymic rats treated with Sugen 5416 (Tamosiuniene *et al*, 2011). This suggests that Treg cells are highly important in modifying the immune response in PAH. Secondly, pre-clinical

studies have resulted in funding to perform a clinical trial examining the effect of rituximab on disease progression in SSc-PAH patients. This is due to compelling pre-clinical data suggesting that rituximab improves lung function and skin thickening in SSc patients and in SLE associated PAH patients (Hennigan *et al*, 2008; Daoussis *et al*, 2010). This trial is currently being undertaken as modulation of the immune system may be an effective strategy for treating SSc-PAH (<http://www.clinicaltrials.gov>, 2012). Previous work determining the involvement of Treg cells and leptin in PAH has also provided evidence to suggest a dysfunctional T cell compartment in IPAH and SSc-PAH patients (Huertas *et al*, 2012). Taken together, these findings emphasise the importance of research in this area. There are however, several limitations to this work, which highlight the challenges faced in determining the role that lymphocytes play in the pathogenesis of PAH.

# Appendix 1

## 1. General reagents

### **AllPrep RNA/Protein Kit**

(80404, Qiagen, Crawley, West Sussex, UK)

---

The kit contained 50 AllPrep Mini Spin Columns, 50 RNeasy® Mini Spin Columns, 50 Protein Cleanup Mini Spin Columns, 50 1.5 mL Collection Tubes, 100 2 mL Collection Tubes, 12 mL Buffer APL, 45 mL Buffer RLT, 45 mL of Buffer RW1, 11 mL of Buffer RPE (prepared by adding 4X 100% ethanol) and 10 mL of RNase-Free Water. All reagents were stored at room temperature.

### **Amicon Ultra-2 (3K device)**

(UFC200324, Millipore Corporation, Massachusetts, USA)

---

The kit contained 24 filtrate collection tubes, 24 filter devices and 24 concentrate collection tubes. Kit contents were all stored at room temperature.

### **Cell trace Violet Proliferation Kit**

(C34557, Invitrogen of Life technologies Ltd, Paisley, UK).

---

5 µL Cell trace violet stock solution (5 mM) made up by dissolving 1 vial cell trace violet stock in 20 µL of DMSO. Stock solution was added at 1 µL / 1 million cells and was stored at –20°C protected from light.

### **DC Protein Assay**

(500-0112, BioRad DC protein assay, Hertfordshire, UK)

---

The kit included 250 mL of REAGENT A (an alkaline copper tartrate solution), 2000 mL of REAGENT B (a dilute Folin Reagent), 5 mL of REAGENT S (surfactant solution) and a bovine serum albumin standard (1.5

mg / mL). All components were stored at room temperature away from direct sunlight. A bovine serum albumin standard (23209, Thermo Fisher Scientific, Epsom, UK) was used (2 mg / mL) along with the DC protein assay kit which was stored at room temperature.

### **Gene-specific primers**

(Applied Biosystems of Life Technologies Ltd, Paisley, UK)

---

Both primers were stored at -20°C.

ATB5B	25 µL 20X mix	HS0096959-ml
HSPA1A (hsp70)	250 µL 20X mix	HS00359163-sl

### **Hsp70 high sensitivity EIA kit**

(ADI-EKS-715, ENZO Life Sciences, Exeter, UK).

---

The kit contained a Hsp70 Clear Microtiter Plate, 50 mL of assay buffer 28, a standard, 100 mL of wash buffer concentrate, 25 µL of Hsp70 High Sensitivity Standard, 10 mL of Hsp70 High Sensitivity EIA Conjugate, 10 mL of Hsp70 High Sensitivity EIA Antibody, 10 mL of TMB Substrate and 10 mL stop solution 2. Stock solutions of wash buffer and Hsp70 Intermediate Standard were prepared as previously described in Chapter 4.2.1. The sensitivity of the kit was determined by interpolation at 2 standard deviations above the mean signal at background (0 ng / mL). The inter-assay coefficient of variation was 12.8% to 19.1% and the intra-assay coefficient of variation was 3.9% to 11.4% for this kit. All reagents were stored at 4°C except the standard which was stored at -20°C.

### **Hsp70 singleplex multibead kit**

(ADI-985-016, ENZO Life Sciences, Exeter, UK)

---

The kit included 200 µL of 25X Hsp70 Capture Bead, 1 vial of HSP/Chaperone Standard Cocktail, 400 µL of 25X Hsp70 Antibody and 400 µL of 25X Streptavidin-PE Conjugate. The HSP/Chaperone MultiBead™ Buffer Pack was also used (ADI-987-002, ENZO Life Sciences, Exeter, UK). Hsp70 Capture Bead, Hsp70 Antibody, Streptavidin-PE Conjugate and the

HSP/Chaperone Standard Cocktail were prepared to a stock solution of 1X before use (as previously described in Chapter 4.2.4.3). All kit reagents were stored at 4°C except the HSP/Chaperone Standard Cocktail which was stored at -20°C.

### **TaqMan® Gene Expression Master Mix**

(4369016, Applied Biosystems of Life Technologies Ltd, Paisley, UK)

---

The TaqMan Gene Expression Master Mix contained AmpliTaq Gold® DNA Polymerase, UP (Ultra Pure), Uracil-DNA glycosylase, dNTPs with dUTP, ROX™ Passive Reference and optimised buffer components. All components were stored at 4°C.

### **Thymidine, [Methyl-<sup>3</sup>H] (<sup>3</sup>H-thymidine)**

(NET027E001MC, PerkinElmer, Buckinghamshire, UK)

---

Thymidine, [Methyl-<sup>3</sup>H] was supplied as a 1 mL solution of 1mCi (37 MBq). 10 µL of isotope was added to 90 µL of PBS giving a stock concentration of 1 µCi. Thymidine, [Methyl-<sup>3</sup>H] was stored at 4°C.

## 2. Cell culture

### Cell lysis buffer

---

Cell lysis buffer was made up using 780  $\mu\text{L}$  of  $\text{dH}_2\text{O}$  added to 10  $\mu\text{L}$  of 1M TRIS.HCl (121.1g TRIS added to 64 - 70 mL concentrated HCl, pH to pH7.4, then made to 1 L with  $\text{dH}_2\text{O}$ ), 10  $\mu\text{L}$  of 100 mM sodium orthovanadate, 100  $\mu\text{L}$  of 10% sodium dodecyl sulfate and 100  $\mu\text{L}$  of protease inhibitor cocktail. Lysis buffer stock solution was stored at  $-20^\circ\text{C}$ . All reagents from Sigma-Aldrich, Dorset, UK)

### Medium 199 (M199 medium)

---

(11150-059, Gibco® of Life Technologies Ltd, Paisley, UK)

Basal stock of M199 medium was prepared under aseptic conditions by adding 450 mL of autoclaved water, 50 mL of 10X M199, 10 mL Bicarbonate, 5 mL of glutamine and 5 mL of a Penicillin (10,000 U)-Streptomycin (10 mg)-L-Glutamine (200 mM) solution (Gibco® of Life Technologies Ltd, Paisley, UK). 80 mL of the basal stock was then added to 10 mL of FCS, 10 mL of newborn calf serum, 100  $\mu\text{L}$  of heparin and 50  $\mu\text{L}$  of endothelial cell growth supplement (Gibco® of Life Technologies Ltd, Paisley, UK). Basal stock of M199 medium and working M199 medium were stored at  $4^\circ\text{C}$ .

### Medium 200 (M200 complete growth medium)

---

(M-200-500, Gibco® of Life Technologies Ltd, Paisley, UK)

Stock M200 medium prepared by adding 500 mL M200 to 5 mL low serum growth supplement 50X (2-003-10, Gibco® via Cascade Biologics of Life Technologies Ltd, Paisley, UK) and 1 vial (1 mL) of gentamicin and amphotericin B 500X (50-0640, Cascade Biologics of Life Technologies Ltd, Paisley, UK). Both low serum growth supplement and gentamicin and amphotericin B vial kept at  $-20^\circ\text{C}$ . Stock solution of M200 complete growth medium was stored at  $4^\circ\text{C}$ .

### **Pulmonary Arterial Endothelial Cells**

(C-008-5C, Cascade Biologics of Life Technologies Ltd, Paisley, UK)

---

Cells were cultured as previously described in Chapter 4.2.4.2. Previous to culture, cells were stored at -150°C.

### **RPMI Media 1640 (RPMI medium)**

(21875-034, Gibco® of Life Technologies Ltd, Paisley, UK)

---

To a 500 mL bottle of RPMI-1640, 5 mL of a Penicillin (10,000 U)-Streptomycin (10 mg)-L-Glutamine (200 mM) solution and 10 mL of FCS were added (both from Gibco® of Life Technologies Ltd, Paisley, UK). Stock solution was stored at 4°C.

### **Trypsin/EDTA**

**2.5% Trypsin (10X), no Phenol Red** (15090, Gibco® of Life Technologies Ltd, Paisley, UK)

**Ethylenediaminetetraacetic acid disodium salt dihydrate** (E5134, Sigma-Aldrich, Dorset, UK)

---

5 mL of 2.5% trypsin was added to 5 mL of 0.2% EDTA (made by adding 0.2g EDTA with 100 mL of ddH<sub>2</sub>O, autoclaved) and 90 mL of PBS. Trypsin/EDTA solution was stored at 4°C.

### 3. Flow cytometry reagents

#### Flow cytometry antibodies and isotype controls

Monoclonal antibodies used in staining of PBMCs isolated from human whole blood samples. All antibodies and isotypes were stored undiluted at 4°C.

Antibody	Clone	Reactivity	Concentration/test number	Catalogue number and Manufacturer
Alexa Fluor® 700 Mouse Anti- Human CD3	UCHT1	Human	0.2 mg / mL (1 µL / test / 1 million cells)	557943, BD Pharmingen™, Oxford, UK
Pacific Blue™ anti-human CD4	RPA-T4	Human, <b>Cross- Reactivity:</b> Chimpanzee	0.5 mg / mL (4 µL / test / 1 million cells)	300521, BioLegend, London, UK
Anti-Human CD25 PE-Cy7	BC96	Human	25 tests (5 µL / test / 1 million cells)	25-0259-42, eBioscience, Hatfield, UK
V500 Mouse Anti- Human CD45	HI30	Human	25 tests (5 µL / test / 1 million cells)	560779, BD Horizon™, Oxford, UK
APC/Cy7 anti- human CD69	FN50	Human, <b>Cross- Reactivity:</b> Chimpanzee, Baboon, Cynomolgus, Rhesus, Pigtailed Macaque	100 tests (20 µL / test / 1 million cells)	310914, BioLegend, London, UK
Alexa Fluor® 488 anti-human CD127 (IL-7Rα)	HCD127	Human	25 tests (5 µL / test / 1 million cells)	317603, BioLegend, London, UK
Anti-Human Foxp3 APC	236A/E7	Human	100 tests (5 µL / test / 1 million cells)	17-4777-42, eBioscience, Hatfield, UK
Alexa Fluor® 488 anti-human CD19	HIB19	Human, Cross- Reactivity: Chimpanzee	100 tests (5 µL / test / 1 million cells)	302219, BioLegend, London, UK
Anti-Human CD8a APC	RPA-T8	Human	100 tests (5 µL / test / 1 million cells)	17-0088-42, eBioscience, Hatfield, UK

Monoclonal isotype controls used in staining of PBMCs from human clinical whole blood.

<b>Antibody</b>	<b>Clone</b>	<b>Concentration/test number</b>	<b>Catalogue number and Manufacturer</b>
Alexa Fluor® 700 mouse IgG1, κ	MOPC-21	0.2 mg / mL (1 µL / test / 1 million cells)	557882, BioLegend, London, UK
Pacific Blue™ mouse IgG1, κ	MOPC-21	0.5 mg / mL (4 µL / test / 1 million cells)	400151, BioLegend, London, UK
Mouse IgG1, κ PE-Cy7	P3.6.2.8.1	100 (5 µL / test / 1 million cells)	25-4714-42, eBioscience, Hatfield, UK
Mouse IgG1, κ APC	P3.6.2.8.1	100 (5 µL / test / 1 million cells)	17-4714-41, eBioscience, Hatfield, UK
APC-Cy7™ Mouse IgG1, κ	MOPC-21	100 tests (20 µL / test / 1 million cells)	400128, BioLegend, London, UK
V500 mouse IgG1, κ	X40	0.2 mg / mL (5 µL / test / 1 million cells)	560787, BD Horizon™, Oxford, UK
AF488 mouse IgG1, κ	MOPC-21	100 tests (5 µL / test / 1 million cells)	400129, BioLegend, London, UK

Monoclonal antibodies used in staining of mouse whole blood, all stored undiluted at 4°C.

<b>Antibody</b>	<b>Clone</b>	<b>Reactivity</b>	<b>Concentration/test number</b>	<b>Catalogue number and Manufacturer</b>
Alexa Fluor® 700 anti-mouse CD3	17A2	Mouse	0.5 mg / mL (1 µL / test / 1 million cells)	100216, BioLegend, London, UK
FITC anti-mouse CD4	RM4-4	Mouse	0.5 mg / mL (0.25 µL / test / 1 million cells)	116004, BioLegend, London, UK
APC anti-mouse CD8a	53-6.7	Mouse	0.2 mg / mL (0.25 µL / test / 1 million cells)	100712, BioLegend, London, UK
PE/Cy7 anti-mouse CD25	PC61	Mouse	0.2 mg / mL (1 µL / test / 1 million cells)	102016, BioLegend, London, UK

Monoclonal isotype controls used in staining of mouse whole blood.

<b>Antibody</b>	<b>Clone</b>	<b>Concentration/test number</b>	<b>Catalogue number and Manufacturer</b>
Alexa Fluor® 700 Rat IgG2b, κ	RTK4530	0.5 mg / mL (1 µL / test / 1 million cells)	400628, BioLegend, London, UK
FITC Rat IgG2b, κ	RTK4530	0.5 mg / mL (0.5 µL / test / 1 million cells)	400606, BioLegend, London, UK
PE/Cy7 Rat IgG1, κ	RTK2071	0.2 mg / mL (1 µL / test / 1 million cells)	400416, BioLegend, London, UK
APC Rat IgG2a, κ	RTK2758	0.2 mg / mL (0.25 µL / test / 1 million cells)	400512, BioLegend, London, UK

### **LIVE/DEAD® Fixable Dead Cell Stain Kit**

(L-23105, Invitrogen of Life Technologies Ltd, Paisley, UK)

---

1 vial of component A (fluorescent reactive dye) was added to 50  $\mu\text{L}$  of component B (anhydrous DMSO), mixed well and 1  $\mu\text{L}$  of fluorescent dye stock solution added to a cell solution of  $1 \times 10^6$  / mL. The fluorescent dye stock solution was stored at  $-20^\circ\text{C}$  and protected from light.

### **Foxp3 / Transcription Factor Staining Buffer Set**

(00-5523-00, eBioscience, Hatfield, UK)

---

This kit contained 30 mL of eBioscience Fixation/Permeabilization Concentrate (4X), 100 mL of eBioscience Fixation/Permeabilization Diluent and 100 mL of eBioscience Permeabilization Buffer (10X). A fixation/permeabilization working solution of 1X was prepared by adding 1 part eBioscience Fixation/Permeabilization Concentrate to 1 part eBioscience Fixation/Permeabilization Diluent. The permeabilization buffer was made by diluting 1 part eBioscience Permeabilization Buffer with 9 parts distilled water. All stocks and working solutions were stored at  $4^\circ\text{C}$ .

### **Cell staining buffer**

---

Cell staining buffer was prepared by adding 10 mL of FCS to 90 mL of PBS after which it was stored at  $4^\circ\text{C}$ .

### **Red Blood Cell Lysis Solution**

(130-094-183, Miltenyi Biotec Ltd, Surrey, UK)

---

Working red blood cell lysis solution was prepared by diluting the 10X red blood cell lysis solution to 1X with ddH<sub>2</sub>O. The working red blood cell lysis solution was stored at  $4^\circ\text{C}$ .

### **Normal mouse serum**

(ab7486, Abcam, Cambridge, UK)

---

Normal mouse serum used as per chapter 2.2.2.1.

### **LSM 1077 Lymphocyte**

(J15-004, PAA, Austria)

---

LSM 1077 Lymphocyte solution was used neat to separate PBMCs from whole blood solution as described in chapter 2.2.2.1.

### **BD CELLFix™**

(340181, BD bioscience, Oxford, UK)

---

A working solution of 1X CELLFix™ was prepared by adding 5 mL of 10X concentrate to 45 mL of distilled water and stored at 4°C.

### **Anti-Mouse Ig, κ/Negative Control Compensation Particles Set**

(552843, BD bioscience, Oxford, UK)

---

1 drop of reagent A (Anti-Mouse Ig, κ) was added to 1 drop of reagent B (FCS) before being added to each anti-human antibody. Compensation Particles Set was stored at 4°C.

### **Anti-Rat and Anti-Hamster Ig κ /Negative Control Compensation Particles Set**

(552845, BD bioscience, Oxford, UK)

---

1 drop of reagent A (Anti-Rat and Anti-Hamster Ig, κ) was added to 1 drop of reagent B (FCS) before being added to each anti-mouse antibody. Compensation Particles Set was stored at 4°C.

### **ArC™ Amine Reactive Compensation Bead Kit**

(A-10346, Invitrogen of Life Technologies Ltd, Paisley, UK)

---

ArC™ Amine Reactive Compensation beads were used as described in chapter 2.2.2.1.

## 4. Animal study reagents

### **Collagenase A from *Clostridium histolyticum* (Collagenase A)**

(10103586001, Roche, Welwyn Garden City, UK)

---

A stock concentration of 0.5 mg / mL of collagenase A was prepared to a working concentration of 0.15% with HBSS (1X) solution (Life Technologies Ltd, Paisley, UK). Working collagenase A solution was stored at -20°C.

### **Crotaline (monocrotaline)**

(C2401-500MG, Sigma Aldrich, Dorset, UK)

---

Crotaline (C<sub>16</sub>H<sub>23</sub>NO<sub>6</sub>) was dissolved in 0.6 mL of 1M Hydrochloric Acid and vortexed for 40 minutes. Sterile water was added to make the volume to 5 mL and the pH adjusted to 7.0 with sterile NaOH. A final solution to 10 mL was made with sterile water. And a dose of 60 mg / kg dose was given to rats weighing approximately 200g at the beginning of the procedure. Crotaline was stored at 4°C prior to use. The control used in the MCT experiments was PBS at the same volume.

### **LEAF™ Purified anti-mouse CD4 Antibody**

(100435, BioLegend, London, UK)

---

LEAF™ Purified anti-mouse CD4 monoclonal antibody (stock solution of Stock solution of 1mg / mL) (clone GK1.5) was administered at a dose of 0.5 mL per mouse per week for 4 weeks. This antibody was stored at 4°C.

### **Normal Rat IgG Control, Rat IgG**

(6-001-A, R & D systems, Abingdon, UK)

---

Normal Rat monoclonal IgG Control, Rat IgG (lyophilised and made up to 1mg / mL in PBS) was administered at a dose of 0.5 mL per mouse per week for 4 weeks. This isotype control was stored at 4°C.

**Paigen diet (atherogenic diet)**

(829110, Special Diet Services, Braintree, Essex, UK)

---

Paigen diet (atherogenic) was made up by mixing distilled water with 500 g diet stock, until it reached the correct consistency. It consisted of 15% fat, 1.25% cholesterol, and 0.5% cholic acid. After preparation, the diet stock was baked overnight on a flat ovenproof baking tray at 80°C, left to cool and broken up into smaller chunks before being used. Diet was kept unprepared at 4°C and prepared (after baking) at -20°C.

**Teklad Global 18% Protein Rodent Diet (Chow diet)**

(2018, Harlan Global Diets, Madison, USA)

---

Chow diet consisted of 6.2% fat and 0% cholesterol. Diet was stored at room temperature.

## 5. Immunohistochemistry buffers and reagents

**Primary antibodies used in immunohistological staining of mouse and rat tissue samples.**

All antibodies were stored at -20°C.

Antibody	Clone	Description/ Reactivity	Catalogue number and Manufacturer	Dilution (in PBS)	Antigen Retrieval step
Anti-Hsp70 antibody	C92F3A-5	Mouse monoclonal <b>Cross reactivity:</b> Rat, Sheep, Rabbit, Chicken, Guinea pig, Hamster, Cow, Dog, Human, Pig, Caenorhabditis elegans, Carp, Fruit fly ( <i>Drosophila melanogaster</i> ), Monkey	ab47455, Abcam, Cambridge, UK	1:500	Citrate buffer
Anti-CD8 antibody	YTS169.4	Rat monoclonal <b>Cross reactivity:</b> Mouse	ab22378, Abcam, Cambridge, UK	1:100	Citrate buffer
Anti-CD4 antibody	mAb51312	Mouse monoclonal <b>Cross reactivity:</b> human	ab51312, Abcam, Cambridge, UK	1:100	Citrate buffer
Anti-IL2 Receptor alpha Antibody (CD25)	AP-MABAP0710	Rat monoclonal, <b>Cross reactivity:</b> mouse	NB110-97867, Novus Biologicals, Cambridge, UK	1:300	Citrate buffer
Anti-Smooth muscle actin	1A4	Mouse monoclonal	M085, DAKO, Ely, UK	1:150	N/A

## **Secondary monoclonal antibodies used in immunohistological staining of mouse tissue samples.**

---

All secondary antibodies were used at a dilution of 1 in 200 in PBS and stored at 4°C.

<b>Antibody</b>	<b>Catalogue number and Manufacturer</b>
Biotinylated goat anti-rat IgG	BA9400 (Vector Laboratories, Peterborough, UK)
Biotinylated goat anti-rabbit IgG	BA1000 (Vector Laboratories, Peterborough, UK)
Biotinylated goat anti-mouse IgG	BA9200 (Vector Laboratories, Peterborough, UK)

## **Acid alcohol**

---

Acid alcohol was prepared with 1% v/v HCl in 70% v/v IMS. This was stored at room temperature away from direct sunlight.

## **Citrate Buffer**

---

500 mL of citrate buffer was made by adding 2.1g of citric acid monohydrate to 900 mL of dH<sub>2</sub>O before adjusting to pH6 with 13 mL of 2M NaOH (25 mL of H<sub>2</sub>O to 2g of NaOH pellets). This solution was then diluted a total volume of 1000 mL using dH<sub>2</sub>O and stored at room temperature away from direct sunlight.

## **Curtis' Modified Van Gieson**

---

Curtis' Modified Van Gieson was prepared by adding 10 mL of 1% w/v Ponceau S [aq] to 90 mL of saturated aq. Picric acid. 1 mL of glacial acetic acid was then added and it was stored at room temperature away from direct sunlight.

### **EDTA buffer**

---

EDTA buffer was made to a 1 mM solution by adding 0.186g of EDTA to 500 mL of dH<sub>2</sub>O before being corrected to pH8. This was stored at room temperature away from direct sunlight.

### **3% Hydrogen peroxide solution**

---

A 3% hydrogen solution was prepared using a 30% stock solution (30 % (w/w) in H<sub>2</sub>O) by diluting 1 mL of stock with 9 mL of PBS. Hydrogen peroxide stock solution was stored at 4°C.

### **Milk blocking buffer**

---

5g of Marvel dried milk (from local supermarket) was added to 500 mL of PBS to make a 1% blocking buffer. Marvel dried milk powder was stored at room temperature.

### **SIGMAFAST™ 3,3'-Diaminobenzidine tablets**

(D4418, Sigma Aldrich, Dorset, UK)

---

1 Urea Hydrogen Peroxide tablet and 1 3,3'-Diaminobenzidine (DAB) tablet was added to 15 mL of water, mixed well and 2 drops of 30% hydrogen peroxide added prior to use to form an active DAB substrate solution. The DAB kit was stored at -20°C.

### **TRIS/EDTA buffer**

---

TRIS/EDTA buffer was made by adding 1.21g of 10 mM TRIS, 0.37g of 1mM EDTA, 0.5 mL of 0.05% Tween20 and 999.5 mL of dH<sub>2</sub>O. The solution was then corrected to pH9 and stored at room temperature away from direct sunlight.

### **VECTASTAIN Elite ABC Kit (Standard\*)**

(PK-6100, Vector Laboratories, Peterborough, UK)

---

Working ABC reagent was prepared by adding 1 drop of Reagent A, 1 drop of Reagent B and 2.5 mL of PBS together. The kit was stored at 4°C.

### **Other reagents**

---

All histological cassettes, moulds, paraffin wax and Millers Elastin stain were purchased from Raymond A Lamb Ltd (now Thermo Fisher Scientific, Epsom, UK) unless otherwise stated. All stains, Polysine™ glass slides, Potassium permanganate, coverslips, DPX resin, alcian blue and Carazzi's Haematoxylin were purchased from VWR International Ltd (Lutterworth, UK) unless otherwise stated. Ethanol and xylene were also from Fisher Scientific. Oxalic acid purchased from Sigma Aldrich (Dorset, UK)

## 6. Patient treatment plans

Patient ID	PAH subtype	Medication at baseline	PAH specific medication given at Visit 1	PAH specific medication given at follow-up
13	IPAH	GTN spray, Simvastatin, Omeprazole, Spironolactone, Metformin, Bisoprolol, Gliclazide, Isosorbide mononitrate, Bumetanide, Ramipril	Bosentan	N/A
19	IPAH	Frusemide, Trimethoprim	Sildenafil	Bosentan, Sildenafil
32	IPAH	Carbimazole, Seretide, Omeprazole, Bendroflumethiazide, Terbutaline, Chlorpheniramine	Sildenafil	Sildenafil
35	IPAH	Levothyroxine, Rosuvastatin, Bimatoprost, Liquifile	Sildenafil	N/A
48	PAH-SSc	Lansoprazole, Prednisolone, Calcichew, Ramipril	Bosentan	Bosentan, Sildenafil
62	IPAH	Simvastatin, Frusemide, Amlodipine	Sildenafil	N/A
64	IPAH	Amlodipine, Bisoprolol, Frumil, Diazepam, Valsartan, Citalopram, Frusemide	Sildenafil	N/A
69	PAH-SSc	Ramipril, Simvastatin, Lansoprazole, Diltiazem	Bosentan, Sildenafil	Bosentan, Sildenafil
84	PAH-SSc	Omeprazole, Ibuprofen, Amlodipine, Dermovate cream, Fucibet	Bosentan	Bosentan
87	PAH-SSc	Salbutamol, Warfarin, Loratidine, Nosonex, GTN spray, Gaviscon, Frusemide, Verapamil, Pregabalin, Quinine, Ramipril, Atorvastatin, Lansoprazole, Paracetamol	Bosentan	Bosentan, Sildenafil
90	IPAH	Methadone, Paracetamol, Clexane, Lansoprazole, Aspirin, Zopiclone, GTN spray, ISMN, Dipyridamole	Bosentan	Ambrisentan
93	PAH-SSc	Aspirin, Bendroflumethiazide, Nifedipine, Atorvastatin, Lansoprazole, Paracetamol, Naproxen	Bosentan	Bosentan
94	PAH-SSc	Digoxin, Warfarin, Omeprazole, Seretide, Salbutamol, Coamoxiclav, Paracetamol, Tiotropium, Carbocisteine	none	N/A
96	IPAH	Aspirin, Diltiazem, Levemir, Novorapid, Digoxin, Doazosin, Olmesartan, Omacor, Olmesartan, Venlafaxine, Warfarin	none	none
131	IPAH	Prednisolone, Lansoprazole, Clexane	Sildenafil	N/A
155	PAH-SSc	Azathioprine, Frusemide, Prednisolone, Lanzoprazole, Ramipril, Amlodipine, Aspirin	Bosentan	Bosentan
163	IPAH	Aspirin, ISMN, Lansoprazole, Simvastatin, Frusemide, Seretide, Ferrous sulphate	Bosentan	N/A
164	PAH-SSc	Frusemide, Ramipril, Omeprazole, Spiriva, Demovate cream, Diclofenac, Tramadol, Salbutamol	Bosentan	Bosentan
165	IPAH	Warfarin, Symbicort, Diltiazem	none	none
171	IPAH	Atorvastatin, Bisoprolol, Citalopram, Thyroxine, Lansoprazole, Bumetanide, Spironolactone	Sildenafil	Sildenafil
175	PAH-SSc	Bisoprolol, Digoxin, Spirinolactone, Warfarin, Ramipril, GTN spray, Simvastatin, Vitamin K	none	none

Cont...

Patient ID	PAH subtype	Medication at baseline	PAH specific medication given at Visit 1	PAH specific medication given at follow-up
183	PAH-SSc	Simvastatin, Frusemide, Pantoprazole, Doxazosin, Tiotropium	Sildenafil	N/A
184	PAH-SSc	Citalopram, Omeprazole, Nifedipine, Ramipril, Ranitidine, Sildenafil	Bosentan, Sildenafil	Bosentan, Sildenafil
189	PAH-SSc	none	Bosentan	Bosentan
193	IPAH	GTN spray, Lansoprazole, ISMN, Digoxin, Thyroxine, Nicorandil, Frusemide, Eplerenone, Perindopril, Allopurinol, Warfarin	Bosentan	Sildenafil
276	PAH-SSc	Warfarin, Simvastatin, Atenolol, Omeprazole, Frusemide	Bosentan	none
277	PAH-SSc	Mycophenolate, Omeprazole, Diltiazem, Ramipril, Prednisolone, Amitriptyline, Paracetamol, Gabapentin	none	none
280	IPAH	Atorvastatin, Aspirin, Cod liver oil, Glucosamine	Sildenafil	Sildenafil
344	IPAH	Aspirin, Atorvastatin, Clopidogrel, Perindopril, Ventolin, Spiriva, GTN, Enoxaparin	Bosentan	N/A
346	PAH-SSc	Lansoprazole, Furosemide, Simvastatin, Nifedipine, Tadalafil, FESO4	Bosentan, Tadalafil	N/A
350	PAH-SSc	Amlodipine, Ramipril, Fexofenadine, Pravastatin, Camellose	Bosentan	N/A
353	IPAH	Cerazette	Bosentan, Sildenafil	N/A
380	IPAH	Warfarin, Bumetanide, Spirinolactone, Simvastatin, Metformin, Bethistine, O2 therapy	Sildenafil	Sildenafil
381	IPAH	ISMN, Aspirin, Azathioprine, Prednisolone, Lansoprazole, Acetylcystene, Adcal d3, Carbocysteine, Alendroninc acid, O2 therapy	Bosentan	N/A
383	IPAH	none	Ambrisentan, Sildenafil	N/A
430	PAH-SSc	Spironolactone, Irbesartan, Bisoprolol, Simvastatin, aspirin, Frusemide, Felodipine, Lansoprazole	Sildenafil	N/A
435	PAH-SSc	Aspirin, Frusemide, Spironolactone, Omeprazole, O2 therapy	Sildenafil	N/A
442	IPAH	Lansoprasole, Adipine, Levothyroxine	Sildenafil	Sildenafil
452	IPAH	Adalat, Disodium,	Bosentan	N/A
456	PAH-SSc	Adalat, Adcal, Alendronic acid, Buprenorphine, Gaviscon, Sertraline, Folic acid, Gabapentin, Hydroxychloroquine, Metoclopramide, Paracetamol	Sildenafil	N/A
460	IPAH	Ramipril, Metformin, Atorvastatin, Humalog insulin, Seretide, Senna, Paracetamol, Salbutamol, Tiotropium, Certirizine, Coamoxiclav	Bosentan, Sildenafil	N/A
467	IPAH	Certirizine	Sildenafil	N/A

### Patient treatment plans from baseline and follow-up visits.

Patient IDs, patient phenotype (IPAH or SSc-PAH) and treatments at baseline, visit 1 and follow-up visits are shown. N/A shown when visit has not been completed.

# Bibliography

- Alessia, A., O. Bistoni., E. Bartoloni., S. Caterbi., B. Bigerna., A. Tabarrini., R. Mannucci., B. Falini and R. Gerli (2012). "IL-17-producing CD4<sup>+</sup>CD8<sup>-</sup> T cells are expanded in the peripheral blood, infiltrate salivary glands and are resistant to corticosteroids in patients with primary Sjögren's syndrome." Annals of the Rheumatic Diseases.
- Ali, K., M. Middleton, E. Pure and D. J. Rader (2005). "Apolipoprotein E suppresses the type I inflammatory response in vivo." Circulation research 97(9): 922-927.
- Ammon-Treiber, S., G. Grecksch, R. Stumm, U. Riechert, H. Tischmeyer, A. Reichenauer and V. Holtt (2004). "Rapid, transient, and dose-dependent expression of hsp70 messenger RNA in the rat brain after morphine treatment." Cell stress & chaperones 9(2): 182-197.
- Amrani, M., N. Latif, K. Morrison, C. C. Gray, J. Jayakumar, J. Corbett, A. T. Goodwin, M. J. Dunn and M. H. Yacoub (1998). "Relative induction of heat shock protein in coronary endothelial cells and cardiomyocytes: implications for myocardial protection." The Journal of thoracic and cardiovascular surgery 115(1): 200-209.
- Antiga, E., P. Quaglino, S. Bellandi, W. Volpi, E. Del Bianco, A. Comessatti, S. Osella-Abate, C. De Simone, A. Marzano, M. G. Bernengo, P. Fabbri and M. Caproni (2010). "Regulatory T cells in the skin lesions and blood of patients with systemic sclerosis and morphoea." The British journal of dermatology 162(5): 1056-1063.
- Archer, S. L., M. Gomberg-Maitland, M. L. Maitland, S. Rich, J. G. Garcia and E. K. Weir (2008). "Mitochondrial metabolism, redox signaling, and fusion: a mitochondria-ROS-HIF-1 $\alpha$ -Kv1.5 O<sub>2</sub>-sensing pathway at the intersection of pulmonary hypertension and cancer." American journal of physiology. Heart and circulatory physiology 294(2): H570-578.
- Ashkar, S., G. F. Weber, V. Panoutsakopoulou, M. E. Sanchirico, M. Jansson, S. Zawaideh, S. R. Rittling, D. T. Denhardt, M. J. Glimcher and H. Cantor (2000). "Eta-1 (osteopontin): an early component of type-1 (cell-mediated) immunity." Science 287(5454): 860-864.
- Atkinson, C., S. Stewart, P. D. Upton, R. Machado, J. R. Thomson, R. C. Trembath and N. W. Morrell (2002). "Primary pulmonary hypertension is associated with reduced pulmonary vascular expression of type II bone morphogenetic protein receptor." Circulation 105(14): 1672-1678.
- Austin, E. D., J. D. Cogan, J. D. West, L. K. Hedges, R. Hamid, E. P. Dawson, L. A. Wheeler, F. F. Parl, J. E. Loyd and J. A. Phillips, 3rd (2009). "Alterations in oestrogen metabolism: implications for higher penetrance of familial pulmonary arterial hypertension in females." The European respiratory journal : official journal of the European Society for Clinical Respiratory Physiology 34(5): 1093-1099.
- Austin, E. D., J. A. Phillips, J. D. Cogan, R. Hamid, C. Yu, K. C. Stanton, C. A. Phillips, L. A. Wheeler, I. M. Robbins, J. H. Newman and J. E. Loyd (2009). "Truncating and missense BMPR2 mutations differentially affect the severity of heritable pulmonary arterial hypertension." Respiratory research 10: 87.
- Austin, E. D., M. T. Rock, C. A. Mosse, C. L. Vnencak-Jones, S. M. Yoder, I. M. Robbins, J. E. Loyd and B. O. Meyrick (2010). "T lymphocyte subset abnormalities in the blood and lung in pulmonary arterial hypertension." Respiratory medicine 104(3): 454-462.
- Bachelet, M., E. Mariethoz, N. Banzet, E. Souil, F. Pinot, C. Z. Polla, P. Durand, I. Bouchaert and B. S. Polla (1998). "Flow cytometry is a rapid and reliable method for evaluating heat shock protein 70 expression in human monocytes." Cell stress & chaperones 3(3): 168-176.
- Balabanian, K., A. Foussat, P. Dorfmüller, I. Durand-Gasselín, F. Capel, L. Bouchet-Delbos, A. Portier, A. Marfaing-Koka, R. Krzysiek, A. C. Rimaniol, G. Simonneau, D. Emile and M. Humbert (2002). "CX(3)C chemokine fractalkine in pulmonary arterial hypertension." American journal of respiratory and critical care medicine 165(10): 1419-1425.
- Banham, A. H. (2006). "Cell-surface IL-7 receptor expression facilitates the purification of FOXP3(+) regulatory T cells." Trends in immunology 27(12): 541-544.

- Banham, A. H., F. M. Powrie and E. Suri-Payer (2006). "FOXP3+ regulatory T cells: Current controversies and future perspectives." European journal of immunology 36(11): 2832-2836.
- Barbara, N. P., J. L. Wrana and M. Letarte (1999). "Endoglin is an accessory protein that interacts with the signaling receptor complex of multiple members of the transforming growth factor-beta superfamily." The Journal of biological chemistry 274(2): 584-594.
- Barnett, A. J., B. D. Tait, M. A. Barnett and B. H. Toh (1989). "T lymphocyte subset abnormalities and HLA antigens in scleroderma (systemic sclerosis)." Clinical and experimental immunology 76(1): 24-29.
- Bauer, H., T. Jung, D. Tsikas, D. O. Stichtenoth, J. C. Frolich and C. Neumann (1997). "Nitric oxide inhibits the secretion of T-helper 1- and T-helper 2-associated cytokines in activated human T cells." Immunology 90(2): 205-211.
- Bedke, T., L. Pretsch, S. Karakhanova, A. H. Enk and K. Mahnke (2010). "Endothelial cells augment the suppressive function of CD4+ CD25+ Foxp3+ regulatory T cells: involvement of programmed death-1 and IL-10." Journal of immunology 184(10): 5562-5570.
- Bellisai, F., G. Morozzi, F. Scaccia, F. Chellini, A. Simpatico, G. Pecetti and M. Galeazzi (2011). "Evaluation of the effect of Bosentan treatment on proinflammatory cytokine serum levels in patients affected by Systemic Sclerosis." International journal of immunopathology and pharmacology 24(1): 261-264.
- Bellosta, S., R. W. Mahley, D. A. Sanan, J. Murata, D. L. Newland, J. M. Taylor and R. E. Pitas (1995). "Macrophage-specific expression of human apolipoprotein E reduces atherosclerosis in hypercholesterolemic apolipoprotein E-null mice." The Journal of clinical investigation 96(5): 2170-2179.
- Bellotto, F., P. Chiavacci, F. Laveder, A. Angelini, G. Thiene and R. Marcolongo (1999). "Effective immunosuppressive therapy in a patient with primary pulmonary hypertension." Thorax 54(4): 372-374.
- Beppu, H., M. Kawabata, T. Hamamoto, A. Chytil, O. Minowa, T. Noda and K. Miyazono (2000). "BMP type II receptor is required for gastrulation and early development of mouse embryos." Developmental biology 221(1): 249-258.
- Bettelli, E., T. Korn and V. K. Kuchroo (2007). "Th17: The third member of the effector T cell Trilogy." Current Opinion in Immunology 19(6):652-657.
- Bevilacqua, M. P., J. S. Pober, M. E. Wheeler, R. S. Cotran and M. A. Gimbrone, Jr. (1985). "Interleukin-1 activation of vascular endothelium. Effects on procoagulant activity and leukocyte adhesion." The American journal of pathology 121(3): 394-403.
- Bhattacharyya, S., P. Sen, M. Wallet, B. Long, A. S. Baldwin, Jr. and R. Tisch (2004). "Immunoregulation of dendritic cells by IL-10 is mediated through suppression of the PI3K/Akt pathway and of IkappaB kinase activity." Blood 104(4): 1100-1109.
- Boehmer, H (2005). "Mechanisms of suppression by suppressor T cells." Nature Immunology 6, 338 – 344.
- Boin, F., U. De Fanis, S. J. Bartlett, F. M. Wigley, A. Rosen and V. Casolaro (2008). "T cell polarization identifies distinct clinical phenotypes in scleroderma lung disease." Arthritis and rheumatism 58(4): 1165-1174.
- Bonnet, S., E. Dumas-de-La-Roque, H. Begueret, R. Marthan, M. Fayon, P. Dos Santos, J. P. Savineau and E. E. Baulieu (2003). "Dehydroepiandrosterone (DHEA) prevents and reverses chronic hypoxic pulmonary hypertension." Proceedings of the National Academy of Sciences of the United States of America 100(16): 9488-9493.
- Bonnet, S., E. D. Michelakis, C. J. Porter, M. A. Andrade-Navarro, B. Thebaud, A. Haromy, G. Harry, R. Moudgil, M. S. McMurtry, E. K. Weir and S. L. Archer (2006). "An abnormal mitochondrial-hypoxia inducible factor-1alpha-Kv channel pathway disrupts oxygen sensing and triggers pulmonary arterial hypertension in fawn hooded rats: similarities to human pulmonary arterial hypertension." Circulation 113(22): 2630-2641.
- Borges, T. J., L. Wieten, M. J. van Herwijnen, F. Broere, R. van der Zee, C. Bonorino and W. van Eden (2012). "The anti-inflammatory mechanisms of Hsp70." Frontiers in immunology 3: 95.
- Born, W. K., C. L. Reardon and R. L. O'Brien (2006). "The function of  $\gamma\delta$  T cells in innate immunity." Current Opinion in Immunology 18(1):31-38

- Botney, M. D., L. Bahadori and L. I. Gold (1994). "Vascular remodeling in primary pulmonary hypertension. Potential role for transforming growth factor-beta." The American journal of pathology 144(2): 286-295.
- Botney, M. D., L. Bahadori and L. I. Gold (1994). "Vascular remodeling in primary pulmonary hypertension. Potential role for transforming growth factor-beta." Am J Pathol 144(2): 286-295.
- Brar, B. K., A. Stephanou, M. J. Wagstaff, R. S. Coffin, M. S. Marber, G. Engelmann and D. S. Latchman (1999). "Heat shock proteins delivered with a virus vector can protect cardiac cells against apoptosis as well as against thermal or hypoxic stress." Journal of molecular and cellular cardiology 31(1): 135-146.
- Broere, F., S. G. Apasov., M. V. Sitkovsky and W. van Eden (2011). "T cell subsets and T cell-mediated immunity," Principles of Immunopharmacology 15-27
- Budhiraja, R., R. M. Tuder and P. M. Hassoun (2004). "Endothelial dysfunction in pulmonary hypertension." Circulation 109(2): 159-165.
- Cacoub, P., R. Dorent, P. Nataf, A. Carayon, M. Riquet, E. Noe, J. C. Piette, P. Godeau and I. Gandjbakhch (1997). "Endothelin-1 in the lungs of patients with pulmonary hypertension." Cardiovascular research 33(1): 196-200.
- Cacoub, P., R. Dorent, P. Nataf, A. Carayon, M. Riquet, E. Noe, J. C. Piette, P. Godeau and I. Gandjbakhch (1997). "Endothelin-1 in the lungs of patients with pulmonary hypertension." Cardiovasc Res 33(1): 196-200.
- Camara, N. O., F. Seville and R. I. Lechler (2003). "Human CD4+CD25+ regulatory cells have marked and sustained effects on CD8+ T cell activation." European journal of immunology 33(12): 3473-3483.
- Caruso, A., S. Licenziati, M. Corulli, A. D. Canaris, M. A. De Francesco, S. Fiorentini, L. Peroni, F. Fallacara, F. Dima, A. Balsari and A. Turano (1997). "Flow cytometric analysis of activation markers on stimulated T cells and their correlation with cell proliferation." Cytometry 27(1): 71-76.
- Chamberlain, J., D. Evans, A. King, R. Dewberry, S. Dower, D. Crossman and S. Francis (2006). "Interleukin-1beta and signaling of interleukin-1 in vascular wall and circulating cells modulates the extent of neointima formation in mice." The American journal of pathology 168(4): 1396-1403.
- Chamberlain, J., S. Francis, Z. Brookes, G. Shaw, D. Graham, N. J. Alp, S. Dower and D. C. Crossman (2009). "Interleukin-1 regulates multiple atherogenic mechanisms in response to fat feeding." PloS one 4(4): e5073.
- Chan, S. Y. and J. Loscalzo (2008). "Pathogenic mechanisms of pulmonary arterial hypertension." Journal of molecular and cellular cardiology 44(1): 14-30.
- Chaouat, A., F. Coulet, C. Favre, G. Simonneau, E. Weitzenblum, F. Soubrier and M. Humbert (2004). "Endoglin germline mutation in a patient with hereditary haemorrhagic telangiectasia and dexfenfluramine associated pulmonary arterial hypertension." Thorax 59(5): 446-448.
- Chazova, I., J. E. Loyd, V. S. Zhdanov, J. H. Newman, Y. Belenkov and B. Meyrick (1995). "Pulmonary artery adventitial changes and venous involvement in primary pulmonary hypertension." The American journal of pathology 146(2): 389-397.
- Chen, Y., V. K. Kuchroo., J. Inobe., D.A. Hafler and H. L. Weiner (1994). "Regulatory T cell clones induced by oral tolerance: suppression of autoimmune encephalomyelitis." Science 265:1237-1240
- Chen, H. M., T. L. Hwang and M. F. Chen (1996). "The effect of gabexate mesilate on pancreatic and hepatic microcirculation in acute experimental pancreatitis in rats." The Journal of surgical research 66(2): 147-153.
- Chen, W., W. Jin, N. Hardegen, K. J. Lei, L. Li, N. Marinos, G. McGrady and S. M. Wahl (2003). "Conversion of peripheral CD4+CD25- naive T cells to CD4+CD25+ regulatory T cells by TGF-beta induction of transcription factor Foxp3." The Journal of experimental medicine 198(12): 1875-1886.
- Christman, B. W., C. D. McPherson, J. H. Newman, G. A. King, G. R. Bernard, B. M. Groves and J. E. Loyd (1992). "An imbalance between the excretion of thromboxane and prostacyclin metabolites in pulmonary hypertension." The New England journal of medicine 327(2): 70-75.
- Christou, H., T. Morita, C. M. Hsieh, H. Koike, B. Arkonac, M. A. Perrella and S. Kourembanas (2000). "Prevention of hypoxia-induced pulmonary hypertension by

- enhancement of endogenous heme oxygenase-1 in the rat." Circulation research 86(12): 1224-1229.
- Chu, J. W., P. N. Kao, J. L. Faul and R. L. Doyle (2002). "High prevalence of autoimmune thyroid disease in pulmonary arterial hypertension." Chest 122(5): 1668-1673.
- Clarke, D., G. Damera, M. B. Sukkar and O. Tliba (2009). "Transcriptional regulation of cytokine function in airway smooth muscle cells." Pulmonary pharmacology & therapeutics 22(5): 436-445.
- Claveau, D., S. L. Chen, S. O'Keefe, D. M. Zaller, A. Styhler, S. Liu, Z. Huang, D. W. Nicholson and J. A. Mancini (2004). "Preferential inhibition of T helper 1, but not T helper 2, cytokines in vitro by L-826,141 [4-[2-(3,4-Bisdifluoromethoxyphenyl)-2-[4-(1,1,1,3,3,3-hexafluoro-2-hydroxypropan-2-yl)-phenyl]-ethyl]3-methylpyridine-1-oxide], a potent and selective phosphodiesterase 4 inhibitor." The Journal of pharmacology and experimental therapeutics 310(2): 752-760.
- Condliffe, R., J. A. Pickworth, K. Hopkinson, S. J. Walker, A. G. Hameed, J. Suntharaligam, E. Soon, C. Treacy, J. Pepke-Zaba, S. E. Francis, D. C. Crossman, C. M. Newman, C. A. Elliot, A. C. Morton, N. W. Morrell, D. G. Kiely and A. Lawrie (2012). "Serum osteoprotegerin is increased and predicts survival in idiopathic pulmonary arterial hypertension." Pulmonary circulation 2(1): 21-27.
- Constant, S. L and K. Bottomly (1997). "Induction of Th1 and Th2 CD4+ T cell responses: The Alternative Approaches." Annual Review of Immunology 15: 297-322
- Cool, C. D., D. Kennedy, N. F. Voelkel and R. M. Tuder (1997). "Pathogenesis and evolution of plexiform lesions in pulmonary hypertension associated with scleroderma and human immunodeficiency virus infection." Human pathology 28(4): 434-442.
- Cool, C. D., J. S. Stewart, P. Werahera, G. J. Miller, R. L. Williams, N. F. Voelkel and R. M. Tuder (1999). "Three-dimensional reconstruction of pulmonary arteries in plexiform pulmonary hypertension using cell-specific markers. Evidence for a dynamic and heterogeneous process of pulmonary endothelial cell growth." The American journal of pathology 155(2): 411-419.
- Corallini, F., E. Rimondi and P. Secchiero (2008). "TRAIL and osteoprotegerin: a role in endothelial physiopathology?" Frontiers in bioscience : a journal and virtual library 13: 135-147.
- Crocker, I. C., R. G. Townley and M. M. Khan (1996). "Phosphodiesterase inhibitors suppress proliferation of peripheral blood mononuclear cells and interleukin-4 and -5 secretion by human T-helper type 2 cells." Immunopharmacology 31(2-3): 223-235.
- Cumming, D. V., R. J. Heads, A. Watson, D. S. Latchman and D. M. Yellon (1996). "Differential protection of primary rat cardiocytes by transfection of specific heat stress proteins." Journal of molecular and cellular cardiology 28(12): 2343-2349.
- Cuttica, M. J., T. Langenickel, A. Noguchi, R. F. Machado, M. T. Gladwin and M. Boehm (2011). "Perivascular T-cell infiltration leads to sustained pulmonary artery remodeling after endothelial cell damage." American journal of respiratory cell and molecular biology 45(1): 62-71.
- Daley, E., C. Emson, C. Guignabert, R. de Waal Malefyt, J. Louten, V. P. Kurup, C. Hogaboam, L. Taraseviciene-Stewart, N. F. Voelkel, M. Rabinovitch, E. Grunig and G. Grunig (2008). "Pulmonary arterial remodeling induced by a Th2 immune response." The Journal of experimental medicine 205(2): 361-372.
- Daoussis, D., S. N. Liossis, A. C. Tsamandas, C. Kalogeropoulou, A. Kazantzi, C. Sirinian, M. Karampetsou, G. Yiannopoulos and A. P. Andonopoulos (2010). "Experience with rituximab in scleroderma: results from a 1-year, proof-of-principle study." Rheumatology 49(2): 271-280.
- Date, T., S. Mochizuki, A. J. Belanger, M. Yamakawa, Z. Luo, K. A. Vincent, S. H. Cheng, R. J. Gregory and C. Jiang (2005). "Expression of constitutively stable hybrid hypoxia-inducible factor-1alpha protects cultured rat cardiomyocytes against simulated ischemia-reperfusion injury." American journal of physiology. Cell physiology 288(2): C314-320.
- Davignon, J. and P. Ganz (2004). "Role of endothelial dysfunction in atherosclerosis." Circulation 109(23 Suppl 1): III27-32.
- Deng, Z., J. H. Morse, S. L. Slager, N. Cuervo, K. J. Moore, G. Venetos, S. Kalachikov, E. Cayanis, S. G. Fischer, R. J. Barst, S. E. Hodge and J. A. Knowles (2000). "Familial primary pulmonary hypertension (gene PPH1) is caused by mutations in the bone

- morphogenetic protein receptor-II gene." American journal of human genetics 67(3): 737-744.
- Dodge, I. L., M. W. Carr, M. Cernadas and M. B. Brenner (2003). "IL-6 production by pulmonary dendritic cells impedes Th1 immune responses." Journal of immunology 170(9): 4457-4464.
- Dorfmüller, P., M. Humbert, F. Perros, O. Sanchez, G. Simonneau, K. M. Müller and F. Capron (2007). "Fibrous remodeling of the pulmonary venous system in pulmonary arterial hypertension associated with connective tissue diseases." Human pathology 38(6): 893-902.
- Dorfmüller, P., F. Perros, K. Balabanian and M. Humbert (2003). "Inflammation in pulmonary arterial hypertension." The European respiratory journal : official journal of the European Society for Clinical Respiratory Physiology 22(2): 358-363.
- Dorfmüller, P., V. Zarka, I. Durand-Gasselín, G. Monti, K. Balabanian, G. Garcia, F. Capron, A. Coulomb-Lhermine, A. Marfaing-Koka, G. Simonneau, D. Emilie and M. Humbert (2002). "Chemokine RANTES in severe pulmonary arterial hypertension." American journal of respiratory and critical care medicine 165(4): 534-539.
- Dumitrescu, R., S. Koebrich, E. Dony, N. Weissmann, R. Savai, S. S. Pullamsetti, H. A. Ghofrani, A. Samidurai, H. Traupe, W. Seeger, F. Grimminger and R. T. Schermuly (2008). "Characterization of a murine model of monocrotaline pyrrole-induced acute lung injury." BMC pulmonary medicine 8: 25.
- Dybdahl, B., A. Wahba, E. Lien, T. H. Flo, A. Waage, N. Qureshi, O. F. Sellevold, T. Espevik and A. Sundan (2002). "Inflammatory response after open heart surgery: release of heat-shock protein 70 and signaling through toll-like receptor-4." Circulation 105(6): 685-690.
- Eddahibi, S. and S. Adnot (2001). "Endothelins and pulmonary hypertension, what directions for the near future?" The European respiratory journal : official journal of the European Society for Clinical Respiratory Physiology 18(1): 1-4.
- Eddahibi, S., M. Humbert, E. Fadel, B. Raffestin, M. Darmon, F. Capron, G. Simonneau, P. Darteville, M. Hamon and S. Adnot (2001). "Serotonin transporter overexpression is responsible for pulmonary artery smooth muscle hyperplasia in primary pulmonary hypertension." The Journal of clinical investigation 108(8): 1141-1150.
- Eddahibi, S., B. Raffestin, I. Pham, J. M. Launay, P. Aegerter, M. Sitbon and S. Adnot (1997). "Treatment with 5-HT potentiates development of pulmonary hypertension in chronically hypoxic rats." The American journal of physiology 272(3 Pt 2): H1173-1181.
- Fallarino, F., U. Grohmann, K. W. Hwang, C. Orabona, C. Vacca, R. Bianchi, M. L. Belladonna, M. C. Fioretti, M. L. Alegre and P. Puccetti (2003). "Modulation of tryptophan catabolism by regulatory T cells." Nature immunology 4(12): 1206-1212.
- Faller, D. V. (1999). "Endothelial cell responses to hypoxic stress." Clinical and experimental pharmacology & physiology 26(1): 74-84.
- Fehervari, Z. and S. Sakaguchi (2004). "CD4<sup>+</sup> Tregs and immune control." The Journal of clinical investigation 114(9): 1209-1217.
- Feng, J., T. Misu, K. Fujihara, S. Sakoda, Y. Nakatsuji, H. Fukaura, S. Kikuchi, K. Tashiro, A. Suzumura, N. Ishii, K. Sugamura, I. Nakashima and Y. Itoyama (2004). "Ibudilast, a nonselective phosphodiesterase inhibitor, regulates Th1/Th2 balance and NKT cell subset in multiple sclerosis." Multiple sclerosis 10(5): 494-498.
- Ferrarini, M., S. Heltai, M. R. Zocchi and C. Rugarli (1992). "Unusual expression and localization of heat-shock proteins in human tumor cells." International journal of cancer. Journal international du cancer 51(4): 613-619.
- Filaci, G., M. Cutolo, M. Scudeletti, C. Castagneto, L. Derchi, R. Gianrossi, F. Ropolo, P. Zentilin, A. Sulli, G. Murdaca, M. Ghio, F. Indiveri and F. Puccio (1999). "Cyclosporin A and iloprost treatment of systemic sclerosis: clinical results and interleukin-6 serum changes after 12 months of therapy." Rheumatology 38(10): 992-996.
- Filaci, G. and N. Suciú-Foca (2002). "CD8<sup>+</sup> T suppressor cells are back to the game: are they players in autoimmunity?" Autoimmunity Reviews 1(5):279–283
- Fishman, A. P. (2000). "Changing concepts of the pulmonary plexiform lesion." Physiological research / Academia Scientiarum Bohemoslovaca 49(5): 485-492.
- Fontenot, J. D., M. A. Gavin and A. Y. Rudensky (2003). "Foxp3 programs the development and function of CD4<sup>+</sup>CD25<sup>+</sup> regulatory T cells." Nature immunology 4(4): 330-336.

- Fortes, M. B. and M. Whitham (2009). "No endogenous circadian rhythm in resting plasma Hsp72 concentration in humans." Cell stress & chaperones 14(3): 273-280.
- Freundlich, B. and S. A. Jimenez (1987). "Phenotype of peripheral blood lymphocytes in patients with progressive systemic sclerosis: activated T lymphocytes and the effect of D-penicillamine therapy." Clinical and experimental immunology 69(2): 375-384.
- Fujita, M., J. M. Shannon, C. G. Irvin, K. A. Fagan, C. Cool, A. Augustin and R. J. Mason (2001). "Overexpression of tumor necrosis factor-alpha produces an increase in lung volumes and pulmonary hypertension." American journal of physiology. Lung cellular and molecular physiology 280(1): L39-49.
- Fujitani, Y., A. Trifilieff, S. Tsuyuki, A. J. Coyle and C. Bertrand (1997). "Endothelin receptor antagonists inhibit antigen-induced lung inflammation in mice." American journal of respiratory and critical care medicine 155(6): 1890-1894.
- Fukuda, A., T. Osawa, H. Oda, T. Tanaka, S. Toyokuni and K. Uchida (1996). "Oxidative stress response in iron-induced acute nephrotoxicity: enhanced expression of heat shock protein 90." Biochemical and biophysical research communications 219(1): 76-81.
- Galie, N., M. M. Hoeper, M. Humbert, A. Torbicki, J. L. Vachiery, J. A. Barbera, M. Beghetti, P. Corris, S. Gaine, J. S. Gibbs, M. A. Gomez-Sanchez, G. Jondeau, W. Klepetko, C. Opitz, A. Peacock, L. Rubin, M. Zellweger and G. Simonneau (2009). "Guidelines for the diagnosis and treatment of pulmonary hypertension." The European respiratory journal : official journal of the European Society for Clinical Respiratory Physiology 34(6): 1219-1263.
- Gantner, F., C. Gotz, V. Gekeler, C. Schudt, A. Wendel and A. Hatzelmann (1998). "Phosphodiesterase profile of human B lymphocytes from normal and atopic donors and the effects of PDE inhibition on B cell proliferation." British journal of pharmacology 123(6): 1031-1038.
- Geroulakos, G. S., B. (2011). Vascular Surgery, Springer.
- Ghiringhelli, F., C. Menard, F. Martin and L. Zitvogel (2006). "The role of regulatory T cells in the control of natural killer cells: relevance during tumor progression." Immunological reviews 214: 229-238.
- Ghods, F. and J. A. Will (1981). "Changes in pulmonary structure and function induced by monocrotaline intoxication." The American journal of physiology 240(2): H149-155.
- Giachelli, C. M., D. Lombardi, R. J. Johnson, C. E. Murry and M. Almeida (1998). "Evidence for a role of osteopontin in macrophage infiltration in response to pathological stimuli in vivo." The American journal of pathology 152(2): 353-358.
- Giaid, A. and D. Saleh (1995). "Reduced expression of endothelial nitric oxide synthase in the lungs of patients with pulmonary hypertension." N Engl J Med 333(4): 214-221.
- Giaid, A. and D. Saleh (1995). "Reduced expression of endothelial nitric oxide synthase in the lungs of patients with pulmonary hypertension." The New England journal of medicine 333(4): 214-221.
- Giaid, A., M. Yanagisawa, D. Langleben, R. P. Michel, R. Levy, H. Shennib, S. Kimura, T. Masaki, W. P. Duguid and D. J. Stewart (1993). "Expression of endothelin-1 in the lungs of patients with pulmonary hypertension." The New England journal of medicine 328(24): 1732-1739.
- Giovannetti, A., E. Rosato, C. Renzi, A. Maselli, L. Gambardella, A. M. Giammarioli, P. Palange, P. Paoletti, S. Pisarri, F. Salsano, W. Malorni and M. Pierdominici (2010). "Analyses of T cell phenotype and function reveal an altered T cell homeostasis in systemic sclerosis. Correlations with disease severity and phenotypes." Clinical immunology 137(1): 122-133.
- Godfrey, D. I., K. J. L. Hammond., L. D. Poulton., M. J. Smyth and A. G. Baxter (2000). "NKT cells: facts, functions and fallacies." Immunology Today 21(11):573-583
- Goodman, M. G., D. E. Chenoweth and W. O. Weigle (1982). "Induction of interleukin 1 secretion and enhancement of humoral immunity by binding of human C5a to macrophage surface C5a receptors." The Journal of experimental medicine 156(3): 912-917.
- Goronzy, J. J. and C. M. Weyand (1990). "Long-term immunomodulatory effects of T lymphocyte depletion in patients with systemic sclerosis." Arthritis and rheumatism 33(4): 511-519.
- Gozzelino, R., V. Jeney and M. P. Soares (2010). "Mechanisms of cell protection by heme oxygenase-1." Annual review of pharmacology and toxicology 50: 323-354.

- Graham, T. K., JR (2011). "Idiopathic Pulmonary Arterial Hypertension." US Respiratory Disease 7(2): 123-132.
- Graven, K. K., L. H. Zimmerman, E. W. Dickson, G. L. Weinhouse and H. W. Farber (1993). "Endothelial cell hypoxia associated proteins are cell and stress specific." Journal of cellular physiology 157(3): 544-554.
- Grossman, W. J., J. W. Verbsky., W. Barchet., M. Colonna., J. P. Atkinson and T. J. Ley (2004). "Human T regulatory cells can use the perforin pathway to cause autologous target cell death." Immunity 21:589.
- Grossman, W. J., J. W. Verbsky, B. L. Tollefsen, C. Kemper, J. P. Atkinson and T. J. Ley (2004). "Differential expression of granzymes A and B in human cytotoxic lymphocyte subsets and T regulatory cells." Blood 104(9): 2840-2848.
- Groux, H., A. O'Garra., M. Bigler., M. Rouleau., S. Antonenko., J. E. de Vries and M. G. Roncarolo (1997). "A CD4+ T-cell subset inhibits antigen-specific T-cell responses and prevents colitis." Nature 389:737.
- Gu, Y. S., J. Kong, G. S. Cheema, C. L. Keen, G. Wick and M. E. Gershwin (2008). "The immunobiology of systemic sclerosis." Seminars in arthritis and rheumatism 38(2): 132-160.
- Guiducci, S., R. Giacomelli and M. M. Cerinic (2007). "Vascular complications of scleroderma." Autoimmunity reviews 6(8): 520-523.
- Guignabert, C., B. Raffestin, R. Benferhat, W. Raoul, P. Zadigue, D. Rideau, M. Hamon, S. Adnot and S. Eddahibi (2005). "Serotonin transporter inhibition prevents and reverses monocrotaline-induced pulmonary hypertension in rats." Circulation 111(21): 2812-2819.
- Gurtner, H. P. (1985). "Aminorex and pulmonary hypertension. A review." Cor et vasa 27(2-3): 160-171.
- Gustafsson, R., T. H. Totterman, L. Klareskog and R. Hallgren (1990). "Increase in activated T cells and reduction in suppressor inducer T cells in systemic sclerosis." Annals of the rheumatic diseases 49(1): 40-45.
- Guzik, K., M. Bzowska, J. Dobrucki and J. Pryjma (1999). "Heat-shocked monocytes are resistant to Staphylococcus aureus-induced apoptotic DNA fragmentation due to expression of HSP72." Infection and immunity 67(8): 4216-4222.
- Guzik, T. J., N. E. Hoch, K. A. Brown, L. A. McCann, A. Rahman, S. Dikalov, J. Goronzy, C. Weyand and D. G. Harrison (2007). "Role of the T cell in the genesis of angiotensin II induced hypertension and vascular dysfunction." The Journal of experimental medicine 204(10): 2449-2460.
- Hahn, B. H., R. Pyare-Singh., A. La Cava., F. M. Ebling (2005). "Tolerogenic treatment of lupus mice with consensus peptide induces Foxp3-expressing, apoptosis-resistant, TGFβ-secreting CD8+ T cell suppressors" Journal of Immunology 175:7728-7737
- Hameed, A. G., N. D. Arnold, J. C. Chamberlain, C. M. H. Newman, D. C. Crossman, S. E. Francis and A. Lawrie (2010). TRAIL deficiency is protective in experimental pulmonary arterial hypertension. British Thoracic Society Winter Conference. London, UK, Thorax. 65.
- Hameed, A. G., N. D. Arnold, J. Pickworth, J. C. Chamberlain, C. M. H. Newman, D. C. Crossman, S. E. Francis and A. Lawrie (2011). TRAIL is a potential novel therapeutic target in pulmonary arterial hypertension. British Thoracic Society Winter Conference. London, UK, Thorax. 66.
- Hameed, A. G., N. D. Arnold, J. Pickworth, J. C. Chamberlain, C. M. H. Newman, D. C. Crossman, S. E. Francis and A. Lawrie (In Press). "Inhibition of Tumor Necrosis Factor Related Apoptosis-Inducing Ligand (TRAIL) reverses experimental pulmonary hypertension." Journal of Experimental Medicine
- Hameed, A. G., J. Chamberlain, N. Arnold, C. Newman, S. Francis, D. Crossman and A. Lawrie (2011). Beneficial Effects Of Inhibiting Trail In Monocrotaline-Induced Experimental Pulmonary Hypertension. American Thoracic Society.
- Hameed, A. G., T. Vinogradova, S. E. Francis, C. M. H. Newman, D. C. Crossman and A. Lawrie (2009). TRAIL expression is increased in the rat monocrotaline model of pulmonary arterial hypertension. Winter Meeting of the British Thoracic Society. London. 64.
- Hampl, V., J. Bibova, V. Povysilova and J. Herget (2003). "Dehydroepiandrosterone sulphate reduces chronic hypoxic pulmonary hypertension in rats." The European

- respiratory journal : official journal of the European Society for Clinical Respiratory Physiology 21(5): 862-865.
- Hanasaki, K., T. Nakano and H. Arita (1990). "Receptor-mediated mitogenic effect of thromboxane A2 in vascular smooth muscle cells." Biochemical pharmacology 40(11): 2535-2542.
- Hansmann, G., V. A. de Jesus Perez, T. P. Alastalo, C. M. Alvira, C. Guignabert, J. M. Bekker, S. Schellong, T. Urashima, L. Wang, N. W. Morrell and M. Rabinovitch (2008). "An antiproliferative BMP-2/PPARgamma/apoE axis in human and murine SMCs and its role in pulmonary hypertension." The Journal of clinical investigation 118(5): 1846-1857.
- Hansson, G. K. (2001). "Immune mechanisms in atherosclerosis." Arteriosclerosis, thrombosis, and vascular biology 21(12): 1876-1890.
- Harris, P. H., D. (1986). The human pulmonary circulation: Its form and function in health and disease, Churchill Livingstone
- Hartigan-O'Connor, D. J., C. Poon, E. Sinclair and J. M. McCune (2007). "Human CD4+ regulatory T cells express lower levels of the IL-7 receptor alpha chain (CD127), allowing consistent identification and sorting of live cells." Journal of immunological methods 319(1-2): 41-52.
- Hassoun, P. M. (2005). "Deciphering the "matrix" in pulmonary vascular remodelling." The European respiratory journal : official journal of the European Society for Clinical Respiratory Physiology 25(5): 778-779.
- Heads, R. J., D. M. Yellon and D. S. Latchman (1995). "Differential cytoprotection against heat stress or hypoxia following expression of specific stress protein genes in myogenic cells." Journal of molecular and cellular cardiology 27(8): 1669-1678.
- Hennigan, S., R. N. Channick and G. J. Silverman (2008). "Rituximab treatment of pulmonary arterial hypertension associated with systemic lupus erythematosus: a case report." Lupus 17(8): 754-756.
- Herve, P., L. Drouet, C. Dosquet, J. M. Launay, B. Rain, G. Simonneau, J. Caen and P. Duroux (1990). "Primary pulmonary hypertension in a patient with a familial platelet storage pool disease: role of serotonin." The American journal of medicine 89(1): 117-120.
- Herve, P., J. M. Launay, M. L. Scrobohaci, F. Brenot, G. Simonneau, P. Petitpretz, P. Poubeau, J. Cerrina, P. Duroux and L. Drouet (1995). "Increased plasma serotonin in primary pulmonary hypertension." The American journal of medicine 99(3): 249-254.
- Hironaka, E., M. Hongo, A. Sakai, E. Mawatari, F. Terasawa, N. Okumura, A. Yamazaki, Y. Ushiyama, Y. Yazaki and O. Kinoshita (2003). "Serotonin receptor antagonist inhibits monocrotaline-induced pulmonary hypertension and prolongs survival in rats." Cardiovascular research 60(3): 692-699.
- Hoepfer, M. M., C. Faulenbach, H. Golpon, J. Winkler, T. Welte and J. Niedermeyer (2004). "Combination therapy with bosentan and sildenafil in idiopathic pulmonary arterial hypertension." The European respiratory journal : official journal of the European Society for Clinical Respiratory Physiology 24(6): 1007-1010.
- Hogquist, K. A., E. R. Unanue and D. D. Chaplin (1991). "Release of IL-1 from mononuclear phagocytes." Journal of immunology 147(7): 2181-2186.
- Hori, S., T. Nomura and S. Sakaguchi (2003). "Control of regulatory T cell development by the transcription factor Foxp3." Science 299(5609): 1057-1061.
- Hoshikawa, Y., N. F. Voelkel, T. L. Gesell, M. D. Moore, K. G. Morris, L. A. Alger, S. Narumiya and M. W. Geraci (2001). "Prostacyclin receptor-dependent modulation of pulmonary vascular remodeling." American journal of respiratory and critical care medicine 164(2): 314-318.
- House, S. D., P. T. Guidon, Jr., G. A. Perdrizet, M. Rewinski, R. Kyriakos, R. S. Bockman, T. Mistry, R. A. Gallagher and L. E. Hightower (2001). "Effects of heat shock, stannous chloride, and gallium nitrate on the rat inflammatory response." Cell stress & chaperones 6(2): 164-171.
- <http://www.clinicaltrials.gov> (2012). "Rituximab for Treatment of Systemic Sclerosis-Associated Pulmonary Arterial Hypertension (SSc-PAH)." <http://www.clinicaltrials.gov/ct2/show/NCT01086540?term=rituximab+pulmonary+hypertension&rank=1Rituximab> N. I. o. A. a. I. Diseases

- <http://www.ic.nhs.uk> (2011). "National Audit of Pulmonary Hypertension 2011." [http://www.ic.nhs.uk/webfiles/Services/NCASP/audits%20and%20reports/NHS\\_IC\\_Pulmonary\\_Hypertension\\_Audit\\_V1.0.pdf](http://www.ic.nhs.uk/webfiles/Services/NCASP/audits%20and%20reports/NHS_IC_Pulmonary_Hypertension_Audit_V1.0.pdf). Clinical Audit Support Unit.
- Huertas, A., L. Tu, N. Gambaryan, B. Girerd, F. Perros, D. Montani, D. Fabre, E. Fadel, S. Eddahibi, S. Cohen-Kaminsky, C. Guignabert and M. Humbert (2012). "Leptin and regulatory T lymphocytes in idiopathic pulmonary arterial hypertension." The European respiratory journal : official journal of the European Society for Clinical Respiratory Physiology.
- Humbert, M., G. Monti, F. Brenot, O. Sitbon, A. Portier, L. Grangeot-Keros, P. Duroux, P. Galanaud, G. Simonneau and D. Emilie (1995). "Increased interleukin-1 and interleukin-6 serum concentrations in severe primary pulmonary hypertension." American journal of respiratory and critical care medicine 151(5): 1628-1631.
- Humbert, M., O. Sitbon, A. Chaouat, M. Bertocchi, G. Habib, V. Gressin, A. Yaici, E. Weitzenblum, J. F. Cordier, F. Chabot, C. Dromer, C. Pison, M. Reynaud-Gaubert, A. Haloun, M. Laurent, E. Hachulla and G. Simonneau (2006). "Pulmonary arterial hypertension in France: results from a national registry." American journal of respiratory and critical care medicine 173(9): 1023-1030.
- Humbert, M. S., R.; Simmoneau, G. (2012). Pulmonary vascular disease, Karger.
- Hunter-Lavin, C., E. L. Davies, M. M. Bacelar, M. J. Marshall, S. M. Andrew and J. H. Williams (2004). "Hsp70 release from peripheral blood mononuclear cells." Biochemical and biophysical research communications 324(2): 511-517.
- Hurdman, J., R. Condliffe, C. A. Elliot, C. Davies, C. Hill, J. M. Wild, D. Capener, P. Sephton, N. Hamilton, I. J. Armstrong, C. Billings, A. Lawrie, I. Sabroe, M. Akil, L. O'Toole and D. G. Kiely (2012). "ASPIRE registry: assessing the Spectrum of Pulmonary hypertension Identified at a REferral centre." The European respiratory journal : official journal of the European Society for Clinical Respiratory Physiology 39(4): 945-955.
- Iannone, F., M. T. Riccardi, S. Guiducci, R. Bizzoca, M. Cinelli, M. Matucci-Cerinic and G. Lapadula (2008). "Bosentan regulates the expression of adhesion molecules on circulating T cells and serum soluble adhesion molecules in systemic sclerosis-associated pulmonary arterial hypertension." Annals of the rheumatic diseases 67(8): 1121-1126.
- Ikeda, U., K. Yamamoto, Y. Maeda, M. Shimpo, T. Kanbe and K. Shimada (1997). "Endothelin-1 inhibits nitric oxide synthesis in vascular smooth muscle cells." Hypertension 29(1 Pt 1): 65-69.
- Ikeda, Y., Y. Yonemitsu, C. Kataoka, S. Kitamoto, T. Yamaoka, K. Nishida, A. Takeshita, K. Egashira and K. Sueishi (2002). "Anti-monocyte chemoattractant protein-1 gene therapy attenuates pulmonary hypertension in rats." American journal of physiology. Heart and circulatory physiology 283(5): H2021-2028.
- Imai, M., C. Goepfert, E. Kaczmarek and S. C. Robson (2000). "CD39 modulates IL-1 release from activated endothelial cells." Biochemical and biophysical research communications 270(1): 272-278.
- Iwaki, K., S. H. Chi, W. H. Dillmann and R. Mestrlil (1993). "Induction of HSP70 in cultured rat neonatal cardiomyocytes by hypoxia and metabolic stress." Circulation 87(6): 2023-2032.
- Jaattela, M., D. Wissing, P. A. Bauer and G. C. Li (1992). "Major heat shock protein hsp70 protects tumor cells from tumor necrosis factor cytotoxicity." The EMBO journal 11(10): 3507-3512.
- Jaffar, Z., M. E. Ferrini, M. C. Buford, G. A. Fitzgerald and K. Roberts (2007). "Prostaglandin I2-IP signaling blocks allergic pulmonary inflammation by preventing recruitment of CD4+ Th2 cells into the airways in a mouse model of asthma." Journal of immunology 179(9): 6193-6203.
- Jais, X., D. Launay, A. Yaici, J. Le Pavec, C. Tcherakian, O. Sitbon, G. Simonneau and M. Humbert (2008). "Immunosuppressive therapy in lupus- and mixed connective tissue disease-associated pulmonary arterial hypertension: a retrospective analysis of twenty-three cases." Arthritis and rheumatism 58(2): 521-531.
- Jammes, Y., J. G. Steinberg, S. Delliaux and F. Bregeon (2009). "Chronic fatigue syndrome combines increased exercise-induced oxidative stress and reduced cytokine and Hsp responses." Journal of internal medicine 266(2): 196-206.

- Janssens, W., V. Carlier, B. Wu, L. VanderElst, M. G. Jacquemin and J. M. Saint-Remy (2003). "CD4+CD25+ T cells lyse antigen-presenting B cells by Fas-Fas ligand interaction in an epitope-specific manner." Journal of immunology 171(9): 4604-4612.
- Joetham, A., K. Takeda, N. Miyahara, S. Matsubara, H. Ohnishi, T. Koya, A. Dakhama and E. W. Gelfand (2007). "Activation of naturally occurring lung CD4(+)CD25(+) regulatory T cells requires CD8 and MHC I interaction." Proceedings of the National Academy of Sciences of the United States of America 104(38): 15057-15062.
- Johnson, A. D. and M. Tytell (1993). "Exogenous HSP70 becomes cell associated, but not internalized, by stressed arterial smooth muscle cells." In vitro cellular & developmental biology. Animal 29A(10): 807-812.
- Joosten, S. A., K. E. van Meijgaarden, N. D. Savage, T. de Boer, F. Triebel, A. van der Wal, E. de Heer, M. R. Klein, A. Geluk and T. H. Ottenhoff (2007). "Identification of a human CD8+ regulatory T cell subset that mediates suppression through the chemokine CC chemokine ligand 4." Proceedings of the National Academy of Sciences of the United States of America 104(19): 8029-8034.
- Jornot, L., M. E. Mirault and A. F. Junod (1991). "Differential expression of hsp70 stress proteins in human endothelial cells exposed to heat shock and hydrogen peroxide." American journal of respiratory cell and molecular biology 5(3): 265-275.
- Kabelitz, D (1992). "Function and specificity of human gamma/delta-positive T cells." Critical Reviews in Immunology 11(5):281-303.
- Kahaleh, B. (2008). "Vascular disease in scleroderma: mechanisms of vascular injury." Rheumatic diseases clinics of North America 34(1): 57-71; vi.
- Kassan, M., M. Galan, M. Partyka, M. Trebak and K. Matrougui (2011). "Interleukin-10 released by CD4(+)CD25(+) natural regulatory T cells improves microvascular endothelial function through inhibition of NADPH oxidase activity in hypertensive mice." Arteriosclerosis, thrombosis, and vascular biology 31(11): 2534-2542.
- Katugampola, S. D. and A. P. Davenport (2001). "Thromboxane receptor density is increased in human cardiovascular disease with evidence for inhibition at therapeutic concentrations by the AT(1) receptor antagonist losartan." British journal of pharmacology 134(7): 1385-1392.
- Kelly, M. E., M. A. Clay, M. J. Mistry, H. M. Hsieh-Li and J. A. Harmony (1994). "Apolipoprotein E inhibition of proliferation of mitogen-activated T lymphocytes: production of interleukin 2 with reduced biological activity." Cellular immunology 159(2): 124-139.
- Kemeny, D. M., A. Noble., B. J. Holmes and D. Diaz-Sanchez (1994). "Immune regulation: a new role for the CD8<sup>+</sup> T cell" Immunology Today 15(3):107-110
- Kessel, A., I. Rosner, M. Rozenbaum, D. Zisman, A. Sagiv, Z. Shmuel, E. Sabo and E. Toubi (2004). "Increased CD8+ T cell apoptosis in scleroderma is associated with low levels of NF-kappa B." Journal of clinical immunology 24(1): 30-36.
- Kim, Y. D. (2011). "Emerging pathogenetic mechanisms of pulmonary arterial hypertension: nitric oxide and more." Korean circulation journal 41(2): 58-60.
- Kim, Y. M., M. E. de Vera, S. C. Watkins and T. R. Billiar (1997). "Nitric oxide protects cultured rat hepatocytes from tumor necrosis factor-alpha-induced apoptosis by inducing heat shock protein 70 expression." The Journal of biological chemistry 272(2): 1402-1411.
- Kohn, G., H. R. Wong, K. Bshesh, B. Zhao, N. Vasi, A. Denenberg, C. Morris, J. Stark and T. P. Shanley (2002). "Heat shock inhibits tnf-induced ICAM-1 expression in human endothelial cells via I kappa kinase inhibition." Shock 17(2): 91-97.
- Ku, I. A., R. Farzaneh-Far, E. Vittinghoff, M. H. Zhang, B. Na and M. A. Whooley (2011). "Association of low leptin with cardiovascular events and mortality in patients with stable coronary artery disease: the Heart and Soul Study." Atherosclerosis 217(2): 503-508.
- Kuhl, A. A., N. N. Pawlowski., K. Grollich., M. Blessenohl., J. Westermann., M. Zeitz., C. Loddenkemper and J. C. Hoffmann (2009). "Human peripheral  $\gamma\delta$  T cells possess regulatory potential". Immunology 128: 580-588.
- Lahm, T., M. Albrecht, A. J. Fisher, M. Selej, N. G. Patel, J. A. Brown, M. J. Justice, M. B. Brown, M. Van Demark, K. M. Trulock, D. Dieudonne, J. G. Reddy, R. G. Presson and I. Petrache (2012). "17beta-Estradiol attenuates hypoxic pulmonary

- hypertension via estrogen receptor-mediated effects." American journal of respiratory and critical care medicine 185(9): 965-980.
- Lamouille, S., C. Mallet, J. J. Feige and S. Bailly (2002). "Activin receptor-like kinase 1 is implicated in the maturation phase of angiogenesis." Blood 100(13): 4495-4501.
- Lane, K. B., R. D. Machado, M. W. Pauciuolo, J. R. Thomson, J. A. Phillips, 3rd, J. E. Loyd, W. C. Nichols and R. C. Trembath (2000). "Heterozygous germline mutations in BMPR2, encoding a TGF-beta receptor, cause familial primary pulmonary hypertension." Nature genetics 26(1): 81-84.
- Launay, J. M., P. Herve, K. Peoc'h, C. Tournois, J. Callebort, C. G. Nebigil, N. Etienne, L. Drouet, M. Humbert, G. Simonneau and L. Maroteaux (2002). "Function of the serotonin 5-hydroxytryptamine 2B receptor in pulmonary hypertension." Nature medicine 8(10): 1129-1135.
- Lawrie, A., A. G. Hameed, J. Chamberlain, N. Arnold, A. Kennerley, K. Hopkinson, J. Pickworth, D. G. Kiely, D. C. Crossman and S. E. Francis (2011). "Paigen diet-fed apolipoprotein E knockout mice develop severe pulmonary hypertension in an interleukin-1-dependent manner." The American journal of pathology 179(4): 1693-1705.
- Lawrie, A., E. Waterman, M. Southwood, D. Evans, J. Suntharalingam, S. Francis, D. Crossman, P. Croucher, N. Morrell and C. Newman (2008). "Evidence of a role for osteoprotegerin in the pathogenesis of pulmonary arterial hypertension." The American journal of pathology 172(1): 256-264.
- Le Pavec, J., F. Perros, S. Eddahibi, B. Decante, P. Dorfmueller, O. Sitbon, D. Lebrec, M. Humbert, M. Mazmanian and P. Herve (2009). "Cirrhosis ameliorates monocrotaline-induced pulmonary hypertension in rats." The European respiratory journal : official journal of the European Society for Clinical Respiratory Physiology 34(3): 731-739.
- Lee, I. Y., E. M. Ko, S. H. Kim, D. I. Jeoung and J. Choe (2005). "Human follicular dendritic cells express prostacyclin synthase: a novel mechanism to control T cell numbers in the germinal center." Journal of immunology 175(3): 1658-1664.
- Lee, S. D., K. R. Shroyer, N. E. Markham, C. D. Cool, N. F. Voelkel and R. M. Tuder (1998). "Monoclonal endothelial cell proliferation is present in primary but not secondary pulmonary hypertension." The Journal of clinical investigation 101(5): 927-934.
- Li, Y., M. Chopp, J. H. Garcia, Y. Yoshida, Z. G. Zhang and S. R. Levine (1992). "Distribution of the 72-kd heat-shock protein as a function of transient focal cerebral ischemia in rats." Stroke; a journal of cerebral circulation 23(9): 1292-1298.
- Liao, D. F., Z. G. Jin, A. S. Baas, G. Daum, S. P. Gygi, R. Aebersold and B. C. Berk (2000). "Purification and identification of secreted oxidative stress-induced factors from vascular smooth muscle cells." The Journal of biological chemistry 275(1): 189-196.
- Libby, P., J. M. Ordovas, K. R. Auger, A. H. Robbins, L. K. Birinyi and C. A. Dinarello (1986). "Endotoxin and tumor necrosis factor induce interleukin-1 gene expression in adult human vascular endothelial cells." The American journal of pathology 124(2): 179-185.
- Libby, P., J. M. Ordovas, L. K. Birinyi, K. R. Auger and C. A. Dinarello (1986). "Inducible interleukin-1 gene expression in human vascular smooth muscle cells." The Journal of clinical investigation 78(6): 1432-1438.
- Lindemann, A., D. Riedel, W. Oster, S. C. Meuer, D. Blohm, R. H. Mertelsmann and F. Herrmann (1988). "Granulocyte/macrophage colony-stimulating factor induces interleukin 1 production by human polymorphonuclear neutrophils." Journal of immunology 140(3): 837-839.
- Lindsey, W. B., M. W. Lowdell, G. E. Marti, F. Abbasi, V. Zenger, K. M. King and L. S. Lamb, Jr. (2007). "CD69 expression as an index of T-cell function: assay standardization, validation and use in monitoring immune recovery." Cytotherapy 9(2): 123-132.
- Liu, Z., S. Tugulea, R. Cortesini and N. Suci-Foca (1998). "Specific suppression of T helper alloreactivity by allo-MHC class I-restricted CD8+CD28- T cells." International journal of Immunology 10:775-783.
- Liu, W., A. L. Putnam, Z. Xu-Yu, G. L. Szot, M. R. Lee, S. Zhu, P. A. Gottlieb, P. Kapranov, T. R. Gingeras, B. Fazekas de St Groth, C. Clayberger, D. M. Soper, S. F. Ziegler and J. A. Bluestone (2006). "CD127 expression inversely correlates with FoxP3 and suppressive function of human CD4+ T reg cells." The Journal of experimental medicine 203(7): 1701-1711.

- Loppnow, H., H. Brade, E. T. Rietschel and H. D. Flad (1994). "Induction of cytokines in mononuclear and vascular cells by endotoxin and other bacterial products." Methods in enzymology 236: 3-10.
- Lord, G. M., G. Matarese, J. K. Howard, R. J. Baker, S. R. Bloom and R. I. Lechler (1998). "Leptin modulates the T-cell immune response and reverses starvation-induced immunosuppression." Nature 394(6696): 897-901.
- Lorenzen, J. M., N. Nickel, R. Kramer, H. Golpon, V. Westerkamp, K. M. Olsson, H. Haller and M. M. Hoepfer (2011). "Osteopontin in patients with idiopathic pulmonary hypertension." Chest 139(5): 1010-1017.
- Luchi, M. E., R. A. Asherson and R. G. Lahita (1992). "Primary idiopathic pulmonary hypertension complicated by pulmonary arterial thrombosis. Association with antiphospholipid antibodies." Arthritis and rheumatism 35(6): 700-705.
- Luo, S. S., K. Sugimoto, S. Fujii, T. Takemasa, S. B. Fu and K. Yamashita (2007). "Role of heat shock protein 70 in induction of stress fiber formation in rat arterial endothelial cells in response to stretch stress." Acta histochemica et cytochemica 40(1): 9-17.
- Luzina, I. G., S. P. Atamas, R. Wise, F. M. Wigley, J. Choi, H. Q. Xiao and B. White (2003). "Occurrence of an activated, profibrotic pattern of gene expression in lung CD8+ T cells from scleroderma patients." Arthritis and rheumatism 48(8): 2262-2274.
- Lynes, M. A., Y. J. Kang, S. L. Sensi, G. A. Perdrizet and L. E. Hightower (2007). "Heavy metal ions in normal physiology, toxic stress, and cytoprotection." Annals of the New York Academy of Sciences 1113: 159-172.
- MacLean, M. R., P. Herve, S. Eddahibi and S. Adnot (2000). "5-hydroxytryptamine and the pulmonary circulation: receptors, transporters and relevance to pulmonary arterial hypertension." British journal of pharmacology 131(2): 161-168.
- Maclean, M. R., E. D. Johnston, K. M. McCulloch, L. Pooley, M. D. Houslay and G. Sweeney (1997). "Phosphodiesterase isoforms in the pulmonary arterial circulation of the rat: changes in pulmonary hypertension." The Journal of pharmacology and experimental therapeutics 283(2): 619-624.
- Majka, S., M. Hagen, T. Blackwell, J. Harral, J. A. Johnson, R. Gendron, H. Paradis, D. Crona, J. E. Loyd, E. Nozik-Grayck, K. R. Stenmark and J. West (2011). "Physiologic and molecular consequences of endothelial Bmpr2 mutation." Respiratory research 12: 84.
- Mallat, Z., H. Ait-Oufella and A. Tedgui (2005). "Regulatory T cell responses: potential role in the control of atherosclerosis." Current opinion in lipidology 16(5): 518-524.
- Marcos, E., S. Adnot, M. H. Pham, A. Nosjean, B. Raffestin, M. Hamon and S. Eddahibi (2003). "Serotonin transporter inhibitors protect against hypoxic pulmonary hypertension." American journal of respiratory and critical care medicine 168(4): 487-493.
- Marsboom, G., P. Pokreisz, O. Gheysens, P. Vermeersch, H. Gillijns, M. Pellens, X. Liu, D. Collen and S. Janssens (2008). "Sustained endothelial progenitor cell dysfunction after chronic hypoxia-induced pulmonary hypertension." Stem cells 26(4): 1017-1026.
- Martin-Romero, C., J. Santos-Alvarez, R. Goberna and V. Sanchez-Margalet (2000). "Human leptin enhances activation and proliferation of human circulating T lymphocytes." Cellular immunology 199(1): 15-24.
- Martin-Ventura, J. L., A. Leclercq, L. M. Blanco-Colio, J. Egido, P. Rossignol, O. Meilhac and J. B. Michel (2007). "Low plasma levels of HSP70 in patients with carotid atherosclerosis are associated with increased levels of proteolytic markers of neutrophil activation." Atherosclerosis 194(2): 334-341.
- Mathai, S. C. and P. M. Hassoun (2011). "Pulmonary arterial hypertension associated with systemic sclerosis." Expert review of respiratory medicine 5(2): 267-279.
- Mathian, A., C. Parizot, K. Dorgham, S. Trad, L. Arnaud, M. Larsen, M. Miyara, M. Hie, J. C. Piette, C. Frances, H. Yssel, Z. Amoura and G. Gorochov (2012). "Activated and resting regulatory T cell exhaustion concurs with high levels of interleukin-22 expression in systemic sclerosis lesions." Annals of the rheumatic diseases 71(7): 1227-1234.
- Mavalia, C., C. Scaletti, P. Romagnani, A. M. Carossino, A. Pignone, L. Emmi, C. Pupilli, G. Pizzolo, E. Maggi and S. Romagnani (1997). "Type 2 helper T-cell predominance and high CD30 expression in systemic sclerosis." The American journal of pathology 151(6): 1751-1758.

- McAllister, K. A., K. M. Grogg, D. W. Johnson, C. J. Gallione, M. A. Baldwin, C. E. Jackson, E. A. Helmbold, D. S. Markel, W. C. McKinnon, J. Murrell and et al. (1994). "Endoglin, a TGF-beta binding protein of endothelial cells, is the gene for hereditary haemorrhagic telangiectasia type 1." Nature genetics 8(4): 345-351.
- McLaughlin, V. V. (2011). "Looking to the future: a new decade of pulmonary arterial hypertension therapy." European respiratory review : an official journal of the European Respiratory Society 20(122): 262-269.
- McLaughlin, V. V. and M. D. McGoon (2006). "Pulmonary arterial hypertension." Circulation 114(13): 1417-1431.
- McLean, P. J., H. Kawamata, S. Shariff, J. Hewett, N. Sharma, K. Ueda, X. O. Breakefield and B. T. Hyman (2002). "TorsinA and heat shock proteins act as molecular chaperones: suppression of alpha-synuclein aggregation." Journal of neurochemistry 83(4): 846-854.
- McMurtry, M. S., S. Bonnet, X. Wu, J. R. Dyck, A. Haromy, K. Hashimoto and E. D. Michelakis (2004). "Dichloroacetate prevents and reverses pulmonary hypertension by inducing pulmonary artery smooth muscle cell apoptosis." Circulation research 95(8): 830-840.
- McNally, A., G. R. Hill, T. Sparwasser, R. Thomas and R. J. Steptoe (2011). "CD4+CD25+ regulatory T cells control CD8+ T-cell effector differentiation by modulating IL-2 homeostasis." Proceedings of the National Academy of Sciences of the United States of America 108(18): 7529-7534.
- Mehta, H. B., B. K. Popovich and W. H. Dillmann (1988). "Ischemia induces changes in the level of mRNAs coding for stress protein 71 and creatine kinase M." Circulation research 63(3): 512-517.
- Meir, K. S. and E. Leitersdorf (2004). "Atherosclerosis in the apolipoprotein-E-deficient mouse: a decade of progress." Arteriosclerosis, thrombosis, and vascular biology 24(6): 1006-1014.
- Mellor, A. L. and D. H. Munn (1999). "Tryptophan catabolism and T-cell tolerance: immunosuppression by starvation?" Immunology today 20(10): 469-473.
- Mestril, R., S. H. Chi, M. R. Sayen, K. O'Reilly and W. H. Dillmann (1994). "Expression of inducible stress protein 70 in rat heart myogenic cells confers protection against simulated ischemia-induced injury." The Journal of clinical investigation 93(2): 759-767.
- Michelakis, E. D., M. S. McMurtry, X. C. Wu, J. R. Dyck, R. Moudgil, T. A. Hopkins, G. D. Lopaschuk, L. Puttagunta, R. Waite and S. L. Archer (2002). "Dichloroacetate, a metabolic modulator, prevents and reverses chronic hypoxic pulmonary hypertension in rats: role of increased expression and activity of voltage-gated potassium channels." Circulation 105(2): 244-250.
- Michiels, C., T. Arnould and J. Remacle (2000). "Endothelial cell responses to hypoxia: initiation of a cascade of cellular interactions." Biochimica et biophysica acta 1497(1): 1-10.
- Milarski, K. L. and R. I. Morimoto (1986). "Expression of human HSP70 during the synthetic phase of the cell cycle." Proceedings of the National Academy of Sciences of the United States of America 83(24): 9517-9521.
- Miyara, M. and S. Sakaguchi (2007). "Natural regulatory T cells: mechanisms of suppression." Trends in Molecular medicine 13(3):108-116.
- Miyata, M., F. Sakuma, M. Ito, H. Ohira, Y. Sato and R. Kasukawa (2000). "Athymic nude rats develop severe pulmonary hypertension following monocrotaline administration." International archives of allergy and immunology 121(3): 246-252.
- Mor, A., G. Luboshits, D. Planer, G. Keren and J. George (2006). "Altered status of CD4(+)/CD25(+) regulatory T cells in patients with acute coronary syndromes." European heart journal 27(21): 2530-2537.
- Morecroft, I., Y. Dempsey, M. Bader, D. J. Walther, K. Kotnik, L. Loughlin, M. Nilsen and M. R. MacLean (2007). "Effect of tryptophan hydroxylase 1 deficiency on the development of hypoxia-induced pulmonary hypertension." Hypertension 49(1): 232-236.
- Morelli, S., M. Giordano, P. De Marzio, R. Priori, A. Sgreccia and G. Valesini (1993). "Pulmonary arterial hypertension responsive to immunosuppressive therapy in systemic lupus erythematosus." Lupus 2(6): 367-369.

- Morrell, N. W., X. Yang, P. D. Upton, K. B. Jourdan, N. Morgan, K. K. Sheares and R. C. Trembath (2001). "Altered growth responses of pulmonary artery smooth muscle cells from patients with primary pulmonary hypertension to transforming growth factor-beta(1) and bone morphogenetic proteins." Circulation 104(7): 790-795.
- Mosmann, T. R and S. Sad (1996). "The expanding universe of T-cell subsets: Th1, Th2 and more." Immunology Today 17(3):138-146.
- Moyer, C. F., D. Sajuthi, H. Tulli and J. K. Williams (1991). "Synthesis of IL-1 alpha and IL-1 beta by arterial cells in atherosclerosis." The American journal of pathology 138(4): 951-960.
- Mukerjee, D., D. St George, B. Coleiro, C. Knight, C. P. Denton, J. Davar, C. M. Black and J. G. Coghlan (2003). "Prevalence and outcome in systemic sclerosis associated pulmonary arterial hypertension: application of a registry approach." Annals of the rheumatic diseases 62(11): 1088-1093.
- Nagaoka, T., K. A. Fagan, S. A. Gebb, K. G. Morris, T. Suzuki, H. Shimokawa, I. F. McMurtry and M. Oka (2005). "Inhaled Rho kinase inhibitors are potent and selective vasodilators in rat pulmonary hypertension." American journal of respiratory and critical care medicine 171(5): 494-499.
- Nakamura, K., A. Kitani and W. Strober (2001). "Cell contact-dependent immunosuppression by CD4(+)CD25(+) regulatory T cells is mediated by cell surface-bound transforming growth factor beta." The Journal of experimental medicine 194(5): 629-644.
- Needleman, B. W., F. M. Wigley and R. W. Stair (1992). "Interleukin-1, interleukin-2, interleukin-4, interleukin-6, tumor necrosis factor alpha, and interferon-gamma levels in sera from patients with scleroderma." Arthritis and rheumatism 35(1): 67-72.
- Newby, A. C., K. M. Southgate and J. W. Assender (1992). "Inhibition of vascular smooth muscle cell proliferation by endothelium-dependent vasodilators." Herz 17(5): 291-299.
- Nijkamp, F. P. and M. J. Parnham (2011). "Principles of Immunopharmacology: 3rd revised and extended edition." ISBN 3-7643-5780-0
- Nollen, E. A. and R. I. Morimoto (2002). "Chaperoning signaling pathways: molecular chaperones as stress-sensing 'heat shock' proteins." Journal of cell science 115(Pt 14): 2809-2816.
- Nunes, A. K., C. Raposo, R. L. Luna, M. A. Cruz-Hofling and C. A. Peixoto (2012). "Sildenafil (Viagra(R)) down regulates cytokines and prevents demyelination in a cuprizone-induced MS mouse model." Cytokine.
- Oehler, R., B. Schmierer, M. Zellner, R. Prohaska and E. Roth (2000). "Endothelial cells downregulate expression of the 70 kDa heat shock protein during hypoxia." Biochemical and biophysical research communications 274(2): 542-547.
- Oh, S. P., T. Seki, K. A. Goss, T. Imamura, Y. Yi, P. K. Donahoe, L. Li, K. Miyazono, P. ten Dijke, S. Kim and E. Li (2000). "Activin receptor-like kinase 1 modulates transforming growth factor-beta 1 signaling in the regulation of angiogenesis." Proceedings of the National Academy of Sciences of the United States of America 97(6): 2626-2631.
- Ong, C., C. Wong, C. R. Roberts, H. S. Teh and F. R. Jirik (1998). "Anti-IL-4 treatment prevents dermal collagen deposition in the tight-skin mouse model of scleroderma." European journal of immunology 28(9): 2619-2629.
- Ormiston, M. L., C. Chang, L. L. Long, E. Soon, D. Jones, R. Machado, C. Treacy, M. R. Toshner, K. Campbell, A. Riding, M. Southwood, J. Pepke-Zaba, A. Exley, R. C. Trembath, F. Colucci, M. Wills, J. Trowsdale and N. W. Morrell (2012). "Impaired natural killer cell phenotype and function in idiopathic and heritable pulmonary arterial hypertension." Circulation 126(9): 1099-1109.
- Ozaki, M., S. Kawashima, T. Yamashita, Y. Ohashi, Y. Rikitake, N. Inoue, K. I. Hirata, Y. Hayashi, H. Itoh and M. Yokoyama (2001). "Reduced hypoxic pulmonary vascular remodeling by nitric oxide from the endothelium." Hypertension 37(2): 322-327.
- Pakala, R., J. T. Willerson and C. R. Benedict (1994). "Mitogenic effect of serotonin on vascular endothelial cells." Circulation 90(4): 1919-1926.
- Papp, G., I. F. Horvath, S. Barath, E. Gyimesi, S. Sipka, P. Szodoray and M. Zeher (2011). "Altered T-cell and regulatory cell repertoire in patients with diffuse cutaneous systemic sclerosis." Scandinavian journal of rheumatology 40(3): 205-210.

- Paternotte, E., C. Gaucher, P. Labrude, J. F. Stoltz and P. Menu (2008). "Review: behaviour of endothelial cells faced with hypoxia." Bio-medical materials and engineering 18(4-5): 295-299.
- Pendergrass, S. A., E. Hayes, G. Farina, R. Lemaire, H. W. Farber, M. L. Whitfield and R. Lafyatis (2010). "Limited systemic sclerosis patients with pulmonary arterial hypertension show biomarkers of inflammation and vascular injury." PLoS one 5(8): e12106.
- Pepke-Zaba, J., M. Delcroix, I. Lang, E. Mayer, P. Jansa, D. Ambroz, C. Treacy, A. M. D'Armini, M. Morsolini, R. Srijder, P. Bresser, A. Torbicki, B. Kristensen, J. Lewczuk, I. Simkova, J. A. Barbera, M. de Perrot, M. M. Hoepfer, S. Gaine, R. Speich, M. A. Gomez-Sanchez, G. Kovacs, A. M. Hamid, X. Jais and G. Simonneau (2011). "Chronic thromboembolic pulmonary hypertension (CTEPH): results from an international prospective registry." Circulation 124(18): 1973-1981.
- Pfister, G., C. M. Stroh, H. Perschinka, M. Kind, M. Knoflach, P. Hinterdorfer and G. Wick (2005). "Detection of HSP60 on the membrane surface of stressed human endothelial cells by atomic force and confocal microscopy." Journal of cell science 118(Pt 8): 1587-1594.
- Piotrowicz, R. S., J. L. Martin, W. H. Dillman and E. G. Levin (1997). "The 27-kDa heat shock protein facilitates basic fibroblast growth factor release from endothelial cells." The Journal of biological chemistry 272(11): 7042-7047.
- Poccia, F., P. Piselli, S. Vendetti, S. Bach, A. Amendola, R. Placido and V. Colizzi (1996). "Heat-shock protein expression on the membrane of T cells undergoing apoptosis." Immunology 88(1): 6-12.
- Pockley, A. G., S. K. Calderwood and G. Multhoff (2009). "The atheroprotective properties of Hsp70: a role for Hsp70-endothelial interactions?" Cell stress & chaperones 14(6): 545-553.
- Pockley, A. G., U. De Faire, R. Kiessling, C. Lemne, T. Thulin and J. Frostegard (2002). "Circulating heat shock protein and heat shock protein antibody levels in established hypertension." Journal of hypertension 20(9): 1815-1820.
- Pockley, A. G. and J. Frostegard (2005). "Heat shock proteins in cardiovascular disease and the prognostic value of heat shock protein related measurements." Heart 91(9): 1124-1126.
- Pockley, A. G., A. Georgiades, T. Thulin, U. de Faire and J. Frostegard (2003). "Serum heat shock protein 70 levels predict the development of atherosclerosis in subjects with established hypertension." Hypertension 42(3): 235-238.
- Pockley, A. G., J. Shepherd and J. M. Corton (1998). "Detection of heat shock protein 70 (Hsp70) and anti-Hsp70 antibodies in the serum of normal individuals." Immunological investigations 27(6): 367-377.
- Post, J. M., J. R. Hume, S. L. Archer and E. K. Weir (1992). "Direct role for potassium channel inhibition in hypoxic pulmonary vasoconstriction." Am J Physiol 262(4 Pt 1): C882-890.
- Pratt, W. B. and D. O. Toft (2003). "Regulation of signaling protein function and trafficking by the hsp90/hsp70-based chaperone machinery." Experimental biology and medicine 228(2): 111-133.
- Pribila, J. T., A. C. Quale, K. L. Mueller and Y. Shimizu (2004). "Integrins and T cell-mediated immunity." Annual review of immunology 22: 157-180.
- Price, L. C., D. Montani, C. Tcherakian, P. Dorfmueller, R. Souza, N. Gambaryan, M. C. Chaumais, D. M. Shao, G. Simonneau, L. S. Howard, I. M. Adcock, S. J. Wort, M. Humbert and F. Perros (2011). "Dexamethasone reverses monocrotaline-induced pulmonary arterial hypertension in rats." The European respiratory journal : official journal of the European Society for Clinical Respiratory Physiology 37(4): 813-822.
- Quarck, R., T. Nawrot, B. Meyns and M. Delcroix (2009). "C-reactive protein: a new predictor of adverse outcome in pulmonary arterial hypertension." Journal of the American College of Cardiology 53(14): 1211-1218.
- Quinn, D. A., H. K. Du, B. T. Thompson and C. A. Hales (1998). "Amiloride analogs inhibit chronic hypoxic pulmonary hypertension." American journal of respiratory and critical care medicine 157(4 Pt 1): 1263-1268.
- Rabinovitch, M. (2008). "Molecular pathogenesis of pulmonary arterial hypertension." The Journal of clinical investigation 118(7): 2372-2379.

- Radstake, T. R., L. van Bon, J. Broen, M. Wenink, K. Santegoets, Y. Deng, A. Hussaini, R. Simms, W. W. Cruikshank and R. Lafyatis (2009). "Increased frequency and compromised function of T regulatory cells in systemic sclerosis (SSc) is related to a diminished CD69 and TGFbeta expression." *PLoS one* 4(6): e5981.
- Rasekaba, T., A. L. Lee, M. T. Naughton, T. J. Williams and A. E. Holland (2009). "The six-minute walk test: a useful metric for the cardiopulmonary patient." *Internal medicine journal* 39(8): 495-501.
- Ray, B. N., N. Y. Lee, T. How and G. C. Blobe (2010). "ALK5 phosphorylation of the endoglin cytoplasmic domain regulates Smad1/5/8 signaling and endothelial cell migration." *Carcinogenesis* 31(3): 435-441.
- Reilly, M. P., S. M. Taylor, C. Franklin, B. S. Sachais, D. B. Cines, K. J. Williams and S. E. McKenzie (2006). "Prothrombotic factors enhance heparin-induced thrombocytopenia and thrombosis in vivo in a mouse model." *Journal of thrombosis and haemostasis* : JTH 4(12): 2687-2694.
- Reindel, J. F. and R. A. Roth (1991). "The effects of monocrotaline pyrrole on cultured bovine pulmonary artery endothelial and smooth muscle cells." *The American journal of pathology* 138(3): 707-719.
- Rhodes, C. J., L. S. Howard, M. Busbridge, D. Ashby, E. Kondili, J. S. Gibbs, J. Wharton and M. R. Wilkins (2011). "Iron deficiency and raised hepcidin in idiopathic pulmonary arterial hypertension: clinical prevalence, outcomes, and mechanistic insights." *Journal of the American College of Cardiology* 58(3): 300-309.
- Rich, S., E. Kaufmann and P. S. Levy (1992). "The effect of high doses of calcium-channel blockers on survival in primary pulmonary hypertension." *The New England journal of medicine* 327(2): 76-81.
- Ritossa, C. (1962). "A new puffing pattern induced and temperature shock and DNP in *Drosophila*." *Experientia*(18): 571-573.
- Robicsek, S. A., D. K. Blanchard, J. Y. Djeu, J. J. Krzanowski, A. Szentivanyi and J. B. Polson (1991). "Multiple high-affinity cAMP-phosphodiesterases in human T-lymphocytes." *Biochemical pharmacology* 42(4): 869-877.
- Rodriguez-Iturbe, B., H. Pons, Y. Quiroz, K. Gordon, J. Rincon, M. Chavez, G. Parra, J. Herrera-Acosta, D. Gomez-Garre, R. Largo, J. Egido and R. J. Johnson (2001). "Mycophenolate mofetil prevents salt-sensitive hypertension resulting from angiotensin II exposure." *Kidney international* 59(6): 2222-2232.
- Romberg, E. (1981). "Ueber Sklerose der Lungen arterie." *Dtsch Archiv Klin Med* 48: 197-206.
- Roncarolo, M. G., S. Gregori., M. Battaglia., R. Bacchetta., K. Fleischhauer and M. K. Levings (2006). "Interleukin-10-secreting type 1 regulatory T cells in rodents and humans." *Immunology* 212:28.
- Roth, R. A., L. A. Dotzlaw, B. Baranyi, C. H. Kuo and J. B. Hook (1981). "Effect of monocrotaline ingestion on liver, kidney, and lung of rats." *Toxicology and applied pharmacology* 60(2): 193-203.
- Roth, R. A. and J. F. Reindel (1991). "Lung vascular injury from monocrotaline pyrrole, a putative hepatic metabolite." *Advances in experimental medicine and biology* 283: 477-487.
- Roumm, A. D., T. L. Whiteside, T. A. Medsger, Jr. and G. P. Rodnan (1984). "Lymphocytes in the skin of patients with progressive systemic sclerosis. Quantification, subtyping, and clinical correlations." *Arthritis and rheumatism* 27(6): 645-653.
- Rubens, C., R. Ewert, M. Halank, R. Wensel, H. D. Orzechowski, H. P. Schultheiss and G. Hoeffken (2001). "Big endothelin-1 and endothelin-1 plasma levels are correlated with the severity of primary pulmonary hypertension." *Chest* 120(5): 1562-1569.
- Rubin, L. J. (2002). "Therapy of pulmonary hypertension: the evolution from vasodilators to antiproliferative agents." *American journal of respiratory and critical care medicine* 166(10): 1308-1309.
- Ruiter, G., S. Lankhorst, A. Boonstra, P. E. Postmus, S. Zweegman, N. Westerhof, W. J. van der Laarse and A. Vonk-Noordegraaf (2011). "Iron deficiency is common in idiopathic pulmonary arterial hypertension." *The European respiratory journal : official journal of the European Society for Clinical Respiratory Physiology* 37(6): 1386-1391.

- Sakaguchi, S. (2004). "Naturally arising CD4+ regulatory t cells for immunologic self-tolerance and negative control of immune responses." Annual review of immunology 22: 531-562.
- Sakaguchi, S., N. Sakaguchi, M. Asano, M. Itoh and M. Toda (1995). "Immunologic self-tolerance maintained by activated T cells expressing IL-2 receptor alpha-chains (CD25). Breakdown of a single mechanism of self-tolerance causes various autoimmune diseases." Journal of immunology 155(3): 1151-1164.
- Sakamaki, F., S. Kyotani, N. Nagaya, N. Sato, H. Oya, T. Satoh and N. Nakanishi (2000). "Increased plasma P-selectin and decreased thrombomodulin in pulmonary arterial hypertension were improved by continuous prostacyclin therapy." Circulation 102(22): 2720-2725.
- Sakao, S., L. Taraseviciene-Stewart, J. D. Lee, K. Wood, C. D. Cool and N. F. Voelkel (2005). "Vascular endothelial growth factor receptor blockade by SU5416 combined with pulsatile shear stress causes apoptosis and subsequent proliferation of apoptosis-resistant endothelial cells." Chest 128(6 Suppl): 610S-611S.
- Sakkas, L. I. and C. D. Platsoucas (2004). "Is systemic sclerosis an antigen-driven T cell disease?" Arthritis and rheumatism 50(6): 1721-1733.
- Saladin, R., P. De Vos, M. Guerre-Millo, A. Leturque, J. Girard, B. Staels and J. Auwerx (1995). "Transient increase in obese gene expression after food intake or insulin administration." Nature 377(6549): 527-529.
- Sallusto, F., J. Geginat and A. Lanzavecchia (2003). "Central memory and effector memory T cell subsets: Function, Generation, and maintenance." Annual Review of Immunology 22: 745-763.
- Sampaio, A. L., G. A. Rae and M. M. Henriques (2000). "Role of endothelins on lymphocyte accumulation in allergic pleurisy." Journal of leukocyte biology 67(2): 189-195.
- Sanchez, O., O. Sitbon, X. Jais, G. Simonneau and M. Humbert (2006). "Immunosuppressive therapy in connective tissue diseases-associated pulmonary arterial hypertension." Chest 130(1): 182-189.
- Sanz, O., A. Estrada, I. Ferrer and A. M. Planas (1997). "Differential cellular distribution and dynamics of HSP70, cyclooxygenase-2, and c-Fos in the rat brain after transient focal ischemia or kainic acid." Neuroscience 80(1): 221-232.
- Schermuly, R. T., Dony, E., Ghofrani, H. A., Pullamsetti, S (2005). "Reversal of experimental pulmonary hypertension by PDGF inhibition." Journal of clinical investigation 115(10):2811-21
- Schubert, L. A., E. Jeffery, Y. Zhang, F. Ramsdell and S. F. Ziegler (2001). "Scurfin (FOXP3) acts as a repressor of transcription and regulates T cell activation." The Journal of biological chemistry 276(40): 37672-37679.
- Scumpia, P. O., M. J. Delano, K. M. Kelly, K. A. O'Malley, P. A. Efron, P. F. McAuliffe, T. Brusko, R. Ungaro, T. Barker, J. L. Wynn, M. A. Atkinson, W. H. Reeves, M. J. Salzler and L. L. Moldawer (2006). "Increased natural CD4+CD25+ regulatory T cells and their suppressor activity do not contribute to mortality in murine polymicrobial sepsis." Journal of immunology 177(11): 7943-7949.
- Serafini, P., K. Meckel, M. Kelso, K. Noonan, J. Califano, W. Koch, L. Dolcetti, V. Bronte and I. Borrello (2006). "Phosphodiesterase-5 inhibition augments endogenous antitumor immunity by reducing myeloid-derived suppressor cell function." The Journal of experimental medicine 203(12): 2691-2702.
- Shen, H., M. Clauss, J. Ryan, A. M. Schmidt, P. Tijburg, L. Borden, D. Connolly, D. Stern and J. Kao (1993). "Characterization of vascular permeability factor/vascular endothelial growth factor receptors on mononuclear phagocytes." Blood 81(10): 2767-2773.
- Shen, L. S., J. Wang, D. F. Shen, X. L. Yuan, P. Dong, M. X. Li, J. Xue, F. M. Zhang, H. L. Ge and D. Xu (2009). "CD4(+)CD25(+)CD127(low/-) regulatory T cells express Foxp3 and suppress effector T cell proliferation and contribute to gastric cancers progression." Clinical immunology 131(1): 109-118.
- Shimoda, L. A. and G. L. Semenza (2011). "HIF and the lung: role of hypoxia-inducible factors in pulmonary development and disease." American journal of respiratory and critical care medicine 183(2): 152-156.
- Shipp, C., E. Derhovanessian and G. Pawelec (2012). "Effect of culture at low oxygen tension on the expression of heat shock proteins in a panel of melanoma cell lines." PloS one 7(6): e37475.

- Simeon-Aznar, C. P., V. Fonollosa-Pla, C. Tolosa-Vilella, G. Espinosa-Garriga, M. Ramos-Casals, M. Campillo-Grau, F. J. Garcia-Hernandez, M. J. Castillo-Palma, J. Sanchez-Roman, J. L. Callejas-Rubio, N. Ortego-Centeno, M. V. Egurbide-Arberas, L. Trapiella-Martinez, M. Gallego-Villalobos, L. Saez-Comet, J. Velilla-Marco, M. T. Camps-Garcia, E. de Ramon-Garrido, E. M. Esteban Marcos, L. Pallares-Ferreeres, C. Hidalgo-Tenorio, J. M. Sabio-Sanchez, R. Gomez-de la Torre, G. Salvador-Cervello, J. J. Rios-Blanco, A. Gil-Aguado and M. Vilardell-Tarres (2012). "Registry of the Spanish network for systemic sclerosis: clinical pattern according to cutaneous subsets and immunological status." Seminars in arthritis and rheumatism 41(6): 789-800.
- Slobodin, G., M. S. Ahmad, I. Rosner, R. Peri, M. Rozenbaum, A. Kessel, E. Toubi and M. Odeh (2010). "Regulatory T cells (CD4(+)/CD25(bright)/FoxP3(+)) expansion in systemic sclerosis correlates with disease activity and severity." Cellular immunology 261(2): 77-80.
- Smolders, J., M. Thewissen, E. Peelen, P. Menheere, J. W. Tervaert, J. Damoiseaux and R. Hupperts (2009). "Vitamin D status is positively correlated with regulatory T cell function in patients with multiple sclerosis." PloS one 4(8): e6635.
- Smyth, M. J., E. Cretney, J. M. Kelly, J. A. Westwood, S. E. Street, H. Yagita, K. Takeda, S. L. van Dommelen, M. A. Degli-Esposti and Y. Hayakawa (2005). "Activation of NK cell cytotoxicity." Molecular immunology 42(4): 501-510.
- Song, Y., L. Coleman, J. Shi, H. Beppu, K. Sato, K. Walsh, J. Loscalzo and Y. Y. Zhang (2008). "Inflammation, endothelial injury, and persistent pulmonary hypertension in heterozygous BMP2-mutant mice." American journal of physiology. Heart and circulatory physiology 295(2): H677-690.
- Soon, E. (2008). "Lymphocyte profiles in idiopathic and chronic thromboembolic pulmonary hypertension." Thorax 63:(Suppl VII): A4-A73.
- Soon, E., A. M. Holmes, C. M. Treacy, N. J. Doughty, L. Southgate, R. D. Machado, R. C. Trembath, S. Jennings, L. Barker, P. Nicklin, C. Walker, D. C. Budd, J. Pepke-Zaba and N. W. Morrell (2010). "Elevated levels of inflammatory cytokines predict survival in idiopathic and familial pulmonary arterial hypertension." Circulation 122(9): 920-927.
- Steiner, M. K., O. L. Syrkina, N. Kolliputi, E. J. Mark, C. A. Hales and A. B. Waxman (2009). "Interleukin-6 overexpression induces pulmonary hypertension." Circulation research 104(2): 236-244, 228p following 244.
- Stenmark, K. R., B. Meyrick, N. Galie, W. J. Mooi and I. F. McMurtry (2009). "Animal models of pulmonary arterial hypertension: the hope for etiological discovery and pharmacological cure." American journal of physiology. Lung cellular and molecular physiology 297(6): L1013-1032.
- Stordeur, P. and M. Goldman (1998). "Interleukin-10 as a regulatory cytokine induced by cellular stress: molecular aspects." International reviews of immunology 16(5-6): 501-522.
- Strom, A., A. Franzen, C. Wangnerud, A. K. Knutsson, D. Heinegard and A. Hultgardh-Nilsson (2004). "Altered vascular remodeling in osteopontin-deficient atherosclerotic mice." Journal of vascular research 41(4): 314-322.
- Su, H., M. S. Longhi, P. Wang, D. Vergani and Y. Ma (2012). "Human CD4+CD25(high)CD127 (low/neg) regulatory T cells." Methods in molecular biology 806: 287-299.
- Summer, R., C. A. Fiack, Y. Ikeda, K. Sato, D. Dwyer, N. Ouchi, A. Fine, H. W. Farber and K. Walsh (2009). "Adiponectin deficiency: a model of pulmonary hypertension associated with pulmonary vascular disease." American journal of physiology. Lung cellular and molecular physiology 297(3): L432-438.
- Sun, J. C., J. N. Beilke and L. L. Lanier (2009). "Adaptive immune features of natural killer cells." Nature 457(7229): 557-561.
- Suzuki, A., D. Nakashima, Y. Miyawaki, J. Fujita, A. Maki, Y. Fujimori, A. Takagi, T. Murate, M. Teranishi, T. Matsushita, H. Saito and T. Kojima (2012). "A novel ENG mutation causing impaired co-translational processing of endoglin associated with hereditary hemorrhagic telangiectasia." Thrombosis research 129(5): e200-208.
- Suzuki, K., Y. Sawa, Y. Kaneda, H. Ichikawa, R. Shirakura and H. Matsuda (1998). "Overexpressed heat shock protein 70 attenuates hypoxic injury in coronary endothelial cells." Journal of molecular and cellular cardiology 30(6): 1129-1136.

- Taams, L. S., J. Smith, M. H. Rustin, M. Salmon, L. W. Poulter and A. N. Akbar (2001). "Human anergic/suppressive CD4(+)/CD25(+) T cells: a highly differentiated and apoptosis-prone population." European journal of immunology 31(4): 1122-1131.
- Taams, L. S., J. M. van Amelsfort, M. M. Tiemessen, K. M. Jacobs, E. C. de Jong, A. N. Akbar, J. W. Bijlsma and F. P. Lafeber (2005). "Modulation of monocyte/macrophage function by human CD4+CD25+ regulatory T cells." Human immunology 66(3): 222-230.
- Tajsic, T. M., NW. (2011). "Smooth Muscle Cell Hypertrophy, Proliferation, Migration and Apoptosis in Pulmonary Hypertension." Comprehensive Physiology 1(1).
- Tamby, M. C., Y. Chanseaud, M. Humbert, J. Fermanian, P. Guilpain, P. Garcia-de-la-Pena-Lefebvre, S. Brunet, A. Servettaz, B. Weill, G. Simonneau, L. Guillevin, M. C. Boissier and L. Mouthon (2005). "Anti-endothelial cell antibodies in idiopathic and systemic sclerosis associated pulmonary arterial hypertension." Thorax 60(9): 765-772.
- Tamby, M. C., M. Humbert, P. Guilpain, A. Servettaz, N. Dupin, J. J. Christner, G. Simonneau, J. Fermanian, B. Weill, L. Guillevin and L. Mouthon (2006). "Antibodies to fibroblasts in idiopathic and scleroderma-associated pulmonary hypertension." The European respiratory journal : official journal of the European Society for Clinical Respiratory Physiology 28(4): 799-807.
- Tamosiuniene, R. and M. R. Nicolls (2011). "Regulatory T cells and pulmonary hypertension." Trends in cardiovascular medicine 21(6): 166-171.
- Tamosiuniene, R., W. Tian, G. Dhillon, L. Wang, Y. K. Sung, L. Gera, A. J. Patterson, R. Agrawal, M. Rabinovitch, K. Ambler, C. S. Long, N. F. Voelkel and M. R. Nicolls (2011). "Regulatory T cells limit vascular endothelial injury and prevent pulmonary hypertension." Circulation research 109(8): 867-879.
- Tang, T. T., Y. J. Ding, Y. H. Liao, X. Yu, H. Xiao, J. J. Xie, J. Yuan, Z. H. Zhou, M. Y. Liao, R. Yao, Y. Cheng and X. Cheng (2010). "Defective circulating CD4CD25+Foxp3+CD127(low) regulatory T-cells in patients with chronic heart failure." Cellular physiology and biochemistry : international journal of experimental cellular physiology, biochemistry, and pharmacology 25(4-5): 451-458.
- Tarantino, G., C. Finelli, A. Colao, D. Capone, M. Tarantino, E. Grimaldi, D. Chianese, S. Gioia, F. Pasanisi, F. Contaldo, F. Scopacasa and S. Savastano (2012). "Are hepatic steatosis and carotid intima media thickness associated in obese patients with normal or slightly elevated gamma-glutamyl-transferase?" Journal of translational medicine 10: 50.
- Taraseviciene-Stewart, L., M. R. Nicolls, D. Kraskauskas, R. Scerbavicius, N. Burns, C. Cool, K. Wood, J. E. Parr, S. A. Boackle and N. F. Voelkel (2007). "Absence of T cells confers increased pulmonary arterial hypertension and vascular remodeling." American journal of respiratory and critical care medicine 175(12): 1280-1289.
- Taraseviciene-Stewart, L., D. K. Scerbavicius, N. Burns, C. D. Cool, M. R. Nicolls and N. F. Voelkel (2005). "The protective role of T-lymphocytes in pulmonary vascular remodeling." Chest 128(6 Suppl): 571S-572S.
- Teichert-Kuliszewska, K., M. J. Kutryk, M. A. Kuliszewski, G. Karoubi, D. W. Courtman, L. Zucco, J. Granton and D. J. Stewart (2006). "Bone morphogenetic protein receptor-2 signaling promotes pulmonary arterial endothelial cell survival: implications for loss-of-function mutations in the pathogenesis of pulmonary hypertension." Circulation research 98(2): 209-217.
- Terness, P., T. M. Bauer, L. Rose, C. Dufter, A. Watzlik, H. Simon and G. Opelz (2002). "Inhibition of allogeneic T cell proliferation by indoleamine 2,3-dioxygenase-expressing dendritic cells: mediation of suppression by tryptophan metabolites." The Journal of experimental medicine 196(4): 447-457.
- Terrier, B., M. C. Tamby, L. Camoin, P. Guilpain, C. Broussard, G. Bussone, A. Yaici, F. Hotellier, G. Simonneau, L. Guillevin, M. Humbert and L. Mouthon (2008). "Identification of target antigens of antifibroblast antibodies in pulmonary arterial hypertension." American journal of respiratory and critical care medicine 177(10): 1128-1134.
- Thomas, H. C., M. W. Lame, D. Morin, D. W. Wilson and H. J. Segall (1998). "Prolonged cell-cycle arrest associated with altered cdc2 kinase in monocrotaline pyrrole-treated pulmonary artery endothelial cells." American journal of respiratory cell and molecular biology 19(1): 129-142.

- Thomson, J. R., R. D. Machado, M. W. Pauciulo, N. V. Morgan, M. Humbert, G. C. Elliott, K. Ward, M. Yacoub, G. Mikhail, P. Rogers, J. Newman, L. Wheeler, T. Higenbottam, J. S. Gibbs, J. Egan, A. Crozier, A. Peacock, R. Allcock, P. Corris, J. E. Loyd, R. C. Trembath and W. C. Nichols (2000). "Sporadic primary pulmonary hypertension is associated with germline mutations of the gene encoding BMPR-II, a receptor member of the TGF-beta family." Journal of medical genetics 37(10): 741-745.
- Thorngate, F. E., L. L. Rudel, R. L. Walzem and D. L. Williams (2000). "Low levels of extrahepatic nonmacrophage ApoE inhibit atherosclerosis without correcting hypercholesterolemia in ApoE-deficient mice." Arteriosclerosis, thrombosis, and vascular biology 20(8): 1939-1945.
- Thornton, A. M., E. E. Donovan, C. A. Piccirillo and E. M. Shevach (2004). "Cutting edge: IL-2 is critically required for the in vitro activation of CD4+CD25+ T cell suppressor function." Journal of immunology 172(11): 6519-6523.
- Thornton, A. M. and E. M. Shevach (1998). "CD4+CD25+ immunoregulatory T cells suppress polyclonal T cell activation in vitro by inhibiting interleukin 2 production." The Journal of experimental medicine 188(2): 287-296.
- Tissieres, A., H. K. Mitchell and U. M. Tracy (1974). "Protein synthesis in salivary glands of *Drosophila melanogaster*: relation to chromosome puffs." Journal of molecular biology 84(3): 389-398.
- Tonelli, A. R., M. Aytakin, A. E. Feldstein and R. A. Dweik (2012). "Leptin levels predict survival in pulmonary arterial hypertension." Pulmonary circulation 2(2): 214-219.
- Trautinger, F., I. Kindas-Mugge, R. M. Knobler and H. Honigsmann (1996). "Stress proteins in the cellular response to ultraviolet radiation." Journal of photochemistry and photobiology. B, Biology 35(3): 141-148.
- Trembath, R. C., J. R. Thomson, R. D. Machado, N. V. Morgan, C. Atkinson, I. Winship, G. Simonneau, N. Galie, J. E. Loyd, M. Humbert, W. C. Nichols, N. W. Morrell, J. Berg, A. Manes, J. McGaughran, M. Pauciulo and L. Wheeler (2001). "Clinical and molecular genetic features of pulmonary hypertension in patients with hereditary hemorrhagic telangiectasia." The New England journal of medicine 345(5): 325-334.
- Trickett, A. and Y. L. Kwan (2003). "T cell stimulation and expansion using anti-CD3/CD28 beads." Journal of immunological methods 275(1-2): 251-255.
- Tuder, R. M., C. D. Cool, M. W. Geraci, J. Wang, S. H. Abman, L. Wright, D. Badesch and N. F. Voelkel (1999). "Prostacyclin synthase expression is decreased in lungs from patients with severe pulmonary hypertension." American journal of respiratory and critical care medicine 159(6): 1925-1932.
- Tuder, R. M., B. Groves, D. B. Badesch and N. F. Voelkel (1994). "Exuberant endothelial cell growth and elements of inflammation are present in plexiform lesions of pulmonary hypertension." The American journal of pathology 144(2): 275-285.
- Tuder, R. M., S. D. Lee and C. C. Cool (1998). "Histopathology of pulmonary hypertension." Chest 114(1 Suppl): 1S-6S.
- Tuder, R. M., Z. Radisavljevic, K. R. Shroyer, J. M. Polak and N. F. Voelkel (1998). "Monoclonal endothelial cells in appetite suppressant-associated pulmonary hypertension." American journal of respiratory and critical care medicine 158(6): 1999-2001.
- Ulrich, S., M. R. Nicolls, L. Taraseviciene, R. Speich and N. Voelkel (2008). "Increased regulatory and decreased CD8+ cytotoxic T cells in the blood of patients with idiopathic pulmonary arterial hypertension." Respiration; international review of thoracic diseases 75(3): 272-280.
- Utsuyama, M., K. Hirokawa, C. Kurashima, M. Fukayama, T. Inamatsu, K. Suzuki, W. Hashimoto and K. Sato (1992). "Differential age-change in the numbers of CD4+CD45RA+ and CD4+CD29+ T cell subsets in human peripheral blood." Mechanisms of ageing and development 63(1): 57-68.
- van Roon, J. A., W. van Eden, J. L. van Roy, F. J. Lafeber and J. W. Bijlsma (1997). "Stimulation of suppressive T cell responses by human but not bacterial 60-kD heat-shock protein in synovial fluid of patients with rheumatoid arthritis." The Journal of clinical investigation 100(2): 459-463.
- Venken, K., N. Hellings, M. Thewissen, V. Somers, K. Hensen, J. L. Rummens, R. Medaer, R. Hupperts and P. Stinissen (2008). "Compromised CD4+ CD25(high) regulatory T-cell function in patients with relapsing-remitting multiple sclerosis is correlated with a

- reduced frequency of FOXP3-positive cells and reduced FOXP3 expression at the single-cell level." Immunology 123(1): 79-89.
- Vieira, P. L., J. R. Christensen, S. Minaee, E. J. O'Neill, F. J. Barrat, A. Boonstra, T. Barthlott, B. Stockinger, D. C. Wraith and A. O'Garra (2004). "IL-10-secreting regulatory T cells do not express Foxp3 but have comparable regulatory function to naturally occurring CD4+CD25+ regulatory T cells." Journal of immunology 172(10): 5986-5993.
- Voelkel, N. F. and R. Tuder (1994). "Interleukin-1 receptor antagonist inhibits pulmonary hypertension induced by inflammation." Annals of the New York Academy of Sciences 725: 104-109.
- Voelkel, N. F. and R. M. Tuder (1995). "Cellular and molecular mechanisms in the pathogenesis of severe pulmonary hypertension." The European respiratory journal : official journal of the European Society for Clinical Respiratory Physiology 8(12): 2129-2138.
- Wagenvoort, C. A. (1960). "Vasoconstriction and medial hypertrophy in pulmonary hypertension." Circulation 22: 535-546.
- Wagenvoort, C. A. (1970). "The pathology of primary pulmonary hypertension." The Journal of pathology 101(4): Pi.
- Wallace, V. A., S. Kondo, T. Kono, Z. Xing, E. Timms, C. Furlonger, E. Keystone, J. Gaudie, D. N. Sauder, T. W. Mak and et al. (1994). "A role for CD4+ T cells in the pathogenesis of skin fibrosis in tight skin mice." European journal of immunology 24(6): 1463-1466.
- Wang, J., A. Ioan-Facsinay, E. I. van der Voort, T. W. Huizinga and R. E. Toes (2007). "Transient expression of FOXP3 in human activated nonregulatory CD4+ T cells." European journal of immunology 37(1): 129-138.
- Wang, J. H., H. P. Redmond, R. W. Watson, C. Condron and D. Bouchier-Hayes (1995). "Induction of heat shock protein 72 prevents neutrophil-mediated human endothelial cell necrosis." Archives of surgery 130(12): 1260-1265.
- Wang, T., Y. Liu, L. Chen, X. Wang, X. R. Hu, Y. L. Feng, D. S. Liu, D. Xu, Y. P. Duan, J. Lin, X. M. Ou and F. Q. Wen (2009). "Effect of sildenafil on acrolein-induced airway inflammation and mucus production in rats." The European respiratory journal : official journal of the European Society for Clinical Respiratory Physiology 33(5): 1122-1132.
- Wang, Z. and W. H. Newman (2003). "Smooth muscle cell migration stimulated by interleukin 6 is associated with cytoskeletal reorganization." The Journal of surgical research 111(2): 261-266.
- Warner, S. J., K. R. Auger and P. Libby (1987). "Interleukin 1 induces interleukin 1. II. Recombinant human interleukin 1 induces interleukin 1 production by adult human vascular endothelial cells." Journal of immunology 139(6): 1911-1917.
- Weiner, H. L. (2002). "Induction and mechanism of action of transforming growth factor- $\beta$ -secreting Th3 regulatory cells" Immunological Reviews 182:207-214
- Welsh, D. J., M. Harnett, M. MacLean and A. J. Peacock (2004). "Proliferation and signaling in fibroblasts: role of 5-hydroxytryptamine<sub>2A</sub> receptor and transporter." American journal of respiratory and critical care medicine 170(3): 252-259.
- White, K., Y. Dempsie, M. Nilsen, A. F. Wright, L. Loughlin and M. R. MacLean (2011). "The serotonin transporter, gender, and 17beta oestradiol in the development of pulmonary arterial hypertension." Cardiovascular research 90(2): 373-382.
- White, K., A. K. Johansen, M. Nilsen, L. Ciucian, E. Wallace, L. Paton, A. Campbell, I. Morecroft, L. Loughlin, J. D. McClure, M. Thomas, K. M. Mair and M. R. Maclean (2012). "Activity of the Estrogen-Metabolizing Enzyme Cytochrome P450 1B1 Influences the Development of Pulmonary Arterial Hypertension." Circulation 126(9): 1087-1098.
- White, K., L. Loughlin, Z. Maqbool, M. Nilsen, J. McClure, Y. Dempsie, A. H. Baker and M. R. MacLean (2011). "Serotonin transporter, sex, and hypoxia: microarray analysis in the pulmonary arteries of mice identifies genes with relevance to human PAH." Physiological genomics 43(8): 417-437.
- Wigren, M., H. Bjorkbacka, L. Andersson, I. Ljungcrantz, G. N. Fredrikson, M. Persson, C. Bryngelsson, B. Hedblad and J. Nilsson (2012). "Low Levels of Circulating CD4+FoxP3+ T Cells Are Associated With an Increased Risk for Development of

- Myocardial Infarction But Not for Stroke." Arteriosclerosis, thrombosis, and vascular biology 32(8): 2000-2004.
- Willers, E. D., J. H. Newman, J. E. Loyd, I. M. Robbins, L. A. Wheeler, M. A. Prince, K. C. Stanton, J. A. Cogan, J. R. Runo, D. Byrne, M. Humbert, G. Simonneau, B. Sztrymf, J. A. Morse, J. A. Knowles, K. E. Roberts, J. J. McElroy, R. J. Barst and J. A. Phillips, 3rd (2006). "Serotonin transporter polymorphisms in familial and idiopathic pulmonary arterial hypertension." American journal of respiratory and critical care medicine 173(7): 798-802.
- Wilson, D. W., H. J. Segall, L. C. Pan, M. W. Lame, J. E. Estep and D. Morin (1992). "Mechanisms and pathology of monocrotaline pulmonary toxicity." Critical reviews in toxicology 22(5-6): 307-325.
- Wing, K., Z. Fehervari and S. Sakaguchi (2006). "Emerging possibilities in the development and function of regulatory T cells." Int Immunol 18(7): 991-1000.
- Wipff, J., A. Kahan, E. Hachulla, J. Sibilia, J. Cabane, O. Meyer, L. Mouthon, L. Guillevin, C. Junien, C. Boileau and Y. Allanore (2007). "Association between an endoglin gene polymorphism and systemic sclerosis-related pulmonary arterial hypertension." Rheumatology 46(4): 622-625.
- Wright, B. H., J. M. Corton, A. M. El-Nahas, R. F. Wood and A. G. Pockley (2000). "Elevated levels of circulating heat shock protein 70 (Hsp70) in peripheral and renal vascular disease." Heart and vessels 15(1): 18-22.
- Xu, Q., Y. Hu, R. Kleindienst and G. Wick (1997). "Nitric oxide induces heat-shock protein 70 expression in vascular smooth muscle cells via activation of heat shock factor 1." The Journal of clinical investigation 100(5): 1089-1097.
- Xu, Q., D. G. Li, N. J. Holbrook and R. Udelsman (1995). "Acute hypertension induces heat-shock protein 70 gene expression in rat aorta." Circulation 92(5): 1223-1229.
- Xu, Q., G. Schett, C. Li, Y. Hu and G. Wick (2000). "Mechanical stress-induced heat shock protein 70 expression in vascular smooth muscle cells is regulated by Rac and Ras small G proteins but not mitogen-activated protein kinases." Circulation research 86(11): 1122-1128.
- Xu, Q., G. Schett, C. S. Seitz, Y. Hu, R. S. Gupta and G. Wick (1994). "Surface staining and cytotoxic activity of heat-shock protein 60 antibody in stressed aortic endothelial cells." Circulation research 75(6): 1078-1085.
- Yagi, H., T. Nomura, K. Nakamura, S. Yamazaki, T. Kitawaki, S. Hori, M. Maeda, M. Onodera, T. Uchiyama, S. Fujii and S. Sakaguchi (2004). "Crucial role of FOXP3 in the development and function of human CD25+CD4+ regulatory T cells." International immunology 16(11): 1643-1656.
- Young, M. R. (2012). "Endothelial cells in the eyes of an immunologist." Cancer immunology, immunotherapy : CII.
- Yu, N., X. Li, W. Song, D. Li, D. Yu, X. Zeng, M. Li and X. Leng (2012). "CD4(+)CD25(+)CD127 (low/-) T Cells: A More Specific Treg Population in Human Peripheral Blood." Inflammation.
- Yuan, J. X., A. M. Aldinger, M. Juhaszova, J. Wang, J. V. Conte, Jr., S. P. Gaine, J. B. Orens and L. J. Rubin (1998). "Dysfunctional voltage-gated K<sup>+</sup> channels in pulmonary artery smooth muscle cells of patients with primary pulmonary hypertension." Circulation 98(14): 1400-1406.
- Yurovsky, V. V., F. M. Wigley, R. A. Wise and B. White (1996). "Skewing of the CD8<sup>+</sup> T-cell repertoire in the lungs of patients with systemic sclerosis." Human immunology 48(1-2): 84-97.
- Zaiman, A. L., M. Podowski, S. Medicherla, K. Gordy, F. Xu, L. Zhen, L. A. Shimoda, E. Neptune, L. Higgins, A. Murphy, S. Chakravarty, A. Protter, P. B. Sehgal, H. C. Champion and R. M. Tuder (2008). "Role of the TGF-beta/Alk5 signaling pathway in monocrotaline-induced pulmonary hypertension." Am J Respir Crit Care Med 177(8): 896-905.
- Zamanian, R. T., G. Hansmann, S. Snook, D. Lilienfeld, K. M. Rappaport, G. M. Reaven, M. Rabinovitch and R. L. Doyle (2009). "Insulin resistance in pulmonary arterial hypertension." The European respiratory journal : official journal of the European Society for Clinical Respiratory Physiology 33(2): 318-324.
- Zanin-Zhorov, A., L. Cahalon, G. Tal, R. Margalit, O. Lider and I. R. Cohen (2006). "Heat shock protein 60 enhances CD4<sup>+</sup> CD25<sup>+</sup> regulatory T cell function via innate TLR2 signaling." The Journal of clinical investigation 116(7): 2022-2032.

- Zanin-Zhorov, A., G. Nussbaum, S. Franitza, I. R. Cohen and O. Lider (2003). "T cells respond to heat shock protein 60 via TLR2: activation of adhesion and inhibition of chemokine receptors." FASEB journal : official publication of the Federation of American Societies for Experimental Biology 17(11): 1567-1569.
- Zanin-Zhorov, A., Bruck, R., Tal, G., Oren, S., Aeed, H., Hershkovich, R., Cohen, I.R. and Lider O (2005). "Heat Shock Protein 60 Inhibits Th1-Mediated Hepatitis Model via Innate Regulation of Th1/Th2 Transcription Factors and Cytokines." Journal of Immunology 174 (6):3227-36.
- Zarpelon, A. C., L. G. Pinto, T. M. Cunha, S. M. Vieira, V. Carregaro, G. R. Souza, J. S. Silva, S. H. Ferreira, F. Q. Cunha and W. A. Verri, Jr. (2012). "Endothelin-1 induces neutrophil recruitment in adaptive inflammation via TNFalpha and CXCL1/CXCR2 in mice." Canadian journal of physiology and pharmacology 90(2): 187-199.
- Zhang, S., I. Fantozzi, D. D. Tigno, E. S. Yi, O. Platoshyn, P. A. Thistlethwaite, J. M. Kriett, G. Yung, L. J. Rubin and J. X. Yuan (2003). "Bone morphogenetic proteins induce apoptosis in human pulmonary vascular smooth muscle cells." American journal of physiology. Lung cellular and molecular physiology 285(3): L740-754.
- Zhao, L., N. A. Mason, N. W. Morrell, B. Kojonazarov, A. Sadykov, A. Maripov, M. M. Mirrakhimov, A. Aldashev and M. R. Wilkins (2001). "Sildenafil inhibits hypoxia-induced pulmonary hypertension." Circulation 104(4): 424-428.
- Zhao, Y. D., D. W. Courtman, Y. Deng, L. Kugathasan, Q. Zhang and D. J. Stewart (2005). "Rescue of monocrotaline-induced pulmonary arterial hypertension using bone marrow-derived endothelial-like progenitor cells: efficacy of combined cell and eNOS gene therapy in established disease." Circulation research 96(4): 442-450.
- Zheng, J., Y. Liu., Y. Lau. and W. Tu (2013). "γδ-T cells: an unpolished sword in human anti-infection immunity." Cellular & Molecular Immunology 10, 50–57.
- Zhou, W., K. Hashimoto, K. Goleniewska, J. F. O'Neal, S. Ji, T. S. Blackwell, G. A. Fitzgerald, K. M. Egan, M. W. Geraci and R. S. Peebles, Jr. (2007). "Prostaglandin I2 analogs inhibit proinflammatory cytokine production and T cell stimulatory function of dendritic cells." Journal of immunology 178(2): 702-710.
- Zhu, J., A. A. Quyyumi, H. Wu, G. Csako, D. Rott, A. Zalles-Ganley, J. Ogunmakinwa, J. Halcox and S. E. Epstein (2003). "Increased serum levels of heat shock protein 70 are associated with low risk of coronary artery disease." Arteriosclerosis, thrombosis, and vascular biology 23(6): 1055-1059.
- Zhu, W., P. Roma, A. Pirillo, F. Pellegatta and A. L. Catapano (1996). "Human endothelial cells exposed to oxidized LDL express hsp70 only when proliferating." Arteriosclerosis, thrombosis, and vascular biology 16(9): 1104-1111.
- Zimmet, P. Z., V. R. Collins, M. P. de Courten, A. M. Hodge, G. R. Collier, G. K. Dowse, K. G. Alberti, J. Tuomilehto, F. Hemraj, H. Gareeboo, P. Chitson and D. Fareed (1998). "Is there a relationship between leptin and insulin sensitivity independent of obesity? A population-based study in the Indian Ocean nation of Mauritius. Mauritius NCD Study Group." International journal of obesity and related metabolic disorders : journal of the International Association for the Study of Obesity 22(2): 171-177.
- Zlotnik, A., D. I. Godfrey., M. Fisher and T. Suda (1992). "Cytokine production by mature and immature CD4-CD8- T cells. Alpha beta-T cell receptor+ CD4-CD8- T cells produce IL-4." The Journal of Immunology 149:4 1211-1215